Terms and Conditions of Use of Digitised Theses from Trinity College Library Dublin

Copyright statement

All material supplied by Trinity College Library is protected by copyright (under the Copyright and Related Rights Act, 2000 as amended) and other relevant Intellectual Property Rights. By accessing and using a Digitised Thesis from Trinity College Library you acknowledge that all Intellectual Property Rights in any Works supplied are the sole and exclusive property of the copyright and/or other IPR holder. Specific copyright holders may not be explicitly identified. Use of materials from other sources within a thesis should not be construed as a claim over them.

A non-exclusive, non-transferable licence is hereby granted to those using or reproducing, in whole or in part, the material for valid purposes, providing the copyright owners are acknowledged using the normal conventions. Where specific permission to use material is required, this is identified and such permission must be sought from the copyright holder or agency cited.

Liability statement

By using a Digitised Thesis, I accept that Trinity College Dublin bears no legal responsibility for the accuracy, legality or comprehensiveness of materials contained within the thesis, and that Trinity College Dublin accepts no liability for indirect, consequential, or incidental, damages or losses arising from use of the thesis for whatever reason. Information located in a thesis may be subject to specific use constraints, details of which may not be explicitly described. It is the responsibility of potential and actual users to be aware of such constraints and to abide by them. By making use of material from a digitised thesis, you accept these copyright and disclaimer provisions. Where it is brought to the attention of Trinity College Library that there may be a breach of copyright or other restraint, it is the policy to withdraw or take down access to a thesis while the issue is being resolved.

Access Agreement

By using a Digitised Thesis from Trinity College Library you are bound by the following Terms & Conditions. Please read them carefully.

I have read and I understand the following statement: All material supplied via a Digitised Thesis from Trinity College Library is protected by copyright and other intellectual property rights, and duplication or sale of all or part of any of a thesis is not permitted, except that material may be duplicated by you for your research use or for educational purposes in electronic or print form providing the copyright owners are acknowledged using the normal conventions. You must obtain permission for any other use. Electronic or print copies may not be offered, whether for sale or otherwise to anyone. This copy has been supplied on the understanding that it is copyright material and that no quotation from the thesis may be published without proper acknowledgement.

Investigation of Autoantibody Profiling to Reveal Biomarkers of Ovarian Cancer

A thesis submitted to the University of Dublin for the degree of Doctor of Philosophy

by

Mairead Anne Murphy (B.Sc.)

Supervisor: Prof. John O'Leary

Department of Histopathology and Morbid Anatomy,

University of Dublin

Trinity College

January 2013

Declaration

I declare that this thesis has not been submitted as an exercise for a degree at this or any other university and it is entirely my own work. I agree to deposit this thesis in the University's open access institutional repository or allow the Library to do so on my behalf, subject to Irish Copyright Legislation and Trinity College Library conditions of use and acknowledgement.

Acknowledgments

My heartfelt thanks to the Emer Casey Foundation and the People of Youghal. I really felt part of your wonderful community and am inspired by your determination and generosity. Your support has been very much appreciated and I hope this work will shed some light on ovarian cancer detection in Emer's memory.

A sincere thanks to my principal supervisor, Professor John O'Leary, your insight and understanding has really helped me over the last three years. Meetings with you were always very motivational, thanks for your positivity and guidance.

Professor Dolores Cahill, thank you very much for your guidance and for the opportunity to work as part of your research group in UCD. You were always very generous with your time and I have learned so much about this research field and beyond thanks to your direction.

A special thanks to Dr David O'Connell for sharing your enthusiasm, knowledge and time. Dave you have been a great support to me over the last three years, both professionally and personally. You've been a fantastic mentor and a great friend, I couldn't have done this without you.

Thanks to Dr Sharon O'Toole for your infinite ovarian cancer knowledge and support! You have been a patient and considerate mentor and have had an invaluable input into

this research.

A big thank you to Dr John O'Brien, I know you have had a lot of late nights and early mornings throughout this project. Your statistical and bioinformatic input is very much appreciated.

Thanks to Professor Orla Shiels and Dr Cara Martin, the two of you have been great sounding boards, thanks for your advice and support over the past few years.

Sara O'Kane, thanks so much for your understanding and humour. Your friendship has seen me through some tough times, I don't think I'll ever be able to get a hot chocolate and not think of our chats!

Thanks to my family who have always been there for me, it has been a long road, all my love to Mam, James, Leah and Mia.

Jay, my wonderful fiancé, thank you for everything. Life starts here.....

For my Family

'...I cried without shame for I love them dear, and I loved them in secret for fear of discovery; yes, I tell you this, for how wrong can you be? And in the closeness of that room I reached out and touched my family..'

Publications Arising from this Thesis

Peer Reviewed Articles

MA. Murphy, JJ. O'Leary, DJ. Cahill. Assessment of the humoral immune response to cancer. *Journal of Proteomics.* 2012 Aug 3;75(15):4573-9. PMID:22300580

MA. Murphy, DJ. O'Connell, SL. O'Kane, JK. O'Brien, S. O'Toole, C. Martin, O. Sheils, JJ. O'Leary, DJ. Cahill. Epitope presentation is an important determinant of the utility of antigens identified from protein arrays in the development of autoantibody diagnostic assays. *Journal of Proteomics.* 2012 Aug 3;75(15):4668-75. PMID:22415278

Book Chapters

S. O'Toole, R. Langhe, DJ. Cahill, MA. Murphy, DJ. O'Connell, C. Martin, M. Gallagher, C. Spillane, O. Sheils, JJ. O'Leary. Non-invasive Diagnostic Biomarkers in Ovarian Cancer. *Cancer Biomarkers.* In preparation. November 2012

Articles in Preparation

MA. Murphy *et al.* Identification of robust ovarian cancer associated autoantibody profiles using high content protein arrays.

Conference Abstracts

MA. Murphy, DJ. O'Connell, JK. O'Brien, S. O'Toole, SL. O'Kane, C. Martin, O. Sheils, JJ. O'Leary, DJ. Cahill. To identify autoantibody biomarkers of ovarian cancer. *4th School of Medicine Postgraduate Research Day, TCD.* Dublin, 2011.

MA. Murphy, DJ. O'Connell, JK. O'Brien, S. O'Toole, SL. O'Kane, C. Martin, O. Sheils, JJ. O'Leary, DJ. Cahill. Autoantibodies: Novel biomarkers of ovarian cancer? *Conway Institute Festival of Research and Innovation 2011, UCD.* Dublin, 2011.

MA. Murphy, DJ. O'Connell, JK. O'Brien, S. O'Toole, SL. O'Kane, C. Martin, O. Sheils, JJ. O'Leary, DJ. Cahill. Autoantibody profiling to determine biomarkers of ovarian cancer. *The 8th International Cancer Conference -State of the Art Cancer Care, TCD.* Dublin, 2011.

MA. Murphy, DJ. O'Connell, JK. O'Brien, S. O'Toole, SL. O'Kane, C. Martin, O. Sheils, JJ. O'Leary, DJ. Cahill. Identification of autoantibodies as novel ovarian cancer biomarkers. *Young Life Scientists Symposium 2011.* Dublin, 2011.

MA. Murphy, DJ. O'Connell, JK. O'Brien, S. O'Toole, SL. O'Kane, C. Martin, O. Sheils, JJ. O'Leary, DJ. Cahill. Autoantibody profiling to determine biomarkers of ovarian cancer. *The Ovarian Cancer Screening Conference.* London, 2011.

MA. Murphy, DJ. O'Connell, JK. O'Brien, S. O'Toole, SL. O'Kane, C. Martin, O. Sheils, JJ. O'Leary, DJ. Cahill. Identification of circulating autoantibodies as novel ovarian cancer biomarkers. *United States and Canadian Academy of Pathology 101st Annual Meeting.* Vancouver, 2012.

MA. Murphy, DJ. O'Connell, JK. O'Brien, S. O'Toole, SL. O'Kane, C. Martin, O. Sheils, JJ. O'Leary, DJ. Cahill. Identification of autoantibodies as novel ovarian cancer biomarkers. *Irish Association for Cancer Research Annual Meeting.* Belfast, 2012.

MA. Murphy, DJ. O'Connell, JK. O'Brien, S. O'Toole, SL. O'Kane, C. Martin, O. Sheils, JJ. O'Leary, DJ. Cahill. Identification of ovarian cancer biomarkers by profiling

the autoantibody repertoire in patients. *British Gynaecological Cancer Society Annual Scientific Meeting.* London 2012

Additional Achievements

Invited Presentation: MA. Murphy. Circulating Autoantibodies as Biomarkers of Ovarian Cancer. *Conway Lecture and Seminar Series - CLASS.* UCD, Dublin, 2011.

Patent Application: Autoantibody Biomarkers of Ovarian Cancer.

Summary

Ovarian cancer is the most deadly gynaecological malignancy and 70% of all women with ovarian cancer die within 5 years of diagnosis. When diagnosed in early stages, ovarian cancer is curable in 90% of cases, however early diagnosis is rare. Over 80% of ovarian cancer patients are diagnosed in late stages when there is only a 30% 5-year survival rate. Ovarian cancer is a relatively asymptomatic disease and biomarkers are unreliable. CA125 is the only routinely used ovarian cancer biomarker, however with a sensitivity of 89% and a specificity of 72% there are many undetected cases. The absence of specific symptoms and a reliable screening tool results in a very poor prognosis for patients. A reliable biomarker of ovarian cancer may improve patient care and survival, especially for tumours which arise from benign precursors such as mucinous tumours. The immune system is an intricate biological system that protects against external agents and regulates internal processes. Autoantibodies are classically associated with autoimmune disease however there is a humoral immune response to antigens released during tumourigenesis. Autoantibodies can arise in advance of clinically detectable disease using conventional diagnostic techniques making them interesting biomarker entities. As ovarian cancer has no reliable biomarkers and has been identified as an immunogenic tumour, assessment of the autoantibody response may provide valuable insight into disease state.

In this study we identified the autoantibody profiles of 74 human serum samples using the hEx1 array. Antigens associated with ovarian disease were selected, expressed,

purified and were interrogated by secondary analyses; protein microarray and ELISA. The most robust autoantibody identified at this stage was the p53 antigen. Autoantibodies to p53 were identified in 20-25% of late stage ovarian cancer patients in all platforms interrogated, which is in-line with published data. Secondary pooled serum hEx1 array screening was compared to previous results to identify robust associated autoantibodies. This identified p53, adducin and endosulfine alpha autoantibodies as ovarian cancer associated. Further validation identified adducin autoantibodies as potential biomarkers of ovarian disease as autoantibodies to this antigen were not identified in non-remarkable controls (n=15). Epitope presentation was identified as an important determinant of antibody binding. This is a significant finding when considering the development of autoantibody diagnostic assays. In addition autoantibody profiles of 20 human serum samples were identified using the Invitrogen ProtoArray. A serum set of non-remarkable controls, benign ovarian disease, early and late stage ovarian cancer patients were screened (benign and malignant tumours were serous histology). Comparison of the ProtoArray and hEx1 serum screening results identified variation between array platforms, highlighting the difference in array platforms and autoantibody binding. Autoantibody profiles were identified as cohort associated, the relatively unknown angiomotin antigen was identified as early stage ovarian carcinoma associated.

In summary this research has identified autoantibodies associated with ovarian cancer using two different protein array platforms. Autoantibodies to p53 have been identified and are consistent with published data which confirms the approach taken. Numerous autoantibodies of interest have been identified, however autoantibodies to adducin and angiomotin are of particular interest and are currently being investigated further. This research advances the field of autoantibody profiling in terms of the consistencies and variances of autoantibody profiling associated with differential experimental platforms.

Abbreviations

AAb Autoantibody

AJCC American Joint Committee on Cancer

ANA Anti-nuclear antibody

APC Antigen presenting cell

APS Ammonium persulfate

ATP Adenosine triphosphate

BRAF V-raf murine sarcoma viral oncogene homolog B1

BRCA1 Breast cancer susceptibility protein 1

BRCA2 Breast cancer susceptibility protein 2

BSA Bovine serum albumin

CA125 Cancer antigen 125

cDNA Complimentary deoxyribonucleic acid

cm Centimetre

dsDNA Double stranded deoxyribonucleic acid

DNA Deoxyribonucleic acid

DTT Dithiothreitol

EMT Epithelial-mysenchymal transition

ELISA Enzyme linked immunosorbent assay

Fab Fragment antigen-binding

Fc Fragment crystallizable

FDA Food drug administration

FIGO International Federation of Gynecology and Obstetrics

GuHCl Guanidine hydrochloride

GST Glutathione S-transferase

HE4 Human epididymis protein 4

HEPES Hydroxyethyl piperazineethanesulfonic acid

hEx1 Human expression library

HRP Horseradish peroxidase

HSP Heat shock protein

IgG Immunoglobulin G

IgM Immunoglobulin M

IL Interleukin

IMAC Immobilised-metal affinity chromatography

IPTG Isopropyl β-D-1-thiogalactopyranoside

KRAS Kirsten rat sarcoma viral oncogene homolog

MAPK Mitogen-activated protein kinase

MDT Multi-disciplinary team

MICA Major histocompatibility complex class I chain-related molecule A

MHC Major histocompatibility complex

ml millilitre

mRNA Messenger RNA

NCBI National Centre for Biotechnology Information

NELF Negative elongation factor

NK Natural killer

OC Ovarian cancer

PAGE Polyacrylimide gel electrophoresis

PBS Phosphate buffered saline

PH Pleckstrin homology

PP2A Protein phosphatase 2A

PTM Post-translational modification

PVDF Polyvinylidene fluoridefp

RA Rheumatoid arthritis

RNA Ribonucleic acid

ROC Risk of ovarian cancer

ROMA Risk of ovarian malignancy algorithm

RT Room Temperature

SCS1 Succinyl coenzyme A synthetase 1

SDS Sodium dodecyl sulfate

SEREX Serological analysis of recombinant cDNA expression libraries

SLE Systemic lupus erythematosus

SNARE Soluble N-ethylmaleimide-sensitive factor attachment protein receptor

STAT Signal transducer and activator of transcription

TEMED N,N,N´,N´-tetramethylethylenediamine

TMB 3,3´,5,5´-tetramethylbenzidine

tRNA Transfer RNA

TSG Tumour suppressor gene

TVU Transvaginal ultrasonography

UKCTOCS United Kingdom collaborative trial of ovarian cancer screening

UTR Untranslated region

VEGF Vascular endothelial growth factor

μ**l** microlitre

Contents

List of Figures

List of Tables

Chapter 1

Introduction

1.1 Cancer

Cancer is an abnormal growth of cells caused by multiple genetic changes leading to a dysreguated balance of cell proliferation and cell death. Benign growths differ from cancer cells as benign tumours grow only locally and cannot invade surrounding tissue and metastasise. Cancer is fast becoming the leading cause of death in the developed world and has replaced heart disease as the leading cause of death in patients younger than 85 years [1] (Figure 1.1). Carcinogenesis is a multistep process whereby normal cells are transformed into cancer cells, usually through multistep somatic mutations in normal cells that lead to tumourigenesis. Cancers are diagnosed more frequently in an older population [2, 3], this is accredited to the accumulation of mutations (outlined in Figure 1.2) as a result of less efficient cellular repair mechanisms as a person ages [4, 5]. For many cancers, precursor lesions have been identified, further supporting the multistep and progressive mutation hypothesis.

1.1.1 Hallmarks of Cancer

Cancer classically has 6 hallmarks that are used to define and differentiate cancer from non-malignant tumours [7]. These hallmarks are:

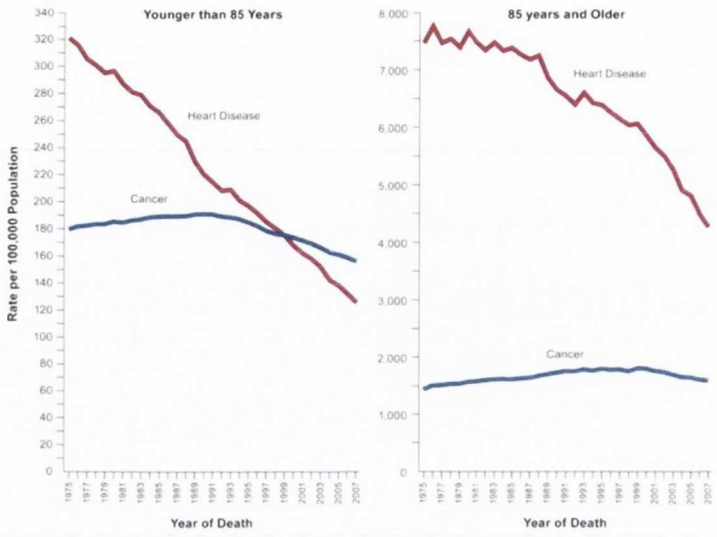

Figure 1.1: Cancer a Leading Cause of Death

This figure outlines the death rates for cancer and heart disease for ages younger than 85 years and 85 years and older, from 1975 to 2006. The rates are age adjusted to the 2000 United States standard population. From this figure it is evident that cancer is the leading cause of death among men and women aged younger that 85 years in the United States. From Jemal *et al*, Cancer statistics, 2010 [6].

Self-sufficiency in growth signals

Cancerous cells provide an autonomous source of growth stimulus to continue to develop and multiply rapidly without environmental stimuli [7, 8]. A proto-oncogene is a normal gene that can become an oncogene as a results of a gain of function mutation leading to increased cellular growth. Proto-oncogenes may be growth factors or receptors, signal transduction proteins, nuclear regulatory proteins or cell cycle regulators and when mutated the resulting oncogene codes for an altered or excessively produced growth control protein. Oncogenes disrupt cell growth signalling resulting in uncontrolled cell proliferation and differentiation . One of the best examples of an oncogene is the Myc gene. The Myc gene promotes a balance of pro- and anti-tumourigenic properties and mutations in Myc can shift this balance [9]. The c-Myc oncoprotein is significantly over-expressed in most human cancers [9, 10, 11] and regulation of Myc transcription

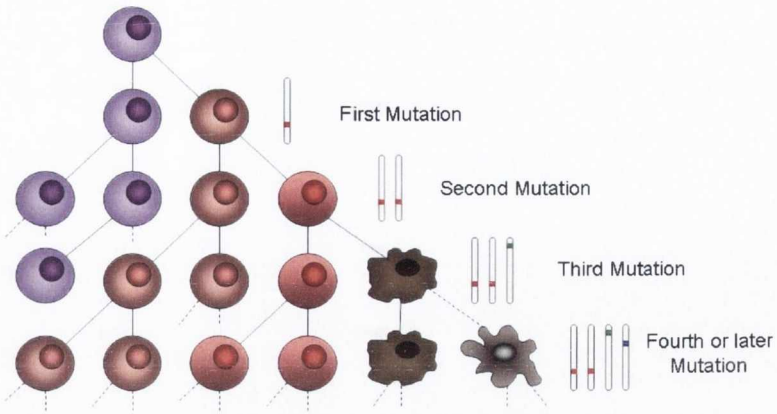

Figure 1.2: The clonal evolution model of carcinogenesis

This figure outlines the somatic evolution model of tumourigenesis where mutations accumulate in cells of the body. With increasing mutations and under selective pressure, damaged cells may undergo transformation and become malignant neoplasms. It has long been postulated that three mutations at least are needed to results in malignant change. Adapted from Cavenee and White, Scientific American 1995 [13].

may be used as a therapeutic strategy [12]. In ovarian cancer, oncogenes such as Kirsten rat sarcoma viral oncogene homolog (kRAS) and v-raf murine sarcoma viral oncogene homolog B1 (BRAF) are used to categorise the disease, this is discussed later in Section 1.7.1.

Insensitivity to anti-growth signals

Cancer cells not only promote their own growth, but also evade antigrowth signals in order to proliferate. In normal cells, there are many antiproliferative signals to maintain tissue homeostasis. Tumour suppressor genes (TSG) are genes that contribute to cancer development in a loss of function manner. These genes act as 'guardians of the genome' and are often involved in maintaining genomic integrity through involvement in deoxyribonucleic acid (DNA) repair and chromosomal segregation [14, 15, 16]. These genes are of vital importance in maintaining genomic health, hence any loss of function in TSGs will result in a mutator phenotype, whereby the risk of developing further

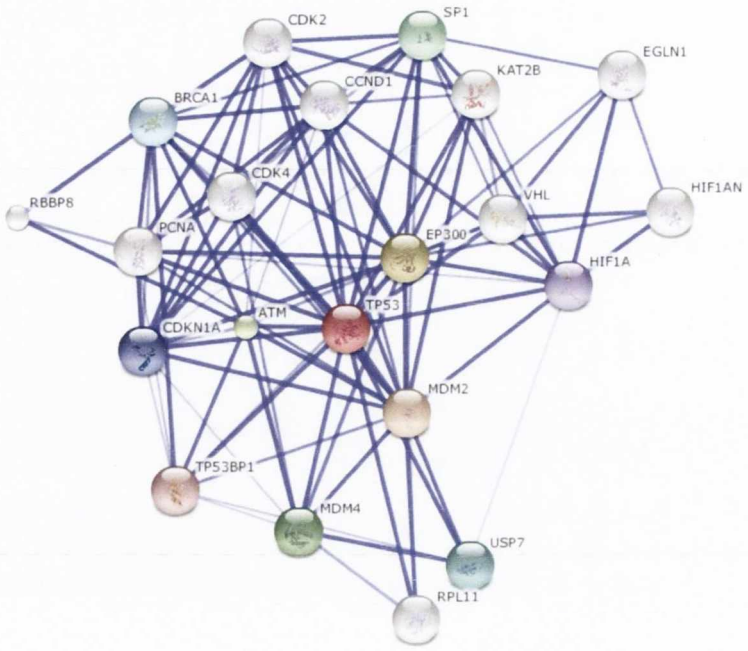

Figure 1.3: Portion of the p53 interaction network

The p53 interaction network is a crucial network that regulates the cell cycle and apoptosis. In this figure, p53 is identified by the red marker. This scaled down interaction network was generated using the String database (http://string-db.org).

mutations is increased. Mutations in TSGs are believed to be the first mutation in the multistep mutation series that leads to cancer (outlined in Figure 1.2).

A classic example of a TSG is the TP53 gene. The p53 protein is a transcription factor that has critical roles in the cellular stress response. p53 is known to protect against tumourigenesis by inducing senescence in cells to facilitate DNA repair, or apoptosis in cells where there is severe or irreparable DNA damage [17, 18]. p53 acts in may ways (Figure 1.3) to prevent malignant transformation and maintain genetic integrity [19] and disruption of this pathway results in unregulated and uninhibited cellular proliferation and avoidance of anti-growth signalling in malignant tumours. TP53 mutation occurs in 80% of high grade ovarian carcinomas [20]. TP53 mutation and ovarian cancer grade are discussed in further detail in Section 1.7.1.

Evading apoptosis

Apoptosis, or programmed cell death is a mechanism which allows for the removal of damaged or potentially oncogenic cells. Apoptosis is a critical defence mechanism against carcinogenesis and inhibition of apoptosis results in a build up of "un-dead" or immortal cells [21]. The Bcl-2 family of proteins regulate cell death by controlling cytochrome c release through mitochondrial membrane permeability [22, 23]. Bcl-2 upregulation has been associated with cancer progression [24, 25] and also resistance to chemotherapy [26, 27]. In ovarian cancer, Bcl-2 expression is associated with improved patient survival [28, 29].

Sustained angiogenesis

Angiogenesis and vasculogenesis are critical for growth and metastasis of solid tumours. New vessels facilitate the supply of oxygen and nutrients to the tumour and remove waste products. Importantly, new vessels also facilitate metastasis by providing "highways" for circulating tumour cell migration. Vascular endothelial growth factor (VEGF) is one of the best characterised and most potent angiogenic factors. VEGF expression is induced by growth factors, cytokines and hypoxia [30, 31]. VEGF and/or its receptor VEGFR, have been shown to be up-regulated/over-expressed in various cancers [32, 33]. Bevacizumab (trade name Avastin, Genetech/Roche) is a humanized monoclonal antibody and was the first Food and Drug Administration (FDA) approved angiogenic inhibitor [34]. Treatment with bevicizumab has shown improved survival in patients with cancers such as colorectal [35] and lung [36] among others cancers [37, 38]. Antivascular agents have also yielded promising results in ovarian cancer treatment [39].

Limitless replicative potential

Telomeres are regions of repetitive nucleotide sequences found at the ends of chromosomes, the function of telomores is to protect and confer stability of chromosome ends. With each cell division telomeres shorten, hence normal cells may only undergo mitosis a finite number of times, but in malignancy cells become immortalised, hence circumventing telomere-dependent pathways of cell mortality [40, 41]. Telomerase is a cellular reverse transcriptase which adds DNA sequence repeats to the 3' end of DNA strands in telomeric regions of chromosomal ends. By elongating telomeres, telomerase acts to prevent cell growth arrest or cell death. In most normal human cells, telomerase is not expressed, however in malignant tumours telomerase is detected in approximately 90% of cases [42, 43]. The immune system is capable of detecting alterations in this system as anti-human telomerase reverse transcriptase autoantibodies (AAbs) have been postulated to be a novel and specific tumour marker [44].

Tissue invasion and metastasis

Invasion is the acquired ability of malignant cells to aggressively invade adjacent tissues. Metastasis involves tumour cell travel through the bloodstream or lymphatic system, to distant sites leading to new clusters of tumour cells growing in a different tissue site. Metastasis is the cause of 90% of deaths from cancer [45, 46]. It is a very complicated process that occurs through a number of steps; loss of cellular adhesion, increased motility and invasiveness, entry and survival in the circulation, exit to a new tissue and colonization at a new site [47]. For metastasis to occur all these steps must proceed without recognition and elimination by the immune system. Numerous models have been proposed to outline how malignant cells evolve molecular metastatic capabilities and at which stages cells gain metastatic competence [48, 49, 50, 47]. Currently the mechanisms and virulence genes that govern metastasis are not fully understood.

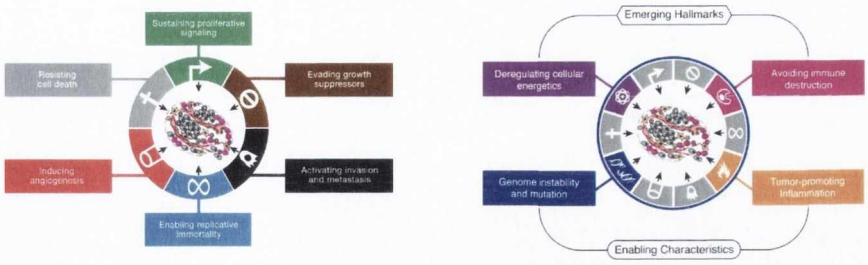

(a) The classic hallmarks of cancer (b) The emerging hallmarks of cancer

Figure 1.4: The hallmarks of cancer

The hallmarks shown are proposed by Hanahan and Weinberg [7, 8]. The classical hallmarks of cancer were proposed over 10 years ago. Two additional hallmarks and enabling characteristics were considered in a publication recently as a result of increased experimentation and understanding of cancer aetiology[8].

Recently, Hanahan and Weinberg have proposed two new, emerging hallmarks of cancer [8]. These emerging hallmarks were proposed as a result of an increasing body of research which suggests their involvement in pathogenesis. These emerging hallmarks are:

Deregulating cellular energetics

In malignant cells, reprogramming and changes in energy metabolism are required to fuel the excessive cell growth and proliferation that is seen in cancers. The discovery that malignant cells exhibit deregulation of metabolic pathways and elevated glycolysis was first documented in the 1930's by Warburg [51]. Under aerobic conditions normal cells do not favour glycolysis as a metabolic pathway, however tumour cells favour aerobic glycolysis producing lactate even in the presence of oxygen [52, 53]. It is now becoming increasingly clear that many oncogenes and tumour suppressor genes (TSG) are important regulators of metabolism. The TSG p53 has been shown to be involved in regulation of numerous metabolic pathways such as glycolysis, oxidative phosphorylation and fatty acid metabolism [54, 55]. High rates of glucose uptake are used in the

clinic to identify cancers, including ovarian, using positron emission tomography (Figure 1.6).

Avoiding immune destruction

It is known that genetic instability and thus genetic heterogeneity, is fundamental to neoplastic progression and underlies the evolutionary theory of cancer progression [56]. Immunoediting is a proposed process outlining how malignant cells avoid immune destruction . In this process, highly immunogenic tumour cells are routinely removed by the immune system leaving behind poorly immunogenic cell variants which may then prosper within the constraints of the host immune system [57]. Studies have also indicated that tumour cells may also exploit the immune system to enhance tumour progression [58, 59]. Although this theory implies tumours should be weakly immunogenic, an AAb response is elicited to tumours. We have recently reviewed this complicated area, however, much more research is needed to determine the nature of the relationship between malignancy and the host immune response [60].

1.2 Ovarian Cancer

Cancer of the ovary is a major clinical challenge in gynaecological oncology, having the highest mortality rate of all gynaecological malignancies and is termed 'the silent killer'. Worldwide approx 200,000 new cases of ovarian cancer are diagnosed each year with over 350 new cases in Ireland (ncri.ie accessed June 2012). The median age of patients presenting with ovarian cancer is 60 years of age and the lifetime risk for development of ovarian cancer is approx 1 in 70 [61]. From Table 1.1, clearly cancers such as breast have high rates of new cases and lower rates of estimated deaths due to the success of screening and tailored therapies. Ovarian cancer has a low rate of new cases, however it

has a relatively high estimated death rate indicating that ovarian cancer carries a very poor prognosis. Due to the anatomical position of the ovaries (Figure 1.5), metastasis to the peritoneal and/or pleural cavity is common.

Although ovarian cancer is a genetic disease, many influences such as hormonal and environmental factors may play direct and indirect roles in disease progression [62]. For the most part, ovarian cancer pathogenesis still poorly understood. Certainly a family history of ovarian cancer is the most significant risk factor, however there are a number of hypotheses that have been proposed to explain the aetiology of ovarian cancer. A family history of ovarian cancer is the most significant risk factor and the hereditary form represents 5-10% of all ovarian cancers[63, 64]. The most commonly mutated genes in hereditary ovarian cancer are breast cancer susceptibility protein 1 and 2 (BRCA1 and BRCA2) [65, 66, 67, 64, 68]. These genes are involved in DNA repair, however there are a number of hypotheses that have been proposed to explain the aetiology of sporadic ovarian cancer [69, 70, 71, 72, 73, 74]. Such hypotheses are the incessant ovulation hypothesis [74] and the gonadotropin hypothesis [70] among others. These hypotheses are not mutually exclusive and are based on evidence that with increasing numbers of ovulatory events, ovarian cancer risk is also increased. It is known that parous, compared to nulliparous women are at a lower risk of ovarian cancer and a late age at menarche and an early age at menopause are weak factors relating to reduced ovarian cancer risk [75, 76]. It is postulated that continual breakage of the ovarian follicle, cell proliferation and post-ovulatory repair of the ovarian surface results in increased cell divisions and mitoses [74, 77]. Therefore, with each ovulatory event there is an increased risk of mutation that may lead to carcinogenesis. Once ovarian cancer is diagnosed, treatment is usually a combination of surgery and chemotherapy [61]. However, ovarian cancer is a particularly refractory disease and many patients exhaust current chemotherapeutic options relatively quickly [78].

Table 1.1: Leading sites of new cancer cases and deaths, 2011 estimates (Female)

This table shows the estimated leading sites of new cancer cases and deaths in American women. *Adapted from "Cancer facts and figures 2011" American Cancer Society. (http://www.cancer.org)*

Estimated New Cases (%)	Estimated Deaths (%)
Breast - 30	Lung and Bronchus - 26
Lung and Bronchus - 14	Breast - 15
Colon and Rectum - 9	Colon and Rectum - 9
Uterine Corpus - 6	Pancreas - 7
Thyroid - 5	***Ovary - 6***
Non-Hodgkin Lymphoma - 4	Non-Hodgkin Lymphoma - 4
Melanoma - 4	Leukaemia - 3
Kidney and Renal Pelvis - 3	Uterine Corpus - 3
Ovary - 3	Liver and Bile Duct - 2
Pancreas - 3	Brain and Nervous System - 2

1.2.1 New Aetiological Findings

More recent morphological, immunohistochemical, and molecular genetic studies have indicated a different origin of epithelial ovarian cancer. It has been proposed that ovarian carcinoma can be divided in two broad categories, "Type I" and "Type II" tumours [79]. The terms, "Type I" and "Type II" refer to different tumorigenic pathways rather than specific histopathologies . "Type I" tumours are typified by somatic mutations in genes encoding protein kinases such as V-Ki-ras2 Kirsten rat sarcoma viral oncogene homolog (kRAS) and v-raf murine sarcoma viral oncogene homolog B1 (BRAF). These growths are often low grade and slow growing, they develop from a well characterized precursor lesion in a step by step fashion. "Type II" tumours are characterized by a high frequency of p53 mutation. "Type II" tumours are high grade with a rapid growth rate and have almost always spread beyond the ovaries at presentation. "Type II" tumours include high-grade serous and endometrioid carcinomas. It has always been assumed that the ovarian surface epithelium is the source of serous carcinomas, however recent

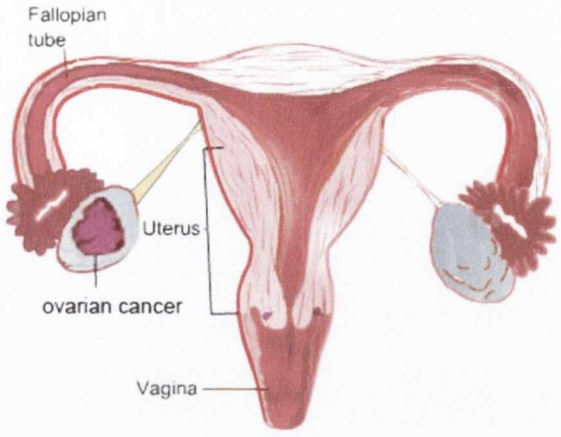

Figure 1.5: The female reproductive system

This diagram shows the position of the ovaries in relation to the rest of the female reproductive system. The ovaries are two almond sized glands located on either side of the uterus. The main function of the ovaries is to release eggs (ova) and hormones.

studies strongly suggest that the fallopian tube epithelium (benign or malignant) that implants on the ovary is the origin of low-grade and high-grade serous carcinoma [80]. Serous tubal intraepithelial carcinomas (STICs) and occult invasive high grade serous carcinomas (HGSC) have been described in the fallopian tube that closely resemble ovarian HGSC, thus it is postulated that these tumours may develop outside the ovary and involve it secondarily [81]. This aetiological theory of ovarian cancer is very recent and relates to this work and an understanding of disease aetiology is needed for experimental design.

1.3 Ovarian Cancer Diagnosis

1.3.1 Symptoms

Symptoms of ovarian cancer are very vague and non-specific. Symptoms include unexplained weight loss or gain, abdominal bloating, early satiety, abdominal cramps, back

pain, urination urgency/frequency, constipation and tiredness [82]. Occasionally, patients with early stage disease may present with pelvic pain as a result of torsion of the ovary [61]. Clearly these symptoms are not solely associated with ovarian cancer and cannot be used alone in diagnosis [83]. The lack of symptoms leads to the majority of patients being diagnosed after the disease has metastasised beyond the ovaries. Ovarian cancer, when diagnosed in early stages, results in over 90% 5-year survival rate, however, when diagnosed in late stages this is much lower at only 30% 5-year survival rate [79]. The ability to diagnose ovarian cancer in the early stages would revolutionise patient care and standard of living.

1.3.2 Biomarkers of Ovarian Cancer

CA 125

Cancer Antigen 125 (CA 125) is the only ovarian cancer biomarker that is routinely used in the clinic. CA 125 is a cell surface glycoprotein that is encoded by the MUC16 gene, the protein has a single transmembrane domain and provides a protective mucosal barrier against foreign particles and infectious agents on the surface of epithelial cells on the surface of the female reproductive tract. [84].

Typically in the clinic values of less than 35 units/mL are considered normal, however elevated CA 125 is also associated with conditions such as pregnancy, endometriosis, adenomyosis, uterine fibroids, pelvic inflammatory disease, menstruation, benign cysts and also other malignancies such as pancreatic, breast, lung, gastric, and colon cancer. [61]. The sensitivity and specificity determine the utility of the test (outlined in Figure 1.7) and for the CA 125 test the sensitivity and specificity is 89%, and 72% respectively [85], it is raised in approximately only 50% of early stage epithelial ovarian cancers and in 75%–90% of patients with advanced disease [85, 86]. CA 125 screening combined with transvaginal ultrasonography (TVU) increases sensitivity and specificity

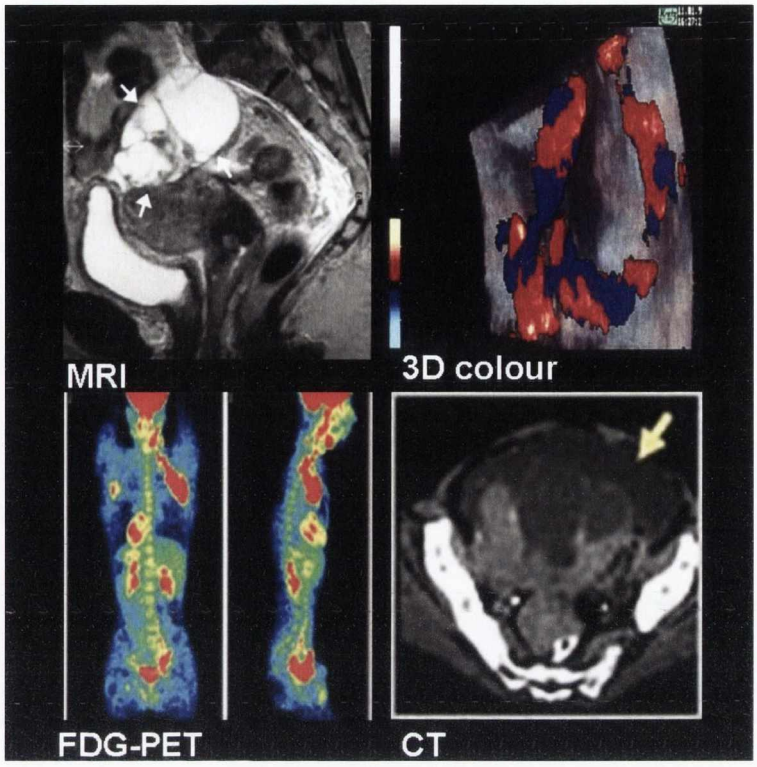

Figure 1.6: Imaging platforms in ovarian cancer

This figures shown the different imaging methodologies used in ovarian cancer diagnosis and monitoring. The mainstay imaging technique of ovarian cancer is transvaginal ultrasonography which may be augmented by 3D colour Doppler, an example of this imaging technique is shown in the top right of this image.

to 89.4% and 99.8% respectively [87].

Algorithms, such as the Risk of Ovarian Cancer (ROC) algorithm and the Risk of Ovarian Malignancy Algorithm (ROMA) have been used in combination with CA 125 to increase sensitivity. Although not routinely used in the clinic, ROMA has recently been approved by the FDA for ovarian cancer diagnosis in patients presenting with a pelvic mass. This algorithm combines serum levels of CA 125 and human epididymis protein 4 (HE4) along with menopausal status in a logistic regression model to identify a patient as low or high risk for having ovarian carcinoma [88]. The HE4 protein is overexpressed in serous and endometrioid ovarian carcinomas [89]. The ROMA algorithm is claimed to have a sensitivity of 93.8% and specificity of 74.9% [88]. However, an independent

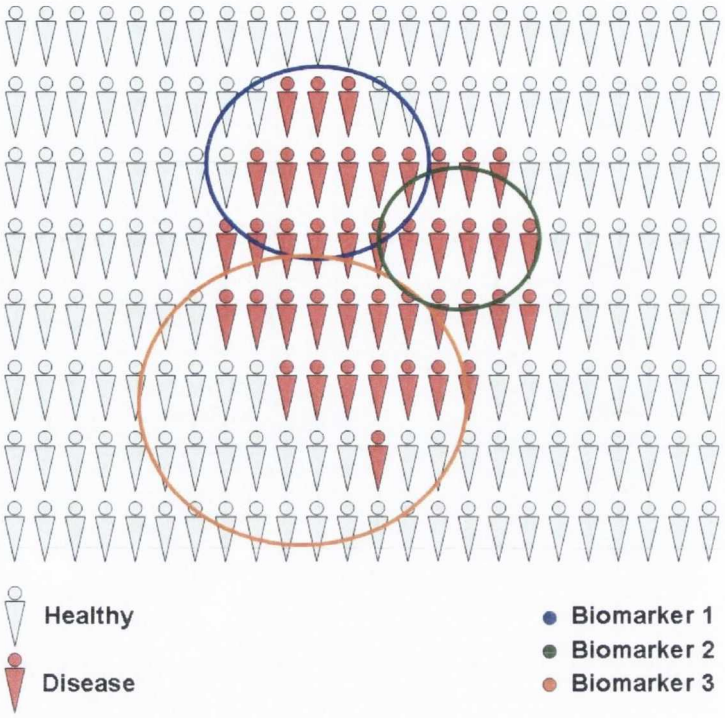

Figure 1.7: Biomarker sensitivity and specificity
Sensitivity is a measure of the proportion of true positives which are correctly identified, while specificity is a measure of the proportion of true negatives which are correctly identified. In this figure, we can see the performance of three biomarkers that may be part of a biomarker panel. Biomarker 2 is ideal in that is increases sensitivity but does not decrease specificity.

study found that ROMA did not increase the detection of malignant disease compared with CA125 alone [90]. A simple, reliable blood based detection method using robust biomarkers, would revolutionise ovarian cancer patient care and survival.

OVA 1

OVA1 (Vermillion, Quest Diagnostics) is the first FDA approved blood test that assists the clinician to determine if an ovarian adnexal mass is malignant or benign prior to planned surgery. The test measures the levels of five different proteins in patient serum, CA 125-II, transthyretin (prealbumin), apolipoprotein A1, beta 2 microglobulin, and transferrin (ova-1.com, accessed June 2012). The levels of these proteins are interpreted

by proprietary software to determine a single numerical OVA1 score . The software algorithm determines a score based on menopausal status, differentiating patients either into a low- or high-risk group [91]. This score is between zero and ten, zero indicating high probability of a benign growth and ten indicating high probability of malignancy. This test is used to determine which patients are at highest risk of malignancy and hence, are most suitable to be referred to a gynaecological oncologist. Surgery performed by an gynaecological oncologist on malignant ovarian adnexal mass results in improved patient survival [92]. OVA1 is claimed to have a sensitivity of 92.5% and a specificity of 42.8%, with a positive predictive value of 42.3% and a negative predictive value of 92.7% [93]. However, OVA1 has not been tested in screening patients for early stage disease [91]. There are also limitations to the use of this test due to assay interference as a result of triglyceride levels and rheumatoid factor levels [93].

1.4 The Immune Response and Cancer

There has been increasing interest in cancer and its interplay with the immune system as an evolving and massively complex process which may have a significant impact on future cancer diagnosis and treatment. It has long been noted that general immune activation is linked to cancer regression. William Coley was one of the first to conduct studies in the area of immune stimulation. Coley's Toxin was a mixture of killed *Streptococcus pyogenes* and *Serratia marcescens* and was used to treat cancer up to the 1960's [94]. The immune system can respond to cancer by recognising tumour antigens, these antigens may arise in several different ways such as, tumour specific mutation, expression, folding, degradation or localisation [95]. Immunosurveillance is a concept where the host immune system (innate and adaptive, Figure 1.8) actively surveys the body from within and recognises pre-cancerous cells and destroys cancer precursors in

most cases [96, 97].

Immunoediting in an updated hypothesis where the selective pressure of the immune system directs tumour growth and immunogenicity leading to immune avoidance [57, 98, 99]. For example, tumour cell shedding is a method that facilitates immune evasion. Major histocompatibility complex class I chain-related molecule A (MICA) shedding is associated with many tumours [100]. MICA is recognised and is bound by the NKG2D receptor, this receptor stimulates natural killer (NK) and T-cells and stimulates anti-tumour immunity [101, 102]. Therefore shedding of MICA by tumour cells facilitates immune evasion [103]. In colorectal cancer, the expression levels of NKG2D ligands decrease with tumour stage. High level expression of ligand, is associated with stage I tumours but ligand expression progressively decreases with tumour stages II, III and IV [104]. This finding is consistent with an immune avoidance mechanism whereby tumour cells expressing NKG2D ligands can be recognised and destroyed by the immune system while tumour cells that lack this ligand are masked more efficiently and evade immune destruction [105, 106]. There is undoubtedly a massive association of the host immune system and tumour development and much evidence now suggests that, in addition to the immune response recognising and preventing the development of cancer, the immune system can interact to promote and direct tumour growth [59, 107]. The interplay between the immune system and pre-cancerous and cancer cells is a vital part of further understanding the cancer-host relationship which we have previously reviewed [60, 99, 108, 109, 110]. Improved and focused studies to progress the understanding of these processes could potentially uncover biomarkers for blood or tissue based diagnosis or targets for treatment.

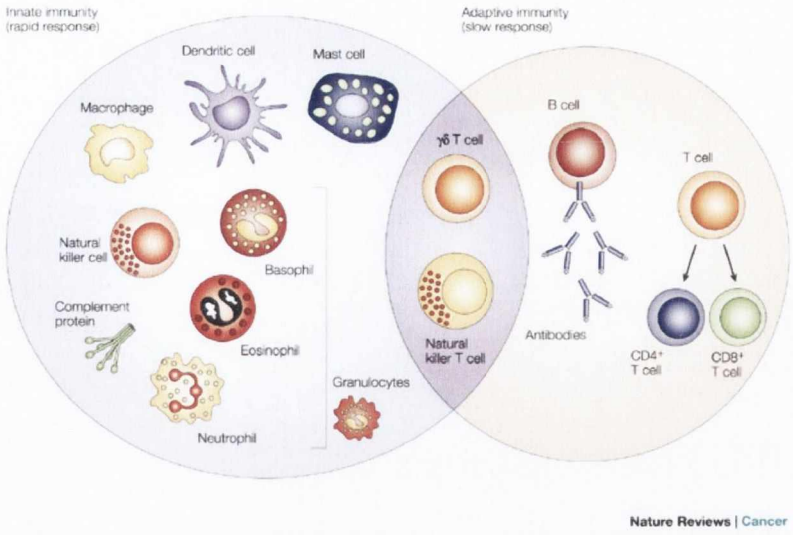

Figure 1.8: Cells of the innate and adaptive immune system

This figure outlines the cells of the innate and adaptive immune system. As evident in this figure, the antibody response is a very large and important part of the adaptive immune response. In this study, the antibody response of cancer patients will be interrogated to identify antibodies associated with disease. Taken from, G Dranoff, 2004 [111].

1.5 Autoantibodies

The robustness of the immune response plays a vital role in maintaining health. The immune system is composed of a variety of interdependent defence mechanisms that collectively defend the body from external agents such as bacterial, parasitic, fungal and viral infections as well as internal processes such as the growth of tumour cells. The humoral immune response is perhaps the most directed arm of the immune response and is mediated by secreted antibodies. Antibodies are large glycoproteins of the immunoglobulin superfamily which are secreted from specialised B-cells termed plasma cells.

Autoantibodies (AAb) are antibodies that are directed against self antigens such as one's own proteins as a result of an inappropriate immune response. Classically autoantibodies are associated with autoimmune disorders such as systemic lupus erythematosus (SLE) and rheumatoid arthritis (RA) [112, 113]. AAbs can be produced

in response to an antigen, or as a result of a cross-reaction to exposure, such as an infection or another stimulating factor [114].

In addition to the induced autoantibody repertoire, natural antibodies are also present in human sera [115, 116]. Natural antibodies, although not fully understood, are antibodies that are thought to arise spontaneously without any prior infection, immunisation or foreign antigen exposure [116]. Typically natural antibodies have low affinity, are generally immunoglobulin M (IgM) or immunoglobulin G3 (IgG3) isotypes and exhibit weak reactivity to multiple self and non-self antigens [117]. Natural antibodies are thought to maintain tissue homeostasis and have important anti-tumourigeneic function, indeed anti-tumour cytotoxic natural antibodies are found in healthy people [118, 119].

Research interrogating antibody profiles is a very challenging field in modern immunology. It is believed that the autoantibody repertoire is determined by a number of different properties such as antigen structure, catabolism, exposure to the immune system after apoptosis/necrosis, and tissue microenvironment [120].

1.5.1 Autoantibodies as Biomarkers

Biomarkers are characteristics that are objectively measured and evaluated as an indicator of normal biologic process, pathogenic process, or pharmacologic responses to a therapeutic intervention [121, 122]. Autoantibodies are used in the clinic for the diagnosis of numerous autoimmune diseases. Autoantibody blood tests such as antinuclear antibody (ANA) tests, are widely used to assist in the diagnosis of autoimmune diseases. For the diagnosis of SLE, an ANA test that identifies autoantibodies to double stranded DNA (dsDNA) is used in the clinic [123]. Autoantibodies to dsDNA are among the most specific for diagnosis of SLE, however they have a relatively low sensitivity for SLE [113]. Similarly to assist in the diagnosis of RA, rheumatoid factor is

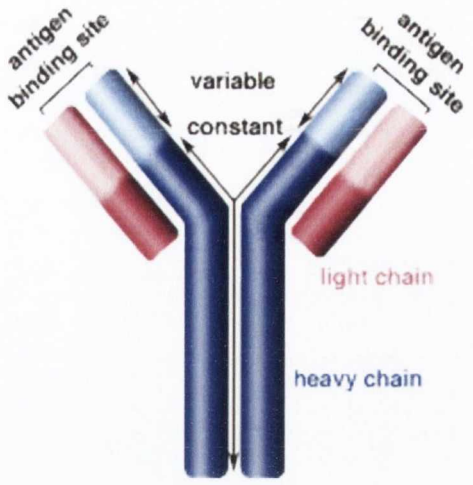

Figure 1.9: Antibody structure

This figure shows the structure of an IgG class molecule. Typically the antibody binds the antigen through the fragment antigen-binding (Fab) region. Detection of IgG by a secondary antibody is usually through the fragment crystallizable (Fc) region. (Taken from www.biology.arizona.edu)

used. Rheumatoid factor is an autoantibody (commonly IgM) that is directed against the fragment crystallizable (Fc) portion of IgG and is most relevant for RA diagnosis [124]. Rheumatoid factor is present in 26% - 90% of patients with RA, however it is also present in other autoimmune diseases such as SLE, Sjögren's syndrome and even in normal, healthy individuals [125]. Ongoing biomarker studies have identified that antibodies to citrullinated antigens are specific for RA with a sensitivity of 41% - 67% and a specificity of 96% - 98% [125], studies of the autoantibody response to citrullinated antigens has also shed light on the aetiology of RA [112].

Compared to other biomarker entities, autoantibodies are particularly attractive and have many appealing characteristics. Accessibility is an important advantage of autoantibody interrogation; autoantibodies are readily accessible in serum or plasma and prevent the need for a more invasive biopsy procedure to confirm diagnosis. Structurally, antibodies are relatively stable entities that do not commonly undergo proteolytic cleavage, making sample handling and storage much easier and cost effective.

The half-life of AAbs is also relatively long ($t\frac{1}{2}$ = 21 days), this minimises fluctuations within a patient on different days [126]. Also in terms of bioassay development, as the primary antibody is present in serum, only a labelled secondary antibody, which detects the Fc region of the primary antibody is required for detection, the antibody structure is detailed in Figure 1.9. This facilitates direct enzyme linked immunosorbent assay (ELISA) bioassay development using readily available commercial reagents in an established diagnostic platform [95].

In terms of the biology of antibody generation and production, antibodies also have advantages over traditional protein approaches. Tumour antigens may only be transient in duration due to short-lived changes in tumours; however, the antibody response may be enduring. Antigens may also be present at low levels in the tissue and the blood and these levels may often be below the detection limits of most diagnostic assays and clinically relevant approaches. The nature of an AAb amplification response to an antigen means that even a relatively small quantity of antigen can trigger a larger immune response that is reflected in relative antibody concentrations [127, 128]. This 'amplification' by their corresponding antibody response makes the antibody a better and easier target to detect. The endurance and amplification provided by the humoral immune system may facilitate discovery of disease-associated antigens and detection over longer periods than the antigen.

1.5.2 Autoantibodies in Cancer

Autoantibodies are indicative of diseases such as cancers, and the specificity and distinction of AAb responses for certain diseases highlight their potential as important tools for improved diagnosis, classification and prognosis. Classically AAbs are associated with autoimmunity, however, in recent years there has been increasing interest in tumour associated AAbs [95, 120, 129, 130, 131, 132, 133, 134]. There is an autoanti-

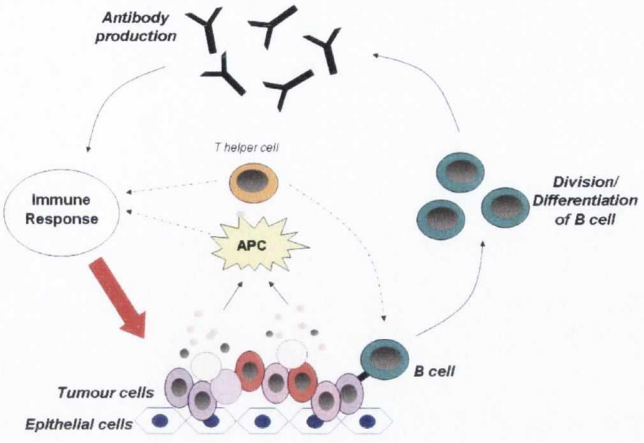

Figure 1.10: Proposed model of autoantibody generation to cancer

This model proposes the generation of circulating autoantibodies in cancer patients. At the site of tumour development, tissue damage and necrosis leads to release of proteins and cellular debris. The antigen presenting cells (APC) then present these proteins to the immune response, ultimately resulting in B cell proliferation and antibody production.

body response that arises as a result of malignancy and due to the development of new technologies, there have been an increasing number of studies that have profiled cancer patient serum for detection of tumour associated antigens [135]. Profiling the antibody repertoire in serum of cancer subjects is performed mainly with a view to discovering biomarkers [136, 137]. The potential use of tumour associated antibodies as biomarkers for diagnosis and prognosis has already yielded promising results, however there is little progression of these result into clinical practice [135, 138].

The p53 protein product is the best characterised cancer related antigen, and mutations (somatic and germline) in this protein have been detected in 50% of human cancers [139]. AAbs to p53 have been identified in cancers such as ovarian, prostate and colorectal cancer [140, 141, 142]. Anti p53 antibodies are present in approximately 30% of patients with a mutated p53 protein and anti-p53 antibodies are found predominantly in cancer patients (approximately 96% sensitivity) [143]. Thus, in cancer patients, antibodies to p53 have increased sensitivity but decreased specificity compared

to mutated protein detection, however, this high sensitivity value shows good potential and indicates that the presence of p53 antibodies is highly correlated with cancer and that the antibody repertoire may provide a valuable resource in identifying high sensitivity biomarker panels. Antibodies directed against p53 have also been uncovered in patients that are at high risk of cancer, even before clinical presentation of disease, however these findings have not been without controversy[144, 145].

Many of the most asymptomatic and common malignancies have been profiled to identify an associated autoantibody repertoire. Studies of prostate cancer have performed serum screening to identify autoantibodies profiles associated with this disease [141, 146, 147, 148, 149]. Studies have also been conducted to identify autoantibodies that are associated with breast cancer. In particular, AAbs to MUC-1, which is an apical cell membrane glycoprotein involved in cellular adhesion, have been characterised in numerous studies [150, 151]. Early CDT-Lung is a blood test that is a commercially available assay that assists in the diagnosis of early stage lung cancer in high risk patients. This test interrogates AAbs to a panel of six tumour-associated antigens, p53, NY-ESO-1, CAGE, GBU4-5, Annexin1 and SOX2 . The test claims a specificity of 90% and a sensitivity of 40% for lung cancer (oncimmune.com, accessed June 2012) [152, 153, 154]. However, it is very difficult to find independent validation data on this assay and there is currently no FDA approval for this diagnostic.

It is only in recent years that better technologies have allowed for the development of high-throughput methodologies that are needed to meaningfully assess and profile the autoantibody repertoire in cancer patients. Cancer is a heterogeneous disease, as are cancer subtypes. As outlined above, ovarian cancer in particular, is a very heterogeneous malignancy [155, 156]. This makes the interpretation of the elicited autoantibody response all the more complex. Currently autoantibody profiling is being undertaken to identify biomarkers of disease, prognostic markers, therapeutic targets

and to shed light on the aetiology of disease.

1.6 Autoantibody Serum Screening

Profiling of the circulating autoantibody repertoire in human serum has been used to identify tumour associated autoantibodies in a wide variety of autoimmune diseases and malignancies [135, 137, 157, 158] among other diseases. Many different approaches have been used to identify components aberrantly expressed in cancer tissues. Mass spectrometry has been used for serum profiling to identify differentially expressed proteins [159]. Gene expression profiling has been used to identify differentially expressed ribonucleic acids (RNA) [160, 161]. However as with all methodologies, there are limitations to these methods, the proteins identified by mass spectrometry technique have low reproducibility, and whether the expression of the genes is reflected at protein level is not clear [162].

Recent improvements in high throughput methodologies have lead to increased autoantibody response profiling studies. A wide variety of discovery platforms are employed to determine autoantibody profiles and within immunoproteomics, numerous methods have been used to assess the humoral immune response to cancer with varying degrees of success. Methods including protein arrays [127, 162, 163], serological analysis of recombinant complimentary DNA (cDNA) expression libraries (SEREX) [158, 164, 165] and other methods of phage display [166, 167] have been used most extensively and the associated methodology and validation techniques have been reviewed extensively [95, 129, 168].

SEREX is perhaps the most widely used screening method to identify AAb profiles in cancer patients. This method uses blotted phage expression libraries derived from tumour cells. These libraries are then probed with patient serum to identify tumour

reactive autoantibodies. This method has many advantages and has been used to identify over 2000 tumour associated autoantigens [95], however this method is limited to interrogation of linear epitopes and some epitopes may be poorly expressed in bacteria.

In phage display, proteins are expressed as fusions with virion capsid proteins. Commonly, phage clones are incubated with healthy patient serum to remove clones reactive in the normal population prior to incubation with disease serum, this is to facilitate identification of disease specific autoantibodies [169]. This method has been used most extensively to profile antibody responses in autoimmune diseases [170, 171]. However, this method has also been used to profile the autoantibody repertoire in patients with many different cancers [165, 169, 172]. Similarly to SEREX, this approach is restricted by epitopes that can be expressed by phage and lacks post-translational modifications and conformational epitopes.

1.6.1 Protein Array Screening

Protein array screening has been used for a variety of purposes such as, protein-protein interaction profiling, small molecule profiling, antibody specificity profiling and enzyme substrate profiling as shown in Figure 1.11. Protein arrays have been used for a number of years to identify targets of serum autoantibodies in autoimmune disorders, however, more recently this technology has been used to identify autoantibody profiles in cancer patients [131, 173, 174, 175].

There are many different protein array platforms that have been used to profile autoantibody responses. Typically to determine autoantibody responses in serum, a reverse-phase or direct methodology is used. This is when an analyte (protein/peptide) is presented on a solid support, these proteins are used to capture autoantibodies in subject serum. The bound autoantibodies are either pre-labelled, or detected with anti-human IgG which may be labelled or there may indeed be a many detection antibodies

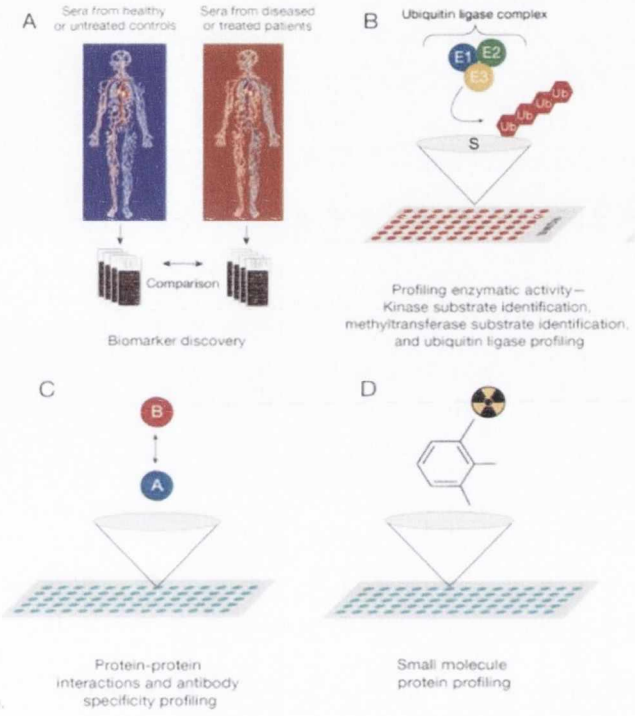

Figure 1.11: Protein array applications

Protein arrays have been used for many different applications, many of these applications have been performed in our research laboratory. In this study, the protein arrays are being used to identify AAb profiles associated with individual patients.

to amplify signal as shown in Figure 1.12.

The source of analyte, which is one of the most important factors for autoantibody profiling, is very variable on different arrays. In general, there is no easy way of generating very large and diverse sets of proteins and content generation very often varies greatly between platforms. The array content may be derived from a cell line [176, 177], or may be derived from human tissue [178, 179]. The proteins on arrays may be purified or non-purified, prokaryotically expressed (not post-translationally modified) or eukaryotically expressed (post-translationally modified), proteins may be spotted onto solid support or may be expressed *in situ* on the array and in some cases, cell free expression is employed [180, 181]. Ultimately the method of content generation also effects protein quantitation, as in cases where proteins are expressed on the array surface, usually the amount of protein that is expressed and present is unknown. Differences in surface chemistry on arrays is also a factor that may impact binding. Slides may have a two or three dimensional surface or may have another surface type which may bind proteins covalently [182]. The surface of the array determines the amount of protein which can be spotted and also the protein orientation. The various array surfaces dictate whether a protein is absorbed, adsorbed, affinity or covalently attached to the array surface. In this research, there were various surfaces used on the different array platforms.

Recently protein array production has improved rapidly, proteins printed on arrays span a sizable proportion of the human proteome and are often full-length and post-translationally modified. It is evident from the above studies that protein array profiling is a very promising technique that allows for the identification of large panels of autoantibody profiles in patients [128, 166, 168, 183, 184]. Although many hundreds of AAbs have been identified to be of interest as biomarkers of malignancy and may shed light on cancer aetiology, few antigens have been validated in secondary platforms. This is due to a variety of factors such as lack of disease serum samples, lack of suitable

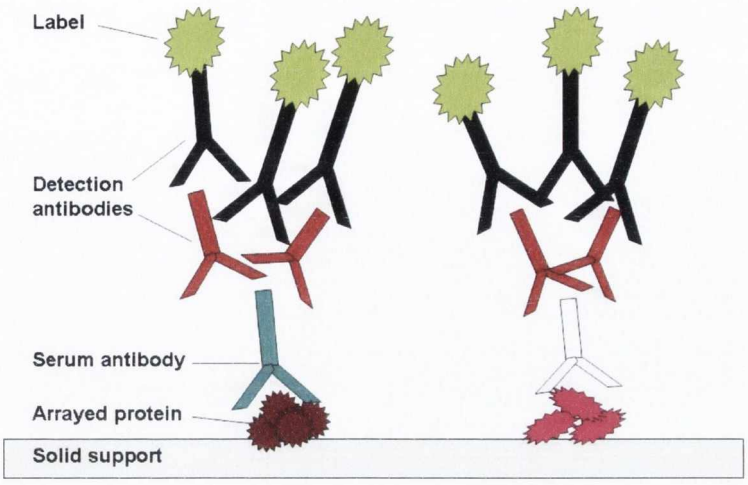

Figure 1.12: Detection of autoantibodies on protein arrays

This figure outlines the methodology used to identify the AAb binding events and hence the AAb profiles associated with patient serum. The AAb in the patient serum recognises and binds the antigen present on the array surface, this binding event is then detected by one (hEx1 protein microarrays, ProtoArrays) or two (hEx1 arrays) secondary antibodies.

healthy serum samples and issues with ELISA optimisation.

1.6.1.1 hEx1 Expression Library and Arrays

Our laboratory has developed and optimised protein array based technology screenings [185, 186] and performed autoantibody profiling in alopecia areata and dilated cardiomyopathy [174, 175], determined binding of antibodies to proteins identified from tumour neovasculature in humans [187], context independent motif identification in the human proteome [188] and identification of novel protein-protein interaction networks [186, 189]. The hEx1 protein array discovery method was employed for this project as many autoantigens and autoantibody repertoires associated with neoplastic events in a wide variety of human cancers have been identified using this method and a very similar method, SEREX [135, 137, 157, 158]. The hEx1 human expression library platform

consists of approximately 37,200 redundant *Escherichia coli* colonies which express over 10,000 non-redundant proteins [179]. This study was the first research to investigate the AAb response in ovarian cancer patient serum using the hEx1 expression library. The availability of the hEx1 expression library on site is a great advantage to this study as well characterised proteins can be expressed and purified in-house for secondary interrogation and validation.

Understanding of the generation of the hEx1 library is an important part of understanding the protein presented for recognition to AAbs in the serum of subjects. The hEx1 protein expression array is the main array platform used in our laboratory and was developed in the late 1990's [179]. To construct the hEx1 library, poly(A)$^+$ RNA was isolated from human brain and cDNA was prepared by oligo(dT)-priming. The resulting products were fractionated by size using gel filtration and the products were directionally (SalI-NotI) cloned into a modified vector for expression of His_6-tagged fusion protein products. Escherichia coli cells were transformed by electroporation, the average insert size for the hEx1 library is estimated to be 1.5 kilobases [179]. The resulting library was plated onto 2xYT-AKG agar plates and used for subsequent array spotting on PVDF membranes. The membranes were probed with an anti-$RGSH_6$ monoclonal antibody to identify which colonies expressed a fusion protein with an N-terminal $RGSH_6$ sequence, of all the arrayed clones approx 20% of the clones were identified in this probe. A subset of these expression clones consisting of 37,200 expression clones were gridded onto the large PVDF membranes in duplicate and incubated on 2xYT-AKG agar at 30°C overnight and induced for protein expression for 3 hours at 37°C on agar plates. The membranes were denatured, neutralised and then air-dried for storage. A flowchart outlines the manufacture and screening of the hEx1 protein arrays as shown in Figure 1.13.

Since the generation of the hEx1 library, further analysis has revealed that there

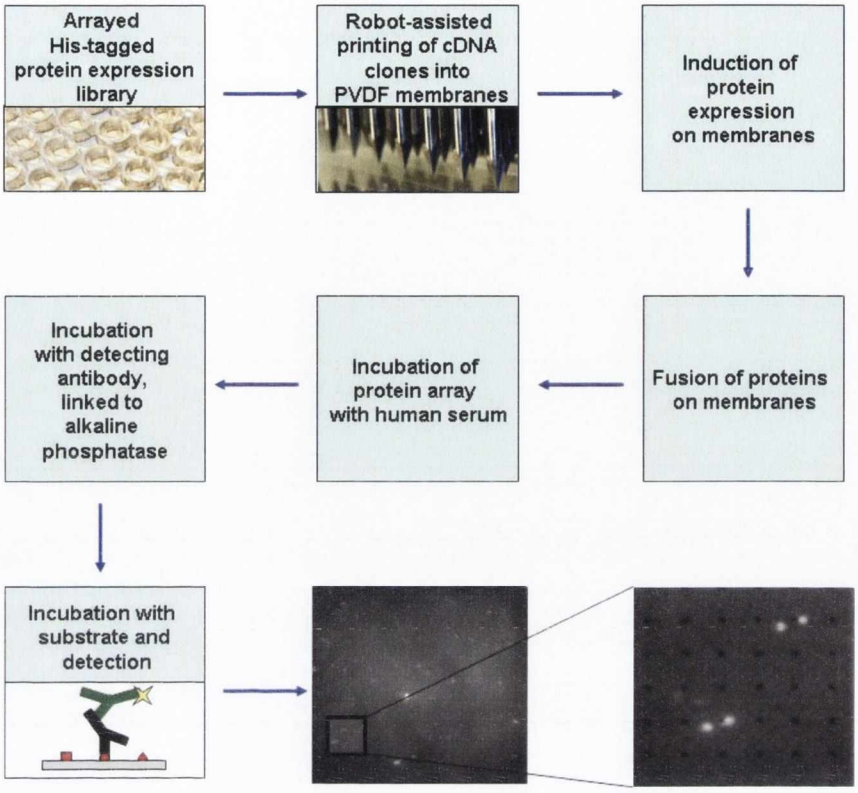

Figure 1.13: hEx1 array production and processing

This flowchart outlines the generation and screening of the hEx1 protein arrays. Bacterial clones are arrayed onto the PVDF membrane, induced for protein expression and then fixed onto the membrane surface. Once the arrays are screened with serum the binding events are detected with anti-human IgG. Positive signals on the array surface are scored manually using Visualgrid software as shown in the bottom right hand corner of this chart. Adapted from www.lifesciences.sourcebioscience.com.

is redundancy within the library and that the majority of the clones represent partial proteins including translated 5' untranslated region (UTR) sequences with roughly one third matching to the human proteome (lifesciences.sourcebioscience.com accessed March 2012). Also the generation of the library is based on poly(A)$^+$ priming of RNA the library is 3' biased and hence protein products may be truncated and will be C-terminus biased.

1.6.1.2 Invitrogen ProtoArray

The Invitrogen ProtoArrays (V5) are a high-density human protein microarray that contain over 9,000 unique human proteins. All proteins are expressed as glutathione S-transferase (GST) fusion proteins in insect cells and are full length, spotted in duplicate and individually purified and arrayed under native conditions to maximise functionality. The structural integrity of the antigens present on the surface of the arrays was an important factor when deciding on the selection of these arrays for serum screening. As the antigens are natively folded and are full length proteins, this array platform is one of the largest collections of endogenous proteins currently available. Proteins present on the array include kinases, phosphatases, G protein coupled receptors, nuclear receptors and proteases. The ProtoArray antigens are spotted on nitrocellulose glass slides. The ProtoArrays also include control proteins in each subarray to assist in gal file alignment and attachment and array analysis (Figure 5.2). The ProtoArrays have been used in a number of studies for various applications including AAb profiling of disease patient serum [137, 189, 190, 191]. Previous studies have also interrogated the results of ProtoArray screening and have concluded that the results of ProtoArray screening can be validated and confirmed using an ELISA format [137].

Gnjatic *et al.* have previously used the Invitrogen, ProtoArray V4.0 consisting of 8277 conformational human proteins. Of this large collection of proteins, 197 proteins were identified as having a greater seroreactivity with a higher fluorescent signal in the ovarian cancer patient cohort compared to healthy controls [137]. As in previous studies, interrogating AAbs in ovarian cancer patients, p53 was identified in the top 15 antigens found in this study. Further validation of the antigens determined in this study is ongoing.

Another group also performed a study of AAbs in ovarian cancer patients also used the ProtoArray V4.0 [173]. In this study pooled ovarian ascites fluid from 30 ovarian car-

cinoma patients was profiled on arrays and compared to non-malignant peritoneal fluid. This identified 10 AAbs that were associated with the ovarian carcinoma patients and one protein (L-aminoadipate semialdehyde dehydrogenase phosphopantetheinyl transferase) which was particularly antigenic was interrogated further. However, further analysis revealed that only ascites fluid in one patient was reactive to this protein, thus studies such as this have highlighted the limitations and concerns of pooling samples.

Similarly an earlier study by Hudson *et al.* used an older version in the ProtoArray (V3.0) to identify AAbs in ovarian cancer patients [162]. This version on the array contains 5,056 non-redundant human proteins, and of these proteins 94 were identified as immunogenic in ovarian cancer patients compared to healthy controls. Interesting some of these antigens overlapped with those identified by Gnjatic *et al.*

The ProtoArray has been used by research groups previously to profile the autoantibody response of many diseases and malignancies, including ovarian cancer. However, to our knowledge this is the first study to interrogate the ovarian cancer immunoproteome using the ProtoArray V5.0, which is the newest version, largest and most complete of the ProtoArray protein microarray versions.

1.7 Autoantibodies in Ovarian Cancer

Recently there has been increasing interest in the area of autoantibody profiling in cancer and there have been a number of studies that have interrogated the autoantibody profile associated with ovarian cancer [137, 162, 192, 193, 194]. Autoantibodies are appealing biomarker entities and as ovarian cancer is one of the most asymptomatic and deadly malignancies, autoantibody profiling of ovarian cancer patient serum to identify biomarkers of disease has the potential to greatly impact patient lives and outcomes. From reviewing the literature, ovarian cancer histotype, grading and staging

are the most important parameters relating to the AAb profile. In the below sections some of the most common autoantigens identified from screening ovarian cancer patient serum are discussed in relation to histotype, grading and staging.

The histology of ovarian neoplasms is linked to the corresponding AAb profile. Histology relates to tumour derivation from coelomic surface epithelial cells, germ cells or mesenchyme and differ in aggressiveness, invasiveness, response to treatment [195, 196]. The vast majority of ovarian cancers (up to 80%) are epithelial in origin [197]. Serous carcinomas are the most common epithelial histotype and are responsible for 70% of deaths from ovarian cancer [198]. They are predominantly discovered as stage III or IV, resulting in a very poor prognosis. Due to the high prevalence of the serous papillary histotype and the strong correlation with presence of p53 AAbs, this histoptype is the main focus of this research. Mucinous, clear cell and endometrioid carcinomas are the other main ovarian carcinoma histoptypes (Figure 1.14). Mucinous carcinomas are characterised by irregular cysts and glands lined by atypical mucinous cells [196, 197], and are usually diagnosed in early stages. Clear cell carcinomas are characterised by clear cells containing cytoplasmic glycogen, comprising of 5%-10% of ovarian cancers and are usually confined to the ovary on clinical presentation. Endometrioid carcinomas are characterised by epithelial elements that resemble those of the endometrium and typically resemble adenocarcinoma of the endometrium. These tumours are solid masses with a soft or fibrous consistency and are often predominantly cystic. At diagnosis, over 50% of endometrioid carcinomas are confined to the ovary [79].

Ovarian cancer staging has also been linked to the AAb profile in patient serum [193]. Staging refers to the spread of the tumour is very important as it is the best indicator of patient prognosis. Diagnosis of ovarian cancer in early stages results in over 90% 5-year survival rate, however if diagnosed in advanced stages 5-year survival is less than 30% (Figure 1.15). The two most commonly used systems of staging an

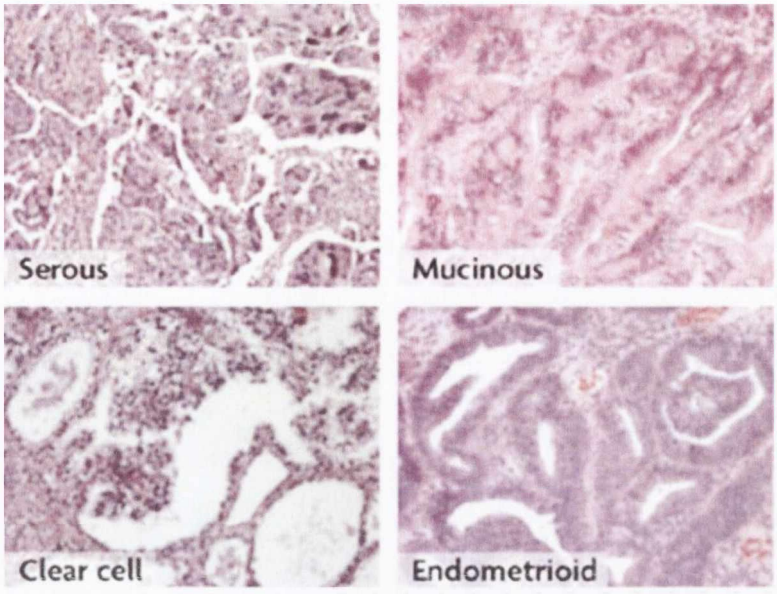

Figure 1.14: Main ovarian cancer histotypes

Shown in this figure are some of the most common ovarian carcinoma histological subtypes. These haemotoxylin and eosin stained images shown the differential staining pattens and the pathology associated with the four ovarian cancer histotypes. Taken from, RC Bast *et al.* The biology of ovarian cancer: new opportunities for translation. Nature Reviews Cancer [27].

ovarian tumour are the American Joint Committee on Cancer (AJCC) system and the International Federation of Gynecology and Obstetrics (FIGO) system. Of these two systems, FIGO is the most commonly used. An outline of staging requirements are listed in Table 1.2

A third classification of ovarian cancer that is related to the AAb profile is tumour grade (discussed in Section 1.7.1). Ovarian cancer grade refers to the degree of cellular dedifferentiation according to histopathological examination. Epithelial-mesenchymal transformation (EMT) is an anaplastic process associated with malignancy whereby the normal epithelial cell phenotype adapts a more mysenchymal or spindle shaped morphology. Also much of the specialised cellular machinery associated with epithelial cells is lost. Cells must undergo EMT to invade and metastasise to other tissues, correspondingly, when a cell settles as a distant site it undergoes mesenchymal-epithelial transformation to adapt and grow at the new site. The grade of a tumour is related

Table 1.2: FIGO ovarian cancer staging

This table lists the criteria obtained after surgery which is used to stage an ovarian cancer. Accurate tumour staging is of great importance as tumour stage is one of the most prognostic indicators of patient long term survivial.

Stage	Notes
Stage I	limited to one or both ovaries
IA	involves one ovary; capsule intact; no tumour on ovarian surface; no malignant cells in ascites or peritoneal washings
IB	involves both ovaries; capsule intact; no tumour on ovarian surface; negative washings
IC	tumour limited to ovaries with any of the following: capsule ruptured, tumour on ovarian surface, positive washings
Stage II	pelvic extension or implants
IIA	extension or implants onto uterus or fallopian tube; negative washings
IIB	extension or implants onto other pelvic structures; negative washings
IIC	pelvic extension or implants with positive peritoneal washings
Stage III	microscopic peritoneal implants outside of the pelvis; or limited to the pelvis with extension to the small bowel or omentum
IIIA	microscopic peritoneal metastases beyond pelvis
IIIB	macroscopic peritoneal metastases beyond pelvis less than 2 cm in size
IIIC	peritoneal metastases beyond pelvis $>$ 2 cm or lymph node metastases
Stage IV	distant metastases to the liver or outside the peritoneal cavity

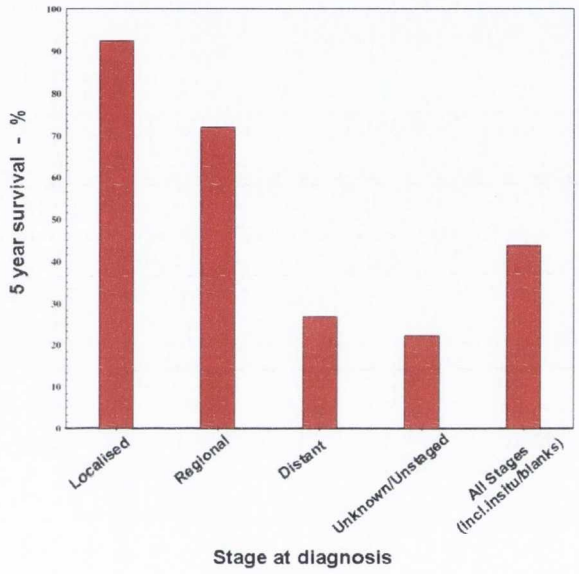

Figure 1.15: Relative ovarian cancer survival by stage (2001-2007)

Ovarian cancer survival correlates well to tumour stage. Indeed stage at diagnosis is the most important indicator of patient survival as patients in early stages with localised disease have over 90% 5-year survival rate. Correspondingly, patients with distant metastases have less than 30% 5-year survival rate. Taken from Surveillance Epidemiology and End Results, http://seer.cancer.gov/canques/survival.html. March 2012.

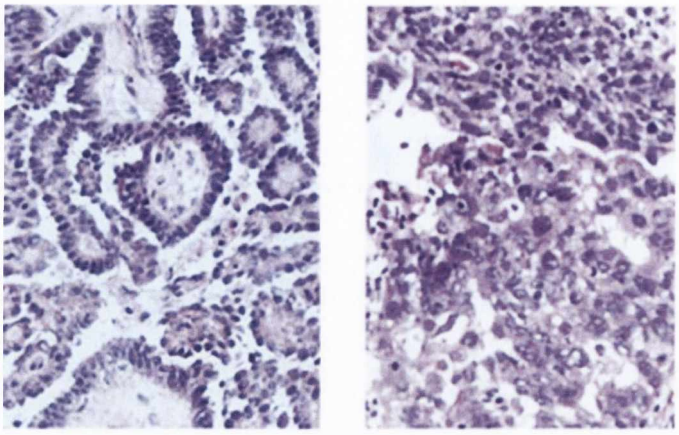

Figure 1.16: Serous ovarian carcinoma grades

Low grade ovarian tumours are typically type I tumours and are thought to derive from invasive foci arising within low malignant potential tumours of the ovary. High grade ovarian tumours are typically type II tumours and are thought to arise without macroscopic premalignant precursors. High-grade serous ovarian cancers are genomically unstable, clinically aggressive and are associated with poor patient survival. Adapted from, DTL Bowtell, The genesis and evolution of high-grade serous ovarian cancer. Nature Reviews Cancer [199].

to how the cells look under a microscope, the lower the grade the closer the malignant cells resemble the normal cells. Grade ranges for ovarian cancer are from 1-3, a grade 1 is well-differentiated, while grade 3 is poorly-differentiated, as shown in Figure 1.16. High grade tumours are more aggressive and associated with a poorer prognosis than low grade tumours.

1.7.1 Anti-p53 Autoantibodies

The best characterised autoantigen/autoantibody relationship is the tumour suppressor protein p53. AAbs to p53 have been identified in the serum of patients with many different cancers [143]. Autoantibodies to p53 have also been identified in ovarian cancer patients in a number of studies [193, 200, 201, 202], p53 autoantibodies have

been identified in approximately 25% of ovarian cancer patients [203, 204].

AAbs to p53 are associated with the 'type' of ovarian tumour and it has been proposed that ovarian carcinoma can be divided in two broad categories, type I and type II tumours [79]. The terms, Type I and Type II refer to different tumorigenic pathways rather than specific histopathologies. Type I tumours are typified by somatic mutations in genes encoding protein kinases such as kRAS and BRAF. These growths are often low grade (relatively well differentiated) and slow growing, they develop from a well characterized precursor lesion in a step by step fashion. Type I growths include, mucinous carcinomas, low-grade endometrioid and low grade serous histotypes. Low grade serous tumours are thought to arise from the ovarian surface epithelium or inclusion cysts, hence this tumour arises in the ovary [205]. Type II tumours are characterized by a high frequency of p53 mutation. Type II tumours are high grade with a rapid growth rate and have almost always spread beyond the ovaries at presentation. "Type II" tumours include high-grade serous and endometrioid carcinomas and as outlined in Section 1.2.1, these tumours are now thought to arise from the fallopian tube. Therefore in contrast to the type I tumour, these tumours do not arise in the ovary. Although this may result in a differential autoantibody profile, autoantibodies may arise to malignant (or even pre-malignant) events in the fallopian tube. Indeed, there is a high association of p53 mutation with type II tumours meaning that anti-p53 autoantibodies are predominantly associated with high grade, hence type II ovarian cancers [206]. Up to 80% of type II tumours exhibit mutated p53 but it is still unclear and there is ongoing investigation into why just a subset (20%-40%) of these cases generate anti-p53 antibodies [207]. Although there is a relatively low frequency of p53 autoantibodies in ovarian cancer, the titre of these antibodies in immunoreactive patient serum is very high. Indeed, ovarian cancers are regarded as one of the most immunogenic tumours inducing anti-p53 AAbs [204]. AAbs to p53 in patient serum have a very high specificity

for cancer at approximately 96% [143], and may be useful as part of a panel of antigens. However, although p53 AAbs have limited clinical utility when used alone as an ovarian cancer biomarker, studies have suggested that p53 AAbs may be used to improve of CA 125 screening [208].

Many studies have interrogated p53 AAbs as prognostic markers of ovarian cancer [200, 204, 209]. Some studies have indicated that p53 AAbs were associated with an improved overall survival [200], while other studies have not found any relationship between p53 AAbs and progression-free survival or overall survival [209, 210]. Similarly studies have found that p53 AAbs were positively correlated with tumour stage [204, 209], while other studies have found that p53 AAbs are not related to tumour stage [211].

1.7.2 Anti-Mesothelin Autoantibodies

Mesothelin is a cell surface glycoprotein which is highly expressed in mesotheliomas and ovarian carcinomas. Mesothelin binds to CA 125 mediating heterotypic cell adhesion, which is believed to contribute to metastasis of ovarian cancer to the peritoneum by initiating cell attachment to the mesothelial epithelium. Although mesothelin has long been implicated in ovarian cancer, AAbs to mesothelin have relatively recently been characterised and are being interrogated for their usefulness in the clinic. In a small study, AAbs to mesothelin have been identified in 41% (10 of 24 patients) of ovarian carcinoma patients and AAbs to mesothelin were not identified in normal healthy control serum [212]. Another study has also identified anti-mesothelin AAbs in 53% of ovarian carcinoma patients (AAbs to mesothelin in 10 of 14 patients with no evidence of disease, and 9 of 21 patients with clinical evidence of disease), however this study also identified AAbs to mesothelin in 26% (6/23) of healthy women [213]. The different frequencies of anti-mesothelin AAbs in the healthy subject serum may in part be due to the very

different ELISA conditions used. Anti-mesothelin AAbs have also been identified in women with increased epidemiological risk of ovarian cancer [214]. There are few studies that have interrogated the utility of AAbs to mesothelin as biomarkers of ovarian cancer. Much of the studies have relatively small numbers of patients and study ovarian carcinoma only. It is not known if AAbs to mesothelin are related to ovarian tumour histology, stage or grade. However, initial results are very positive and further study is certainly warranted to determine the clinical usefulness of anti-mesothelin AAbs.

1.7.3 Anti-NY-ESO-1 Autoantibodies

NY-ESO-1, also known as cancer testis antigen, is expressed in the testis and ovary and in a wide variety of cancers. AAbs to NY-ESO-1 have been identified in many studies that have interrogated the autoantibody profile of ovarian cancer patients [207, 215, 216, 217]. AAbs to NY-ESO-1 have been identified in 12.5% of ovarian carcinoma patients in one study [217], 26% of serous high grade ovarian cancer patients in another study [215] and AAbs to NY-ESO-1/LAGE 1 have been identified in 30% of ovarian carcinoma patients in another study [216]. AAbs to NY-ESO-1 have also been linked to tumour stage, specifically late stage [193]. Similarly to p53 AAbs, AAbs to NY-ESO-1 have been suggested to be associated with type II tumours [208]. However, AAbs to NY-ESO-1 have also been identified in other cancers, such as melanoma [217] and breast cancer [218].

1.7.4 Anti-HSP 90 Autoantibodies

Several different heat shock proteins have been identified to be associated with malignancy and have been proposed as targets for cancer therapy [219]. Heat shock protein 90 (HSP-90) is a molecular chaperone that promotes the maturation, structural main-

tenance and proper regulation of specific target proteins involved in cell cycle control and signal transduction. AAbs to HSP-90 have been implicated in the pathogenesis of diseases such as SLE [220], and RA [221], and also in malignancies such as osteosarcoma [222] and ovarian cancer [223]. A study carried out by Luo *et al.* revealed AAbs to HSP-90 in 32% of late stage ovarian carcinoma patients, 10% of stage I-II ovarian carcinoma patients and between 2.7% and 7.7% in patients with other malignancies and benign ovarian disease [224]. However, another study interrogating AAbs to HSP-90 in ascites fluid identified that 7.1% of stage III ovarian cancer patients were immunoreactive, while 58.8% of stage IV ovarian cancer patients were immunoreactive [223]. Vidal *et al.* have postulated that AAbs to HSP 90 is tumour associated and stage specific [223]. Anti-HSP 90 autoantibodies of the IgA class have also been linked to ovarian cancer [225].

1.7.5 Anti-Survivin Autoantibodies

Survivin is encoded by the BIRC5 gene and is a component of the chromosomal passenger complex that acts as a key regulator of mitosis. Survivin is ubiquitously expressed in a variety of cancers and has been identified as a potential target of anticancer therapy [226]. Autoantibodies to survivin have been identified in the serum of patients with various cancers including head and neck cancer [227], lung cancer [228, 229] and breast cancer [230]. AAbs to survivin have also been identified in two studies of ovarian cancer patient sera. Taylor *et al.* have identified AAbs to survivin in ovarian cancer patients and noted that reactivities to this antigen were significantly greater in advanced stage compared to early stage ovarian cancer. However, in this study they also noted that patients with lung and colon cancer reacted strongly with survivin [193]. Li *et al.* identified that AAbs to survivin were present in 21.9% of ovarian cancer patients and in none of the normal control serum [203]. In this study, they interrogated AAbs to

survivin as part of a panel of antigens, AAbs to survivin and 6 other antigens (p53, p16, cyclin B1, cyclin D1, cyclin A and cyclin E) were identified to have a sensitivity of up to 62.5%, and in specificity of 90.2% for ovarian cancer. Certainly AAbs to survivin are not specific to ovarian cancer, however they may be of use in a AAb biomarker panel, perhaps in ovarian cancer staging [193].

1.8 Hypothesis and Aims of this Work

The study hypothesis

- There is a ovarian cancer associated autoantibody profile present in patient serum
- Autoantibodies can be used as biomarkers of ovarian cancer
- Autoantibodies identified by protein array screening can be adapted to secondary platforms

To test this hypothesis the study aims were

- To screen ovarian cancer, benign ovarian disease and non-remarkable subject serum samples on protein arrays
- To identify AAb profiles associated with ovarian cancer
- To investigate the identified AAb profiles using secondary methodologies
- To investigate the identified AAb profiles using additional serum samples

Study Outline

The aim of this research is to profile the autoantibody repertoire of early and late stage ovarian cancer patient serum, benign ovarian disease and healthy control serum. This study used well characterised serum cohorts that were collected as part of an ovarian

cancer research consortium - Discovary. The samples were screened against very large collections of human proteins on two different array platforms. Firstly, we profiled the autoantibody repertoire of ovarian cancer patient and control cohort serum using the hEx1 protein arrays. From this work, autoantibodies were identified to be associated with disease. These results were interrogated in secondary platforms, including a translational platform which is routinely used in the clinic (ELISA). The autoantibody profile in ovarian cancer patient and control cohort serum was also determined using the Invitrogen ProtoArrays. The results of ProtoArray screening was compared to previous profiles identified using the hEx1 array. Autoantibodies associated with disease were identified and pathway analysis was also performed to determine if autoantibodies can be indicative of pathway dysregulation associated with malignancy.

Chapter 2

Materials and Methods

2.1 Materials

Material	Source	Catalog
Acrylamide/bis-acrylamide 30% solution	Sigma Aldrich, UK	A3574
Agar	Sigma Aldrich, UK	A5054
Ammonium persulfate (APS)	Sigma Aldrich, UK	A7460
Ampicillin	Sigma Aldrich, UK	A9518
Attophos substrate	Roche, UK	11681982001
Bovine serum albumin (BSA)	Sigma Aldrich, UK	A2153
Bromophenol Blue	Sigma Aldrich, UK	B5525
Coomassie brilliant blue	Molekula, UK	M10947360
Dithiothreitol (DTT)	Sigma Aldrich, UK	D9163
Ethanol	Sigma Aldrich, UK	E7023
Glacial acetic acid	Sigma Aldrich, UK	320099
Glucose	Sigma Aldrich, UK	G7528
Glycerol	Sigma Aldrich, UK	G6279
Glycine	Sigma Aldrich, UK	G8898
Guanidine hydrocloride (GuHCl)	Sigma Aldrich, UK	G4505
Human protein microarray (hEx1)	Imagenes GmbH, Berlin, Germany	IMA- PROT-ARR
Hydrochloric acid (HCl)	Sigma Aldrich, UK	258148
Hydroxyethyl piperazineethanesulfonic acid (HEPES)	Sigma Aldrich, UK	H7006
Isopropanol	Sigma Aldrich, UK	59304
Kanamycin	Sigma Aldrich, UK	K4000
Magnesium chloride ($MgCl_2$)	Sigma Aldrich, UK	63072
Methanol	Sigma Aldrich, UK	24229
Ni-NTA agarose beads	Merck, UK	70666-4
N,N,N´,N´-tetramethylethylenediamine (TEMED)	Sigma Aldrich, UK	T981
Overnight express media	Novagen (Merck), UK	71491

Material	Source	Catalog
Polypropylene columns	Qiagen, UK	34924
Polyvinylidene fluoride (PVDF)	Amersham (GE Healthcare), UK	RPN303F
Potassium chloride (KCl)	Sigma Aldrich, UK	P9541
Potassium dihydrogen phosphate (KH_2PO_4)	Sigma Aldrich, UK	30407
Skimmed milk powder	Sigma Aldrich, UK	70166
Sulfuric acid (H_2SO_4)	Sigma Aldrich, UK	84736
Sodium Chloride ($NaCl_2$)	Sigma Aldrich, UK	S9888
Sodium dihydrogen phosphate (NaH_2PO_4)	Sigma Aldrich, UK	S3139
Sodium dodecyl sulfate (SDS)	Sigma Aldrich, UK	L3771
Sodium phosphate dibasic (Na_2HPO_4)	Sigma Aldrich, UK	S3264
Tris-HCl	Sigma Aldrich, UK	T5941
Triton X 100	Sigma Aldrich, UK	X100
Trizma base	Sigma Aldrich, UK	T1503
Tryptone	Formedium, UK	TRP03
Tween 20	Riedel-de Haën (Sigma Aldrich), Germany	63158
Urea	Sigma Aldrich, UK	U5378
Yeast extract	Formedium, UK	YEA02
2-mercaptoethanol	Sigma Aldrich, UK	M3148
3,3´,5,5´-Tetramethylbenzidine (TMB)	Sigma Aldrich, UK	T8665

2.2 Serum Sample Collection

Approval for this study was obtained from St. James's Hospital and Adelaide and Meath incorporating the National Children's Hospital research ethics committee. Serum samples and clinical information was obtained with informed consent from patients attending St James's Hospital undergoing surgery for possible ovarian neoplasm. All blood samples in this study were obtained pre-operatively from patients undergoing cytoreductive surgery, all patients were treatment naive. The blood was collected into a non-heparinised tube and allowed to clot. The blood was then spun at 400 x g for 10 minutes. The serum supernatant was removed and dispensed into labelled cryovial tubes. Serum was stored at $-80°C$ until further use. The serum samples obtained were stored as part of the Discovary Bioresource, which was formed to specifically address issues in relation to ovarian and endometrial cancer diagnostics and prognostics

and supports the development of translational research in Ireland. This research was gratefully funded by the Emer Casey Foundation, who support ovarian, uterine and endometrial cancer research in Ireland and abroad.

2.3 hEx1 Array Screening and Analysis

2.3.1 hEx1 Array Serum Screening

As described previously, the human expression library 1 was made from mRNA, extracted from human brain tissue. The cDNA was prepared from poly(A)$^+$RNA by oligo(dT)-priming. Products were size fractionated by gel filtration and directionally cloned into a commercial vector (modified pQE-30 vector from Qiagen). The vector was then transformed into *E. coli* cells (SCS1 cells from Stratagene). The library contains 37,200 clones, which are spotted in duplicate [179, 175, 231]. The hEx1 arrays were purchased from Imagenes GmbH, (Berlin, Germany).

The hEx1 arrays, which consist of two separate PVDF membranes, (pt 8 and pt 9) were activated by soaking in ethanol for 1 minute. They were then rinsed in deionised water and washed in TBS-T-T (500mM sodium chloride, 20mM Tris-HCL pH 7.5, 0.05% v/v Tween 20, 0.5% v/v Triton X 100). The dessicated bacterial colonies that had expressed the proteins *in situ*, were then removed with a tissue and the arrays washed with TBS-T-T for 10 minutes, TBS-T (500mM Sodium chloride, 20mM Tris-HCL pH 7.5, 0.05% v/v Tween 20) for 10 minutes and TBS (150mM NaCl, 10 mM Tris-HCL pH 7.5) for 10 minutes, all on fast rocker (35 rpm). The arrays were blocked on a slow rocker (7 rpm) for 2 hours at room temperature using 2% w/v skimmed milk powder in TBS. The arrays were then incubated in serum (thawed on ice) by addition of 200μl serum in 20ml 2% w/v BSA (Bovine Serum Albumin) TBS-T. A dilution factor of 1:100 was used, this dilution was selected as its the most commonly used in diagnostic

labs. The dish containing the hEx1 arrays were was wrapped in cling film to prevent evaporation. The arrays were placed on a slow rocking see-saw rocker (Stuart SSL4) overnight at room temperature.

The arrays were washed 3 times for 30 minutes in TBS-T (total of 90 minutes). Monoclonal mouse anti-human IgG (Sigma Aldrich UK, Cat no: I6260) was diluted 1:5000 in 2% w/v BSA TBS-T, and the arrays were incubated with the antibody for 1 hour at room temperature on a slow rocker. The arrays were then washed 3 times, each for 30 minutes in TBS-T.

Polyclonal goat anti-mouse alkaline-phosphatase conjugate IgG (Sigma Aldrich UK, Cat no: A1418) was also diluted 1:5000 in 2% w/v BSA TBS-T. The arrays were incubated with the antibody for 1 hour at room temperature. The arrays were then washed twice in TBS-T for 30 minutes and once in TBS for 15 minutes.

The arrays were equilibrated in attophos buffer (100mM Tris-HCL pH 9.5, 1mM $MgCl_2$) with slow rocking for 10 minutes, then transferred to a 1:40 dilution of attophos substrate (Roche,UK, Cat no: 1 681 982) in attophos buffer. In the diluted substrate solution, the arrays were incubated in the dark for 5 minutes, and were imaged using a Fuji LAS3000 imager, using tray position 3, filter 3 and 460nm blue light. The resultant TIFF image was saved for further analysis.

2.3.2 hEx1 Array Scoring

Visualgrid (GPC Biotech) software was used for hEx1 array scoring. A grid was superimposed onto the TIFF image of the screened human protein array. Central circles were used to align up guide dots, around which 12 clones were arrayed in duplicate in a 5x5 pattern. The positive signals were identified on the grid and then scored by intensity (1 to 3, 3 being the most intense). Once the array was scored, results were exported and saved for analysis.

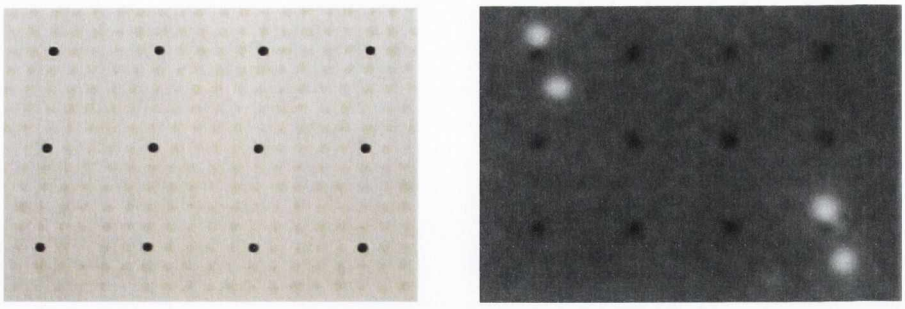

(a) Pre-screen hEx1 array (b) Post-screen hEx1 array

Figure 2.1: Images of hEx1 protein arrays

Subfigure A is an image of a subsection of the Imagenes hEx1 array prior to processing. Evident in this image is the bacterial colonies that are spotted, grown and induced for protein expression on the surface of the PVDF membrane sheets. These colonies are removed prior to AAb probing. Subfigure B is an image of a subsection of the arrays taken with a CCD camera after serum screening and array processing. Clearly evident are the positive signals that indicate an AAb binding event. In both subfigures, the black dots are ink guide dots which are used for orientation during image analysis.

2.3.3 Analysis of hEx1 Array Serum Screening Results

The aim of the analysis was to develop panels of clones to distinguish between various cohorts of subjects (typically a patient group and a control group). As the numbers of possible panels was systematically too large to assess, an iterative approach was adopted.

To seed the process, a pool of clones that were identified as reactive by any serum sample in the study was listed. From this pool, a list of all possible pairs of clones was generated. For each pair the sensitivity, specificity and p-value was calculated. Pairs of clones with p-values below a value of 0.05 were retained, while pairs of clones with higher p-values were discarded. From the pool of clones, a third clone was added to each remaining pair and the calculations repeated. This procedure was repeated until no improvement was seen in the metrics, or a score of 1 was achieved in sensitivity and specificity. A combination of Perl scripts (http://www.perl.org/) was used to build the panels and to calculate sensitivities and specificities, and an R script (http://www.r-

project.org/) was used to calculate p-values. General data management was based on a PostgreSQL (http://www.postgresql.org/) database.

2.4 hEx1 Protein Production and Analysis

2.4.1 Bacterial Clone Sequencing

Once the panels of clones were identified and assigned p-values, the top ranked panels for each cohort were selected and the clone identification numbers collated. The listed of clones of interest were used to inoculate agar plates for sequencing as follows.

Under sterile conditions, 100μl of 2xYT-AKG agar (per litre 15g agar, 16g tryptone, 10g yeast extract, 5g NaCl, after autoclave the following are added, 2% glucose, 25μg/ml kanamycin, 50μg/ml ampicillin) was aliquoted per well in a 96 well plate. The agar plate was left at room temperature to solidify. 384 well microplates, corresponding to the identified clones of interest were removed from the -80^{o}C freezer and placed on dry ice in a biosafety hood. Autoclaved filter paper with a central hole was placed over the well to protect surrounding colonies and a sterile pipette tip was used to remove some of the frozen bacterial media from the denoted well. The tip with frozen media was then used to inoculate a 100μl agar well in the microplate. At least one negative control well was included in every agar plate, this well was not inoculated with a pipette tip. The plate was incubated at 37°C overnight to promote bacterial growth. The following day the visual inspection was carried out to ensure that the colonies had grown satisfactory. The plate was then sealed with a breathable microplate seal, the lid placed on top and was packaged in a bubble padded envelope for courier transport to LCG genomics in Berlin, Germany. For Sanger sequencing a pQE-F (CATTGAGAGGATCGCATCAC) primer was used. Results were accessed online and downloaded as an ABI chromatogram file.

2.4.2 Sequence Open Reading Frame Analysis

From the chromatogram files, the start codon was identified and the sequence was copied from this start codon to the end of the sequence. The copied sequence was then pasted into the open reading frame (ORF) finder (www.ncbi.nlm.nih.gov/projects /gorf/orfig.cgi) on the National Centre for Biotechnology Information (NCBI) website. The ORF finder program was then used to analyse the sequences and only products in the +1 reading frame were used for further analysis. The +1 reading frame product was ran through the Basic Local Alignment Tool (BLAST) to identify homologous sequences and proteins. The identity of the product was determined usually by taking the *Homo sapiens* protein with the most significant alignment. The protein product for each bacterial clone was recorded with the bacterial clone identifier and the predicted protein product size was obtained by inputting the ORF sequence into an online peptide molecular weight calculator (www.biopeptide.com/PepCalc/).

2.4.3 Induction of hEx1 Bacterial Clones

Wells from the collection of 384 well plates that correspond to the in frame bacterial clones of interest were identified. Plates were removed from the -80^{o}C freezer and placed on dry ice. In a biosafety hood, autoclaved filter paper with a central hole was placed over the well to protect surrounding colonies and a sterile pipette tip used to remove some frozen bacterial media from the well. This tip with frozen media was then used to inoculate a 1ml solution of 2xYT-AKG (per litre 16g tryptone, 10g yeast extract, 5g NaCl, after autoclave the following are added, 2% glucose, 25μg/ml kanamycin, 50μg/ml ampicillin) media in a sterile 15ml tube. Inoculation and procedures were performed under sterile conditions and a negative control of 2xYT-AKG was included for every lot of media inoculated. The inoculated media was then agitated for 16 hours

on an orbital shaker (220rpm) at 37°C to promote bacterial growth.

The following inoculation steps were performed under sterile conditions in a biosafety hood. Of these 1ml starter cultures, 100μl was used to inoculate 10ml of sterile 'Overnight Express' autoinduction media (Novagen Cat no: 71491-5) with antibiotics as before. For bacterial clones that were poor protein expressors 500ul of the starter culture was used to inoculate 50ml of autoinduction media to improve protein yield. The solutions were placed on an orbital shaker at 37°C for 20-22 hours to promote growth. The bacterial cultures were spun at 2135 x g for 35 minutes at 4°C, the supernatant was decanted off and the waste autoclaved before disposal. The pellet was stored at −80°C for over one hour to lyse the bacteria.

2.4.4 His-Tagged Protein Purification

Bacterial pellets were removed from −80°C and allowed to thaw on the bench, 2ml of lysis buffer A (100mM NaH_2PO_4, 10mM Tris-HCl, 6M GuHCl, pH 8) was added to promote bacterial lysis. The pellet was resuspended by pipetting and vortexing. Resuspended pellets in buffer A were then placed on a rocker on slow rock (15 rpm) for 1 hour.

Labelled polypropylene columns (Qiagen, Cat no: 34924) were set up in a rack above a catchment tray. Nickel-nitrilotriacetic agarose beads (Ni-NTA, Merck UK, Cat no: 70666-4) were inverted repeatedly to ensure the beads were homogenous in the solution. 400μl (for 10ml cultures) or 1ml (for 50ml cultures) of the Ni-NTA beads were aliquoted into 2ml microcentrifuge tubes. These tubes were then centrifuged at 400 x g for 2 minutes and the storage solution supernatant removed. The Ni-NTA pellets were resuspended in 1ml of lysis buffer A solution and centrifuged at 400 x g for 2 minutes, the supernatant was removed. This nickel bead wash step with lysis buffer A was repeated 3 times.

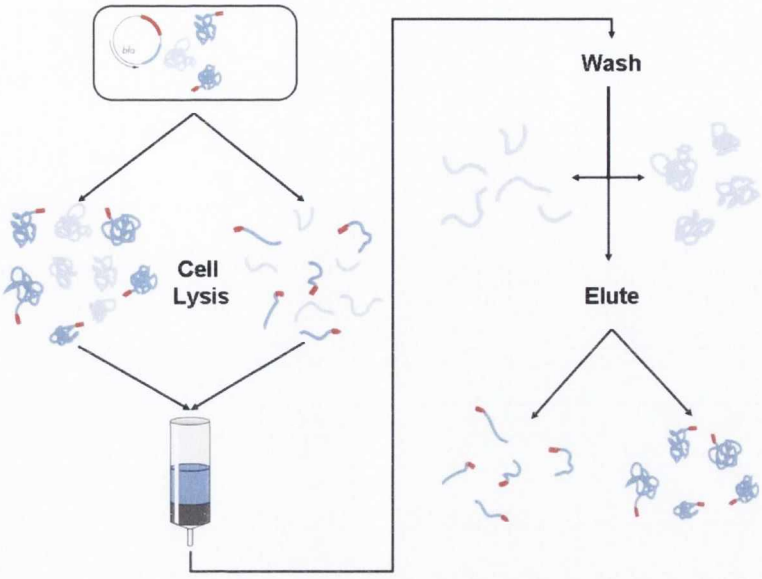

Figure 2.2: 6xHis-tagged protein purification

This diagram shows the principles of 6xHis-tagged protein purification using immobilised metal affinity chromatography (IMAC). Proteins can be purified under native or denaturing conditions using this method as outlined in this figure. Using Adapted from "*The QIAexpressionist*"- Fifth Edition .

The resuspended bacterial pellets were transferred to 2 ml microcentrifuge tubes and centrifuged at 16,100 x g for 25 minutes at 4°C. The resultant supernatant was removed and saved while the bacterial pellet was discarded. The supernatant was then used to resuspend the Ni-NTA beads and this was then placed on a slow rocker to allow his-tag binding. After 30 minutes the resuspended beads/lysate was aliquoted into a stoppered polypropylene column. After 5 minutes, when the solution had settled, the column stopper was removed and the run-off discarded. The columns were then washed with 2 x 4mls of wash buffer C (100mM NaH_2PO_4, 10mM Tris-HCl, 8M Urea, pH 6.3) and the run-off discarded. Columns were then stoppered and 200μl of elution buffer E (100mM NaH_2PO_4,10mM Tris-HCl, 8M Urea, pH 4.5) was added to the columns. After 10 minutes, the stopper was removed and the run-off was discarded. 500μl of elution buffer E was added to the columns and the run-off was collected and stored in a low retention microcentrifuge tube at 4°C until further use.

2.4.5 Protein Quantitation using BCA Protein Assay

Protein quantitation was carried out using a Pierce BCA protein assay kit, (Pierce, UK, Cat no: 500-0002). One part elution buffer E was added to two parts deionised water and this diluent was used to make up the bovine serum albumin standards. BSA standards prepared were 2mg/ml, 1.5mg/ml, 1mg/ml, 0.75mg/ml, 0.5mg/ml, 0.25mg/ml, 0.125mg/ml, 0.025mg/ml and a blank of diluent was also included in the standards. 20μl of proteins to be tested were diluted in 40μl deionised water and vortexed. 25μl of the BSA standards were aliquoted in triplicate and 25μl of the test proteins were aliquoted in duplicate in a 96 well microplate. Working reagent was prepared by mixing 50 parts of BCA reagent A with 1 part of BCA reagent B. 200μl of working reagent was added to both standard and test wells in the microplate. The plate was shaken briefly and then incubated at 37°C for 30 minutes. The plate was then left to cool for 2 minutes. The absorbance was measured using a microplate reader (Wallac Victor) at 540nm, and readings were recorded. A standard curve of the BSA standards was generated using the equation of a polynomial curve. The equation of this curve was then used to determine the concentration of the diluted test proteins. Only concentration values that were within the range of the standard curve were used. The determined concentration of the diluted test proteins was then multiplied by the dilution factor (usually 3) to determine the concentration of the original test proteins.

2.4.6 Protein Quantitation at A280nm with Ultraviolet Light

For proteins that could not be analysed using the BCA method due to incompatibility with buffers or small sample volumes, quantitation with a Nanodrop spectrophotometer was performed. To quantify protein the "ProteinA280" setting was employed. Firstly the nanodrop was cleaned, with the sampling arm open 1μl of 0.5M HCl solution was

pipetted onto the lower measurement pedestal. The sampling arm was closed and pressed downward so that the droplet is drawn upwards and held between the arms by surface tension. The acid was left for 1 minute to clean the pedestal, after this time the acid was wiped away with a soft tissue. This process was then repeated with ultrapure water to rinse the pedestal. Once cleaned and rinsed 1μl of the sample protein to be tested was pipetted into the lower arm and the upper arm was closed (and not pressed downwards in this case). Measurement was initiated using the operating software on the PC. After this initiation the sample arm slightly compressed drawing the droplet between the arms. The spectral measurement was then made and quantitation was made based on the tightly controlled path length of 1mm. Once this measurement was recorded the pedestal was wiped with a soft tissue. 1μl of the same test protein was then again pipetted onto the pedestal as before and the measurement repeated. Three replicate measurements for each test protein was performed and the average of these measurements was used for further analysis. The nanodrop was cleaned and rinsed between different protein samples.

2.4.7 Polyacrylimide Gel Electrophoresis Analysis (PAGE)

All polyacrylamide gels were 12% acrylamide and 1mm thick. The running phase and stacking phase were prepared as follows:

Running phase: 2.1ml of dH2O, 3.75ml of 1M Tris-HCL pH 8.9, 4ml of Acrylamide/bis-acrylamide 40% solution, 100μl of 10 % SDS solution, 5μl of TEMED, 50μl of APS.

Stacking phase: 2.66ml of dH2O, 1.575ml of 0.4M Tris-HCL pH 6.8, 660μl of Acrylamide/bis-acrylamide 40% solution, 50μl of 10 % SDS solution, 5μl of TEMED, 50μl of APS.

When the gel was set, 2X loading buffer (4% w/v SDS, 20% v/v glycerol, 0.05% w/v

(a) Genetix QArray spotting robot

(b) Robot arm, pinhead and pins

Figure 2.3: hEx1 protein microarray spotting

Shown here in subfigure A is the Genetix spotting robot used in hEx1 protein microarray generation. Subfigure B is a close up image of the robot arm with the print head and the eight pins used in the microarray spotting.

Bromophenol Blue, 126mM Tris-HCL pH 6.8, 5% v/v 2-mercaptoethanol) and an equal quantity of protein was pipetted into microcentrifuge tubes and denatured by heating to 95°C for 5 minutes and then cooled and centrifuged on short spin to collect condensate. The gels were set up in the electrophoresis tank, and running buffer (25mM Trizma base, 192mM glycine, 0.1% w/v SDS) added to fill the 'dam' cover the electrode at the bottom of the tank. Each of the protein samples were then pipetted into the wells of the gel along with a molecular weight marker standard. The gels were electrophoresed at 15mA per gel through the stacking phase and 20mA per gel through the running phase. The gels were transferred to coomassie stain solution (0.2% w/v Coomassie brilliant blue, 7.5% v/v glacial acetic acid, 50% v/v ethanol) for 2 hours on slow rock and then destain solution overnight (10% v/v glacial acetic acid, 30% v/v ethanol), also on a slow rocker. The gels were then scanned and the images stored for subsequent analysis.

2.5 Secondary Serum Screening Methodology

2.5.1 hEx1 Protein Microarray Screening and Analysis

2.5.1.1 hEx1 Protein Microarray Spotting

A Genetix QArray spotting robot was used for microarray spotting (as shown in Figure 2.3). Before use the machine was cleaned thoroughly using lens cleaning tissue (Whatman,GE Healthcare, UK. Cat no: 2105841) and 70% ethanol to remove dust. The pin-head was removed from the robot arm and the head and pins were sonicated in a ultrasonic bath (Grant XB2) containing aQu Clean pin cleaning fluid (Genetix, Cat no: K2505, diluted as per manufacturers instructions in filtered/autoclaved deionised water) for 15 minutes. The pin-head and pins were then sonicated in filtered/autoclaved deionised water for a further 15 minutes. The pin head and pins were then sprayed with isopropanol and left to air dry. The pins were left to air dry suspended in cut-off pipette tips.

A 384 well microplate layout was generated by the QSoft software (Genetix) to result in the desired spotting layout. The spotting layout consisted of two fields with eight blocks in each field (Figure 2.4). Field 1 contained four duplicate blocks (totaling 8 blocks), and in each block antigens were spotted in duplicate and adjacent to each other, control proteins were spotted in quadruplicate (Figure 2.5a). As in field 1, field 2 contained four duplicate blocks (totaling 8 blocks), however, in each block antigens were spotted randomly and all antigens and controls were spotted in triplicate (Figure 2.5b). Hence, in total each antigen of interest was spotted 10 times on each microarray. To assist with gal file alignment repeats of Cy3 labelled IgG and buffer were included for spotting in each block. Additional controls and normalisation proteins were included also, these were dilutions of unlabelled IgG, anti-human IgG, a purified eluate as expressed by an empty bacterial clone (no insert present as identified by sequence), buffer (PBS) and a hEx1 protein to which no serum was reactive (as determined by previous

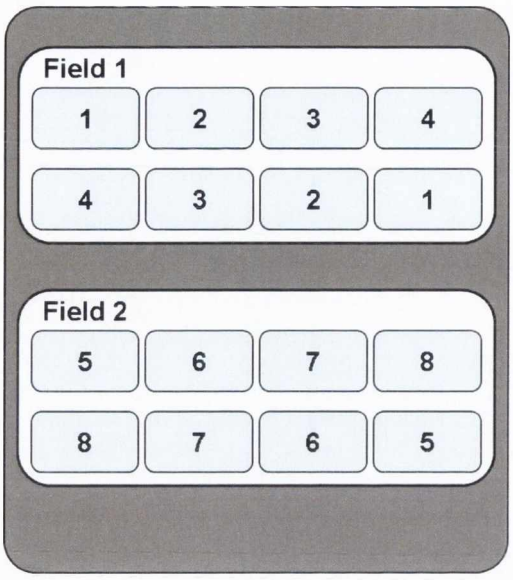

Figure 2.4: hEx1 microarray slide layout

Two fields were spotted on each slide, each field consisted of 4 blocks spotted in duplicate. Hence, each block was spotted in duplicate per field, in total eight unique blocks were spotted on each slide.

hEx1 array screening).

Using the results of BCA assay protein quantitation, the hEx1 proteins were diluted with PBS (137mM NaCl, 2.7mM KCl, 4.3mM Na_2HPO_4, 1.47mM KH_2PO_4, pH 7.4) to give a final protein concentration of 250μg/ml. Proteins that were too dilute to be spotted at this concentration were spotted undiluted. The generated 384 microplate layout was followed and 20μl of the hEx1 proteins and controls were pipetted into predetermined wells in the 384-well low retention polypropylene microplates. All microplates to be used for spotting were made in one sitting from the same diluted stock concentration to ensure minimum variation. The microplates were then stored at $-20°$C short term until further use.

Spotting was performed with 150μm solid pins (blunted ends) 8 pins were used – in 2x4 format in print head, with each slide containing a total of 10 replicates per protein spot. For spotting, a humidity of over 60% was maintained. Once spotted the slides

were left in the machine for 20 minutes to dry. Slides were stored at 4°C until further use.

2.5.1.2 hEx1 Protein Microarray Screening

The slides were removed from 4°C and equilibrated to room temperature on the bench for 10 minutes. Arrays were then washed (all washing steps took place on a fast rocker - 35rpm, in a multislide glass holder) for 10 minutes in PBS (137mM NaCl, 2.7mM KCl, 4.3mM Na_2HPO_4, 1.47mM KH_2PO_4, pH 7.4). Blocking (all blocking and incubation steps took place on a slow rocker, 7rpm) in 2% w/v BSA-PBS was performed for 1 hour, also in a multislide glass holder.

For the anti-histidine incubation a 1:1000 dilution of anti-histidine mouse monoclonal antibody (Qiagen Cat no: 34610) in 2% BSA PBS was used. 100µl of the diluted antibody was pipetted on the nitrocellulose surface and a coverslip was placed on top. The slides were incubated, on slow rocker for 2 hours in a humidity chamber to ensure the microarrays remained moist and did not dry out. This was followed by 3 washes for 10 minutes each with PBS-T (0.01% v/v Tween 20). The slides were incubated for 90 minutes with 1:1000 Cy3 conjugated AffiniPure Goat Anti-Mouse IgG (Jackson Immunoresearch Europe, Cat:115-165-003) in 2% BSA-PBS.

For the serum incubation, the following steps took place after the blocking step: The serum was diluted to a 1:100 dilution in 2% BSA-PBS. 100μl of the diluted serum was pipetted on the nitrocellulose surface and a coverslip was placed on top. The arrays were placed on a slow rock for 2 hours in the humidity chamber. The slides were then washed 3 times each for 10 minutes in PBS-T. The detection antibody, Cy3 conjugated goat anti-human IgG (Jackson Immunoresearch Europe, Cat:109-165-088) was diluted 1:1000 in 2% BSA PBS was then incubated over the arrays for 90 minutes.

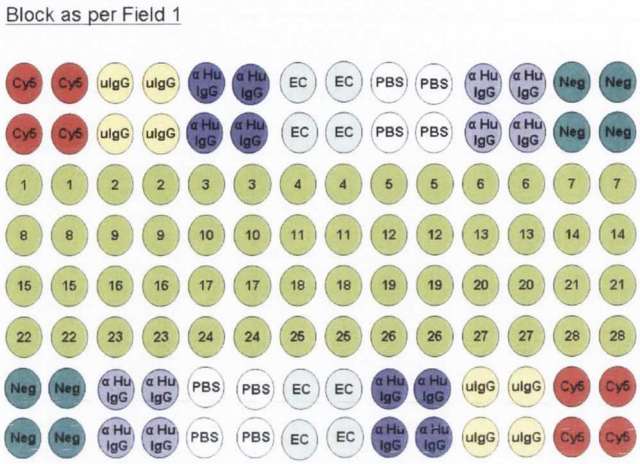

(a) Block spotting layout as in Field 1

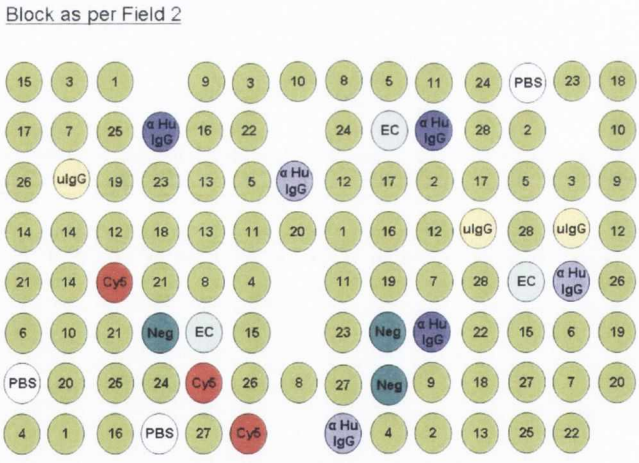

(b) Block spotting layout as in Field 2 - Random

Figure 2.5: hEx1 microarray spotting layout

In field 1, antigens were spotted in duplicate and control proteins were spotted in quadruplicate. In field 2 all antigens and controls were spotted in triplicate in a random pattern.

All slides where then washed 3 times for 10 minutes in PBS-T, once for 5 minutes in PBS and once for 5 minutes in deionised water. Arrays were dried by centrifugation at 500 x g for 2 minutes at 4°C. Arrays were scanned immediately after screening and stored at room temperature.

2.5.1.3 hEx1 Protein Microarray Scanning

Microarray scanning was performed using a GenePix 4000B Axon set to scan at the ratio wavelength setting of 532nm and 635nm. GenePix Pro 5.0 software was used to analyse the scanned protein array images. A gal file was created and attached to the image, this allowed the generation of a grid of empty spots labelled with the protein ID, which was laid over the image identifying the spots on the array. The gal file was overlaid on the image, ensuring good alignment to the image and to all spots on the array, the gal file was then fitted to the image, using the software. Individual spot alignment and re-adjustment was performed at this stage if necessary using feature mode. Spots that were not of sufficient quality for analysis were flagged as 'bad'. The image was then analysed using the GenePix Pro 5.0 software and results for each serum was saved as a gpr file.

This procedure was also followed for the second field on each of the arrays, except a different gal file corresponding to the amended spotting layout was created and attached.

2.5.1.4 Analysis of hEx1 Protein Microarray Serum Screening Results

Spots that were flagged as bad with a flag value of -100 were omitted at the first stage of collating the raw data for analysis. The gpr file gives raw data readouts on two different channels, however all analysis was performed on the 532 channel as the detection fluoraphore is Cy3. For background subtraction, the background mean value

attained from the Genepix Pro 5.0 software was subtracted from the foreground mean value. For instances where background had a higher mean value than the foreground mean value, this negative value was reassigned a value of 1.

For data normalisation, the anti-hu IgG (1:1000) spot was used as a normalisation control, block normalisation was carried out by dividing the average value for the anti-hu IgG (1:1000) spots into the values of the hEx1 spots in the relevant block. This results in 10 normalised values for each of the different hEx1 antigens spotted on the array. The top and bottom 20% of these 10 values were discarded at this stage, leaving 6 normalised values remaining. Of the hEx1 antigens spotted on the array, the overall mean and standard deviation of all these normalised values was calculated. The antigens that had a signal two standard deviations greater than the overall mean of all hEx1 antigens spotted on the arrays was determined for all screened serum samples. These top signal antigens were identified as the positive results for each screened serum sample.

2.5.2 Western Immunoblotting

As for PAGE analysis, gels were loaded and proteins electrophoresed. A PVDF membrane was cut to size (9cm x 6.5cm) and activated in ethanol for 2 minutes. The membrane was then washed in dH_2O and equilibrated in transfer buffer (20mM Tris-HCl pH 8.5, 150mM glycine, 0.01% w/v SDS and 20% methanol). Filter papers were also cut to size (10cm x 7.5cm) and equilibrated in transfer buffer. The electrophoresed gel was placed on the PVDF membrane, sandwiched between four filter papers and two blotting sponges. The rig was set up with an ice insert and stirring bar to keep the buffer cool. The tank was filled with transfer buffer and ran at 100 volts for 1 hour to transfer proteins from the gel to the membrane. The blot was removed from rig and rinsed in TBS-T (150mM NaCl, 10mM Tris-HCL pH 7.5, 0.05% v/v Tween 20). Blots were blocked in 5% milk-TBS-T for 1 hour at room temperature, then incubated in

diluted serum in 2% milk TBS-T for 2 hours on slow rock. Blots were washed 3 times for 10 minutes in TBS-T and incubated in anti-human alkaline phosphatase conjugated IgG (Sigma Aldrich UK, Cat no: A1543), at 1:5000 dilution in 2% milk TBS-T for 1 hour. The blot was washed twice for 10 minutes in TBS-T and once for 10 minutes in TBS. Next the blot was equilibrated in attophos buffer for 10 minutes and then incubated in diluted attophos substrate solution (1:40 dilution of attophos substrate in attophos buffer) for 7 minutes in the dark. The blot was imaged using a LAS3000 Fuji imager, using tray position 1, filter 3 and 460nm blue light usually at a 1 second exposure. Images were saved for analysis.

2.5.3 Enzyme-Linked Immunosorbent Assay (E.L.I.S.A.)

Maxisorb microplates (Nunc UK, Cat no: 456537) were washed in deionised water and left inverted to dry. Antigens were diluted in deionised water to a final concentration of 1ng/ul. 50μl of diluted antigens were aliquoted into wells in the maxisorb plate. The plate was left overnight at 4°C to coat. The plate was washed 3 times with TBS-T (150mM NaCl, 10 mM Tris-HCL pH 7.5, 0.1% v/v Tween 20). All microplate washes were performed in a microplate washer (Biochrom Anthos Fluido 2). Next, 400μl of 5% milk TBS-T was aliquoted into each well and the wells were blocked for 2 hours. The plate was washed 3 times with TBS-T. Serum was diluted 1:100 in 5% milk TBS-T and 50μl of diluted serum was added to each well, this was incubated on a plate shaker for 2 hours at RT. The plate was washed 5 times with TBS-T. Goat anti-human horseradish peroxidase (HRP) conjugate IgG (Sigma Aldrich UK, Cat no: A0170) was diluted to 1:5000 dilution in 5% milk TBS-T. 50μl of diluted antibody was aliquoted into wells and left to incubate for 1 hour at RT. Plate was washed 5 times with TBS-T. Next, 50μl of TMB substrate was added to wells and incubated for 30 minutes in the dark. The reaction was then stopped by addition of 25μl of 1N sulfuric acid to wells and the

plate shaken briefly to mix the contents. The absorbance was read at 450nm using a microplate reader (Wallac, Victor).

To determine the ELISA cut-off value, the mean absorbance value and the standard deviation for all results (absorbance values for all serum for tested antigen and negative protein) in each lot of ELISAs was determined. The cut-off value was equal to the mean absorbance value plus two standard deviations. The cut-off value for each ELISA was indicated on the graphed results as a horizontal black line.

2.5.4 Dot-Blot Immunoblotting

PVDF membranes were cut to size and activated in ethanol for 2 minutes and washed in dH_2O for 2 minutes. Protein antigens were diluted in dH_2O to a final concentration of 10ng/μl. The PVDF membrane was kept humidified on PBS soaked filter paper while 2μl of the diluted antigens were spotted on the membrane in a grid like layout. The membranes were then carefully removed from the soaked filter paper and placed on a dry filter paper for 20 minutes until dry. The membranes were then reactivated in ethanol for 2 minutes, rinsed in dH_2O for 2 minutes and rinsed in TBS-T (150mM NaCl, 10 mM Tris-HCL pH 7.5, 0.05% v/v Tween 20) for 2 minutes. Dot blots were blocked in 5% milk-TBS-T for 1 hour at room temperature, then incubated in diluted serum in 2% milk TBS-T for 2 hours on slow rock. Blots were washed 3 times for 10 minutes in TBS-T and incubated in anti-human alkaline phosphatase conjugated IgG (Sigma Aldrich, UK, Cat no: A1543), at 1:5000 dilution in 2% milk TBS-T for 1 hour. The blot was washed twice for 10 minutes in TBS-T and once for 10 minutes in TBS. Next, the blot was equilibrated in attophos buffer for 10 minutes and then incubated in diluted attophos substrate solution (1:40 dilution of attophos substrate in attophos buffer) for 7 minutes in the dark. The blot was imaged using a LAS3000 Fuji imager, using tray position 1, filter 3 and 460nm blue light usually at a 1 second exposure.

Images were saved for analysis.

2.6 ProtoArray Screening and Analysis

The Invitrogen ProtoArrays (V5) consist of over 9,000 unique human proteins which are spotted in duplicate. The spotted proteins are GST fusion proteins that are full length, purified and also retain functionality.

2.6.1 ProtoArray Serum Screening

The Invitrogen ProtoArrays were removed from $-80°C$ and equilibrated to $4°C$ for 20 minutes. Arrays were placed in a petri dish and blocked in 20 mls of blocking buffer (50nM HEPES, 25% v/v glycerol, 0.08% v/v Triton X-100, 200mM NaCl, 2% w/v skimmed milk powder, 1mM DTT) for 1 hour at $4°C$ on an orbital shaker on slow rock. The arrays were washed in wash buffer (137mM NaCl, 2.7mM KCl, 4.3mM Na_2HPO_4, 1.47mM KH_2PO_4, 0.1% Tween 20, 2% w/v skimmed milk powder) for 5 minutes at 4^oC at a faster rocking speed. Serum was diluted at a 1:500 dilution in wash buffer to result in 20mls total volume. The diluted serum was poured over the array and incubated for 90 minutes at $4°C$. Arrays were then washed with 20mls of wash buffer for 5 minutes for a total of 5 washes. Alexa fluor 647 goat anti-human IgG (Invitrogen, UK, Cat: A21445) was diluted 1:2000 in wash buffer and incubated over the array for 90 minutes. Arrays were washed with 20mls of wash buffer for 5 minutes for a total of 5 washes. Arrays were then dipped in deionised water 3 times to remove salt and were then dried by centrifugation at 300 x g for 3 minutes. Scanning was performed using a GenePix 4000B Axon scanned at a wavelength of 647nm. The individual gal file for the array was downloaded from the invitrogen.com website and overlaid on the ProtoArray TIFF file image.The gal file was fitted to the image and the resultant gpr file was created.

2.6.2 ProtoArray Analysis with Prospector

The Invitrogen Prospector software was used to analyse the array results. The gpr files were opened within the software program and were analysed using the "Immune Response Profiling" application.

2.6.3 ProtoArray Pathway Analysis

After performing analysis using Invitrogen Prospector software the significantly reactive proteins (based on z-factor) for each serum sample were saved as ranked lists in microsoft excel files. These lists of proteins were analysed using the innate database pathway analysis tool (innatedb.com). The "Data Analysis" tab was selected and accession numbers were inputted into the web form and uploaded. The column was then specified as "Cross-reference ID" and the database was selected as "Refseq". A list of pathways was selected and the pathway over-representation tool was used to identify the pathways of interest. The analysis algorithm and p-value correction method selection was performed with recommended algorithms (Hypergeometric) and correction methods (Benjamini Hochberg). Results were arranged first by corrected p-value (ascending), then by number of uploaded genes in annotated pathway (descending). The generated results were saved as ranked lists in microsoft excel files. All pathways with a corrected p-value of less than 0.05 was considered significant and was highlighted for further analysis.

2.7 Statistical Analyses

As outlined in sections 2.3.3and 2.5.1.4 statistical analyses were performed inhouse. In the case of section 2.3.3 regarding the analysis of the hEx1 arrays, this methodology

was developed in association with the Centre for Support and Training in Analysis and Research (CSTAR). Whereas in section 2.5.1.4, this analysis has been used routinely for microarray analysis within our research group and is used to control for variations associated with inter and intra array variation.

Regarding sample size calcuation, this was initially performed in association with Prof. Leslie Daly (University College Dublin), further refinement of sample size was performed by Dr. John O'Brien in collaboration with Dr. Gloria Crispino and CSTAR. The sample size calculation is based on the primary analysis, the sensitivity of detecting a positive case of ovarian cancer. To determine if a panel has any diagnostic ability beyond chance (i.e. has a sensitivity >50%), the sample size calculation is based on the minimally acceptable value for sensitivity (true positive rate), which has been set at 70% with a desirable value of 80%. With 80% power at a two-sided level of 5%, a sample of 153 cases and at least 153 healthy subjects (at least the same number of controls as cases) would be sufficient to detect such sensitivity.

In this study, 26 healthy/non remarkable, 28 benign ovarian disease, 34 late stage ovarian cancer and 20 early stage ovarian cancer were interrogated, giving a total of 108 subject sera that were interrogated. The sample size in this study is relatively small, in our current data set and the sensitivities and specificities produced for these panels are descriptive rather than prescriptive. Our aim is to further assess the significance, specificities and sensitivities of the identified panels using a larger testing cohort. However, this study serves as an important reference for ongoing work as it interrogates the ability of differential methodologies to provide the same result.

Chapter 3

Autoantibody Identification by hEx1 Array Serum Screening and Validation

3.1 Introduction

The immune system can recognise and destroy pre-malignant cells, and the immune system is capable of sensing aberrant location, function and structure of cellular components and machinery that may be involved in tumourigenesis. As outlined in the introduction, autoantibodies are known informative reporters of the immune system [132]. It has been identified that there is a humoral immune response to tumour associated antigens and, in some cases (p53), that AAbs to these antigens may arise in advance of clinically detectable disease. As ovarian cancer is an assymptomatic disease with no reliable biomarkers, AAb profiling of this disease has the potential to dramatically improve patient quality of life and survival.

To profile the AAb repertoire of selected subjects, the hEx1 arrays were employed. Our research group has optimised autoantibody serum profiling and has many years of experience regarding protein array generation and screening. Access to the hEx1 expression subset of 37,200 *E. coli* expression clones is one of the main advantages of this research project. This access allows expression of the same bacterially produced proteins that are present on the surface of the hEx1 arrays.

Serum Sample Selection

In this study, the early and late stage ovarian cancer patient sera used were clinically defined, categorised and diagnosed by a multi-disciplinary team (MDT), as is the gold standard in cancer care, in St. James's Hospital, Dublin 8. The MDT uses information such as tumour invasion and spread - as determined by imaging platforms, and also histological methodologies which identify morphological changes in cells and the architectural "pattern" of the cells and their nuclear content (e.g., DNA "ploidy) and also in some cases p53 mutation status. All serum used in this study was obtained prior to planned surgery, prior to chemotherapy and/or radiotherapy and all sera was collected and stored identically. Cancer patient serum was not included in this study if patients had a previous history of cancer, or if an autoimmune disease had been clinically diagnosed. The ovarian cancer serum samples, selected for this work were early and late stage ovarian cancer. The early stage ovarian cancer patients are of mixed histologies, the advantage to profiling a hetero-histologicial cohort is that, a biomarker, if identified, will be very informative, as ovarian cancer, by nature is a very heterogenous disease. However, a disadvantage is that it may be more difficult to identify an AAb pattern in a diverse group, than a more homogenous group. As early stage ovarian cancer is a very rare and heterogenous disease and there are relatively few serum samples available, it was decided to screen an increased number of heterogenous patients for this study. The late stage ovarian cancer patients assessed in this study are all serous papillary histology, this is reflective of disease presentation, as serous papillary is the most common subtype and typically presents at stage III-IV. It was decided to screen a more homogenous patient cohort of late stage ovarian cancer patients as numbers of patients were not an issue for this disease stage.

The selection of control serum samples in this study was very important. Many studies are now using patients with benign diseases as a control cohort [232], this may

be a more appropriate control group than "normal" or "healthy" controls, as it is often very difficult to identify a truely healthy person and subjects from the normal population may have malignancies or other conditions that have yet to present clinically. In this study serum from healthy subjects, non-remarkable subjects, benign ovarian disease patients and primary peritoneal carcinoma patients were screened as control cohorts to determine AAb responses that are specific to ovarian cancer. The healthy cohort are a commercially available serum cohort purchased from Percision Med (http://www.precisionmed.com). All patients in this cohort were gender matched. These samples were from patients that were assured to be healthy and are tracked over time, serum samples are not released for a period after serum collection to ensure subject health. Screening of these healthy serum on the hEx1 arrays was performed by a different researcher in our lab group prior to the start of this project. The non-remarkable serum cohort was obtained from a group of age matched women from the general population, these subjects have not been previously diagnosed with malignancy. The benign ovarian disease subjects were clinically defined, categorised and diagnosed by the MDT in St. James's Hospital. Benign patients were selected for AAb serum profiling, as tissue remodelling and damage at the site of the ovarian growth may induce an autoantibody response. This response needs to be interrogated to ensure it does not overlap with the tumour AAb profile. As outlined in Section 1.2.1, new findings have indicated that this may be unlikely, as the benign and malignant growths arise in different tissues. However, benign patients are still one of the most widely used and accepted control groups and so were included in this study.

Primary peritoneal carcinoma patient serum was also screened in this study. Primary peritoneal carcinoma is a cancer of the peritoneal membrane that forms the lining of the abdominal cavity , this malignancy carries a very poor prognosis, largely due to lack of symptoms. Patients are managed similarly to late stage ovarian cancer patient

and like the majority of ovarian carcinomas, primary peritoenal carcinoma has a serous papillary histology and the peritoneum may also arise from the same mesodermal embryonic origin as the ovaries. As primary peritoneal carcinoma and ovarian cancer may arise from the same origin, this may result in very similar AAb profiles. Also, due to the close proximity of the ovaries to the peritoneal membrane, metastasis from the ovary to the peritoneal lining is very common. Therefore, because of proximity, similar presentation and histology it was decided to use this disease a control cohort. Peritoneal cancinoma can be difficult to distinguish from serous papillary ovarian carcinoma and an autoantibody response that interrogates this may be useful in the clinic for patient stratification. The primary peritoneal subject sera used in this study was also clinically defined, categorised and diagnosed by the MDT in St. James's Hospital. Sera from primary peritoneal carcinoma patients was screened as a control to determine AAbs that may be associated with malignant tumours of serous histology that are not exclusive to ovarian cancer

3.2 Aims

- To use the hEx1 protein arrays to identify autoantibody profiles in healthy and disease serum.
- To identify autoantibodies that are associated with ovarian cancer.
- To validate the results of hEx1 screening using secondary experimental platforms.

3.3 Materials and Methods

3.3.1 Serum Samples and hEx1 Array Screening

The hEx1 arrays were used to profile the AAb repertoires of the serum samples indicated in Table 3.1. A breakdown of these individual serum sample details is outlined in Table A.1. Five different serum cohorts were screened for this study.

Following serum screening on the hEx1 arrays, array scoring for each individual serum was carried out as outlined in Section 2.3.2, and two results files for each serum sample was generated. 148 results files, corresponding to the 74 serum samples screened were sent to Dr. John O'Brien for analysis.

Table 3.1: Serum for hEx1 array screening

Number of Samples	Stage	Histology	Mean Age
13	Early OC (I-II)	Mixed Histology	54
20	Late OC (III-IV)	Serous Papillary Adenocarcinoma	63
5	Primary Peritoneal Carcinoma	Serous Histology	65
10	Benign Ovarian Disease	Mixed Histology	51
9	Non-Remarkable	-	64
17	Healthy	-	67

3.3.2 Selection and Expression of Antigens of Interest

3.3.2.1 Selection of hEx1 Antigens of Interest

The files were sent for statistical analysis to Dr. John O'Brien. Dr John O'Brien developed the statistical methodology for analysis of the hEx1 array results as outlined in Section 2.3.3 This analysis was independently analysed, by Dr Tim Grant and Dr. Gloria Crispino-O'Connell, director of the Centre for Support and Training in Analysis and Research (CSTAR) and their analysis confirmed and supported the previous methodology. The top ranked panels of clones identified to be associated with early

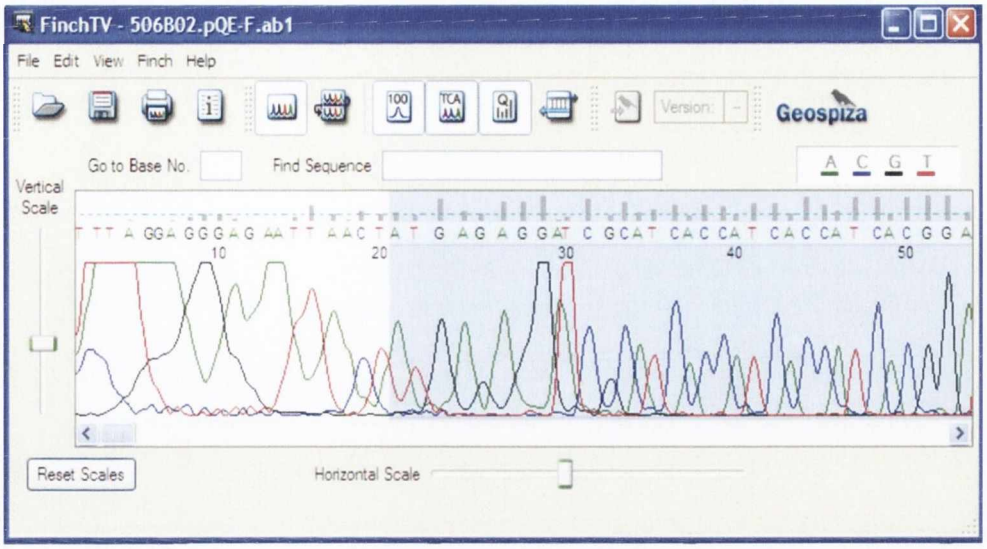

Figure 3.1: Sequence Analysis

This figure shows the results of sequncing anaysis for clone 506B02. To interrogate the sequence further the section from the start codon is selected through to the end of the sequence read and then inputted into the open reading frame finder on the NCBI website. The classical "AGAGGATCGCATCACCATCACCATCAC" sequence is clearly visible in this image and this encodes the $RGSH_6$tag.

stage ovarian cancer only, late stage ovarian cancer only, late and early stage ovarian cancer only, benign ovarian disease and primary peritoneal carcinoma were selected for further analysis. From these lists of panels, the individual clone identities were collated into lists of clones of interest. These clones were sequenced and interrogated to identify clones that express a His-tagged protein product in the +1 ORF. The sequence was selected from the start codon as outlined in Figure 3.1 and ORF analysis was performed as in Section 2.4.2.

3.3.2.2 Production of hEx1 Antigens of Interest

Clones that expressed a His-tagged protein product in the +1 ORF were picked, grown and induced for protein expression as in Section 2.4.3. The protein products were purified as in Section 2.4.4 and five microlitres of each protein was mixed with SDS-sample loading buffer and boiled for 5 minutes to denature the protein prior to analysis

by PAGE (Section 2.4.7). Following PAGE analysis the proteins were quantified as in Section 2.4.5.

3.3.3 Secondary Validation

To analyse the results of hEx1 array screening, secondary validation techniques were performed. An initial hEx1 protein microarray analysis was performed as a relatively high-throughput secondary screening methodology. ELISA analysis was also carried out as an additional secondary screening technique as this platform is used in a diagnostic setting, which is the ultimate goal of autoantibody profiling.

3.3.3.1 hEx1 Protein Microarray

The hEx1 protein microarrays were generated as in Section 2.5.1.1. Proteins were diluted to the required concentration with deionised water, enough diluted antigen was made up to make five master plates from which to spot, hence the same dilutions were used on each array spotted. Once the master plates were aliquoted, they were stored short-term at $-20°C$ until use. Four lots of 25 slides were spotted on 4 different days totalling 100 slides spotted. Twenty five slides were spotted per lot as the Genetix QArray robotic arm has a relatively short transfer time from the masterplate to the array, this prevents protein evaporation and improves spotting quality. The layout of the slides is outlined in Figures 2.4 and 2.5.

Quality Control Analysis

For quality control analysis, one randomly selected slide from each lot was probed with anti-histidine antibody as outlined in Section 2.5.1.2. The slides were scanned as outlined in Section 2.5.1.3. The resultant gpr files were sent for analysis to Dr.

John O'Brien. The normalised mean for each individual hEx1 protein across all 5 anti-histidine probed slides was determined and plotted to identify variation.

hEx1 Protein Microarray Serum Screening

The 73 serum chosen for autoantibody screening on the hEx1 protein microarrays is outlined in Table 3.2. The breakdown of individual serum is outlined in Table A.4. The serum was randomly selected for probing on different lots of slides. The serum was screened as outlined in Section 2.5.1.2 and the slides were scanned as outlined in Section 2.5.1.3. The resultant gpr files were sent for analysis to Dr. John O'Brien. The results files were analysed as outlined in Section 2.5.1.4 to identify the reactive antigens in each serum sample.

Table 3.2: Serum for hEx1 microarray screening

Number of Samples	Stage	Histology	Mean Age
20	Early OC (I-II)	Mixed histology	57
23	Late OC (III-IV)	Mixed histology	61
20	Benign Ovarian Disease	Mixed histology	45
15	Non-Remarkable	-	64

ELISA Optimisation

ELISA optimisation was performed using antigen coating concentrations of 125ng/well, 62.5ng/well, 31.3ng/well, 15.6ng/well and 7.8ng/well. For optimisation hEx1 p53 protein, commercial recombinant p53 and hEx1 negative control protein (tenascin) was probed with a serum sample (Late stage TCDOG 55) that was identified as having AAbs to p53 by hEx1 array and hEx1 protein microarray. The optimisation ELISAs were processed as in Section 2.5.3.

ELISA Processing

ELISA analysis was performed on the overlapping serum that was assessed in the hEx1 array screening (Table 3.1) and the hEx1 protein microarray screening (Table 3.2). The sera used for ELISA analysis are outlined in Table 3.3. In total six antigens were selected for ELISA analysis. Three antigens were selected for ELISA analysis as they exhibited similar binding patterns in hEx1 array and hEx1 protein microarray screening. Two antigens were selected for ELISA analysis as they exhibited strong binding in hEx1 array platform only, while one antigen was selected as it exhibited strong binding in the hEx1 protein microarray only.

Table 3.3: Serum for ELISA Analysis

Number of Samples	Stage	Histology	Mean Age
12	Early OC (I-II)	Mixed histology	57
20	Late OC (III-IV)	Serous Papillary Adenocarcinoma	63
10	Benign Ovarian Disease	Mixed histology	51
9	Non-Remarkable	-	64

3.4 Results

3.4.1 Results of hEx1 Array Screening

Once serum screening has been performed and the hEx1 arrays have been imaged, the positive signals identified as duplicate spots, can be easily seen as shown in Figure 3.2.

Analysis by Dr. John O'Brien identified the top ranked panels of clones as are listed as in Table A.2. This table outline the identities of clones in each panel and the cohort which has been identified to be associated with the panel. Following sequence analysis of all these bacterial clones only clones with His-tagged protein products in the +1 ORF, as performed as in Section 2.4.2, were selected for further analysis. The bacterial clones selected for further analysis are outlined in TableA.2 as highlighted blue text. Approximately one third of bacterial clones listed in the panels of interest were identified as not having an insert in the correct open reading frame this is in agreement with the previous analysis of the hEx1 library [179, 233]. Seventy four bacterial clones were selected for further investigation.

3.4.2 Assessment of Antigens of Interest

The selected 74 expression clones were assessed using the BLAST program on the NCBI website. The clone identifier and human protein expression product in the +1 ORF is listed in Table A.3. Many of these clones are associated with more than one cohort, for instance, clone 592F05 has been shown to be associated with the benign and the primary peritoneal cohort. This list of protein products is redundant and many of the expressed proteins are partial products.

A simple analysis was carried out to identify the serum reactivities for each of the 74 expression clones identified by hEx1 screening. This analysis is outlined in Figure 3.3. The coloured boxes indicate if a patient serum was identified as reactive to an

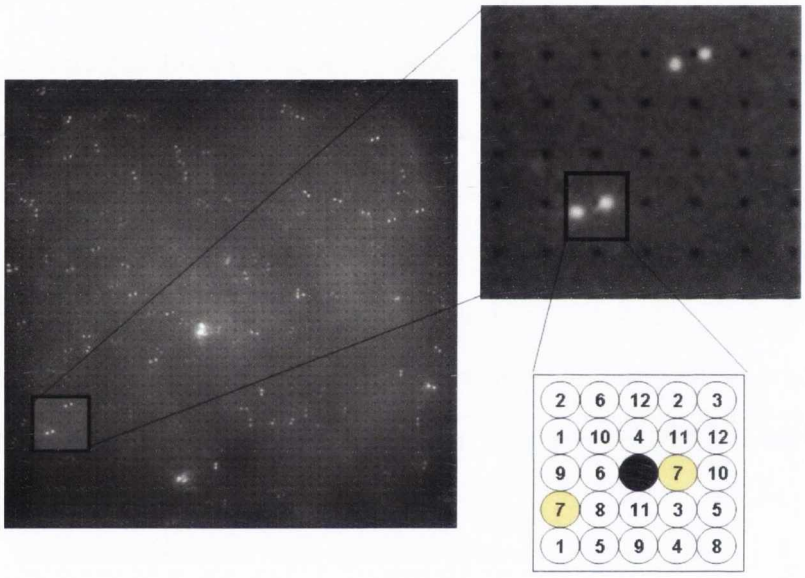

Figure 3.2: Image analysis of a screened hEx1 array

This image is of a processed hEx1 array incubated with ovarian cancer serum (part 8). The duplicate spots are clearly visible around the black guide spots. The grid shows the position of the antigens and around the black guide spot. In this instance, there is a positive signal at position 7. Positive signals are then referenced to a master grid and the exact bacterial expression clone is determined [179].

antigen by hEx1 screening. As detailed in Section 2.3.2 there are three different scoring intensities for signals on the hEx1 arrays, the strongest intensity is "3" and the weakest is "1". In the Figure 3.3, the brown colour represents the strongest intensity signal of "3" with the lightest orange colour representing the weakest signal of "1". From this image, it is clear that the most reactive serum cohort for these antigens is the "Late" stage cohort, this is indicated by a larger proportion of coloured boxes in this section. The least reactive cohorts, having a lower proportion of boxes are "Peritoneal" and "Healthy". This is as expected as the 74 clones were identified and selected to have a stronger association with ovarian cancer.

After growing the 74 expression clones, the protein products were purified and analysed by PAGE analysis. The results of PAGE analysis are shown in Figure 3.4. From PAGE the purity of the proteins could be assessed, from the PAGE images it is clear that protein expression varied greatly but overall was very successful. PAGE also confirmed that the purification methodology worked well as for the majority of proteins a single clear banding pattern is visible. The mass of the proteins by PAGE analysis was compared to the mass as determined by sequence analysis (Table A.3). As antigens were sized using two different methodologies, by sequence and by PAGE, there are some discrepancies for some antigens. This may be due to a number of factors, such as inhibition of protein migration through the gel as a results of charge or protein aggregation, both factors will lead to a heavier than expected protein sizing on PAGE compared to sequence analysis. DNA sequencing was used to determine the identity of all antigens using the BLAST algorithm, however sizing could not be obtained for all antigens as in a few cases the sequencing did not maintain sufficient integrity up to a stop codon.

Protein quantitation identified that 26% of the 74 protein products were below a concentration of 250μg/ml and hence could not be spotted at this concentration on the

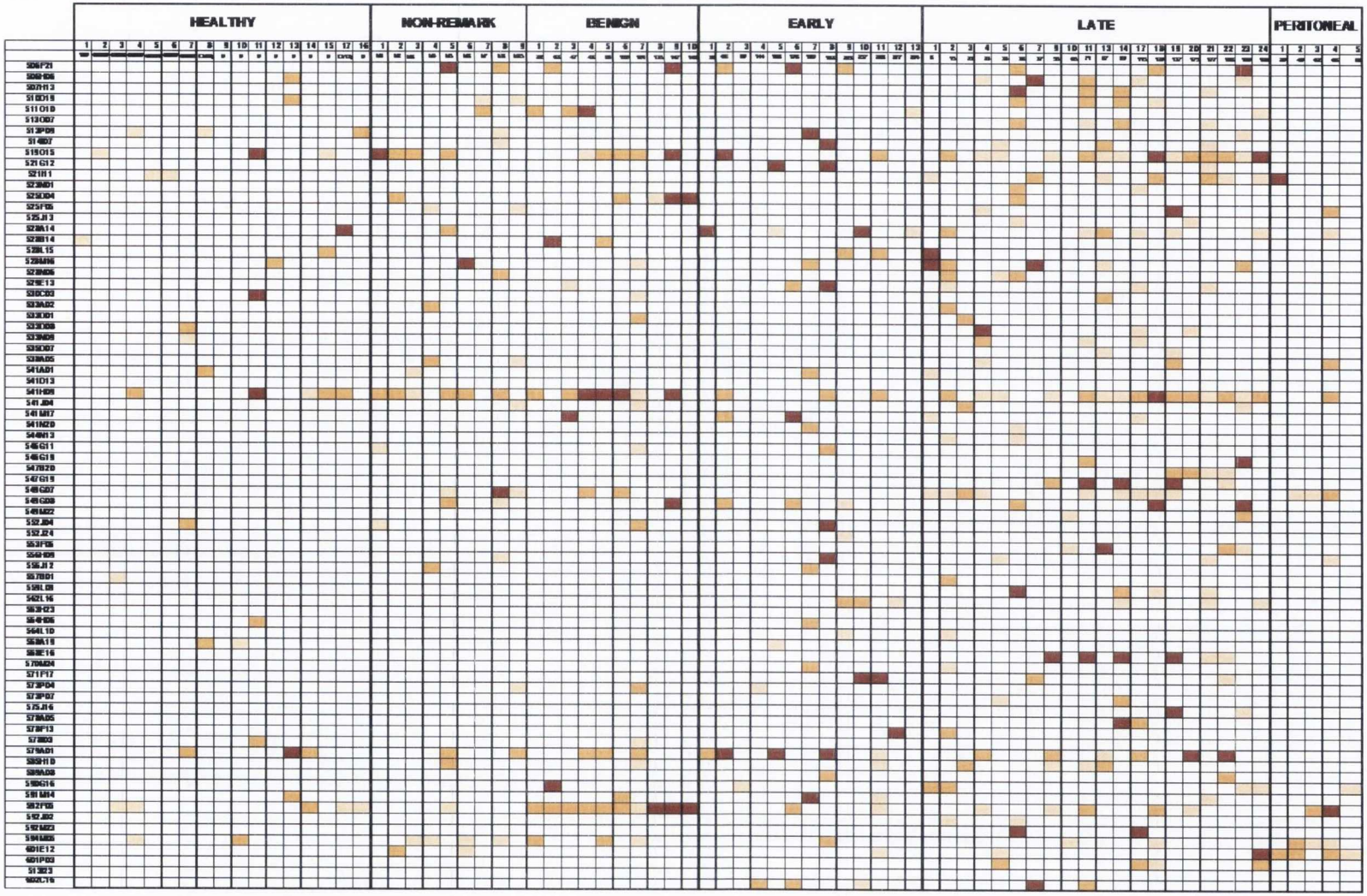

Figure 3.3: Frequency and intensity of antigenic clones in hEx1 array screened serum

This figure outlines the frequency of AAb detection, and the associated intensity of this binding event on the surface of the Imagene hEx1 array. The light orange boxes indicate a weaker intensity spot, while the brown boxes indicate a strong intensity spot.

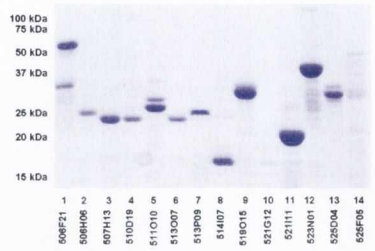

(a) Antigens 1-14

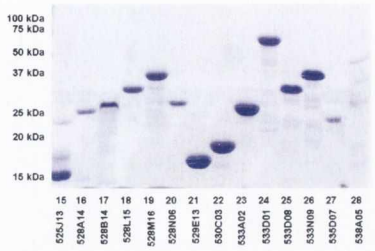

(b) Antigens 15-28

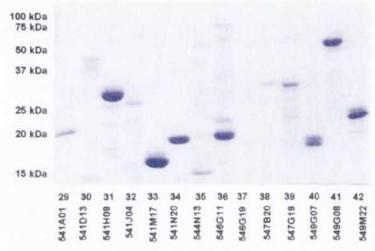

(c) Antigens 29-42

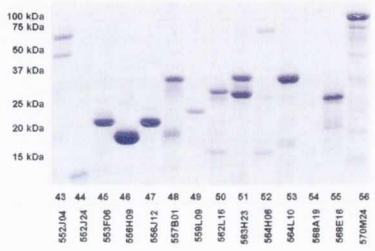

(d) Antigens 43-56

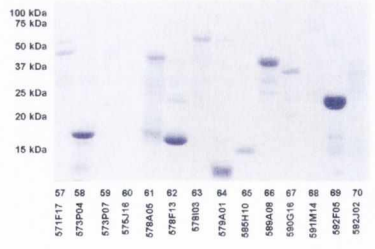

(e) Antigens 57-70

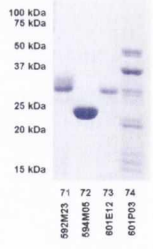

(f) Antigens 71-74

Figure 3.4: PAGE analysis of 74 antigens of interest

These images of PAGE analysis on the 74 antigens provide information on antigen purity, antigen expression and sizing. From these PAGE images it is evident that the vast majority of proteins are expressed well and have a good purity level. In some cases there are multiple bands that may correspond to the protein of interest. However these proteins were retained for further analysis without any further preparation to retain the high throughput nature of this research.

protein microarrays. The average concentration of the 19 protein products below this threshold was 111μg/ml

3.4.3 Secondary Validation

3.4.3.1 hEx1 Protein Microarray

Quality Control Analysis

The microarrays were spotted in-house as detailed in Section 2.5.1.1 and to ensure that the microarray spotted were of reproducible quality and that the generated results would be reliable, basic quality control analysis was performed.

One slide from each lot of spotted arrays was randomly selected for probing with an anti-histidine antibody. The anti-histidine antibody binds all the hEx1 proteins spotted on the arrays as all the hEx1 are his-tagged fusion proteins, as shown in the images of the screened microarrays in Figure 3.5. Analysis of the anti-histidine probed slides will determine the quality of the spotting in each lot of arrays and also determine the reproducibility of the spotting on the slides. The anti-histidine antibody probed slides were analysed in the same way as the serum screened slides, as outlined in Section 2.5.1.4. Once the 6 normalised values for each of the clones were remaining, the mean value and standard deviation for individual antigens across all the slides was calculated and graphed (Figure 3.6). From the analysis of the anti-histidine probed slides it is evident that there is variation in the fluorescence values for each antigen across individual lots, however this variation is reasonable, with an average fluorescence per spot of 1.35, and an average standard deviation of 0.2. Thus, it was determined that the in-house microarray spotting was reproducible and meaningful data could be obtained across lots of slides.

An array screen without any primary antibody was also performed to identify any antigens that may bind the secondary antibody directly or potentially autofluoresce.

Figure 3.5f shows the result obtained for this screen. There is very little hEx1 antigen fluorescence evident from this screen, indicating positive signals attained from serum screening are as a results of AAb recognition in subject serum.

It is evident from Figures 3.5c and 3.5f that the array slides spotted at Lot 3 exhibit three large fluorescent spots in the second field of the arrays. These spots correspond to the same protein (not a hEx1 protein). It is evident that this protein has spread out on the surface of the nitrocellulose, the exact reason for this is unknown. However this is a known disadvantage of using a nitrocellulose array surface [234], this may be due to changes in humidity during spotting. It only happened for one protein, and is probably related to the properties of the individual protein. For gal file alignment on the lot 3 arrays, feature mode was selected and these spots, and any surrounding spots that were affected by this spreading were not included in analysis.

hEx1 Protein Microarray Serum Screening

Following the assessment of the quality of the protein microarray spotting and confirmation that the spotting reproducibility was sufficient, serum screening was performed. Figure 3.7 shows a subset of images of serum screened hEx1 protein microarrays. The top signal antigens for each screened serum sample was identified and are outlined in Figure 3.8. As previous analysis, the coloured boxes indicate if a patient serum was identified as reactive to an antigen. Although array screening was performed on a slightly altered serum cohort, the trend of ovarian cancer association does not seem to be as evident from the results of protein microarray screening.

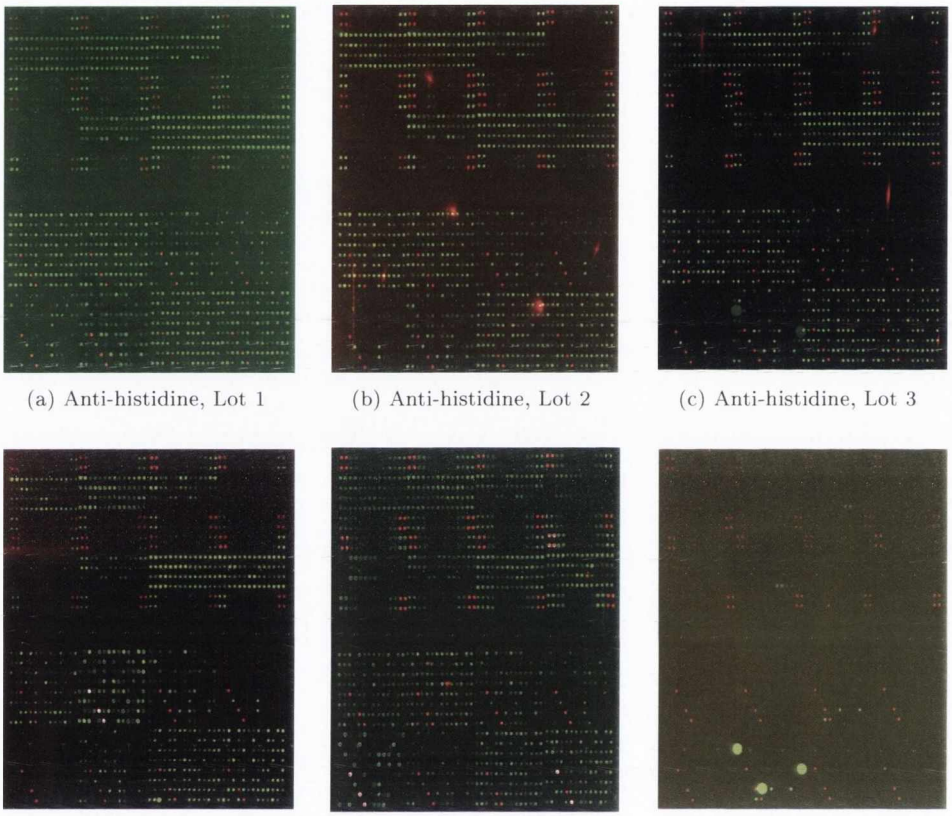

(a) Anti-histidine, Lot 1 (b) Anti-histidine, Lot 2 (c) Anti-histidine, Lot 3

(d) Anti-histidine, Lot 4 (e) Anti-histidine, Lot 5 (f) Anti-IgG only, Lot 3

Figure 3.5: Anti-histidine screened hEx1 microarray slides

These figures show the results of anti-histidine antibody screening and anti-IgG antibody screening only on the hEx1 protein microarrays. The red spots represet Cy5 dye which is spotted for GAL file alignment, the green spots here identify the binding events which have been detected using a Cy3 labelled detection antibody. From these images we can see that there a good and general binding pattern as a result of anti-histidine screening, especially for the randomised field 2 printed on the lower half of the images. Notably, a subset of arrays printed in lot three show protein spreading for one protein in field 2. This may be due to a change in conditions, however, spreading of spotted proteins is known to be associated with nitrocellulose surface chemistry.

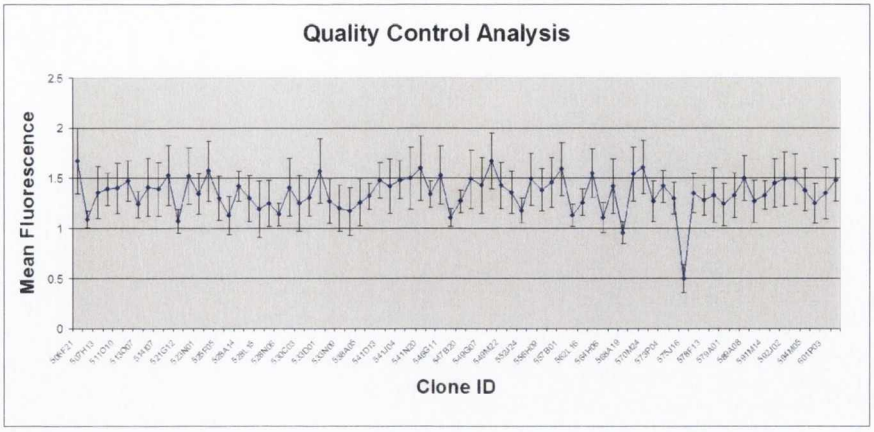

Figure 3.6: Quality control and reproducibility analysis of hEx1 microarrays

This analysis identifies the flourescence variation of the individual clones across the different lots of slides spotted. Variation is noted across the lots of slides, however for an in-house spotted microarray this variation is relatively small, the variation noted was considered to be acceptible. Notably, the antigen corresponding to clone 575J16 has a very low mean value compared to other values. From the results of PAGE and quantitaion analysis there is little or no antigen present in this sample. Although it was included as an undiluted sample for microarray spotting, as mean signal for this antigen is very different from the others it was concluded that there was little or no protein present.

Comparative Analysis of hEx1 Array and hEx1 Microarray Analysis for 74 Antigens

Both the hEx1 arrays and the hEx1 protein microarray platforms differ greatly in their surface chemistry and antigen purity, however as hEx1 antigens are used in both array platforms it was expected that there would be a large overlap between the platforms. In particular where there was a strong signal (intensity 3) to an antigen in the hEx1 array platform, it was assumed that there would also be a strong signal to an antigen on the protein microarrays. The results of hEx1 array serum screening and hEx1 microarray serum screening were compared to assess the different AAb patterns identified in both platforms, this analysis is outline in Figure 3.9. This image is an overlap figure of Figure 3.3 and Figure 3.8 for common serum samples screened on both array platforms. As previous, the different shades of orange/brown boxes represent the positive identification of an AAb response by hEx1 arrays screening, while the green boxes represent

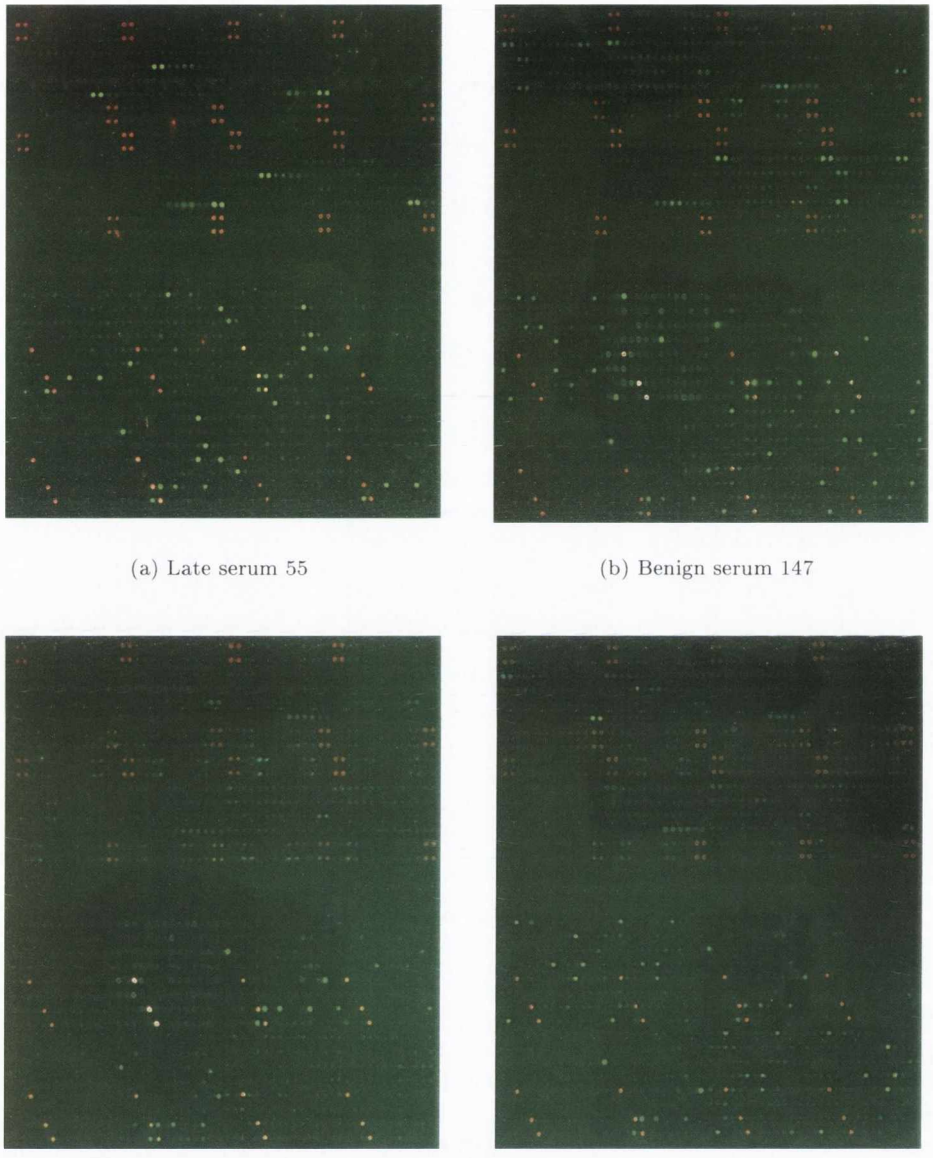

(a) Late serum 55

(b) Benign serum 147

(c) Benign serum 151

(d) Non-remarkable serum N8

Figure 3.7: Selection of serum screened hEx1 microarray slides

Shown in this figure are images of hEx1 protein microarrays screened with human serum. The red Cy5 spots used for gal file alignment are clearly seen and positive recognition of hEx1 proteins by AAbs in serum are indicated by the positive green Cy3 signals.

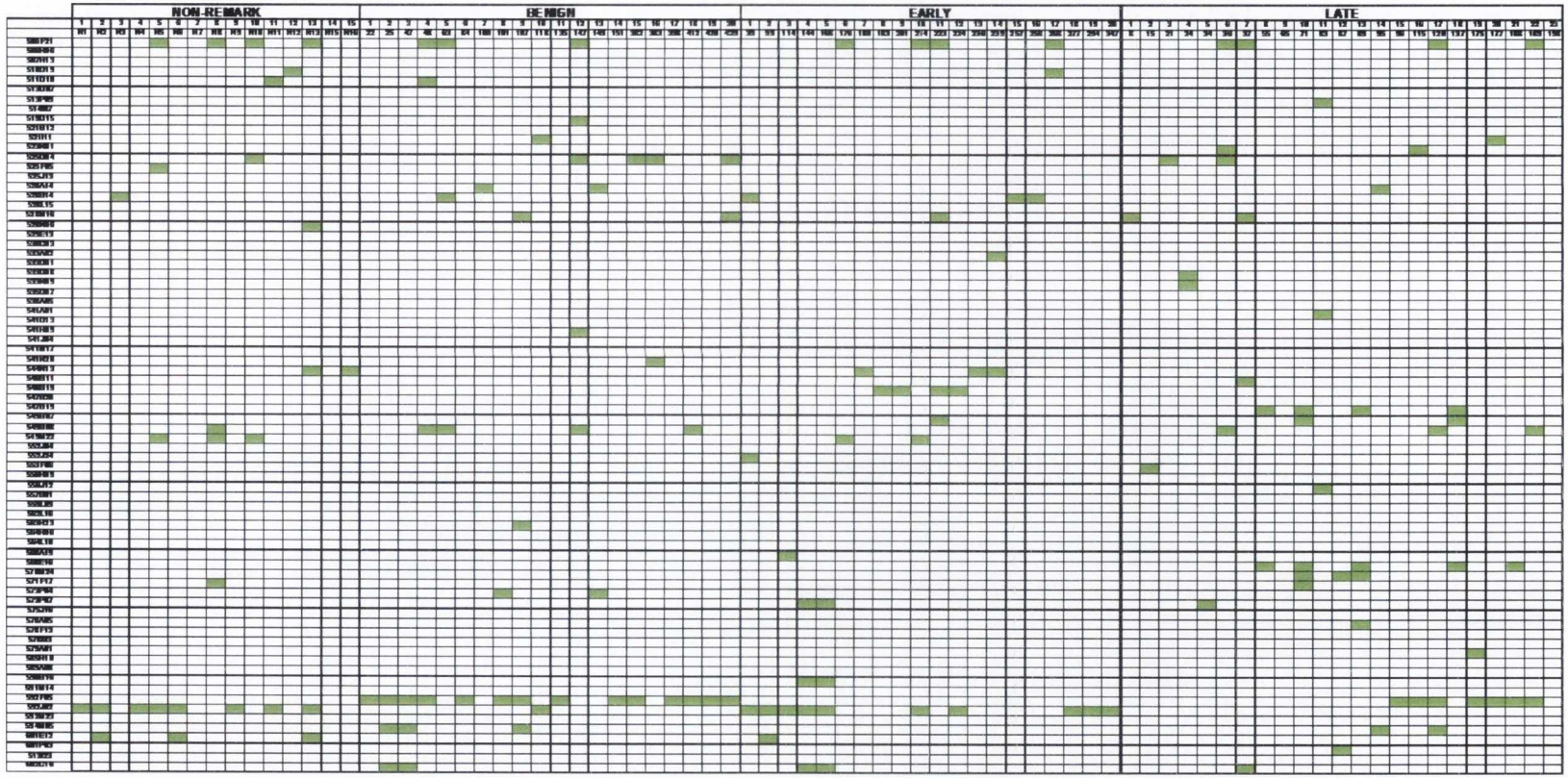

Figure 3.8: Highly reactive antigens identified by microarray serum screening

Shown in this figure are the results of hEx1 protein microarray analysis. The green boxes indicate when AAbs in a serum sample were identified to a recombinant purified protein. On the left of this figure, the expression clone identities which express the protein are listed. The serum was identified as positive for AAbs to an antigen when the normalised mean fluorescence value of the antigen is greater than the normalised average fluorescence value of all spotted antigens, plus two standard deviations.

the positive identification of an AAb response by hEx1 protein microarray screening. The blue boxes represent the identification of an AAb response by both of the array platforms.

From Figure 3.9 it is clear that there is a modest overlap in AAb identification between the two array platforms. The majority of AAb identified as common to both platforms are identified predominantly in the late stage cohort of ovarian cancer patients, disappointingly there are very few AAb that were identified in both platforms in the early stage ovarian cancer cohort. From reviewing Figure 3.9 it is clear that AAb identification may be platform associated as AAbs to some antigens are identified in the majority of the serum screened. This seems to be the case for the hEx1 array in particular. However, these antigens may be associated with the natural AAb profile, as it is known that there is an autoantibody response that arises in normal individuals in the absence of deliberate immunization with any antigen [235, 116]. Hence it is predicted that AAbs to antigens will be identified that are common to numerous individuals across all cohorts, these autoantibodies may be part of the natural autoantibody repertoire.

3.4.3.2 ELISA Analysis

ELISA has a relatively high throughput compared to other assay formats and is clinically relevant. AAb detection using an indirect (reverse-phase) ELISA has been used in previous AAb studies [230, 236, 237]. Antigens that are identified as immunoreactive in patient serum in both of these platforms and also antigens that seemed to be biased towards one of the array platforms were investigated by ELISA analysis. An ELISA format was selected for antigen validation at this stage as this is the classical 'gold standard' diagnostic platform.

In total six antigens were assessed by ELISA. Three of these antigens exhibited similar binding patterns in hEx1 array and hEx1 protein microarray screening, these

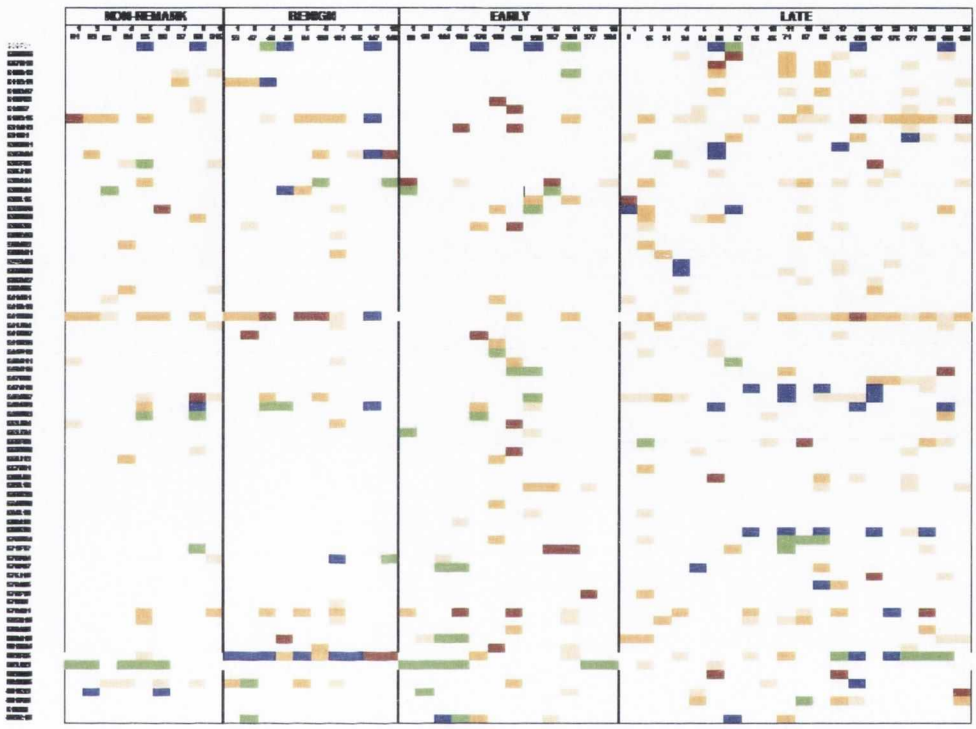

Figure 3.9: Comparison of positives identified using different array platforms

This figure is a comparative analysis of Figure 3.3 and Figure 3.8. The increasing intensities of orange squares reflect the increasing intensity associated with antigen binding of AAbs on the surface of the hEx1 array. The green squares reflect antigens that bound AAbs and ellicited a fluorescence that was greater than the average fluorescence plus two standard deviations on the surface of the hEx1 protein microarray. The overlap between these two experiments is identified as blue boxes.

antigens were selected as they were thought to be relatively straightforwardly adapted into an ELISA format. Two antigens were selected for ELISA analysis as they exhibited strong binding in the hEx1 array platform only, while one antigen was selected as it exhibited strong binding in the hEx1 protein microarray only. Figure 3.10 is a adapted from Figure 3.9 and outlines the AAb

The six antigens selected for further ELISA analysis were p53, FAM161A, complexin 1, myosin light chain 6B, DBB/CUL4 asasociated factor 6 and BACH2. As outlined previously (Sections 1.1.1, 1.7.1) p53 is a very well known cancer associated protein, as are the AAbs to the p53 protein. The identification of AAbs to p53 in this study is an important finding as this gives strength and credence to the method of antigen and AAb identification.

Many of the other antigens of interest identified in this study also show potential to be cancer or disease associated. The FAM161A protein has not been associated with cancer previously, however it is implicated in a retinitis pigmentosa subtype [238, 239]. High levels of this protein are expressed in highest levels in the retina and also in the testis. The FAM161A protein is a very novel protein and AAbs to this protein have not been characterised.

Complexin 1 is involved in the Soluble N-ethylmaleimide-sensitive factor attachment protein receptor (SNARE) complex in vesicle exocytosis, this protein is mainly expressed in the hippocampus and cerebellum, however it is also expressed in the pancreatic beta-cells where it is involved in insulin secretion [240]. The complexin 1 gene (CPLX1) is differentially expressed in an ovarian cancer cell line [241] and has been identified as loosely cancer associated in one study [242]. Our study is the first study in which AAbs to complexin 1 have been characterised.

Myosin light chain 6B (MYL6B) is the regulatory light chain of myosin that does not bind calcium. This protein has been implicated in different cancers [243, 244, 245],

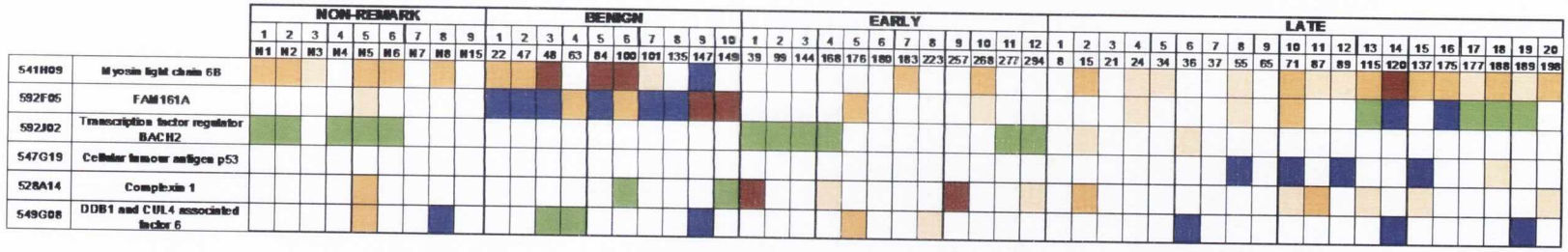

Figure 3.10: Six antigens selected for ELISA analysis

This image is a sub-image of Figure 3.9, six antigens were selected for further ELISA analysis. The six antigens were selected to investigate the different hEx1 array screening methodologies. Antigens 541H09 and 528A14 were selected due to strong intensity binding in the Imagenes hEx1 array screening, while antigen 592J02 was selected due to strong intensity binding in the in-house hEx1 protein microarray screening. The remaining three selected antigens were investigated as they exhibited strong AAb binding in both of these platforms, which may be most likely to be validated in the ELISA platform.

however this protein has not been implicated in ovarian cancer. In a recent study of lung cancer patients, higher expression of MYL6B was noted compared to controls, the same research group are also continuing with work to identify AAbs to MYL6B in the serum of lung cancer patients [246].

The DBB/CUL4 associated factor 6 (DCAF6) is a nuclear protein known to interact with the androgen receptor, this protein is highly expressed in skeletal muscle and in the testis [247, 248]. This protein has been implicated in oncogenic pathways in cancers such as prostate, [249], cervical [250] and has been identified in ovarian cancer patient tissue [248].

Transcriptional regulator BACH2 is a B-cell specific protein that is critical for class switch recombination to induce secretion of different antibody classes [251]. BACH2 has also been shown to act as a transcriptional repressor to induce cell death upon oxidative stress and to act as a negative regulator of cell proliferation [252]. The BACH2 gene has been to identified to be of interest in various malignancies [253, 254, 255], including ovarian [65, 256].

ELISA Optimisation

As optimization is an extremely important part of assay development, a commercial p53 protein which is a full length, wild-type recombinant protein that has been purified and refolded was used as a positive control. As the autoimmune response ellicted is polyclonal, the wild-type p53 protein acts as a good antigen for immunoreactive serum. The mutated hotspots of the p53 protein are near the N and C terminals [257, 258] studies have shown that patients that exhibit AAbs to p53, mainly generate AAbs to the non mutated regions . Hence, it is determined that the increased half-life of p53 gives rise to its immunogenicity [259, 260, 261]). For this reason, the wild-type protein was selected as a positive control, which was needed for a reference for the optimization

steps to ensure optimal binding of the AAbs in serum.

From reading the published literature on development of an ELISA to identify AAb profiles in patient serum, there is much variation in the parameters used, for instance antigen concentration and serum dilution vary massively. Some studies have used a very low antigen coating concentration per well, less than 0.005 nanograms of antigen [262], while other studies use a high concentrations of 250 nanograms of antigen per well [263].

ELISA optimization was performed to determine the optimum antigen coating concentration. The results of antigen coating optimisation are shown in Figure 3.11. From this image it is evident that there is a very good similarity between the two different p53 proteins. From this experiment, the antigen coating concentration was determined to be 50 nanograms per well, this results in a strongly positive signal but is not a maximal signal. Also, the hEx1 negative control protein does not exhibit binding of AAbs in serum. From this experiment it was determined that the hEx1 negative control protein was suitable for use as a negative control.

p53 Antigen ELISA

Cellular tumour antigen p53 (p53) is a tumour suppressor gene which regulates the cell cycle and plays an important role in DNA repair, as detailed in Section 1.1.1. This is one of the best characterised tumour suppressor proteins and also one of the best characterised proteins that elicit an immune response in cancer patients [142, 143, 202, 264, 265]. A number of studies have demonstrated that the half-life of mutated p53 (several hours) is markedly increased compared to wild-type (several minutes) which may result in its accumulation in the cell nucleus and the accumulation of protein rather than the mutations has been suggested as the immunogenic trigger that results in autoantibody generation [266]. Anti-p53 antibodies are found in cancer patients with

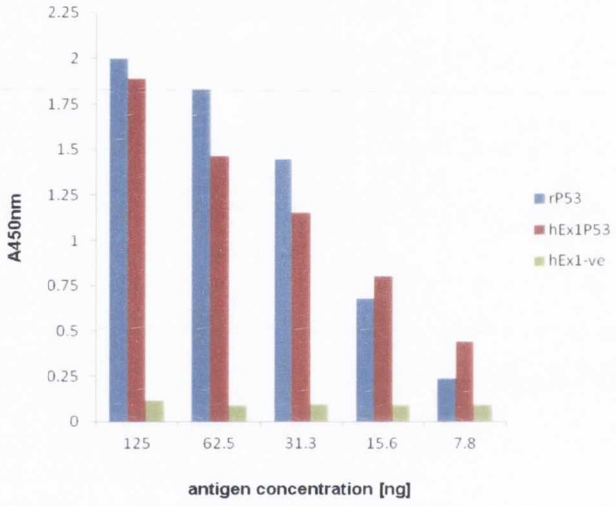

Figure 3.11: ELISA optimisation analysis

The antigen coating concentration is determined using the commercial p53 protein (indicated in blue) as a reference, the hEx1 p53 product (red) is identified as having a similar reactivity compared to the commercial protein. A negative protein, which is also a hEx1 expressed and purified protein is also included to identify any potential reactivity to *E-coli* proteins as a negative control.

a specificity of 96%, however, the sensitivity of anti-p53 antibodies for cancer is only 30% [143], the frequency and utility of AAbs to p53 have been outlined in Section 1.5.2. AAbs to p53 have also been determined and interrogated in ovarian cancer patients, details on some of the more relevant studies are discussed in Section 1.7.1.

As mentioned, p53 was selected for further analysis using the ELISA platform. AAbs to p53 were identified in 5/20 late stage ovarian cancer patients by hEx1 array screening and 4/20 late stage ovarian cancer patients in protein microarray screening. Hence, 4/20 late stage ovarian cancer patient sera were identified to have AAbs to p53 in both array platforms. The results of hEx1 p53 ELISA analysis are shown in Figure 3.12, from this image it is clear that the same 4 late stage serum are reactive to the p53 protein. All of the p53 immunoreactive serum are in the late stage serum cohort which are all high grade serous papillary adenocarcinomas. This finding confirms previously published results where AAbs to p53 are associated with type II ovarian tumours [79, 208], our findings indicate that AAbs to p53 are found in 20% of late stage ovarian carcinoma patients using all three methodologies. From Figure 3.10 we can also see that AAbs to p53 are identified by both array formats (indicated with blue boxes), therefore we can confirm that the AAb response induced to p53 is robust and has been validated in three different platforms to be present in the same serum samples. The results of this p53 ELISA also show a clear AAb response to p53, in this platform there is a clear qualitive difference between the serum that are definitively positive for AAbs to p53 and those that are definitively negative.

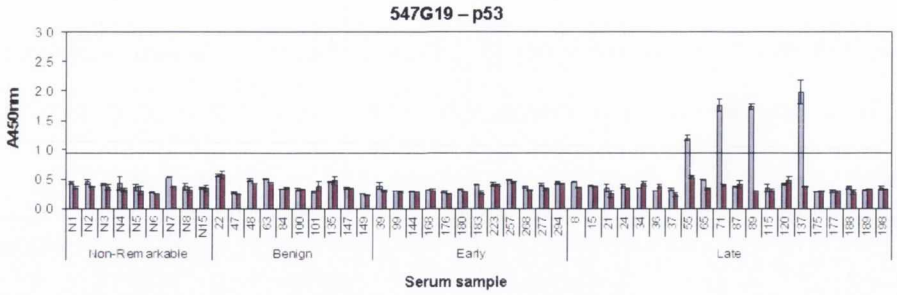

Figure 3.12: hEx1 p53 ELISA analysis

In this figure the hEx1 p53 absorbance values are indicated as blue columns, another hEx1 protein expressed, purified and normalised in the same manner, identified as tenascin protein was included as a negative control. The absorbance values for this negative control protein are indicated as purple columns. The error bars in this figure are representative of the standard deviation attained from duplicate wells in this experiment.

Additional Antigen ELISA

The ELISA protocol was optimised primarily using the hEx1 p53 protein and a commerial recombinant p53 protein (Section 3.4.3.2), however, other hEx1 antigens were also interrogated in the ELISA optimisation stage and the conditions were confirmed to be suitable for these antigens also. Following the confirmation and validation of the p53 ELISAs that identified AAbs to p53 in late stage ovarian cancer patients ELISA analysis was performed on the remaining five antigens selected for further investigation. As with the p53 protein, 2 of these selected 5 antigens were shown to have a good overlap between the two different array formats and were hence expected to be robust AAb markers.

FAM161A protein (592F05) was identified from Figure 3.10 to show a good overlap between the two array formats, although this was thought to identify a robust profile this results was not replicated in the ELISA platform. For this antigen 8 of 51 sera were identified to have AAbs using both hEx1 array screening platforms. However from the results of ELISA analysis the results are unclear. The ELISA results do not identify

any definitive positive results indicating AAbs in serum. Although serum samples 63, 34 and 87 are just above the cut-off threshold, the high absorbance readings of the corresponding negative control protein indicates that these are not true positives. There seems to be only one positive AAb response identified in serum sample 120. This value is above the threshold and the corresponding negative control has a lower value. AAbs in this serum sample were also identified in the hEx1 array and protein microarray platform.

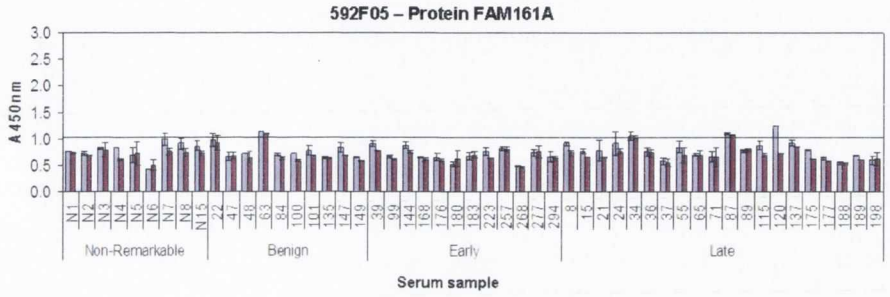

Figure 3.13: hEx1 FAM161A ELISA analysis

In this figure the hEx1 FAM161A absorbance values are indicated as blue columns. The absorbance values for a negative control protein (details outlined in 3.12) are indicated as purple columns. The error bars in this figure are representative of the standard deviation attained from duplicate wells in this experiment.

AAbs to DDB1 and CUL4 associated factor 6 (549G08) were identified by both array formats also, for this antigen 5 of the 51 sera were identified to have AAbs in both array platforms. From the results of ELISA analysis (Figure 3.14) there are two serum that are identified as immunoreactive to this antigen (Late 36, 120). These two immunoreactive serum were identified as such by both of the array platforms. Two additional serum also appear to have borderline immunoreactivity (Non-remarkable serum N5 and late serum 189). Both of these serum are not above the predetermined ELISA cut-off, however sample AAbs to this antigen were identified in sample N5 by hEx1 array screening only, while AAbs were identified in sample 189 by both array

screening platforms.

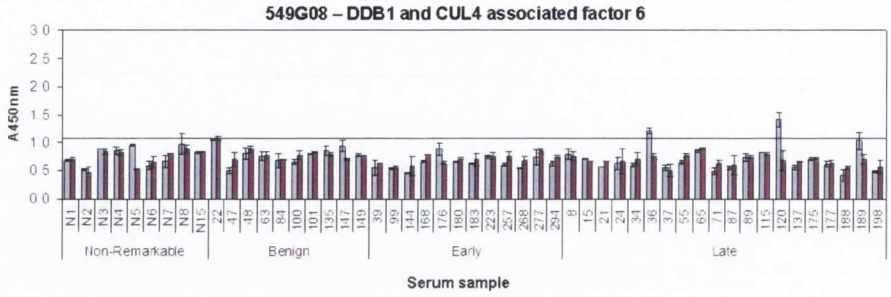

Figure 3.14: hEx1 DDB1 and CUL4 associated factor 6 ELISA analysis

In this figure the hEx1 DDB1 and CUL4 associated factor 6 absorbance values are indicated as blue columns. The absorbance values for a negative control protein (details outlined in 3.12) are indicated as purple columns. The error bars in this figure are representative of the standard deviation attained from duplicate wells in this experiment.

AAbs to the complexin 1 (528A14) protein was identified in patient serum by the hEx1 array primarily (11 AAb positive serum of varying intensity, in 51 screened samples), however, additional serum samples exhibited reactivity using the hEx1 protein microarray platform (2 AAb positive serum of 51). The results of ELISA analysis, shown in Figure 3.15, indicate that 4 of the 51 serum are positive for AAbs to complexin. Of the 4 immunoreactive serum identifiedby ELISA, one serum (non-remarkable - N3) was not previously identified as immunoreactive by either of the array screens. From ELISA, two sera (Early 39 and 257) of the four immunoreactive sera were identified to be immunoreactive on the Imagenes hEx1 arrays, while the remaining one serum of the four ELISA identified immunoreactive sera was identified to be immunoreactive on the in-house hEx1 protein microarrays. From reviewing Figure 3.15, two additional serum also appear to have borderline immunoreactivity, (Non-remarkable N2 and Late 15). No previous screens identified AAbs to this antigen in serum N2, while AAbs were identified in late stage serum 15 using hEx1 array screening.

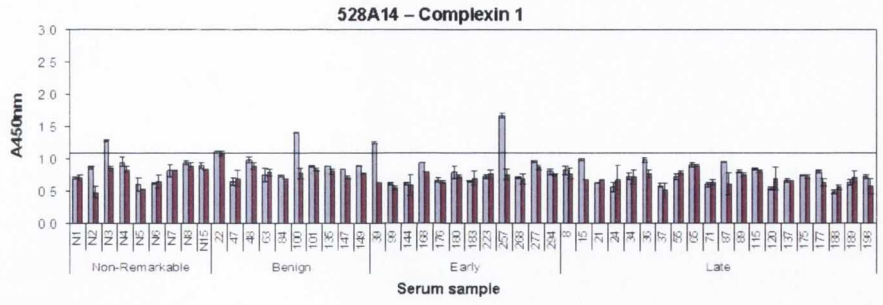

Figure 3.15: hEx1 Complexin 1 ELISA analysis

In this figure the hEx1 complexin 1 absorbance values are indicated as blue columns. The absorbance values for a negative control protein (details outlined in 3.12) are indicated as purple columns. The error bars in this figure are representative of the standard deviation attained from duplicate wells in this experiment.

AAbs to the myosin light chain 6B (541H09) protein were identified in patient serum by the hEx1 array primarily, (30 AAb positive serum in 51 screened serum samples). However, only one serum sample was identifed as immunoreative to this antigen using the in-house hEx1 protein microarray. This single serum sample was identified by both array platforms. As with previous ELISAs, the ELISA results for this antigen are not clear as there are no definitive positives. Although serum samples 22, 63, 34 and 87 are just above the cut-off threshold, the high absorbance readings of the corresponding negative control protein indicates that these are not true positives. There seems to be only one positive AAb response identified in serum sample 147 (Figure 3.16). This value is above the threshold and the corresponding negative control has a lower value. AAbs to this antigen in this serum sample were identified in the hEx1 array and protein microarray platform. No serum samples appear to have borderline immunoreactivity to this antigen as the absorbance values for the negative control and the test antigen are very similar.

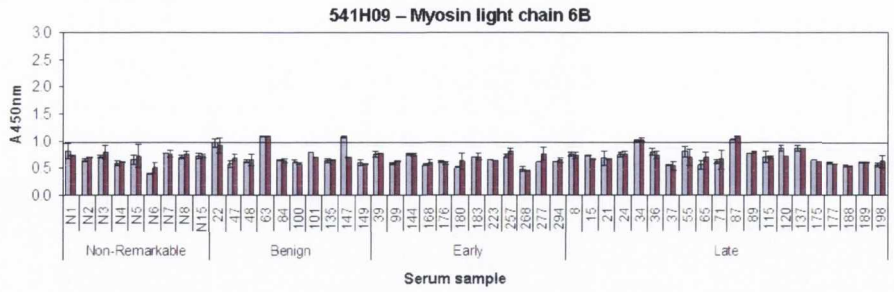

Figure 3.16: hEx1 Myosin light chain 6B ELISA analysis

In this figure the hEx1 myosin light chain 6B protein absorbance values are indicated as blue columns. The absorbance values for a negative control protein (details outlined in 3.12) are indicated as purple columns. The error bars in this figure are representative of the standard deviation attained from duplicate wells in this experiment.

AAbs to transcription regulator BACH2 (592J02) were identified predominantly using the in-house hEx1 protein microarray. However, the results of the hEx1 array screening could not be replicated in the ELISA format for this antigen. As with previous ELISAs, the results for this antigen are not clear as there are no definitive positives (Figure 3.17). Although serum samples 22, 63, 34 and 87 are just above the cut-off threshold, the high absorbance readings of the corresponding negative control protein indicates that these are not true positives. This ELISA analysis did not detect AAbs to this antigen in any of the serum samples screened.

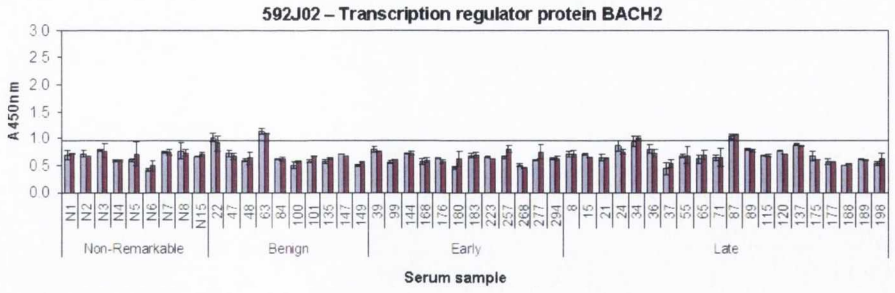

Figure 3.17: hEx1 transcription regulator BACH2 ELISA analysis

In this figure the hEx1 transcription regulator protein BACH2 absorbance values are indicated as blue columns. The absorbance values for a negative control protein (details outlined in 3.12) are indicated as purple columns. The error bars in this figure are representative of the standard deviation attained from duplicate wells in this experiment.

From the ELISA results it is clear that AAbs against p53 perform far better than any of the other AAbs to the antigens tested. The p53 ELISA results clearly indicate definite positive serum with AAbs to p53 and the remaining serum are definitively negative. From the results of the p53 ELISA outlined in Section 3.4.3.2 it is clear that there is a strong AAb response in 20% of late stage ovarian cancer patients. The p53 AAb response was the most consistent AAb response and was identified in 4 of 20 late stage ovarian cancer patient serum in all three platforms tested.

Outlined is Section 3.4.3.2 are the ELISA results of the other 5 antigens of interest. The complexin 1 ELISA seems to identify definitive positive and negative results, from these results AAbs to this antigen are present in a non-remarkable patient, a benign patient and two early stage ovarian cancer patients. This seems to discredit AAbs to this antigens being interrogated further as they are present in the same number of non-malignant serum as malignant serum. The ELISA results for FAM161A protein indicate that AAbs to this antigen are present in one late stage ovarian cancer patient serum. As this AAb response is limited to only one ovarian cancer patient serum of the 32 ovarian cancer patient serum interogated by ELISA it is very unlikely that AAbs

are ovarian cancer associated. The ELISA results for determination of AAbs to DDB1 and CUL4 associated factor 6 are difficult to discern. i.e. it is difficult to identify which serum are definitively negative and which are definitively positive. However, there are two positives identified using the ELISA cut-off (late stage serum 36 and 120) and one borderline positive (late stage serum 189). This may show potential as AAbs to this antigen are only identified in the late stage ovarian cancer samples, however from reviewing Figure 3.14, there seems to be an AAb response in a non-remarkable serum (N5). Although this response was not above the cut-off value, the absorbance difference between the antigen coated wells and the negative protein coated wells indicate the potential immunoreactivity of this serum to DDB1 and CUL4 associated factor 6. AAbs to this antigen may be of interest however the difficulty in distinguishing positive from negative sera will need to be addressed first. The ELISA results for myosin light chain 6B and transcription regulator protein BACH2 do not indicate an AAb response in any of the ovarian cancer patient serum sampled by ELISA. These antigens do not warrant further interrogation.

The ELISA results shown in Figures 3.12-3.17, are not easy to define and the 'cut-off', indicated by a horizontal line is not an ideal reference for some of the assayed antigens. The cut-off value was equal to the mean absorbance values (absorbance values for all serum for tested antigen and negative protein) plus two standard deviations. Previous, to the employment of this method of determining the cut-off value a two sample t-test was used to compare the absorbance values of the tested antigen to the negative protein for a single serum sample. However, due to the very small standard deviations associated with this method, this statistical analysis identified the majority of comparisons as positive results, this did not match previously published results and was not used for determination of reactivity in serum. The method used (mean +2 standard deviations) is the general method of determining positive ELISA results and is relatively

standard. The limitations of cut-off determination may be due to different factors such as the concentration of AAbs in the various patient serum, which may range from 5.5mg/ml to 22 mg/ml of IgG. Initially the total IgG concentration of patient serum was interrogated, however this was very problematic due to the large dilution factors used in performing the assay, leading to large variations between results. At this stage of validation the main focus is on qualitative analysis, hence it was determined that all serum samples should be used at a standard dilution. This is also favourable for a diagnostic assay as it results in less expense and quicker assay processing.

Notably serum samples 22, 63, 34 and 87 were frequently above the cut-off threshold and although these serum had high absorbance readings for nearly all antigens, they also had high absorbance readings for the corresponding negative control protein. This indicates that these samples are reactive serum and may have increased reactivity to bacterial proteins which are present in the hEx1 protein products. The differences in serum reactivity and binding has been noticed throughout this work with different serum samples exhibiting different background binding. This is the reason a hEx1 protein which was expressed and purified in the same way as the test antigens was included in the protein microarray and in ELISA.

3.5 Discussion

The ultimate aim of autoantibody serum screening is to identify biomarkers of disease. To achieve this goal, AAb profiles identified by protein array screening need to be relatively easily adapted into an ELISA or other widely used clinical assay format. The results of the above serum screening on hEx1 arrays and the secondary investigation by hEx1 protein microarray and ELISA indicate that AAb responses to antigens are identified with different frequencies in different platforms. The two array platforms used in this research are very different. The hEx1 arrays are commercially made arrays subject to rigorous quality control testing and comprised of over-expression bacterial cell lysates on PVDF membranes. The in-house hEx1 protein microarrays are spotted purified and normalised human proteins on a nitrocellulose pad and are not subject to rigourous commercial quality control production. Although both of these array platforms comprise of hEx1 proteins, there are many differences between the arrays which may result in differential AAb binding and rectivity profiles. However, there was a small number of overlapping AAbs identified in serum by both array formats. From investigating the overlaps between platforms it was identified that AAb responses to antigens in both of the hEx1 array platforms are more likely to be robust AAb responses and have increased likelyhood to be validated in an ELISA format. This was the case for p53 AAbs which were identified in the same patients by both array platforms.

From the ELISA results it is clear that AAbs against p53 perform far better than any of the other 5 antigen/AAb responses tested. Autoantibodies to the p53 antigen were identified in ovarian cancer patients with a frequency similar to published data [143, 203, 204]. However the results of the remaining antigens seems to discredit AAbs to these antigens being interrogated further, as they are present in equal numbers of non-malignant serum as malignant serum. This finding highlights the importance of a high-throughput secondary screening methodology to identify the most likely candidates

for further investigation.

3.6 Conclusion

As outlined in the aims of this chapter, the hEx1 protein arrays were used to identify autoantibodies to antigens in non-remarkable, benign and ovarian cancer patient serum. Using secondary methodologies, protein microarray and ELISA, AAbs to p53 were identified in 20% of late stage ovarian cancer patient serum. This AAb response was the only consistent response and was identified in all three platforms used for AAb assessment. Five other AAb responses were also identified to be of potential interest, however they were not consistent in all platforms. AAbs to these antigens did not validate as ovarian cancer associated by ELISA. Although, autoantibodies were identified using this methodology, further refinement is needed to identify antigens that have a more robust profile in the discovery platform compared to the end-stage platform, ELISA.

Chapter 4

Identification of Robust Autoantibody Responses and Validation in Additional Patient Serum.

4.1 Introduction

This research aims to uncover a robust autoantibody profile associated with ovarian cancer that can be consistently adapted into other platforms. From the previous chapter it is clear that there is variation between the results of the hEx1 array screening, hEx1 microarray screening and ELISA analysis. The differences between the platforms, for the same serum samples needed to be interrogated further to improve identification of AAb responses that will validate in an ELISA format.

In an attempt to identify a cohort of highly reproducible autoantibodies an amended protocol for hEx1 array screening was developed, this protocol has extremely rigourous blocking and washing steps. The increased rigour of this protocol was developed to decrease the number of false positives identified in this platform, meaning that any positives on the array would have an increased likelyhood of being robust in other platforms. This amended array screening using more rigourous screening methodology was performed with pooled serum.

Serum pooling has been used in many biomarker discovery platforms and AAb profiling studies have also been performed using pooled and non-pooled serum. Some studies have indicated that screening of pooled serum needs to be undertaken with caution [174, 173]. This is because high titres of antibodies, to a particular antigen in one patient serum may bias the results of the entire pooled batch of sera. Low titres of antibodies to a particular antigen in the majority of patient sera may be masked by high titres of antibodies in a single patient serum. However, other studies have indicated that screening of pooled serum has numerous benefits and is a viable method of serum screening [267, 268]. Biomarker discovery is a very costly part of biomarker identification and serum pooling can serve to reduce costs while improving statistical power (by screening larger patient numbers), if performed correctly. In this study, pooled serum screening was performed with a view to enrich and strengthen the results of the individual serum screening to identify the most robust antigens for further validation.

4.2 Aims

- To identify robust autoantibody profiles associated with ovarian cancer.
- To validate these profiles using secondary experimental platforms in an additional cohort of ovarian cancer patient serum.

4.3 Materials and Methods

4.3.1 Pooled Serum Screening on hEx1 Arrays

4.3.1.1 Serum Selection

Three serum cohorts were used for pooled screening, the sera are outlined in Table 4.1. A subset of 4 early stage ovarian cancer sera were used from the larger cohort of 13 early stage ovarian cancer patients. Only four sera were selected here as these early stage ovarian cancer serum were all of the same histology, this was performed to limit variation that may arise as a results of differential AAbs responses due to various malignant ovarian histologies. An increased number of non-remarkable controls were used for pooled serum screening. The 20 late stage ovarian cancer patient sera are the same sera that have been used in previous hEx1 array screens.

Table 4.1: hEx1 screened pooled serum

Number of Samples	Stage	Histology	Mean Age
4	Early OC (I-II)	Serous Papillary Adenocarcinoma	65
20	Late OC (III-IV)	Serous Papillary Adenocarcinoma	63
15	Non-Remarkable	-	64

4.3.1.2 hEx1 Array Screening Using Pooled Serum

As for previous hEx1 array screening detailed in Section 2.3.1, arrays were activated, rinsed in dH_2O and bacterial colonies were removed. Arrays were washed in TBS-T-T and TBS-T as previous. The arrays were blocked for 2 hours in 5% w/v skimmed milk powder in TBS-T (150mM NaCl, 10 mM Tris-HCL pH 7.5, 0.05% v/v Tween 20). Serum was thawed on ice and 20μl of each serum was added to a 50ml tube. The sera was diluted in 5% milk TBS-T to a final volume of 20mls. This ensured that all sera was diluted to 1:1000 dilution factor. The arrays were then incubated overnight

as outlined in Section 2.3.1.The arrays were washed 3 times for 30 minutes in TBS-T. Monoclonal mouse anti-human IgG (Sigma Aldrich, UK, Cat no: I6260) was diluted 1:5000 in 5% w/v milk TBS-T, and the arrays were incubated with the antibody for 1 hour at room temperature on a slow rocker. The arrays were then washed 3 times, each for 30 minutes in TBS-T. Polyclonal goat anti-mouse alkaline-phosphatase conjugate IgG (Sigma Aldrich, UK, Cat no: A1418) was also diluted 1:5000 in 5% w/v milk TBS-T. Arrays were incubated with the antibody for 1 hour at room temperature. The arrays were then washed twice in TBS-T for 30 minutes and once in TBS for 20 minutes. The arrays were equilibrated in attophos buffer and substrate, then imaged as outlined in Section 2.3.1 and scored as outlined in Section 2.3.2.

4.3.2 Selection and Expression of Antigens of Interest

A simple analysis was performed to identify antigenic bacterial clones that were immunoreactive in the ovarian cancer cohort only. Expression clones that were identified to be immunogenic in ovarian cancer sera and not in the non-remarkable sera, as determined by the individual serum screening performed in Section 3.3.1, were collated. Expression clones that were identified to be immunogenic in the pooled ovarian cancer sera and not in the non-remarkable pooled sera (Outlined in Section 4.3.1), were also collated. The expression products of the collated lists of clones were determined (as outlined in Section 2.4.2) and antigens that were present in both lists were selected for further investigation.

The bacterial clones which express these antigens were identified and the corresponding bacterial clones were picked and induced for protein expression as outlined in Section 2.4.3. Proteins were purified, analysed by PAGE analysis and quantified as in Sections 2.4.4, 2.4.7 and 2.4.5.

4.3.3 Secondary Validation

4.3.3.1 Western Immunoblotting

Commercial recombinant p53 Western Blot Analysis

SDS-gels were loaded with 200ng/well or 50ng/well of commercial recombinant p53 protein and electrophoresed. The proteins on the gel were transferred to a PVDF membrane at 100 volts for 1 hour. The blot was rinsed in TBS-T (150mM NaCl, 10mM Tris-HCl pH 7.5, 0.05% v/v Tween), then blocked in 5% milk-TBS-T for 1 hour at room temperature. The blots were then incubated in human serum. Serum was diluted (1:870 dilution for 200ng/lane blots or 1:100 dilution for 50ng/lane blots) in 10ml 2% milk-TBS-T blots were incubated overnight on slow rock at RT. The blots were washed 3 times for 10min in TBS-T and then incubated in mouse anti-human antibody at a 1:5000 dilution in 10ml 2% milk TBS-T for 1 hour. The blots were washed 2 times for 10 min in TBS-T and once for 10 min in TBS.

To compare effect of different imaging approaches a standard horseradish peroxidise detection with chemiluminescence and X-ray film was also used for some Western blots to compare to results obtained with alkaline phosphatase/attophos detection. For this a Mouse anti-human Fc spec IgG HRP-conjugate antibody was used as a detection antibody after the serum incubation step (Figure B.2).

hEx1 Protein Western Blot Analysis

These blots were as per previous blot with the following exceptions: SDS-gels were loaded with 500ng/well of protein and electrophoresed. Serum was diluted 1:100 dilution for the hEx1 proteins identified to be immunogenic in . Blots were incubated for 2 hours in serum. The blot was washed 3 times for 10 min in TBS-T and then incubated in goat anti-human Fc AP conjugate antibody (Sigma Aldrich, UK, Cat no: A1418) at a 1:5000 dilution in 10ml 2% milk TBS-T for 1 hour. Blot was washed 2 times for 10 min

in TBS-T and once for 10 min in TBS. The blot was then treated with attophos buffer and substrate and imaged as in Section 2.5.2.

4.3.3.2 ELISA Analysis

ELISA coating concentrations of 50ng/well and 100ng/well were compared using the commercial p53 protein. For coating of hEx1 antigens 50ng/well concentrations were used. ELISA analysis was performed as per 2.5.3.

4.3.3.3 Extended Serum Cohort

The additional serum cohorts selected for validation was a cohort of late stage serous papillary ovarian cancer patient sera, and a cohort of benign ovarian disease (of various histology) patient sera, as with all other sera, these sera were obtained from the Discovary Bioresource. The details of the sera are outlined in Table 4.2.

Table 4.2: Additional seum cohort

Number of Samples	Stage	Histology	Mean Age
28	Benign	Mixed Histology	48
14	Late OC (III-IV)	Serous Papillary Adenocarcinoma	62

4.4 Results

4.4.1 Results and Overlap of hEx1 Array Serum Screening

Expression products that were identified to be immunogenic in the ovarian cancer cohort sera and not in the non-remarkable sera, as determined by the individual serum screening are listed in Table B.1. Expression products that were identified to be immunogenic in the pooled ovarian cancer sera and not in the non-remarkable pooled sera are listed in Table B.2. Three antigens were identified to be present in both lists. These antigens were p53, adducin alpha and endosulfine alpha (Outlined in Table 4.3). These antigens were postulated to be highly immunoreactive, with a high AAb titre in late stage ovarian cancer serum and hence had good promise as robust AAb indicators and were selected for further interrogation using secondary methods.

Table 4.3: Overlap from hEx1 screening methods

Three antigens were identified in both hEx1 screening methods. These three antigens are of particular importance as they represent strong reactivity in patient serum and are also specific to the cancer cohort.

Cellular tumour antigen p53
Adducin alpha
Endosulfine alpha

Following identification of the three antigens associated with the ovarian cancer cohort, an analysis was performed to determine the proportion of patients with AAbs to the antigens in each cohort as identified by hEx1 array screening. The results of this analysis is outlined in Table 4.4. hEx1 array screening identified AAbs to p53 in 25% of late stage ovarian cancer patients, AAbs to p53 were not identified in early ovarian cancer patients or the non-remarkable controls. hEx1 array screening also identified AAbs to adducin alpha in 15% of late stage ovarian cancer patients, 23% of early stage ovarian cancer patients. AAbs to adducin alpha were not identified in the non-remarkable control sera. hEx1 array screening also identified AAbs to endosulfine alpha in 20% of late stage ovarian cancer patients and AAbs to endosulfine alpha were not

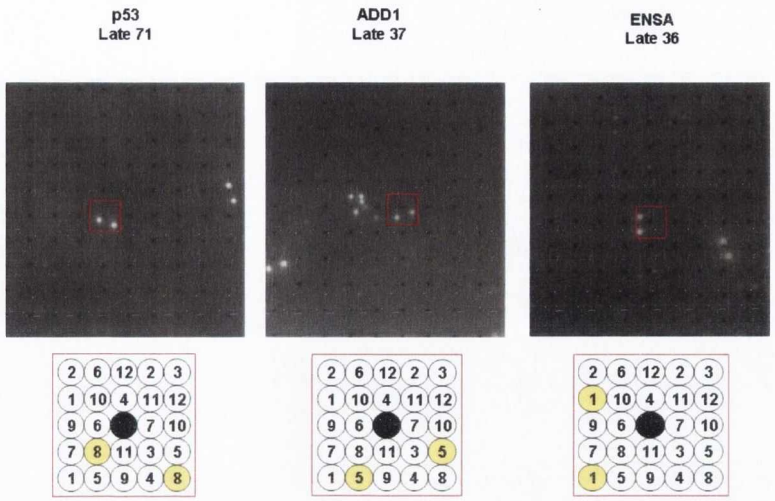

Figure 4.1: Serum recogniton of antigens of interest

Shown here are immunoreactive late stage ovarian cancer serum 71, 37 and 35 and the positive signals resulting from AAb binding to the hEx1 expression clones for p53, adducin alpha and endosulfine alpha respectively. The antigen spotting panel is outlined below the hEx1 array images. This layout is used for hEx1 array scoring of postive antigen signals.

identified in early ovarian cancer patients or the non-remarkable control sera.

4.4.2 Assessment of Overlap Antigens

After growing of the 3 expression clones and the negative hEx1 control protein, the protein products were purified and analysed by PAGE analysis. The results of PAGE analysis are shown in Figure 4.2. From PAGE the purity of the proteins could be

Table 4.4: Frequency of Autoantibodies Identified by hEx1 Array Screening

This table outlines the numbers of subjects that were identified as having AAbs to the relevant antigens in each cohort as determined by hEx1 array screening. Notably, from hEx1 array screening none of these antigens were identifed as reactive to AAbs in non-remarkable subjects.

	Late OC	Early OC	Non Remarkable
p53	5/20 (25%)	0/13 (0%)	0/15 (0%)
Adducin alpha	3/20 (15%)	3/13 (23%)	0/15 (0%)
Endosulfine alpha	4/20 (20%)	0/13 (0%)	0/15 (0%)

Table 4.5: Protein sizing by sequence for antigens and negative protein

	ENSA	ADD1	NEG	TP53
sizing by sequence	19 kDa	39 kDa	39 kDa	28 kDa

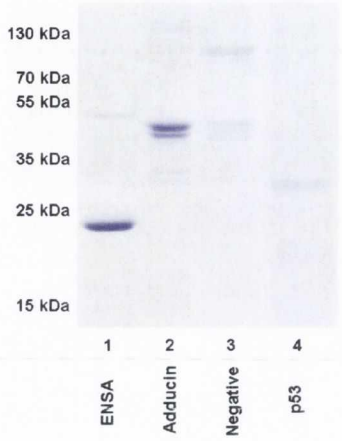

Figure 4.2: PAGE analysis of three antigens and negative protein

assessed, from the PAGE images it is clear that protein purification was quite successful. The antigens were all assessed by sequence and by PAGE analysis to determine protein molecular weight, as outlined in Table and Figure 4.2 the sizings determine by the two methods agreed well.

4.4.2.1 Cellular tumour antigen p53 (TP53)

The identification of AAbs to p53 in this analysis was a very positive and reassuring finding. This confirmed that the screening methodologies and analysis were sufficient to determine AAb profiles that have been previously identified to be associated with ovarian cancer. This selection method may also have the capacity to identify AAb profiles that have not been previously identified to be ovarian cancer associated. These novel AAb profiles are of particular interest as they hold the most potential to be used in the development of a diagnostic assay. AAbs to p53 have been found in cancer patients with a specificity of 96% and a sensitivity of 30% [143], however additional AAb profiles

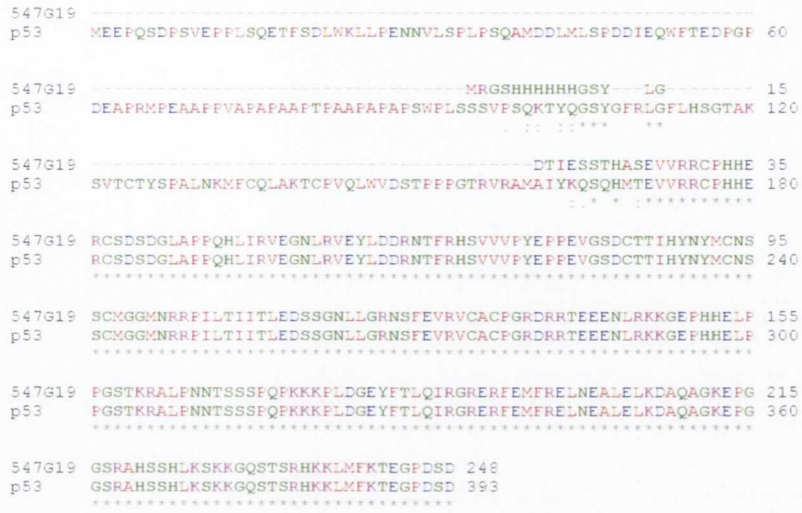

Figure 4.3: p53 sequence alignment

Sequence alignment of the hEx1 p53 expression clone (547G19) and the wild type full length p53 protein (p53). The hEx1 p53 protein has approximately 60% coverage of the full length p53 protein. The hEx1 expression library is C-terminal biased, this is clearly diplayed here where the hEx1 sequence matches to the C-terminal of the full length p53 protein.

are needed to increase the sensitivity value.

ELISA analysis of the p53 protein had been previously performed and is outlined in Section 3.4.3.2, however further interrogation and analysis of patient reactivity to the p53 protein was undertaken to validate previous results and also to ensure the correctness of the methodology used. To interrogate the hEx1 p53 expression clone, the protein FASTA sequence attained from analysis of the open reading frame was compared to the FASTA sequence of the full length wild type p53 protein. The sequence alignment was performed using the ClustalW2 tool, the alignment results are shown in Figure 4.3. This alignment shows that the hEx1 protein overlaps with 60% of the full length, wild type p53 protein, this analysis also confirms the C-terminus bias of the hEx1 library.

4.4.2.2 Adducin alpha (ADD1)

Adducin alpha (adducin 1) is an ubiquitously expressed membrane-cytoskeleton-associated protein that is localised at the spectrin-actin junction and is known to play a crucial role in membrane skeletal assembley in erythrocytes [269, 270], and also known to regulate platelet morphology during activation [271, 272]. It is known to bind to calmodulin and is an *in vivo* substrate for protein kinase C and Rho-associated kinase [273]. Previous publications have linked adducin and malignancy [274], in particular adducin in known to localise to cell-cell contacts [275, 276], and membrane protrusions such as lamellipodia [277, 278]. Recently adducin alpha has also been implicated in mitosis [279]. These processes, such as cytoskeletal reorganisation, cell-cell contact and cell motility all have important and very direct links to malignancy, hence adducin and autoantibodies may have important links to malignancy.

Autoantibodies to adducin have not been previously characterised in ovarian cancer. However recently autoantibodies to adducin have been identified in prostate cancer patients [146, 280, 281]. In these publications, AAbs to adducin were considered an important immune reponse and were featured in the top ranked autoantigens [146], and were identified in an antigen subset with the highest likelyhood ratio for differentiating prostate cancer patients versus controls [281]. This is an interesting finding, these cancers can be linked, as increased risk of prostate and ovarian cancer (among others), has been linked to BRCA1 and BRCA2 mutations [67, 68].

As with the hEx1 p53 expression clone, the protein FASTA sequence attained for the Adducin alpha expression clone, was compared to the FASTA sequence of the full length adducin alpha protein. The sequence alignment was performed as previous and results are outlined in Figure 4.4. This analysis shows a relatively fragmented overlap of the full length adducin alpha protein, with an overlap of 34%. Again, the overlap between these two sequences is biased towards the C-terminus, as is evident with the

p53 overlap.

4.4.2.3 Endosulfine alpha (ENSA)

Endosulfine alpha is a protein phosphatase inhibitor that is encoded by the ENSA gene. Endosulfine alpha specifically inhibits protein phosphatase 2A (PP2A) during mitosis. When phosphorylated at Ser-67 during mitosis, it specifically interacts with PPP2R2D (PR55-delta) and inhibits its activity, leading to inactivation of PP2A, this is essential to keep cyclin-B1-CDK1 activity high during M phase [282]. In mammals endosulfine alpha also acts as a stimulator of insulin secretion by interacting with sulfonylurea receptor (ABCC8), thereby preventing sulfonylurea from binding to its receptor and reducing K(ATP) channel currents [283]. However recently the function and roles of endosulfine alpha have been linked to oocyte maturation in *Drosophila* [284], and also to cognitive function due to blocking of ATP-sensitive potassium [285].

Endosulfine alpha is a novel molecule and AAbs to endosulfine alpha have been identified before in a previous publication based on the same hEx1 array platform [175]. However AAbs to endosulfine alpha have not been identified in ovarian cancer patients previously. The protein FASTA sequence attained from analysis of the open reading frame of the endosulfine alpha expression clone was compared to the FASTA sequence of the full length endosulfine alpha protein. The results of sequence alignment are outlined in Figure 4.5. The hEx1 endosulfine alpha sequence overlaps 100% with the wild-type, full length protein sequence. However, from this analysis it is clear that there is an extra section of translated UTR section included in the hEx1 expression product.

Figure 4.4: Adducin alpha sequence alignment

Sequence alignment of the hEx1 adducin alpha expression clone (602C16) and the wild type full length adducin alpha protein (AdducinAlpha). Like the p53 sequence alignments, this alignment is also more C-terminal biased. However, this sequence is relatively fragmented with inclusions and deletions. The hEx1 adducin alpha FASTA sequence was compared to three different isoforms of adducin alpha, isoform 1 (shown here) shows the best alignment of 34%.

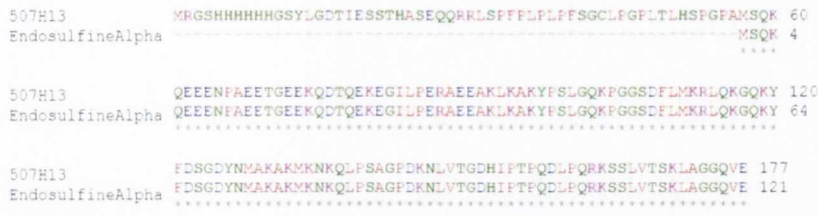

Figure 4.5: Endosulfine alpha sequence alignment

Sequence alignment of the hEx1 endosulfine alpha expression clone (507H13) and the full length endosulfine alpha protein (EndosulfineAlpha). From this alignment it is clear that the hEx1 expression product contains the sequence of the full endosulfine alpha sequence. The histidine tag and a short section of the 5' UTR are also included in the hEx1 expression product.

4.4.3 Secondary Validation by Western Blot and ELISA

4.4.3.1 Characterisation of Anti - p53 Autoantibodies

A comparative analysis of ELISA and Western results was performed to interrogate the reproducibility and performance of the different platforms. In the previous chapter ELISA analysis had been optimised at 50 ng/well concentration, however Western immunoblotting had been optimised at 200ng/lane for commercial p53 and 500ng/lane for hEx1 proteins. For this analysis the serum samples that were identified as reactive to the p53 protein were interrogated by ELISA and Western immunoblot at comparable concentrations (50ng total protein). This was performed to confirm comparable results in both platforms using different antigen concentrations. From the results of this analysis, it is clear that even at comparable concentrations, that Western blot appears to have improved sensitivity compared to ELISA, shown in Figure 4.6. Traditionally ELISA is thought to be a more sensitive detection technique, however our research shows that the Western blot technique exhibits improved antigen recognition by AAbs. Once the relative platform methodologies were optimized, late, early and non-remarkable sera were interrogated using ELISA and Western immunoblotting, the results of these different methods varied greatly for each of the antigens and are summarised in Table 4.6.

From reviewing the results table, p53 AAbs were detected in 4/20 (20%) of the

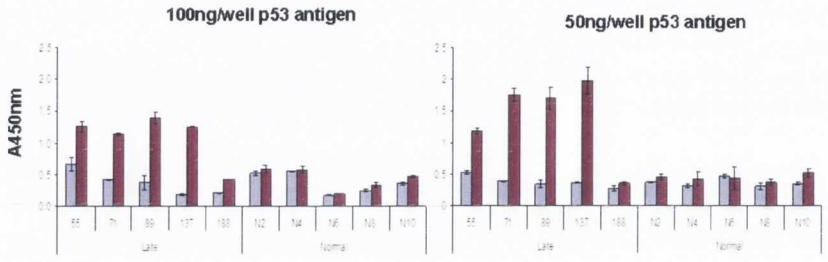

(a) ELISA antigen coating comparison

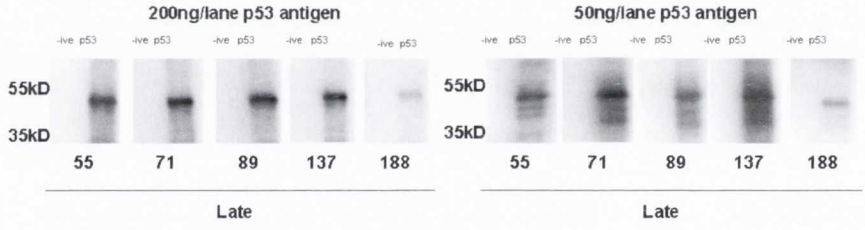

(b) Western blotting antigen concentration comparison

Figure 4.6: Comparative commercial p53 antigen concentrations

This figure shows the results of different methodologies to identify AAbs to the p53 antigen. Subfigure A shows the results of ELISAs using different antigen coating concentrations, notably the lower coating concentration provides a better signal to noise ratio. Subfigure B shows the results of Western immunoblotting using different amounts of antigen. The results of western immunoblotting show little difference between the different antigen amounts. However, there seems to be a increased lower molecular weight banding in the 50ng/lane immunoblots, this is most likely due to degradation during antigen storage.

late stage ovarian cancer sera by ELISA. The ELISA positive sera matched 4 of 5 sera identified as positive by hEx1 array screening. Western immunoblots identified p53 AAb immunoreactivity in 5/20 (25%) of late stage patient sera (Figure 4.7a). The sera positive for p53 immunoreactivity by Western blot matched exactly the sera positive for p53 immunoreactivity by hEx1 array screening. AAbs to p53 were also identified in 2/20 (10%) of an extended early stage ovarian cancer serum cohort by Western immunoblot only. Neither the hEx1 arrays nor the ELISA analysis identified a p53 AAb response in an early stage serum. AAbs to p53 were not identified in any of the non-remarkable patient sera in any of the methodologies used.

AAbs to p53 have long been identifed as having very high specificity for cancer patients at 96%, [134, 143], and although AAbs to p53 are not used for ovarian cancer detection, the high specificity of AAbs to p53 for cancer patients has the potential to be exploited in a larger panel of AAbs to diagnose ovarian cancer. In this study, it was confirmed that anti-p53 autoantibodies are not present in the non-remarkable patient cohort and that AAbs to p53 are present in 25% of late stage ovarian cancer patients. This is a reassuring finding and matches very well with previously published results which state that 25-30% of ovarian carcinoma patients have circulating AAbs to the p53 protein [143, 210]. As mentioned previously there is an increased sensitivity associated with the Western blotting platform which may be antigen associated. For instance, although AAbs to p53 are identified in comparable numbers in both platforms, in total 4 positive sera were identified by ELISA, while 7 positive sera were identified by Western blot. Hence there is more sensitive detection associated with Western blotting.

4.4.3.2 Characterisation of Anti - Adducin Alpha Autoantibodies

AAbs to adducin alpha have not been previously characterised in ovarian cancer. However overexpression of the ADD1 gene in OVCA cells has been associated with tumour

Table 4.6: Comparison of Autoantibody Frequency in Differential Methodologies

This table outlines the numbers of subjects that were identified as having AAbs to the relevant antigens in each cohort using ELISA and Western immunoblotting. Comparison of the numbers of serum identifying positive for AAbs to the relevant antigens are higher with Western immunoblotting compared to ELISA.

	Late OC		Early OC		Non Remarkable	
	ELISA	**Western Blot**	**ELISA**	**Western Blot**	**ELISA**	**Western Blot**
p53	4/20 (20%)	5/20 (25%)	0/20 (0%)	2/20 (10%)	0/15 (0%)	0/15 (0%)
Adducin alpha	1/20 (5%)	6/20 (30%)	0/20 (0%)	4/20 (20%)	0/15 (0%)	0/15 (0%)
Endosulfine alpha	1/20 (5%)	3/20 (15%)	0/20 (0%)	2/20 (10%)	0/15 (0%)	2/15 (13%)

suppressive effects, such as reduced cellular proliferation, colony formation and invasion [286]. It is postulated that this effect may be mediated via supression of mobility in cancer cells. Adducin alpha has been linked to general malignant processes, particularly in epithelial cells where it has been found to localise cell-cell contact and membrane protrusions such as lamellipodia [279]. Adducin alpha, which has been implicated in cell motility and invasiveness and the identification of AAbs to this protein may be indicative of immune system reporting malignant transformation [132].

In this study we detected adducin alpha AAbs in 1/20 (5%) of the late stage ovarian cancer group by ELISA (Table 4.6and Figure 4.8a). The ELISA positive serum matched 1 of 3 sera identified as positive by array screening. Western immunoblots identified AAbs to adducin alpha in 6/20 (30%) of the late stage patient group. The sera positive for adducin alpha immunoreactivity by Western blot contained those sera that were positive for alpha adducin immunoreactivity by hEx1 array screening. In the extended early stage ovarian cancer group we failed to detect adducin alpha AAbs in any of the 20 patient sera by ELISA. By contrast, we detected adducin alpha AAbs in 4/20 (20%) of early stage patient samples by Western immunoblot (Figure 4.7b). The four sera that were immunoreactive to alpha adducin by Western immunoblotting were from the

original 13 patient samples which were screened individually on the hEx1 arrays. AAbs to adducin alpha were not identified in any of the non-remarkable patient sera by any of the methodologies used.

From the results table, there is a general trend of increased sensitivity associated with the Western blotting platform compared to ELISA. AAbs to Adducin alpha are identified in very different numbers in both platforms. In total 1 positive serum was identified by ELISA, while 10 positive sera were identified by Western blot. As with AAbs to p53, more sensitive detection is associated with Western blotting. Certainly ELISA may be a preferred diagnostic application as it is a higher thoughput platform and also uses less serum, however the increased sensitivity of the Western blotting platform is an interesting finding that may impove the sensitivity of a panel of cancer associated AAbs.

4.4.3.3 Characterisation of Anti - Endosulfine Alpha Autoantibodies

AAbs to endosulfine alpha have not been previously characterised in ovarian cancer patients. However, endosulfine alpha is an inhibitor of PP2A and PP2A inhibitors are aberrantly expressed in a wide variety of cancers [287]. This aberrant espression may result in an AAb response that may be more easily detected compared to the antigen. Hence AAbs to PP2A inhibitors such as endosulfine alpha may be indicative of cancers, such as ovarian.

In this study, we detected AAbs to endosulfine alpha in 1/20 (5%) of the late stage ovarian cancer patient sera by ELISA (Table 4.6 and Figure 4.8b). The ELISA positive serum matched 1 of the 4 sera identified as positive by hEx1 array screening. Western immunoblot identified endosulfine alpha AAbs in 3/20 (15%) of the late stage patient sera (Figure 4.7c). The 3 sera identified as positive by Western matched those identified in the hEx1 array screen. In the expanded early stage ovarian cancer group we failed

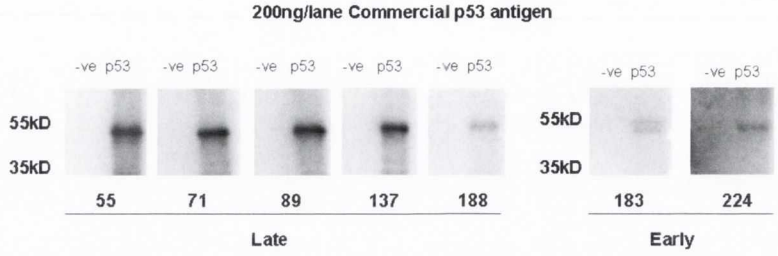

(a) Positive Western immunoblots for Commercial p53

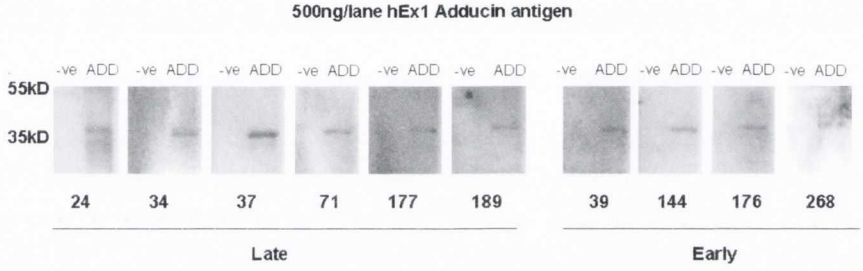

(b) Positive Western immunoblots for hEx1 adducin alpha

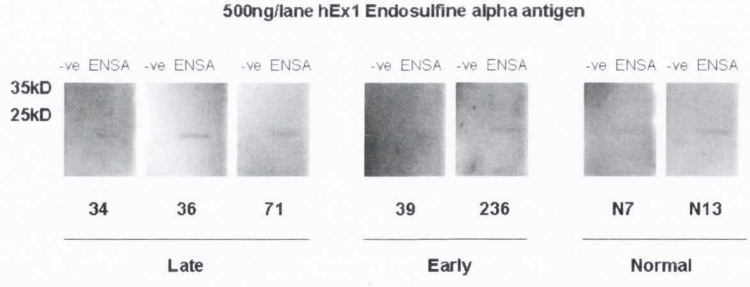

(c) Positive Western immunoblots for hEx1 endosulfine alpha

Figure 4.7: Positive Western immunoblots

This figure shows images of Western immunoblots that have been screened with human serum to identify AAbs to the three selected antigens. It is evident from these subfigures that the p53 antigen ellicits a very strong AAb response in the majority of sera identified as p53 AAb positive.

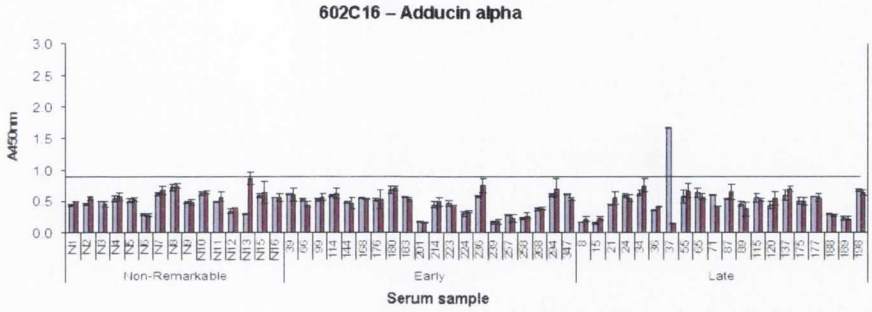

(a) Adducin Alpha ELISA Analysis

This figure shows the hEx1 Adducin alpha absorbance values, indicated as blue columns. The absorbance values for a negative control protein (as used throughout this work) are indicated as purple columns. The error bars in this figure are representative of the standard deviation attained from duplicate wells in this experiment. From this analysis it is clear that only one serum was identified to have autoantibodies to Adducin Alpha, late stage serum 37.

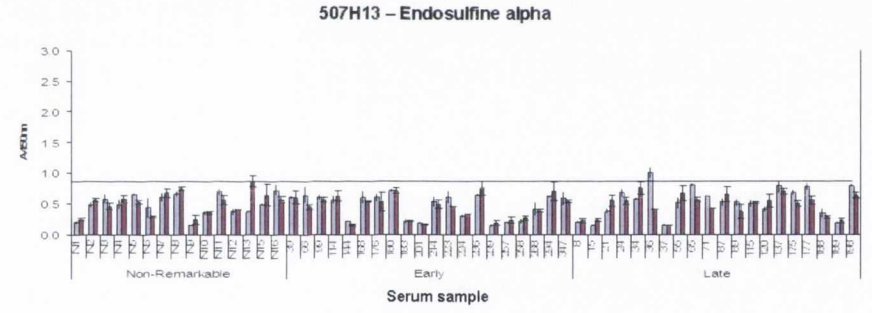

(b) Endosulfine Alpha ELISA Analysis

This figure shows the hEx1 Endosulfine alpha absorbance values, indicated as blue columns. Again, the negative control values (as used throughout this work) are indicated as purple columns. The error bars in this figure are representative of the standard deviation attained from duplicate wells in this experiment. From these results only one patient serum is above the cut-off value for this experiment, which is late stage serum sample 36.

Figure 4.8: ELISA results for identification of Autoantibodies to Adducin Alpha and Endosulfine Alpha

to detect endosulfine alpha AAbs in any of the 20 patient sera by ELISA. In contrast we detected endosulfine alpha AAbs in 2/20 (10%) of the early stage patient samples by Western immunoblots. Of the two early stage sera that were immunoreactive to endosulfine alpha by Western immunoblotting one was from the original 13 patient samples screened on the hEx1 array and one was a serum sample fromthe additional 7 early ovarian cancer sera. AAbs to endosulfine alpha were not identified in any of the non-remarkable patient sera using the hEx1 arrays and ELISA. However, AAbs to endosulfine alpha were identified in 2/15 (13%) of the non-remarkable subject sera by Western immunoblotting.

On reviewing Table 4.6, AAbs to endosulfine alpha were detected by Western immunoblot with relatively similar frequencies (15% in late stage, 10% in early stage, 13% in non-remarkable). Thus AAbs to endosulfine alpha are not of interest in differentiating between ovarian cancer and non-remarkable controls. Regarding endosulfine alpha AAbs, the general trend of increased sensitivity associated with the Western blotting platform compared to ELISA is also evident for this antigen. In total 1 serum was identified as positive for AAbs to endosulfine alpha by ELISA, while 7 positive sera were identified by Western blot, this indicates more sensitive detection is associated with Western blotting.

4.4.4 Validation on Additional Serum Samples

Experimentation was performed to investigate AAbs to the three antigens in an additional serum cohort. Western immunoblotting and ELISA was performed on individual serum samples to assess the AAb response in an additional cohort of 42 serum samples - 28 benign ovarian disease patients and 14 late stage ovarian cancer patients. The results are outlined in Table 4.7.

In the additional serum cohort, AAbs to p53 were identified in 3/14 (21%) of late

stage ovarian cancer patients by ELISA. Western blotting also identified the same 3/14 (21%) of late stage patient sera as immunoreactive to the p53 protein. Neither ELISA nor Western blotting identified AAbs to p53 in the 28 benign ovarian disease serum subjects. Therefore in the total grouping of 97 sera samples interrogated, 7 sera were identified as immunoreactive to p53 using the ELISA immunoassay platform, while 10 sera were identified as immunoreactive to p53 using the Western immunoblot. Hence a better performance was noted for Western immunoblotting for detecting AAbs to p53 in patient sera compared to ELISA. By Western immunoblotting AAbs to p53 were detected in 8 of 34 of late stage ovarian cancer patients. AAbs to p53 were detected in 2 of 20 of early stage ovarian cancer patients, one patient had a clear cell tumour, grading was not available for this subject, while the other had an endometrioid tumour, grade 2, these histological types are compatable with Type II tumour subtypes.

In the additional serum cohort, AAbs to adducin alpha were identified in 0/14 of the late ovarian cancer patient sera by ELISA. However, Western blotting identified AAb to alpha adducin in 3/14 (21%) of the late stage patient sera. AAbs to adducin alpha were identified in 1/28 (4%) of the benign ovarian disease subject sera by ELISA (as shown in Figure 4.9a), and 9/28 (32%) of this sera cohort by Western blot. Therefore, a total grouping of 97 sera samples interrogated, 2 sera were identified as immunoreactive to adducin alpha using the ELISA platform, while 22 sera were identified as immunoreactive to adducin alpha using Western immunoblot. Hence, as with the p53 antigen, a better performance was noted for Western immunoblotting for detecting AAbs in patient sera compared to ELISA. By Western immunoblotting AAbs to adducin alpha were detected in 9 of 34 (27%) of late stage ovarian carcinoma patients, this is a novel finding as AAbs to adducin alpha have not been interrogated in ovarian cancer patients previously. However AAbs to adducin alpha were not deemed to be ovarian cancer specific as they were detected in 9 of 28 (32%) benign ovarian disease patients by Western

immunoblotting. AAbs to adducin alpha have not been identified previously in ovarian cancer patients.

In the additional serum cohort, AAbs to endosulfine alpha were identified in 0/14 late stage ovarian cancer patient sera by ELISA (as shown in Figure 4.9b). In contrast, AAbs to endosulfine alpha were identified in 7/14 (50%) of late stage ovarian cancer patient sera by Western immunoblotting. AAbs to endosulfine alpha were identified in none of 28 benign ovarian disease serum by ELISA, but were identified in 14/28 (50%) benign ovarian disease serum by Western blot. For endosulfine alpha, of the total grouping of 97 sera samples interrogated, 1 serum was identified as immunoreactive to endosulfine alpha using the ELISA immunoassay platform, while 28 sera were identified as immunoreactive to endosulfine alpha using the Western immunoblot. As with previous antigens, the increased sensitivity of AAb detection is noted in the Western immunoblotting platform. Notably, the Western blotting result images for endosulfine alpha (Figure 4.7c) compared to the other two antigens identify that there appears to be little AAb binding to endosulfine alpha resulting in faint banding. This was the case for all of the serum samples screened for AAbs to endosulfine alpha. As AAbs to the endosulfine alpha antigen are unlikely to be of interest for use as a disease diagnostic.

The analysis of the additional patient sera data presented in Table 4.7, validates the results obtained in the previous serum cohorts which identified that each antigen has unique performance characteristics and that Western blotting is more sensitive than ELISA in identifying AAb responses. This additional serum cohort analysis identified AAbs to adducin as present in benign ovarian disease serum. Hence these AAbs are not specific to patients with malignant ovarian masses. However, AAbs to adducin alpha were not identified in the non-remarkable subject sera, which implies that AAbs to adducin alpha may be associated with an ovarian mass or perhaps inflammation. AAbs to endosulfine alpha are also identified in large proportions in these additional

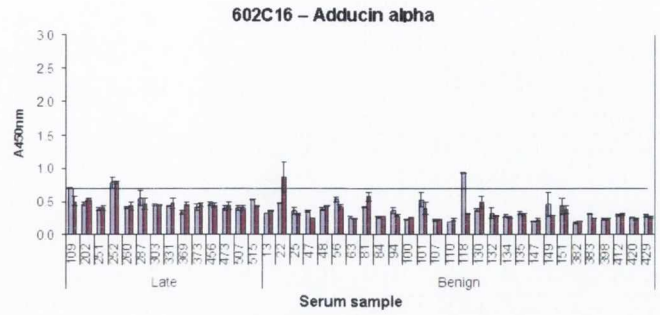

(a) Adducin Alpha ELISA analysis on additional serum samples

As before, the hEx1 Adducin alpha absorbance values are indicated as blue columns. The absorbance values for a negative control protein are indicated as purple columns. The error bars in this figure are representative of the standard deviation attained from duplicate wells in this experiment. From this analysis, only one serum was identified to have autoantibodies to Adducin Alpha, late stage serum 118. Although late stage serum sample 252 is above the cut-off value it was not deemed a true result as the negative control is also above this level.

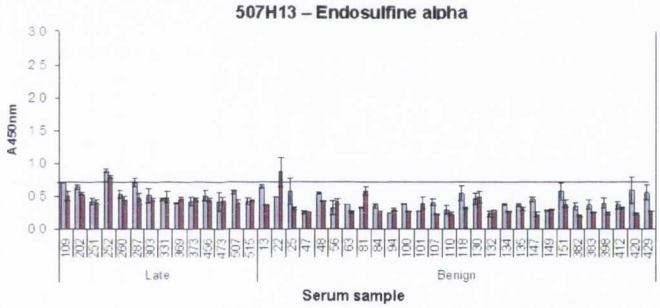

(b) Endosulfine Alpha ELISA analysis on additional serum samples

As before, the hEx1 Endosulfine alpha absorbance values are indicated as blue columns. The absorbance values for a negative control protein are indicated as purple columns. The error bars in this figure are representative of the standard deviation attained from duplicate wells in this experiment. From this analysis, no serum sample was identified to have autoantibodies to this protein. One late stage serum sample 252 is above the cut-off value, however as in the Adducin alpha analysis it was not deemed a true result as the negative control is also above this level.

Figure 4.9: ELISA results for identification of Autoantibodies to Adducin Alpha and Endosulfine Alpha

cohorts, including the benign cohort, this suggests that AAbs to endosulfine alpha may be associated with the natural AAb response.

Table 4.7: Additional Cohort Autoantibody Frequency

This table outlines the numbers of subjects that were identified as having AAbs to the relevant antigens in additional serum cohorts using ELISA and Western immunoblotting. As noted previously, the numbers of serum identifying positive for AAbs to the relevant antigens are higher with Western immunoblotting compared to ELISA.

	Late OC		Benign	
	ELISA	**Western Blot**	**ELISA**	**Western Blot**
p53	3/14 (21%)	3/14 (21%)	0/28 (0%)	0/28 (0%)
Adducin alpha	0/14 (0%)	3/14 (21%)	1/28 (4%)	9/28 (32%)
Endosulfine alpha	0/14 (0%)	7/14 (50%)	0/28 (0%)	14/28 (50%)

Shown in Figure 4.7 are all the Western immunoblots that were identified as positive and outlined in Table 4.6. Notably, the serum that was identified as strongly immunoreactive in the Western blotting platform can be validated by ELISA, while the serum identified as weakly immunoreactive by Western blot with a weaker banding pattern, are not likely to validate in the ELISA platform. The ELISA and Western blot comparative analysis with 50ng of antigen (Figure 4.6) identified that antigen presentation also appears to be an important factor as Western immunoblotting was identified to exhibit improved sensitivity [192]. In total for this study, 28 benign ovarian disease, 34 late stage ovarian cancer, 20 early stage ovarian cancer and 15 non-remarkable subject serum samples were interrogated, giving a total of 97 subject sera that were interrogated by ELISA and Western immunoblot. From the data it is clear that each antigen has different performance characteristics using conventional ELISA format and Western immunoblot. For the candidate tumour associated AAbs studied we see a disconnect between the results of the array data, the results of ELISA immunoassay and the results of Western immunoblot.

4.5 Discussion

The hEx1 platform has been used in previous studies to identify AAb profiles in cancer patients [131, 146, 288, 289, 290, 291, 292], however this is the first study to employ this screening platform to identify AAb profiles associated with ovarian cancer.

Regarding the identification of an AAb response to the p53 antigen, a better performance was noted for Western immunoblotting for detecting AAbs to p53 in patient sera compared to ELISA. By Western immunoblotting AAbs to p53 were detected in 24% of late stage ovarian cancer patients, which is in line with published data [143]. AAbs to p53 were detected in 10% of early stage ovarian cancer patients, although this is lower than the proportion of p53 reactive serum in the late stage cohort and is lower than previously published data [211, 204], in light of the varying histological dfferences in the early stage cohort, this is perhaps not surprising. Typically AAbs to p53 are associated with Type II tumours, these tumours are typified by agressive growth and high grade [205]. All of the late stage ovarian cancers interrogated in this study were late stage serous papillary adenocarcinoma and are almost invariably grade 3 growths. The early stage ovarian cancers interrogated in this study are a more heterogeneous group and have varying histologies, including mucinous and low grade tumours, these tumours are Type I tumours and are hence less associated with p53 mutation and AAbs to p53 [205]. As mentioned previously, two early stage patients were identified to be immunoreactive to p53, one patient had a clear cell tumour, grading was not available for this subject, while the other had an endometrioid tumour, grade 2, these histological types are compatable with Type II tumour subtypes.

AAbs to adducin alpha have not been identified previously in ovarian cancer patients, however they have been interrogated in patients with prostate cancer. In a recent study Maricque et al. used a phage based methodology to identify autoantigens associated with prostate cancer, of these autoantigens adducin alpha was identified in

an antigen subset that has the highest individual positive likelihood ratio for prostate cancer compared to controls [281]. Adducin alpha was interrogated in this study after being previously identified in a study profiling the AAb response in patients with prostatitis [293]. Hence AAbs to adducin alpha may arise due to inflammation or the inflammatory process and AAbs to adducin alpha may be associated with benign conditions. Further interrogation of AAbs to adducin alpha in a larger cohort of ovarian cancer patients, benign patients and healthy controls may be of interest as AAbs to this antigen may be indicative of an ovarian mass and may also reveal details of disease aetiology.

The status of endosulfine alpha as a candidate autoantigen is considerably altered by the of detection of autoantibody immunoreactivity in benign ovarian disease and control subject sera. As with previous antigens, the increased sensitivity of AAb detection is noted in the Western immunoblotting platform. As AAbs to the endosulfine alpha antigen have been identified in patients in the non-remarkable cohort and in the benign ovarian disease cohort, AAbs to this antigen are not likely to be of interest for use in a disease diagnostic.

The results of this study identified differential AAb binding was identified in the same serum using different methodologies and thus, identified that antigen presentation also appears to be an important factor as Western immunoblotting was identified to exhibit improved sensitivity [192]. The antigen conformation on the surface of the hEx1 array platform, which was used to identify these AAbs in patient serum is unknown. However it is assumed, as the antigens are denatured using guanidine hydrochloride that the antigens are unfolded or perhaps partially re-folded. In the case of the antigens presented in this ELISA, there may be increased re-folding which hence leads to differential epitope recogntion. An epitope, or an antigenic determinant, is typically between 5 and 8 amino acids long, with between 2 and 5 critical residues and can be

either linear or conformational [294]. Figure 4.10 outlines these two different epitope structures. Linear epitopes are recognised by antibodies through a linear sequence of amino acids, i.e. identification is of the antigens primary structure. Classically, antibodies to linear epitopes are generated once the antigen is digested by macrophages and presented as short peptides to the major histocompatibility complex (MHC). However, conformational epitopes are recognised by antibodies through a non-linear sequence of amino acids, in this case the antibody recognises the tertiary structure of the antigen. Antibodies to conformational epitopes are generated when antigens are presented in a non-digested manner. The results of this study identified differential AAb binding was identified in the same serum using different methodologies (Figure 4.6).

Allowing for the small size of the study cohort this data is compelling and indicates that the presentation of the epitope is a significant factor in autoantigen recognition by autoantibodies. The poor performance of the ELISA assay is in marked contrast to the Western blot for adducin in particular and appears to be associated with optimal recognition of a linear epitope in the Western immunoblot. It is likely that proteins which are expressed in E-Coli, denatured and immobilised in situ on protein arrays, as is the case for hEx1 proteins, represented highly unfolded polypeptides. Upon expression, purification and dilution for coating the wells of ELISA plates there is a significant opportunity for the polypeptide to refold, the immunoreactive epitopes may then be buried and not be available for recognition for the AAbs in patient serum. This may result in reduced sensitivity of this assay. In preparation for Western blotting, antigens are heat denatured and linearised by SDS-polyacrylamide electrophoresis resulting in the antigen being completely denatured and transferred as a linear polypeptide to the membrane prior to incubation with the patient serum. This platform enhances linear epitope presentation and may increase the sensitivity of this assay.

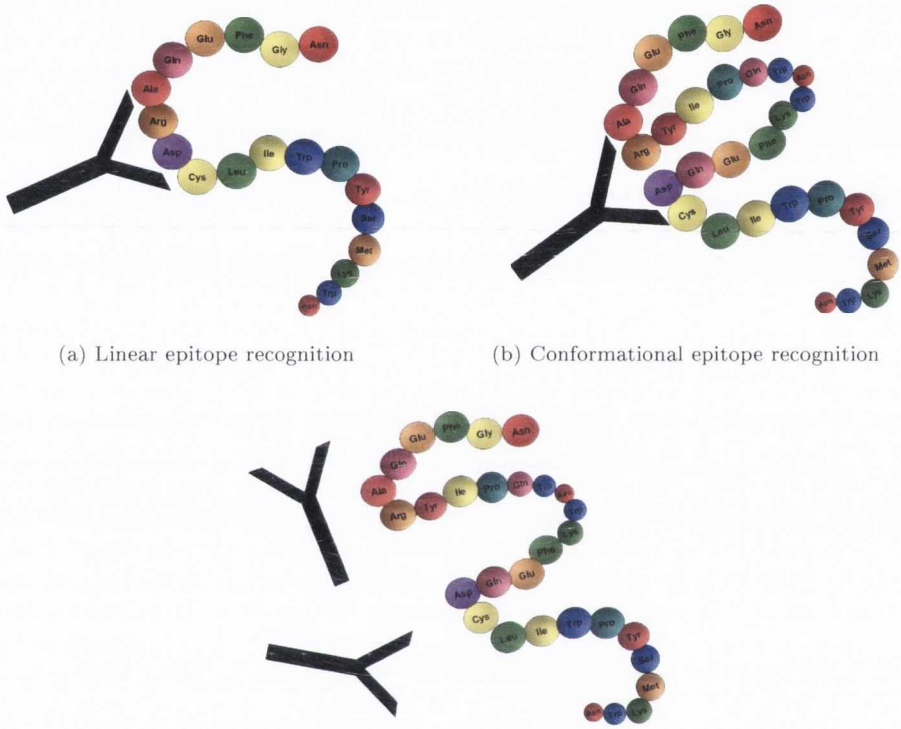

(a) Linear epitope recognition

(b) Conformational epitope recognition

(c) Conformational epitope recognition

Figure 4.10: Antibody recognition of linear and conformational epitopes

Shown in this figure are the different methods of epitope recognition. In both cases the same amino acid sequence is being recognised, however as shown in sub-figure 4.10a the amino acids are in a linear sequence, however in sub-figure 4.10b the amino acid sequence is not linear and antigen conformation is needed to result in epitope recognition. In sub-figure 4.10c the amino acid sequence is not recognised by the antibodies as the epitope is only presented when the antigen is conformational, however in this image the antigen is linear.

4.6 Conclusion

Robust autoantibody profiles to p53 and adducin alpha have been identified and validated in secondary platforms, to be ovarian cancer and ovarian disease associated respectively, this fulfills the chapter aims. In the case of adducin alpha, this is the first study to identify AAbs to adducin alpha in ovarian cancer and benign ovarian disease patients. Further investigation is warranted to determine the adducin alpha AAb profile in a larger and diverse cohort of patient samples. AAbs to the antigens investigated in this study have exhibited improved sensitivity using Western immunoblot. A more complete analysis, to determine the exact immunogenic epitope is merited to afford the optimal presentation in diagnostic assay format. Presentation of short peptide sequences of specific antigens has the potential to perform with a higher level of specificity and sensitivity than we have seen to date with existing modalities. Better knowledge of epitope recognition and superior presentation of the epitope to which AAbs bind would greatly influence AAb profiling and validation methodologies.

Chapter 5

Autoantibody Identification by ProtoArray Serum Screening

5.1 Introduction

Previous results indicate variation and differences in the results of AAb profiling that may be due to differential epitope presentation and recognition by AAbs that are related to the difference profiling methodologies used. Previously we have hypothesised that the AAb profiles identified from hEx1 array screening may be linear epitope biased, as this technology presents denatured protein fragments for binding [192]. As the AAb response identified may be linear epitope biased this may have led to the differences noted between the results of the ELISA immunoassay and Western immunoblotting platforms. The identification of AAb profiles using an array that presents antigens in a native protein structure may be used to identify AAb profiles that are biased towards recognition of comformational epitopes. However an AAb response can also recognise both linear and conformational antigenic epitopes, hence it is hypothesised that AAbs present in both of these platforms will have the greatest potential for further validation using different secondary validation techniques. The ProtoArrays were selected for additonal serum screening. These arrays offer a very different screening platform for AAb profiling, the arrayed proteins are purified, full length, functionally folded and post-translationally modified. It may be expected that autoantibodies will recognise

antigens present in both platforms, one platform or in neither platform. The ability of the autoantibodies to recognise the antigens in each platform may be indicative of the epitope presentation due to the conformation of the antigen on the array surface. Unfortunately, the p53 protein is not spotted on the ProtoArrays. Throughout this research the p53 AAb response was assessed as a positive control and as a "gold standard" autoantigen and AAb response, however, the assessment of the p53 AAb response in ProtoArray screened sera could not be compared to the p53 AAb response using other methodologies. The ability to compare the previous p53 AAb results to the ProtoArray screening results would have acted as a good reference point for optimisation and signal value cut-off determination.

For ProtoArray analysis, a small cohort of well matched serum samples were selected for screening. Serous papillary ovarian cancers are the most common histotype and also carry the poorest prognosis, for that reason the malignant serum screened on the ProtoArrays were all of this histology. As control cohorts, benign ovarian disease patient serum and non-remarkable were screened. All of the benign ovarian disease patient serum screened were serous histology. Screening of these samples was performed to ensure less variation in the dataset. It is thought that high grade serous papillary ovarian cancer does not arise from a benign serous tumour (as discussed in Section 1.2.1). There is no easily identifyable precursor of high grade serous papillary carcinomas, and there are different hypotheses proposing these malignancies arise from surface epithelial inclusion glands with p53 mutation [295], but it is most likely that they may arise from fallopian tube epithelium [80, 81, 296]. In this study, high grade early and late stage ovarian cancer patient serum were selected for investigation. Up until relatively recently, early stage high grade serous papillary carcinomas were thought to lead to late stage disease. This study was designed to determine the AAb profiles associated with serous papillary ovarian carcinoma, and to interrogate the changes in the AAb profile as ovarian

carcinoma progresses from early to late stage disease. Although, recent findings have identified that early stage ovarian cancer is unlikely to progress to late stage disease, the study design was left unchanged, as for slow growing ovarian malignancies, such as mucinous and low grade serous papillary, it is likely that late stage ovarian cancer arises from an early stage precursor.

It is well known that pathway deregulation is associated with malignancy and analysis of the immunogenic antigens identified in this screening was performed to identify an AAb response in patients may be indicative of malignant pathway dysregultion [297, 288]. As evident from previous results, the AAb response tends to have high specificity but low sensitivity for cancer. This means that an AAb response to a tumour associated antigen may or may not arise, as is the case with p53. Although AAbs to a particular antigen may not be generated, AAbs to other antigens present in a signalling pathway may be generated, this may increase the sensitivity associated with AAb profiling. Also the dataset generated from ProtoArray analysis is extremely large and a 'systems approach' of pathway and interaction network identification was considered to condense and refine the data, generating pathways/interactions common to different patient cohorts [298]. Innate database was selected for this analysis and is a manually-curated knowledgebase of genes, proteins and particularly, the interactions and signalling responses involved in the mammalian innate immune system [299].

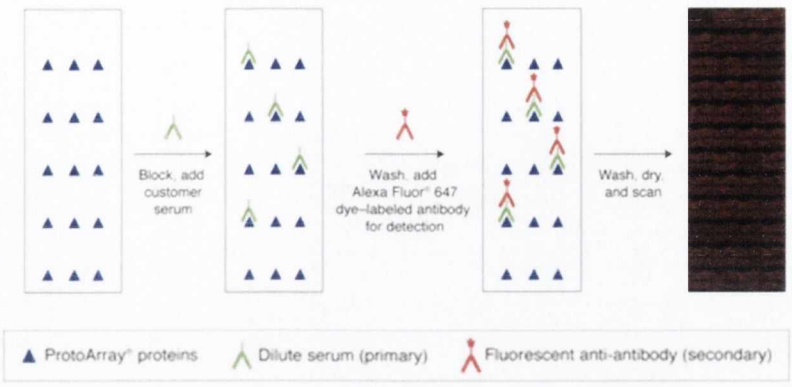

Figure 5.1: ProtoArray Serum Screening

This figure shows how serum autoantibodies recognise and bind to specific antigens on the surface of the ProtoArrays. The antibodies present in the serum bind to the recognised protein with very high specificity and are detected by a labelled anti human IgG. This is the principle employed in hEx1 array screening also.

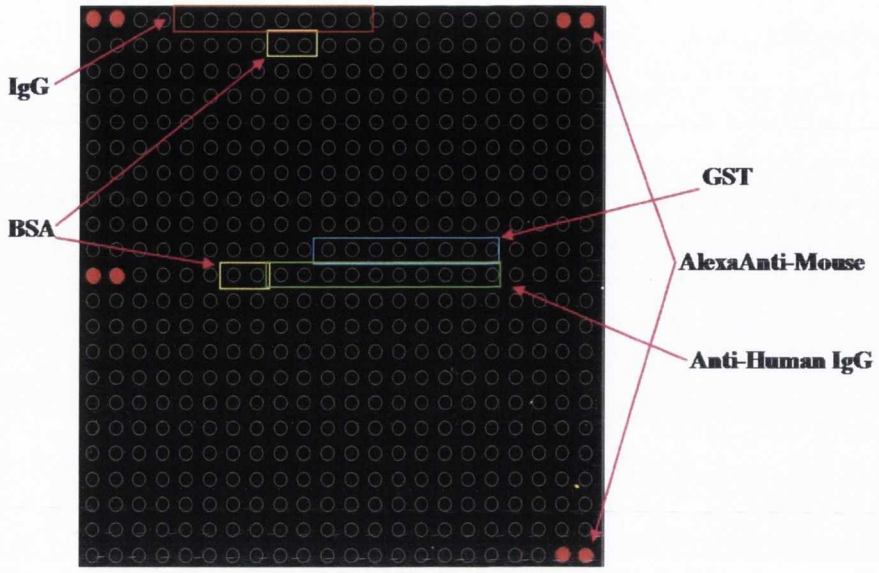

Figure 5.2: ProtoArray field layout

This figure outlines the field layout of the Invitrogen ProtoArray. Numerous control proteins are spotted in each field and their locations and identities are shown above.

5.2 Aims

- To use the ProtoArrays to identify autoantibody profiles in healthy and disease serum.
- To identify autoantibodies that are associated with ovarian cancer.
- To compare the results of previous array screening to ProtoArray screening.
- To identify pathway dysregulation associated with ovarian cancer.

5.3 Materials and Methods

5.3.1 ProtoArray Serum Screening

For ProtoArray screening 20 serum samples from the Discovary biobank were selected for screening. The samples chosen for screening are outlined in Table 5.1. The ProtoArrays were screened as outlined in Section 2.6.1.

Table 5.1: Serum screened on ProtoArrays

Sample	Identifier	Histology	Age	Grade	Stage
Normal					
1	N1	n/a	60	n/a	n/a
2	N3	n/a	56	n/a	n/a
3	N5	n/a	63	n/a	n/a
4	N15	n/a	62	n/a	n/a
5	N16	n/a	48	n/a	n/a
Benign					
1	382	Serous cystadenoma	58	n/a	n/a
2	383	Serous cystadenoma	42	n/a	n/a
3	398	Serous cystadenoma	31	n/a	n/a
4	420	Serous cystadenoma	57	n/a	n/a
5	429	Serous cystadenoma	43	n/a	n/a
Early					
1	176	Serous papillary adenocarcinoma	57	2	IA
2	223	Serous papillary adenocarcinoma	49	3	IC
3	257	Serous papillary adenocarcinoma	61	3	IC
4	268	Serous papillary adenocarcinoma	64	3	IC
5	347	Serous papillary adenocarcinoma	50	3	IC
Late					
1	87	Serous papillary adenocarcinoma	60	3	3C
2	89	Serous papillary adenocarcinoma	44	3	3A
3	120	Serous papillary adenocarcinoma	60	3	3C
4	189	Serous papillary adenocarcinoma	59	2-3	3C
5	198	Serous papillary adenocarcinoma	55	3	4

The ProtoArrays were analysed using Invitrogen's Prospector software, as outlined in 2.6.2 to identify antigens that were immunogenic in each serum sample screened. A more stringent analysis was also performed in parallel for each serum sample. Antigens that had the highest signal values was selected to identify the most immunogenic AAb response to antigens in each serum sample.

5.3.2 Comparative Analysis of ProtoArray Screening

5.3.2.1 Comparison to Published Results

Section 1.7 outlines AAb responses which have been identified in previously published results to be ovarian cancer associated. The 3 antigens investigated in Chapter 4 were also investigated in this manner. As above, and analysis was performed to determine if AAbs to these previously published antigens were also identified in any of the 20 subject sera screened on the ProtoArrays.

5.3.2.2 Comparison to hEx1 Array Results

The 74 antigens identified to be ovarian cancer and ovarian disease associated in Chapter 3 from hEx1 array screening were investigated to determine if the antigens are present on the surface of the ProtoArray. The AAb responses to the antigens common to both platforms were assessed to determine any overlaps between hEx1 and ProtoArray screening.

5.3.3 Identification of Immunogenic Antigens

Using the results attained from the stringent highest signal values for antigens, a comparative analysis was performed to identify AAb profiles that are associated with each subject cohort. AAb responses were identified as cohort associated if they were present in 40% (2/5) or above of cohort serum, and present in 20% (1/5) or less of serum from other cohorts. This cut-off was selected as 2 of 5 (40%) patients in a cohort was deemed to be in-line with previous results which identify AAbs to p53 in approx 30% of cancer patients.

5.3.4 Identification of Immunogenic Pathways

Pathway analysis for each screened serum was performed as outlined in Section 2.6.3. Pathways that were identified in 60% (3 of 5) or above of patients in a cohort and present in 20% (1/5) or less of serum from other cohorts were deduced to be cohort associated and were collated into cohort associated files. An overlap analysis of these files was performed to identify pathways that are unique to the different cohorts assessed.

5.4 Results

5.4.1 Prospector Identified Autoantibody Responses

After identification of immunogenic antigens using Prospector analysis software, on average 2,815 (Standard deviation 1,702) statistically significant autoantigens were identified per individual screened serum. The breakdown of the mean number of "hits" and the associated standard deviation per individual serum cohort is outlined in Table 5.2. In many of the screened serum, a very large proportion of the antigens present on the ProtoArrays were identified to have a corresponding AAb, i.e. early stage serum sample 347 was identified to have 7,248 antigens out of a possible ~10,000 identified as immunogenic.

Table 5.2: Reactivities of screened serum cohorts

This table gives an overview of the mean number and standard deviation of positives for each cohort. From reviewing the standard deviation values, it is evident that there is a lot of variation in the number of antigens that bind AAbs in subject serum.

Cohort	Mean Number of "Hits"	Standard Deviation
Non-Remark	3469	1535
Benign	1797	623
Early	3457	2356
Late	2539	1742

5.4.1.1 Comparison to Published Autoantibody Responses

As outlined in Section 1.7 a number of AAbs have been previously identified to be associated with ovarian cancer. These AAbs and autoantigens have been identified using many different screening methodologies, including ProtoArray serum screening. The three antigens identified from the hEx1 array screening in Chapter 4 were also included in this analysis. Hence 7 antigens were selected for further interrogation these antigens were, p53, adducin alpha, endosulfine alpha, mesothelin, HSP-90, NY-ESO-1 and survivin. After investigation to determine if the antigens present on the ProtoArray,

the antigens p53 and NY-ESO-1 could not be interrogated further as they were not present. Hence analysis was carried out on the 5 antigens (adducin alpha, endosulfine alpha, mesothelin, HSP-90 and survivin) that were present on the ProtoArrays to determine if AAb responses were generated in the screened patient serum. The results of this analysis are summarised in Table 5.3. The "Y" marked in this table indicate the antigens to which sera were immunoreactive. Some of the antigens detailed in this table have one or more transcript variant present on the surface of the ProtoArrays, notably, endosulfine alpha has three transcript variants present on the surface of the array, while survivin has two transcript variants. Transcript variants of all the antigens were included to provide a complete analysis.

From reviewing Table 5.3 it is clear that by ProtoArray screening, AAbs to adducin alpha were only identified in one non-remarkable serum sample and in none of the disease sera. This is in contrast to the previous hEx1 adducin protein which was no immunogenic in any of the non-remarkable patients and was immunogenic in benign disease and early and late stage ovarian cancer. In the case of endosulfine alpha, there are both overlapping and unique AAb profiles for the different transcript variants. Comparison of the serum identified as endosulfine alpha immunoreactive by ProtoArray screening to the serum identified as immunoreactive by Western immunoblotting revealed no overlap between these two methodologies, i.e. the sera identified as immunoreactive in Table 5.3 were not identified as such by Western immunoblotting. Regarding the remaining antigens (mesothelin, HSP-90, survivin, survivin variant 1) these antigens had not been previously investigated in this research. However from reviewing the serum immunoreactivities in Table 5.3 these antigens to not seem to be strongly associated with any of the serum cohorts. AAbs to mesothelin were identified in equal serum proportions in the non-remarkable cohort and the early stage ovarian cancer cohort. AAbs to HSP-90 were identified in relatively equal proportions in all cohorts (40% non-remarkable,

20% benign, 40% early, 40% late). AAbs to survivin were identified in 60% of non-remarkable subjects, 20% of benign subjects, 80% of early stage patients and 60% of late stage patients. AAbs to this antigen may be of interest as they are present in relatively low proportions of benign subjects compared to early stage ovarian cancer patients, however as the sample size is small this will need to be interrogated in a larger sample cohort before this can be validated. AAbs to survivin variant 1 were identified in 40% of the non-remarkable subjects, none of the benign disease patients and in 20% of the early and late stage patients respectively. This seems to indicate that AAbs to this antigen may be associated with the non-remarkable cohort, however this needs to be investigated further in a larger serum cohort.

These results outlined in Table 5.3 for the adducin alpha and endosulfine alpha antigen identify that there are differences between this discovery platform and the previously used methodologies. However this is not surprising as there are many differences between all the platforms used for AAb identification. The antigens present on the surface of the ProtoArrays are all full length and are post-translationally modified which affects antibody binding. As discussed in the previous chapter, epitope presentation is very important in AAb binding and as the ProtoArray antigens are structurally folded this will also result in differential AAb recognition and binding. further investigation of short peptide sequences is needed to confirm this.

5.4.1.2 Autoantibody Response to hEx1 Identified Antigens

Previously, in Chapter 3 AAb to 74 potential autoantigens were identified as associated with ovarian cancer and disease patients. The hEx1 arrays have been validated in previous screening experiments, therefore a comparative analysis was performed to identify AAbs that have been identified to be disease associated in both the hEx1 array and the ProtoArray platform. Of the 74 antigens identified in Chapter 3 to be associated

Table 5.3: Autoantibody frequency of previously identified antigens

The frequency of AAbs to antigens identified to be of interest in this and other studies was determined in our screened set of 20 sera.

	Non-Remarkable					Benign					Early OC					Late OC				
	N1	N3	N5	N15	N16	382	383	398	420	429	176	223	257	268	347	87	89	120	189	198
Adducin alpha					Y															
Endosulfine Alpha Variant 3	Y	Y	Y									Y	Y	Y	Y	Y				Y
Endosulfine Alpha Variant 7				Y							Y	Y		Y	Y					Y
Endosulfine Alpha Variant 8				Y											Y					Y
Mesothelin				Y											Y					
HSP-90		Y		Y					Y				Y		Y	Y				Y
Survivin	Y	Y			Y				Y			Y	Y	Y	Y	Y			Y	Y
Survivin Variant 1	Y			Y											Y					Y

with ovarian disease, 64 of these antigens were non-redundant. Analysis of these 64 antigens identified 35 of these antigens were present in the ProtoArrays, i.e. 55% of the 64 antigens were present on the ProtoArrays. Of the 35 antigens identified to be present on the ProtoArrays, two of these antigens have been analysed earlier in this chapter (adducin alpha and endosulfine alpha), hence AAbs to 33 antigens previously identified in this study were compared to the results of ProtoArray screening. Figure 5.3 outlines the sero-reactivity, as identified by ProtoArray serum screening, of the 33 antigens. In this figure the blue highlighted boxes are indicative of a positive AAb response to an antigen. It is clear from this figure that the vast majority of antigens are bound by a very large proportion of the serum samples. In some cases, antigens were identified to ellicit an AAb response in all serum samples screened.

Previous knowledge of the cancer associated AAb response has identified that AAbs have low sensitivity and high specificity as cancer biomarkers. Classically in the case of p53, AAbs are present in 30% of cancer patient serum with a specificity of 96% [143]. However from reviewing Figure 5.3, AAb responses were identified in high proportions of all serum cohorts. This might be indicative of the natural AAb response where AAbs may be present in higher proportions of subject serum and not disease associated. However it may also be associated with a high false positive rate using the Invitrogen Prospector software. The goal of serum screening is to identify ovarian cancer associated AAb responses that can be validated by secondary methologies that can be used in the clinic. Further analysis was performed to select the most robust AAb responses which have the greatest potential to translate into a different platform.

5.4.2 Highest Signal Autoantibody Responses

As outlined in the previous section, the classical cancer associated AAb response is one with low sensitivity and high specificity. The results outlined in Figure 5.3 are not

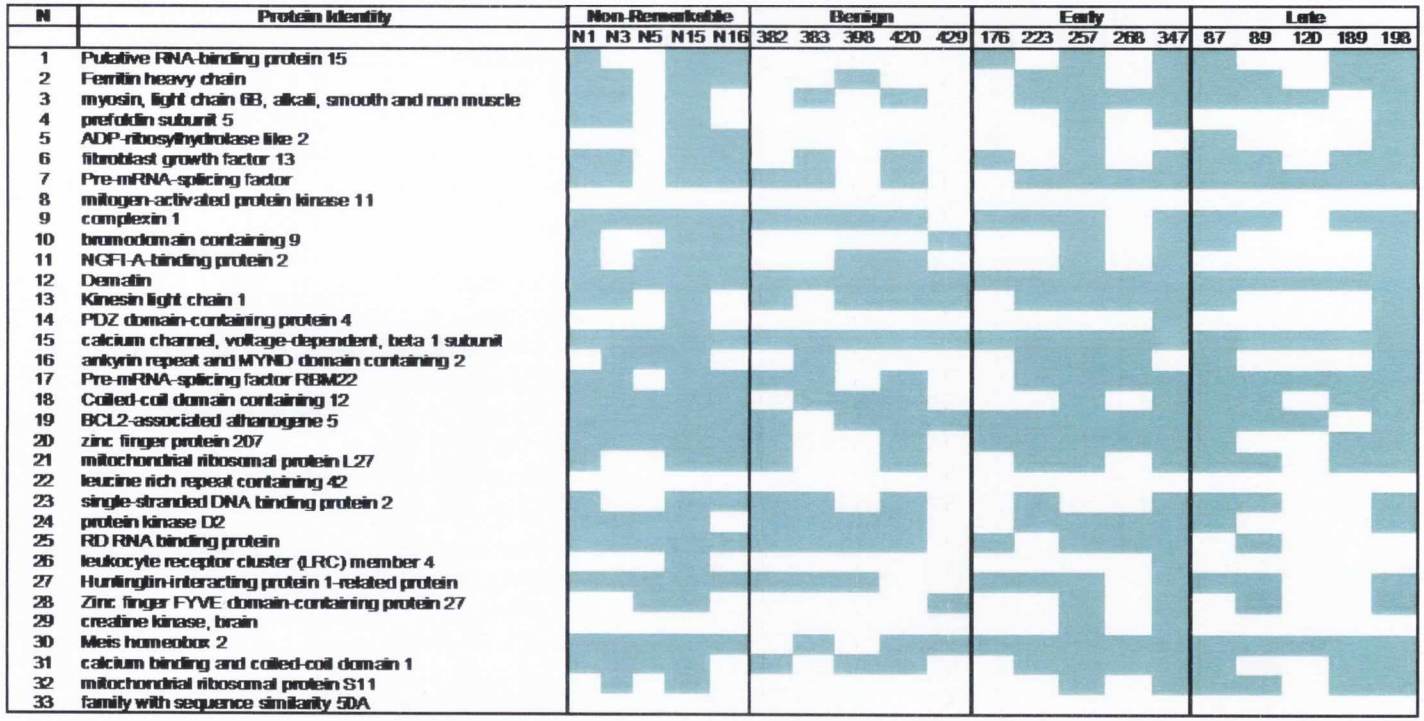

Figure 5.3: Analysis of 33 overlap antigens

In this figure the serum samples deemed to have a statistically significant AAb response are identified by blue boxes.

specific to any cohort and hence it was decided to amend the cut-off of the antigens identified as immunogenic to only select the AAb profiles that are very strongly reactive. A more stringent cut-off value was employed to ensure identification immunogenic antigens that are robust in other platforms.

To determine which cut-off value was most suitable, the signal intensities for all antigens identified by the Prospector software for each serum sample were graphed. This was performed for all serum samples screened on the ProtoArrays. Shown in Figure 5.4 are the graphed results for the late stage ovarian cancer cohort only. The antigens which exhibited the highest signal value were deemed to be of greatest interest and would be more likely to be reproduced in other platforms. From the graphed signal values (Figure 5.4) the antigens that had a signal value of over 1000 units were selected for further analysis.

Following the more stringent cut-off value, analysis was performed to identify the numbers of AAb/antigens identified to have a high signal value. The reanalysed data is outlined in Table 5.4, clearly this is a much more rigorous cut-off as the number of posotive AAb responses are very small compared to the numbers identified previously in Table 5.2. Interestingly there are similarities between these two analyses, the early stage serum cohort has the highest number of "hits" and also the highest standard deviation value compared to all other cohorts in both analyses. This may reflect increased tumour immunogenicity in early stages, increased immunogenicity in early stages compared to later stages of tumourigenesis has been postulated by the immunoediting hypothesis of cancer and may be exploited to identify early stage malignancies [57, 98, 109]. Certainly the variation in the numbers of immunogenic antigens is very high in the early stage cohort. However, this is a relatively small study with only 5 patients sera assessed in each cohort, therefore any findings drawn from this analysis need to be validated using a larger cohort of patient serum samples.

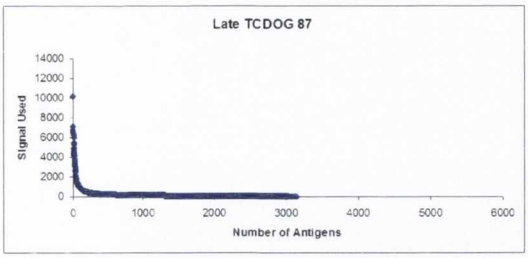

(a) Late stage serum 87

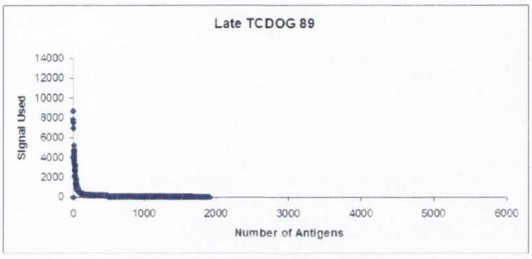

(b) Late stage serum 89

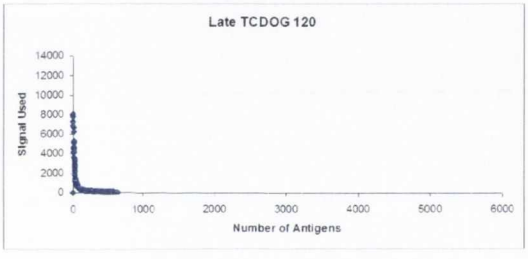

(c) Late stage serum 120

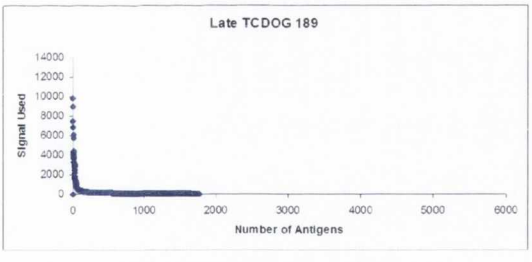

(d) Late stage serum 189

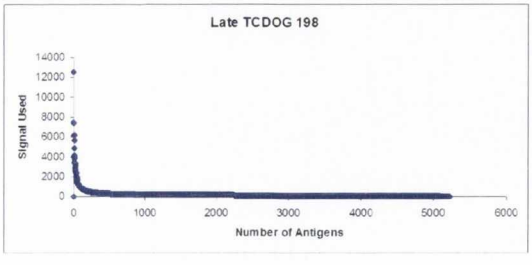

(e) Late stage serum 198

Figure 5.4: Signal values for antigens in late stage sample cohort

Table 5.4: Reactivities of reanalysed screened serum cohorts

This table gives an overview of the mean number and standard deviation of 'positives' for each cohort following the more rigorous analysis. Similarly to the previous analysis in Table 5.2 the standard deviation values are relatively high. However,

Cohort	Mean Number of "Hits"	Standard Deviation
Non-Remark	88	28
Benign	89	26
Early	163	105
Late	62	22

To compare the results of this reanalysed dataset, the previous analyses which compared the published autoantibody responses (as in Figure 5.3) to the hEx1 identified autoantibody responses (as in Figure 5.3) were again performed using the more stringent analysis. As in Figure 5.3, the analysis was re-performed, however in this instance AAb to these 5 antigens (8 antigens including variants) were not identified in any of the serum samples screened on the ProtoArrays.

5.4.2.1 Comparison to hEx1 Identified Autoantibody Responses

As in Figure 5.3 the analysis of the 33 antigens was re-performed using the new cut off value. Figure 5.5 shows the results of this reanalysis. These results are very different to the previous set of analyses, as there are now very few antigens identified as elliciting an AAb response. Most of the AAb responses identified are present in very low proportions of the patient serum cohorts. One antigen which may be of interest is 'RD RNA binding protein' (also known as negative elongation factor E (NELF-E)). AAbs to this antigen were identified in 40% (2/5) of the early stage ovarian cancer patients and in no other cohort, which is the first time that AAbs to NELF-E have been identified. This antigen is a member of the negative elongation factor (NELF) complex which causes transcriptional pausing and NELF is involved in inhibition of oestrogen-dependent growth of breast cancer cells [300]. Although a component of the

NELF complex (COBRA1) is a known cofactor of BRCA1, there have been very few studies that investigated the role of the NELF complex in ovarian cancer.

A comparative analysis was performed by comparing the results of hEx1 array screening (outlined in Figure 3.3) to determine the overlap between the hEx1 array results and the ProtoArray results (Figure 5.5) The resultant AAb responses, as determined by the two array platforms, for the common screened serum are indicated in Figure 5.6. This analysis was performed to determine AAb profiles in sera that were identified using both platforms. However, it is clear from this figure that there are very few overlapping results (indicated in purple). Only three positive AAb responses were identified as present in the two platforms.

5.4.3 Identification Autoantibodies Associated with Cohorts

To interrogate the results of ProtoArray screening further, the antigens that had the highest signal values for each serum sample were further analysed as outlined in Section 5.3.3. The resultant lists of cohort associated antigens were then compared to each other to identify AAb responses that may be associated with each of the cohorts interrogated. This analysis is represented as a venn diagram in Figure 5.7.

From the analysis in Figure 5.7 we can see that there is a very large number of immunogenic antigens identified in the early stage cohort, with relatively small numbers of antigens associated with the remaining cohorts. Notably, there is an antigen that is common to the late and early stage ovarian cancer cohorts, this antigen is angiomotin which is an angiostatin binding protein involved in the regulation of endothelial cell migration [301, 302]. Further investigation of the frequency of angiomotin AAbs in this study identified AAbs were present in 20% (1/5) of the non-remarkable cohort, none of the benign cohort, 80% (4/5) of the early stage cohort and 40% (2/5) of the late stage cohort. The angiomotin protein is a known inhibitor of angiogenesis and has

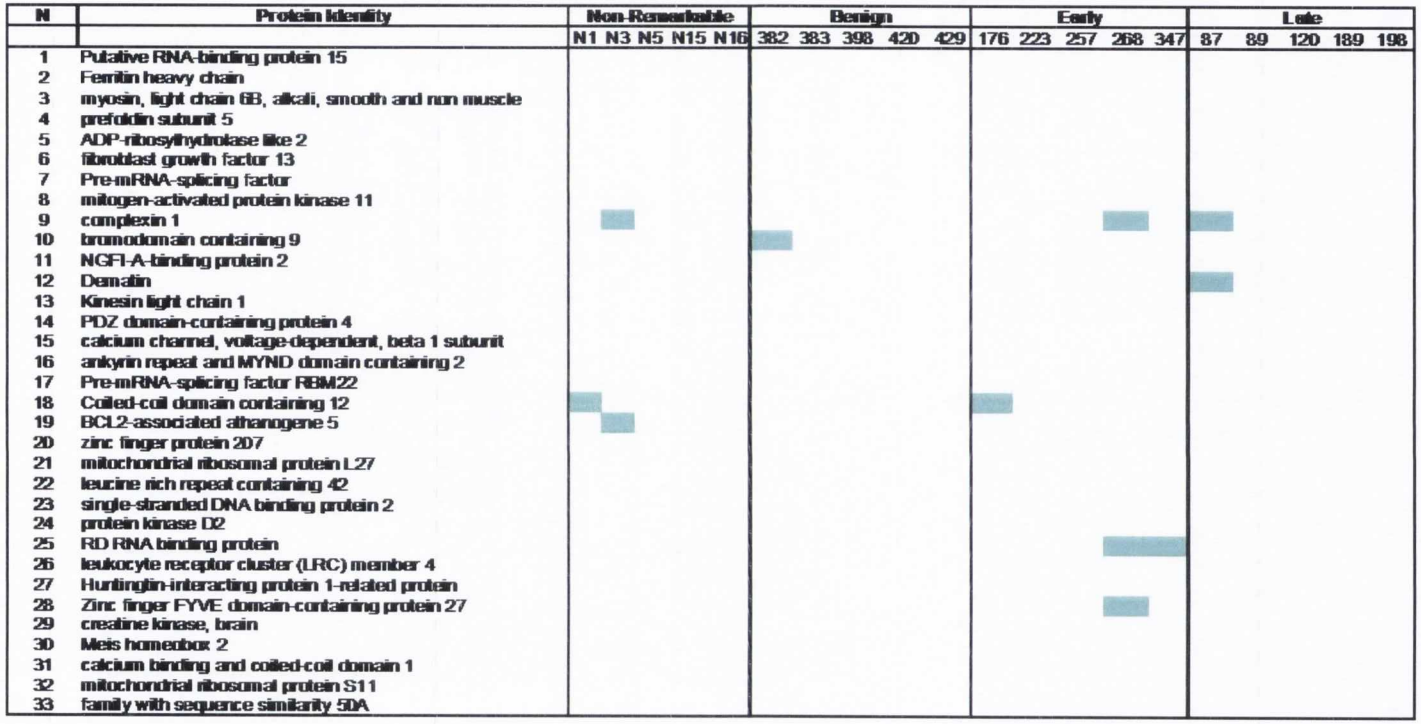

N	Protein Identity	Non-Remarkable					Benign					Early					Late				
		N1	N3	N5	N15	N16	382	383	398	420	429	176	223	257	268	347	87	89	120	189	198
1	Putative RNA-binding protein 15																				
2	Ferritin heavy chain																				
3	myosin, light chain 6B, alkali, smooth and non muscle																				
4	prefoldin subunit 5																				
5	ADP-ribosylhydrolase like 2																				
6	fibroblast growth factor 13																				
7	Pre-mRNA-splicing factor																				
8	mitogen-activated protein kinase 11																				
9	complexin 1																				
10	bromodomain containing 9																				
11	NGFI-A-binding protein 2																				
12	Dematin																				
13	Kinesin light chain 1																				
14	PDZ domain-containing protein 4																				
15	calcium channel, voltage-dependent, beta 1 subunit																				
16	ankyrin repeat and MYND domain containing 2																				
17	Pre-mRNA-splicing factor RBM22																				
18	Coiled-coil domain containing 12																				
19	BCL2-associated athanogene 5																				
20	zinc finger protein 207																				
21	mitochondrial ribosomal protein L27																				
22	leucine rich repeat containing 42																				
23	single-stranded DNA binding protein 2																				
24	protein kinase D2																				
25	RD RNA binding protein																				
26	leukocyte receptor cluster (LRC) member 4																				
27	Huntingtin-interacting protein 1-related protein																				
28	Zinc finger FYVE domain-containing protein 27																				
29	creatine kinase, brain																				
30	Meis homeobox 2																				
31	calcium binding and coiled-coil domain 1																				
32	mitochondrial ribosomal protein S11																				
33	family with sequence similarity 50A																				

Figure 5.5: Reanalysis of 33 overlap antigens

In this figure identified with blue boxes are the antigens that were deemed to have induced a very strong AAb response in the relevant serum.

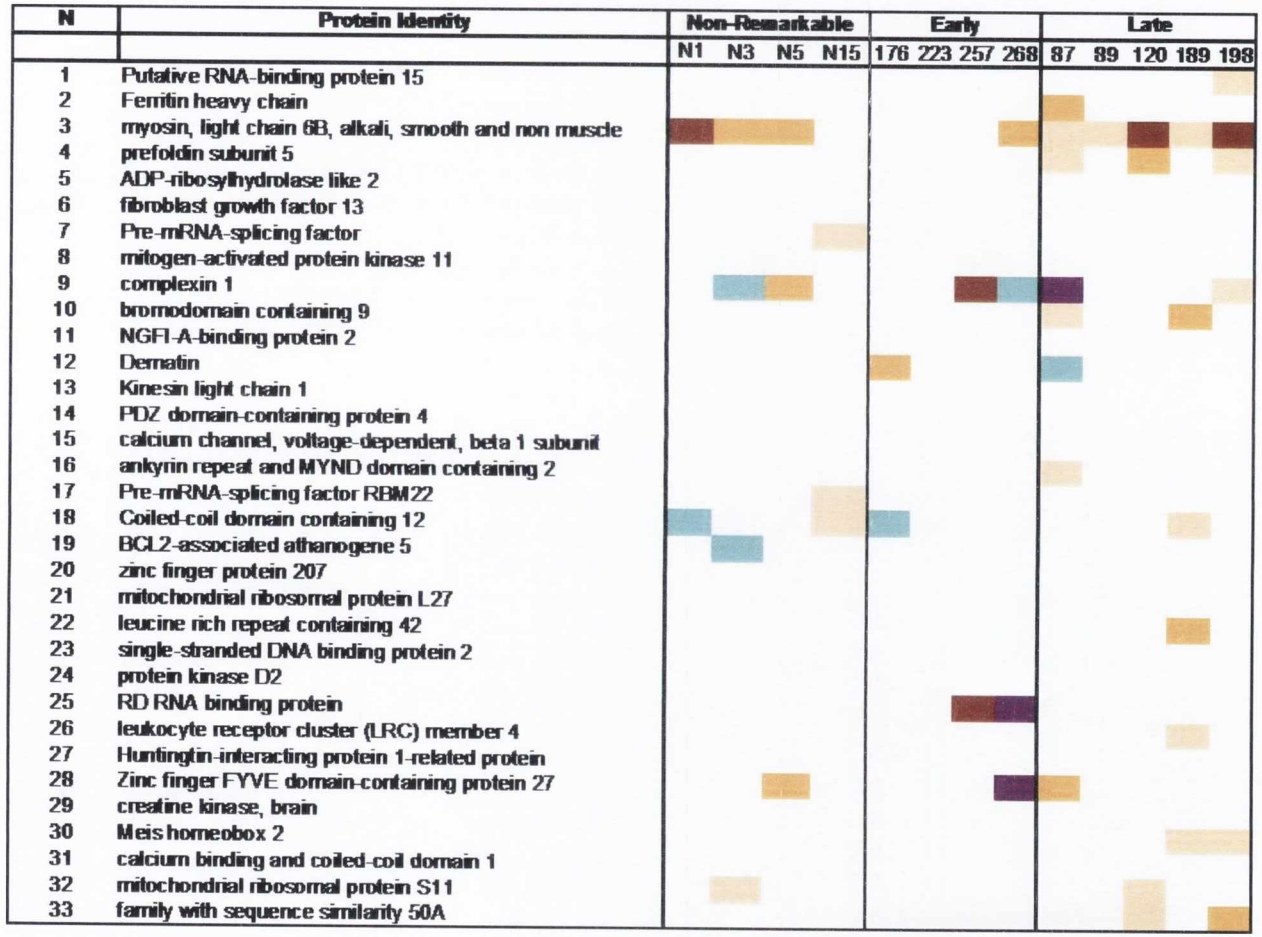

Figure 5.6: Assessment of common hEx1 and ProtoArray autoantibody profiles

In this figure identified with blue boxes are the antigens that were deemed to have induced a very strong AAb response using ProtoArray screening. The different shades of orange/brown boxes identify the antigens that were deemed to induce an AAb response using the hEx1 array. The antigens identified by the purple boxes were identified to induce an AAb response in both of these platforms.

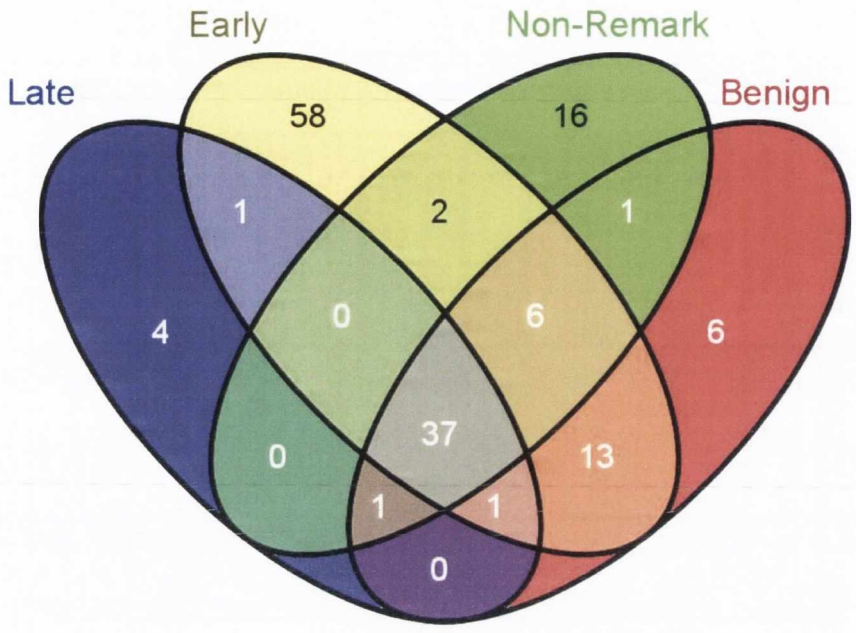

Figure 5.7: Overlap analysis of top antigens in cohorts

been shown to be linked to aggressive growth of breast tumours and also poor long term survival of breast cancer patients [303]. Experimental data on the effect that angiomotin exerts on ovarian tumours and hence the effects on patient survival is not available. However, from the results of this screening this would be an interesting future experiment. Also AAbs to angiomotin have not been previously described, however experimentation into a DNA vaccination targeting angiomotin has been shown to inhibit angiogenesis and tumour growth in mice [304]. Indeed, very recent findings by the same research group have shown that the titre of anti-angiomotin antibodies generated as a result of DNA vaccine correlates with tumour inhibition. This study also indicated that this tumour inhibition was associated with increase in tumour vessel diameter and permeability, formation of lacunar spaces, massive tumour perivascular necrosis and an effective epitope spreading that induces an immune response against other tumour associated antigens. The effect of chemotherapy (doxorubicin) was also shown to be

improved, presumably due to increased vessel permeability which aided delivery [305]. This data is very promising and although this data is based on a relatively small patient cohort the identification of AAbs to angiomotin in 80% of the early stage patient serum is a very exciting finding that should be interrogated in a larger patient cohort. It may also be the case that the relatively newly discovered angiomotin protein plays a very important role in ovarian cancer progression. Hence it is important to further investigate the role of AAbs to angiomotin in ovarian cancer. Although angiomotin AAbs may be indicative of disease they may also relate to patient prognosis and may play a role in slowing disease progression.

A list of the antigens that were identified as immunogenic in each of the four different cohorts were identified also (outlined in Table C.1), in the late stage ovarian cancer serum, four AAb identified to be late stage ovarian cancer associated. From investigation of these four antigens there seems to be a common link between these antigens relating to the cytoskeleton. Notably, 'pleckstrin homology domain-containing family O member 2', 'ral GEF with PH domain and SH3 binding motif 1' and 'annilin' antigens are all proteins that contain a pleckstrin homology (PH) domain. This domain, which is common in three of the four identified antigens, is known to occur in a variety of proteins involved in intracellular signalling or as constituents of the cytoskeleton [306, 307, 308]. The "annilin" antigen is also known to be required for completion of the cleavage furrow during cytokinesis [309]. Overexpression of PH domain containing proteins have been identified in ovarian carcinomas in previous studies [310]. This may indicate that these antigens or other antigens may have induced an AAb response that may be associated with the PH domain. Certainly of the 4 antigens that have been identified to be associated with the late stage ovarian cancer, 3 of these antigens contain a PH domain, this is a very high proportion (75%) and hence unlikely to have happen by chance. From Table 5.5 the frequency of these late stage associated antigens in all

the sera in all cohorts is outlined. From this figure is evident that there is a different profile for all of the antigens, even for the three antigens that contain the PH domain. This indicates that the AAb binding may not be PH domain specific, it may also be related to differential antigen domains, however this will need to be interrogated further utilising an overlapping peptide experiment to identify the immunogenic antigens.

Additional analyses, similar to Table 5.5 were also performed for the benign disease, early stage ovarian cancer and non-remarkable subject cohorts and are outlined in the Appendix in Tables C.3, C.4 and C.5 respectively.

In addition to the antigens associated with the individual serum cohorts, the identity of antigens that were present in all cohorts were also deemed of interest. Table C.2 lists the 37 antigens that were identified to be associated with all cohorts, as identified by the overlap of all ellipses in Figure 5.7. These antigens seem to be mainly associated with the secondary antibody binding as they are predominantly IgG regions, as listed in Table C.1. This is as expected as the detection antibody is anti-human IgG (H+L), which would interact with many of these IgG portions. The identification of these proteins in this study is as expected and confirms that the detection antibody is performing correctly.

5.4.4 Results of Pathway Analysis

Pathway analysis was performed to determine the over-represented pathways associated with each patient serum (5 sera in 4 cohorts, 20 sera in total), as in Section 2.6.3. Firstly analysis was carried out to identify the pathways that were present in 60% and above of each cohort, the overlap of these results are shown in Figure 5.8. The antigens corresponding to the numbers in Figure 5.8 are outlined in Table 5.6 for each of the four cohorts.

An additional analysis was carried out to identify the pathways that were present in

Table 5.5: Autoantibody frequency of late stage associated antigens

The frequency of AAbs to late stage associated antigens as determined in the screened set of 20 sera. As evident from this table, AAbs to these antigens are mainly associated with the late stage ovarian cancer cohort.

	Non-Remarkable					Benign					Early OC					Late OC				
	N1	N3	N5	N15	N16	382	383	398	420	429	176	223	257	268	347	87	89	120	189	198
Pleckstrin homology domain-containing family O member 2		Y															Y			Y
Ral GEF with PH domain and SH3 binding motif 1						Y											Y			Y
anillin, actin binding protein																		Y		Y
glial fibrillary acidic protein																	Y			Y

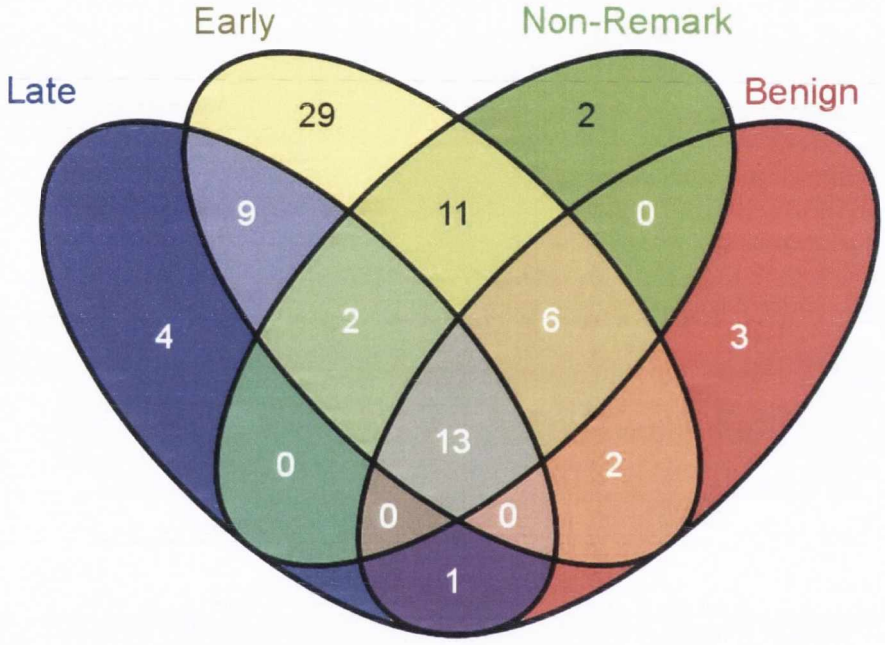

Figure 5.8: Overlap analysis of top pathways in cohorts

60% (3 of 5) or above of patients in a cohort and present in 20% (1/5) or less of serum from other cohorts. The pathways that fulfilled these criteria were deemed to be cohort associated. The results of this analysis are outlined in Table 5.6.

From the results of the overlap analysis to identify pathways over 60% in each cohort, (shown in Figure 5.8) and Table 5.6 outlines a subsection of these pathway that are identified in 20% or less of the other cohorts examined. It is evident from both these analyses that early stage ovarian cancer has a larger number of immunogenic pathways (n = 29) compared to the other cohorts examined. From the overlap analysis in Figure 5.8 the other cohorts have relatively few associated immunogenic pathways. Classically pathway dysregulation is thought to increase as a malignancy progresses from early to late stage, however the pathways identified in this study identify increased dysregulation in the early stages. This finding may be related to the immunoediting hypothesis of tumours [57, 98], this theory postulates that a tumour is more immunogenic in the early stages of tumour development compared to later stages [59, 97].

Outlined in Table 5.6 are the 9 pathways that were identified from all of the 82 pathways in Figure 5.8 to be present in 60% or above of patients in a cohort and in 20% or less of other cohorts. Hence only 11% of pathways first identified were identified to be truely cohort associated. Of these 9 pathways identified, 8 were early stage ovarian cancer associated.

The pentose phosphate pathway was identified to be an early stage ovarian cancer pathway in this study. This pathway generates nicotinamide adenine dinucleotide phosphate (NADPH) and pentoses in the cytoplasm of the cell. This pathway has not been identified to be ovarian cancer associated however it has been previously associated with oocyte maturation [311]. This pathway has also been identified to be associated with other malignancies [312]. The p38 mitogen-activated protein kinase (MAPK) cascade is a cellular stress induced response, hypoxia induced activation of this pathway

Table 5.6: Identification of pathways associated with cohorts

Shown in Figure 5.8 are the numbers of pathways associated with individual and overlapping cohorts. This table outlines the identities of the pathways that are specific to the individual cohorts. Notably, there seems to be very diverse pathway dysregulation associated with early stage ovarian cancer, compared to the other conditions.

Association	Pathway	Late OC	Early OC	Non-Remarkable	Benign
Early OC	Pentose phosphate pathway (hexose monophosphate shunt)	1/5 (20%)	4/5 (80%)	1/5 (20%)	1/5 (20%)
Early OC	P38 cascade (BMP2 signaling(through TAK1))	0/5 (0%)	3/5 (60%)	1/5 (20%)	1/5 (20%)
Early OC	JNK cascade (TNFR1 signaling pathway)	0/5 (0%)	4/5 (80%)	1/5 (20%)	0/5 (0%)
Early OC	TGF beta receptor I degradation signaling (TGF-beta super family signaling pathway(canonical))	1/5 (20%)	3/5 (60%)	1/5 (20%)	0/5 (0%)
Early OC	AKT(PKB)-GSK3 beta signaling	1/5 (20%)	4/5 (80%)	1/5 (20%)	0/5 (0%)
Early OC	IL5 signalling	0/5 (0%)	3/5 (60%)	1/5 (20%)	1/5 (20%)
Early OC	IL1 signalling	0/5 (0%)	3/5 (60%)	0/5 (0%)	0/5 (0%)
Early OC	ATF-2 transcription factor network	1/5 (20%)	3/5 (60%)	1/5 (20%)	0/5 (0%)
Benign	PDGFR-beta signaling pathway	1/5 (20%)	0/5 (0%)	0/5 (0%)	3/5 (60%)

is associated with ovarian cancer [313, 314]. A similar, stress induced pathway associated with early stage ovarian cancer was the c-Jun N-terminal kinase (JNK) cascade. The differential activation of this pathway has been shown to play a role in ovarian cancer cell viability following chemotherapy [315]. The particular signalling pathway, tumor necrosis factor receptor 1 (TNFR1), identified as part of this cascade has been identified to promote ovarian tumour progression [316]. TNFR1 is an antigen that is shed from the surface of ovarian cancer cells, it is proposed that this may facilitate tumour escape [317], in this study this shed antigen may have induced an AAb response. The TGF beta receptor I degradation signaling pathway and AKT(PKB)-GSK3 beta signaling were also identified as early stage ovarian cancer associated, these pathways have been linked as TGF-beta signalling is regulated through PKB/Akt [318]. Both these pathways have long been linked to various malignancies, including ovarian cancer [319, 320, 321, 322, 323, 324]. Two interleukin signaling pathways, IL1 and IL5, were identified as early ovarian cancer associated also. Publications relating to the association between IL1 and ovarian cancer are conflicting, with some studies indicating that IL1 is not ovarian cancer associated [325, 326], while other studies have found an association [327, 328]. There are relatively few studies that have investigated levels of IL5 and ovarian cancer association. However one study has identified that increased levels of IL5 are associated with high grade and advanced disease [206]. In this study all ovarian cancer patients are high grade, however IL5 signalling was predominantly associated with early stage disease. The activating transcription factor 2 (ATF-2) network, also identified as early stage ovarian associated in this study, has been previously identified as cancer associated [329]. The previously discussed p38 pathway can activate ATF-2 and ATF-2 also forms a homodimer or heterodimer with c-Jun and stimulates CRE-dependent transcription, linking it to other pathways identified in this study.

Only one pathway was identified in this study to be associated with a cohort other

than early stage ovarian cancer. That was the PDGFR-beta signaling pathway which was identified as benign ovarian disease assocaited. However this pathway has been long associated with cancer [330, 331].

The results of the immunogenic pathway analysis outlined here must be interpreted with caution. Although the samples are selected with care, the sample size is small with only 5 patients in each cohort. The non-remarkable patients that were profiled in this study are representative of the normal population, they have not been examined or determined to be cancer free, this is a limitation of this study. Also classical pathway analysis is used to identify pathways which are upregulated, downregulated or dysregulated, however from AAb profiling these conditions cannot be commented upon with any certainty. Although, in the case of AAb responses to some antigens, upregulation of an antigen is sufficient to trigger an AAb response, this is certainly not the case for all antigens. The pathways indicated in this study are referred to as "immunogenic", the exact reason why the antigens that make up these pathways are immunogenic is not determined. As mentioned previously, limited studies have interrogated signalling pathways identified from AAb profiling. Certainly, this approach may have the potential to identify minute and subtle alterations in pathway signalling through immunogenic triggering that identifies abnormalities in individuals. Interesting comparisons can be made, however the utility of interrogating signalling pathways identified by autoantibody profiling has yet to be determined.

5.5 Discussion

The Invitrogen ProtoArrays are a very powerful platform and one of the largest collections of arrayed proteins available. The ProtoArrays were used in this study to identify AAb profiles in well characterised cohorts of non-remarkable, benign ovarian disease, early and late stage ovarian cancer patient serum.

From the results of ProtoArray screening there are a number of potentially interesting antigens that have been identified to be associated with ovarian cancer. The patient serum samples used in this study were all very well characterised and collected uniformly, thus limiting variation associated with sample collection and storage. However the sample size is relatively small which may result in misleading results in some cases. Additional cohorts of serum are needed to confirm and validate the results obtained in this study. The validation would need to be performed on a large cohort of ovarian cancer patient serum, encompassing all histological subtypes, but in particular papillary serous histology as this was the histotype interrogated in this research. Also, serum from patients with other benign conditions and malignancies would need to be included in the validation to determine ovarian cancer specificity of the AAb responses. In relation to interrogation of angiomotin AAbs, as this profile was associated with early stage serous papillary ovarian cancer serum, additional serum from this subtype of ovarian cancer would also be needed. This serum is very rare as ovarian cancer is not usually diagnosed in early stage.

In general it is thought that the AAb response is enduring and that AAbs that arise during the early stages of cancer development may also be present in late stage ovarian cancer patient sera. However in this study there is a trend that an increased number of antigens and pathways have been associated with the early stage ovarian cancer cohort compared to the late stage cohort. This may relate to the immunoediting hypothesis of cancer, whereby early stage tumours are proposed to more immunogenic

than their late stage counterparts, this is an evolutionary model of tumorigenesis [99, 57, 98, 109]. However, in the case of the classic tumour protein p53, studies have identified a relationship between the p53 AAb response and tumour status as patients undergo treatment [332, 333, 201]. AAb titres to the p53 protein have been shown to decrease or even disappear in patients with different types of cancer once the malignant tumour had been surgically removed [334, 335, 336]. Monitoring of the titres of p53 AAbs have also been shown to correlate well with patient response during treatment [337, 335]. It seems likely that an AAb reponse generated to an early stage antigen may not be present when the tumour is in the later stages, assuming that a late stage tumour arose from the early stage tumour (which may not always be the case in ovarian cancer, outlined in Secion 1.2.1). All potential tumour associated AAb responses are inevitiably compared to the p53 AAb response, however different antigens may induce very different immunogenic responses. The AAb response to certain antigens may remain, although that antigen is no longer presented to the immune system, however AAb responses to other antigens may decline once the antigen is no longer present. Interrogation into the AAb response in patients that is ellicited as a result of tumourigenesis is very poorly understood, indeed the mechanism by which the best known immunogenic cancer antigen, p53 is presented to the immune system is still unknown [259, 338].

5.6 Conclusion

The Invitrogen ProtoArrays were employed in this study to identify ovarian cancer associated AAb profiles in patient serum. AAbs to angiomotin were identified as early stage ovarian cancer associate, this finding partially fulfills the aim of this study, unfortunately a late stage ovarian cancer profile as robust as the early stage disease was not identified in this study. However, these results will need to be investigated in a

larger early stage ovarian cancer cohort. Very little is known about AAb generation in response to malignancy, however in this research early stage ovarian cancer shows a tendency to ellicit a more diverse AAb response. This may uncover details of AAb generation and malignant tumour progression.

This research aimed to outline the differences between the AAb responses identified by two different array profiling methodologies. The results identify differences in AAb profiles, depending on the platform used for serum screening. Care must be taken when comparing discovery platforms as differences in antigen expression, length, structure and purity will all impact AAb recognition and binding. Minimising the differences between platforms may assist in increasing AAb profile validation in additional patient serum.

Chapter 6

General Discussion

6.1 Introduction

Biomarkers or human disease markers are proteins or molecules that can be measured in a patient's tissue or body fluid as a measure of biologic state or specific state and therefore may be indicative of pathological processes [121]. Autoantibodies - antibodies directed against the individuals own proteins, may also be indicative of diseases such as cancers, and the specificity and distinction of autoantibody responses for certain diseases highlight their potential as important tools for improved diagnosis, classification and prognostication [95, 339]. As ovarian cancer is classically diagnosed at a late stage and is particularly refractory, the development of a routine test for earlier diagnosis of ovarian cancer has the potential to transform ovarian cancer patient survival and care. AAbs to ovarian tumour associated antigens have been identified in cancer patient serum in previous studies [140, 162, 340], but as of yet an AAb based diagnostic test for ovarian cancer has yet to materalise in the hands of the clinician.

Generation of protein array platforms and screening of human serum for detection of disease associated AAb profiling has been performed previously in this research group [174, 175, 179, 187, 192, 233, 341], and this experience was exploited to profile ovarian cancer patient serum. The aim of this study was to identify ovarian cancer associated AAb profiles, and to investigate these profiles to determine if AAbs may be used in a di-

agnostic assay format to identify ovarian malignancy. Profiling of the AAb response was successfully performed in serum from ovarian cancer patients, benign disease subjects and non-remarkable controls. AAb profiles that were associated with ovarian cancer were also successfully identified using all discovery platforms assessed in this study. A limited number of autoantibody responses were validated by secondary methodologies, the p53 AAb response was identified to be the most robust response identified. The lack of reproducibility and validation in secondary validation platforms was disappointing and highlighted the high attrition rate associated with biomarker identification and validation (As outlined in Figure 6.1). The study hypothesis was confirmed that AAb profiles do exist in ovarian cancer patients, however, the hypothesis that AAb responses could be validated in secondary platforms is only partially confirmed. In this research a small number of AAb responses were validated in secondary platforms, although IgG interactions are specific in nature, conversion of protein array AAb profiling to secondary platforms is very challenging. Further investigation is needed to streamline this process, as outlined here secondary screening may assist is identifying the most robust AAb responses for further interrogation.

6.2 Additions to Current Knowledge of the Tumour Associated Autoantibody Profile

In this study three different high-content protein array platforms were used as AAb discovery tools, the Imagenes hEx1 expression library, the in-house hEx1 protein microarray and the Invitrogen ProtoArray platform. The hEx1 expression library and the ProtoArray have been validated for identification of biomarkers by different groups [233, 174, 131, 173, 137]. In this research, secondary platforms were also used for interrogation of the identified AAb profiles. This study, to our knowledge was the first to examine the AAb profile in ovarian cancer patients using the hEx1 array platform and

the ProtoArray V5 platform. This study was also the first to employ a direct ELISA to interrogate an AAb response as identified by hEx1 array screening. AAb profiles were identified in the different methodologies used, there were common and diverse profiles which were dependent on the platform used. However, it was expected that AAb profiles that were common to both platforms would have the greatest potential for adaptation into ELISA format.

6.2.1 Epitope Presentation

This research has investigated many different protein platforms to assess the AAb profile in human serum. Our results have indicated that AAb profiles may be platform specific and hence will not be easily adapted into a secondary platform in most cases. As mentioned above, many research groups have used the hEx1 arrays to identify AAb profiles associated with malignancy and report very high sensitivity and specificity values. However secondary validation is not carried out in many of these studies and validation using ELISA has not been reported. Although AAb biomarkers of malignancy hold great promise, as of yet they have not translated to the clinic. We have outlined in this study that it is very difficult to adapt AAb profiles identified using the hEx1 array, into another platform such as ELISA, protein microarray or Western immunoblot.

For all antigens assessed, Western immunoblotting exhibited the highest sensitivity for detection of AAbs in patient serum, while ELISA exhibited the lowest sensitivity, the hEx1 array screening exhibited an intermediate sensitivity. The various AAb sensitivities in the different platforms seems to reflect the antigen structure and hence epitope presentation. Western immunoblotting presents a fully denatured and linearised peptide sequence, while antigens in the ELISA platform, following dilution prior to coating, may refold. It is likely that the hEx1 array proteins which are denatured and immobilised on membranes *in situ* are highly unfolded polypeptides. Previous studies of the

classic p53 AAb response indicated that recognition of p53 epitopes by specific AAbs is preferentially, non conformational [342, 343, 344]. This reflects the results of this study where Western immunoblotting, which presents non-conformational epitopes is the most sensitive methodology. This research has highlighted various AAb binding profiles in different platforms, which also differs depending on the antigen assessed. It is of great importance to consider the antigenic determinant to which the AAb binds when identified using high throughput array for discovery.

The differences in AAb profiles to antigens between the hEx1 array platform and the ProtoArray platform are very evident in this study also. However these two array platforms are very different and it is perhaps not surprising that diverse AAb profiles are identified. Post-translational modifications (PTM) are known to affect AAb recognition and binding [112], the ProtoArrays were the only platform used in this study that contained antigens that were post-translationally modified. The different platforms, methodologies and antigens presented all contribute to antibody binding, hence the complexity of autoantibody profiling of patient serum is compounded.

6.2.2 Autoantibodies to p53

The classic p53 AAb response is the most interrogated AAb profile associated with cancer. Our research corresponds with previously published results which identify p53 AAbs in 25% of the late stage ovarian cancer patients [206, 209, 345]. This AAb was by far the most robust response identified in this research. AAbs to the p53 protein were identified with very similar frequency in all the platforms researched, and in the majority of patient sera there was a clear distinction between sera that was p53 AAb positive and sera that was p53 AAb negative. However there were also differences between platforms for this antigen, it is known that the immunogenic p53 epitopes are predominantly linear and our research identified that Western immunoblotting was the

most sensitive platform to identify p53 immunoreactivity in patient serum. As AAbs to p53 have been proposed as clinically useful cancer biomarkers, this study highlights the importance of assay development and optimum epitope presentation to ensure reliable and sensitive detection of p53 AAbs in patient serum.

Previous studies that have interrogated the relationship between the p53 AAb response and tumour grade have been conflicting, some studies have not found a relationship between the p53 AAb response and tumour grade [204, 345], while others have [208, 209, 205]. Our research has identified AAbs to p53 predominantly in high grade tumours, this agrees with the majority of recent publications.

6.2.3 Autoantibodies to Adducin

This study was the first, to our knowledge, that identified adducin alpha AAbs in ovarian cancer patient serum. From our results AAbs to adducin alpha were identified in a subset of patients with ovarian tumours (benign and malignant) and in none of the non-remarkable control subjects. Although this study has a relatively small sample size there is an indication that AAbs to adducin may be of use as an ovarian tumour biomarker. In particular AAbs to this antigen, unlike the p53 AAb response, are present in comparable proportions of all of the disease serum samples. This in particular may indicate the alpha adducin AAbs may not be tumour stage or type associated. Further analysis of AAbs to the adducin alpha product is needed to determine if these AAbs are present in all ovarian cancer histotypes and stages, and also in the serum of patients with other types of cancer and benign conditions.

6.2.4 Autoantibodies to Other Novel Antigens

Many hundreds of AAbs have been identified to be potentially associated with ovarian cancer in this study. AAbs to DDB1 and CUL4 associated factor were identified from hEx1 array screening to be of interest. ELISA analysis confirmed that AAbs to this antigen are present in 10% of late stage ovarian cancer patients. AAbs to this antigen have not been previously identified to be ovarian cancer associated. Further validation on a larger serum sample cohort is needed to determine the sensitivity and specificity of AAbs to this antigen.

Using ProtoArray screening, AAbs to angiomotin were identified in 80% of early stage serous papillary ovarian cancer patients. To our knowledge, this is the first study to identify an AAb response to the angiomotin protein. In this study, AAbs to angiomotin were present in early stage ovarian cancer patient with high sensitivity. Although the sample size in this study is small, this is a promising result as early stage ovarian cancer diagnosis, particularly for high grade lesions would dramatically improve patient survival rates.

This research has consistently identified early stage ovarian cancer as having a higher number of immunoreactive antigens. This is an interesting finding that, to our knowledge may have been identified but has not been discussed on other AAb profiling studies. This finding should be interrogated further as AAbs, which are important reporters of the immune system may provide insight into tumour immunology.

6.3 Future Directions

This study has identified ovarian cancer associated AAb profiles, the ultimate goal of AAb profiling research is to identify AAb biomarkers of disease for use in a diagnostic assay format. However there are many hurdles to overcome as assay development is a

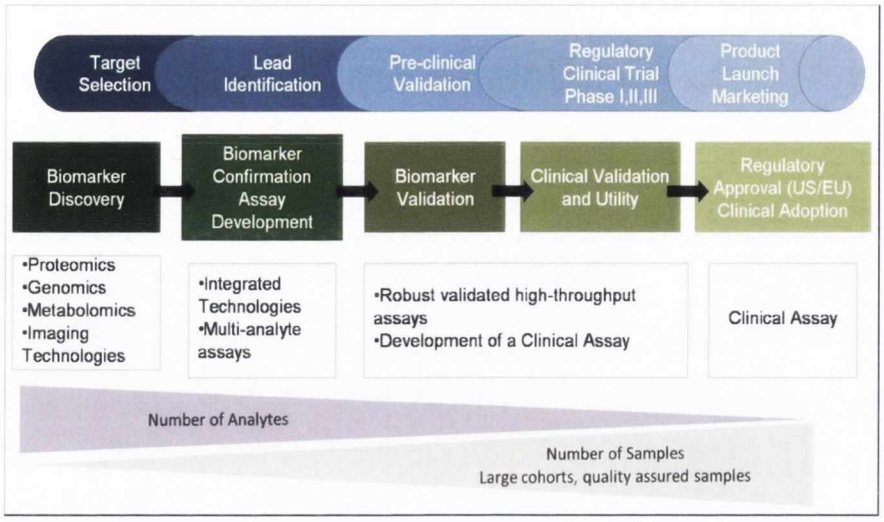

Figure 6.1: Classical biomarker identification and assay development pathway
This flowchart outlines the biomarker assay development pathway. This process starts with biomarker discovery, which was performed in this work and moves onto biomarker confirmation and assay development. As part of this research, lead identification was performed and an assay for detection of autoantibodies to p53 was developed. There are many other antigens that may be of biomarker utility that were identified in this study, further validation for these antigens is needed.

laborious and difficult process (Figure 6.1).

To investigate the AAb profiles identified in this study, further additional, well characterised ovarian disease and cancer patient serum is needed for validation. Ovarian cancer is quite an uncommon disease. In Ireland there are only 350 new cases diagnosed each year, this is relatively few when compared to more common cancers such as breast (2,518 cases in Ireland per year). As ovarian cancer is frequently diagnosed in the latter stages of the disease, early stage ovarian cancer serum, is rare and very precious. Currently our research group is in negotiations with the United Kingdom Collaborative Trial of Ovarian Cancer Screening (UKCTOCS) to gain access to a larger serum sample cohort. The ongoing UKCTOCS trial has recruited over 200,000 women, samples attained from this trial could be used for interrogation and validation of the identified AAb profiles. The UKCTOCS trial serum samples have been attained from patients prior to clinical presentation of ovarian cancer. It is hoped that the AAb profile

has the ability to identify malignant transformation prior to clinical presentation of the disease, this has been shown for p53 AAbs in different cancers [143, 264], but has not been investigated in ovarian cancer. As we have optimised an ELISA that detects p53 AAbs in patient sera this could be performed effectively and efficiently in our research group. Additional AAb profiles may also be validated in this manner to determine when a malignant associated AAb profile first manifests. This study may assist in the identification of an AAb biomarker that identifies ovarian malignancy prior to clinical presentation when patients are most curable and may also enhance and further the understanding of the AAb profile and its generation. Along with further investigation of the p53 AAb response, further investigation of the AAb responses to adducin alpha, DDB1 and CUL4 associated factor and angiomotin in particular is warranted. These AAb responses were identified to be of particular interest in ovarian tumour patients, late stage ovarian cancer patients and early stage ovarian cancer patients respectively.

This study has outlined the difficulties involved in transferring results from one platform to another. Peptide arrays are of great interest and importance when it comes identifying the individual epitopes that are immunoreactive in the antigen [234]. Determination of the immunogenic epitopes and the use of these peptides in secondary platforms could act to increase the concordance between platforms and hence ease the validation of the AAb responses in the various secondary platforms. Identification of the immunogenic epitopes could also reveal the method of immune presentation.

The AAb response is still very poorly understood, throughout this research we have used the p53 AAb response as a benchmark on which to base our results. However, even in the case of the p53 AAb response, nothing is known about the generation of this response. AAb profiling has been used predominantly to identify AAb or antigen biomarkers of disease, however the lack of knowledge about AAb generation compounds the complexity of the AAb profile. Future studies that profile the AAb response in

animal models at different stages during tumour development would provide insight into the alterations in the AAb profile during tumour progression. Ultimately further knowledge of the tumour associated AAb profile will assist in the employment of the AAb repertoire as a biomarker.

Bibliography

[1] R. Siegel, E. Ward, O. Brawley, and A. Jemal. Cancer statistics, 2011: the impact of eliminating socioeconomic and racial disparities on premature cancer deaths. *CA - A Cancer Journal for Clinicians*, 61(4):212–36, 2011.

[2] B. D. Smith, G. L. Smith, A. Hurria, G. N. Hortobagyi, and T. A. Buchholz. Future of cancer incidence in the united states: burdens upon an aging, changing nation. *Journal of Clinical Oncology*, 27(17):2758–65, 2009.

[3] C. Erikson, E. Salsberg, G. Forte, S. Bruinooge, and M. Goldstein. Future supply and demand for oncologists : challenges to assuring access to oncology services. *Journal of Oncology Practice*, 3(2):79–86, 2007.

[4] I. Bozic, T. Antal, H. Ohtsuki, H. Carter, D. Kim, S. Chen, R. Karchin, K. W. Kinzler, B. Vogelstein, and M. A. Nowak. Accumulation of driver and passenger mutations during tumor progression. *Proceedings of the National Academy of Sciences of the United States of America*, 107(43):18545–50, 2010.

[5] A. Marusyk and J. DeGregori. Declining cellular fitness with age promotes cancer initiation by selecting for adaptive oncogenic mutations. *Biochimica Biophysica Acta*, 1785(1):1–11, 2008.

[6] A. Jemal, R. Siegel, J. Xu, and E. Ward. Cancer statistics, 2010. *CA, A Cancer Journal for Clinicians*, 60(5):277–300, 2010.

[7] D. Hanahan and R. A. Weinberg. The hallmarks of cancer. *Cell*, 100(1):57–70, 2000.

[8] D. Hanahan and R. A. Weinberg. Hallmarks of cancer: the next generation. *Cell*, 144(5):646–74, 2011.

[9] M. T. Hemann, A. Bric, J. Teruya-Feldstein, A. Herbst, J. A. Nilsson, C. Cordon-Cardo, J. L. Cleveland, W. P. Tansey, and S. W. Lowe. Evasion of the p53 tumour surveillance network by tumour-derived myc mutants. *Nature*, 436(7052):807–11, 2005.

[10] S. Pelengaris, M. Khan, and G. Evan. c-myc: more than just a matter of life and death. *Nature Reviews, Cancer*, 2(10):764–76, 2002.

[11] C. V. Dang, A. Le, and P. Gao. Myc-induced cancer cell energy metabolism and therapeutic opportunities. *Clinical Cancer Research*, 15(21):6479–83, 2009.

[12] J. D. Kessler, K. T. Kahle, T. Sun, K. L. Meerbrey, M. R. Schlabach, E. M. Schmitt, S. O. Skinner, Q. Xu, M. Z. Li, Z. C. Hartman, M. Rao, P. Yu, R. Dominguez-Vidana, A. C. Liang, N. L. Solimini, R. J. Bernardi, B. Yu, T. Hsu, I. Golding, J. Luo, C. K. Osborne, C. J. Creighton, S. G. Hilsenbeck, R. Schiff,

C. A. Shaw, S. J. Elledge, and T. F. Westbrook. A sumoylation-dependent transcriptional subprogram is required for myc-driven tumorigenesis. *Science*, 335(6066):348–53, 2012.

[13] W. K. Cavenee and R. L White. The genetic basis of cancer. *Scientific American*, March:72–79, 1995.

[14] D. W. Meek. Tumour suppression by p53: a role for the dna damage response? *Nature Reviews, Cancer*, 9(10):714–23, 2009.

[15] Y. Yin and W. H. Shen. Pten: a new guardian of the genome. *Oncogene*, 27(41):5443–53, 2008.

[16] D. P. Lane. Cancer. p53, guardian of the genome. *Nature*, 358(6381):15–6, 1992.

[17] A.J. Levine. p53, the cellular gatekeeper review for growth and division. *Cell*, 88:323–331, 1997.

[18] N. Stewart, G. G. Hicks, F. Paraskevas, and M. Mowat. Evidence for a second cell cycle block at g2/m by p53. *Oncogene*, 10(1):109–15, 1995.

[19] V. Zuckerman, K. Wolyniec, R. V. Sionov, S. Haupt, and Y. Haupt. Tumour suppression by p53: the importance of apoptosis and cellular senescence. *Journal of Pathology*, 219(1):3–15, 2009.

[20] R. Vang, M. Shih Ie, and R. J. Kurman. Ovarian low-grade and high-grade serous carcinoma: pathogenesis, clinicopathologic and molecular biologic features, and diagnostic problems. *Advances in Anatomic Pathology*, 16(5):267–82, 2009.

[21] C. A. Pettigrew and T. G. Cotter. Deregulation of cell death (apoptosis): implications for tumor development. *Discovery Medicine*, 8(41):61–3, 2009.

[22] M. H. Kang and C. P. Reynolds. Bcl-2 inhibitors: targeting mitochondrial apoptotic pathways in cancer therapy. *Clinical Cancer Research*, 15(4):1126–32, 2009.

[23] Y. Wei, S. Pattingre, S. Sinha, M. Bassik, and B. Levine. Jnk1-mediated phosphorylation of bcl-2 regulates starvation-induced autophagy. *Molecular Cell*, 30(6):678–88, 2008.

[24] W. J. Placzek, J. Wei, S. Kitada, D. Zhai, J. C. Reed, and M. Pellecchia. A survey of the anti-apoptotic bcl-2 subfamily expression in cancer types provides a platform to predict the efficacy of bcl-2 antagonists in cancer therapy. *Cell Death & Disease*, 1:e40, 2010.

[25] Y. Lin, J. Fukuchi, R. A. Hiipakka, J. M. Kokontis, and J. Xiang. Up-regulation of bcl-2 is required for the progression of prostate cancer cells from an androgen-dependent to an androgen-independent growth stage. *Cell Research*, 17(6):531–6, 2007.

[26] H. J. Cho, J. K. Kim, K. D. Kim, H. K. Yoon, M. Y. Cho, Y. P. Park, J. H. Jeon, E. S. Lee, S. S. Byun, H. M. Lim, E. Y. Song, J. S. Lim, D. Y. Yoon, H. G. Lee, and Y. K. Choe. Upregulation of bcl-2 is associated with cisplatin-resistance via inhibition of bax translocation in human bladder cancer cells. *Cancer Letters*, 237(1):56–66, 2006.

[27] R. C. Bast, B. Hennessy, and G. B. Mills. The biology of ovarian cancer: new opportunities for translation. *Nature Reviews, Cancer*, 9(6):415, 2009.

[28] R. Henriksen, E. Wilander, and K. Oberg. Expression and prognostic significance of bcl-2 in ovarian tumours. *British Journal of Cancer*, 72(5):1324–9, 1995.

[29] J. J. Herod, A. G. Eliopoulos, J. Warwick, G. Niedobitek, L. S. Young, and D. J. Kerr. The prognostic significance of bcl-2 and p53 expression in ovarian carcinoma. *Cancer Research*, 56(9):2178–84, 1996.

[30] F. Iovino, F. Ferraraccio, M. Orditura, G. Antoniol, F. Morgillo, T. Cascone, M. R. Diadema, G. Aurilio, G. Santabarbara, R. Ruggiero, C. Belli, E. Irlandese, M. Fasano, F. Ciardiello, E. Procaccini, F. Lo Schiavo, G. Catalano, and F. De Vita. Serum vascular endothelial growth factor (vegf) levels correlate with tumor vegf and p53 overexpression in endocrine positive primary breast cancer. *Cancer Investigation*, 26(3):250–5, 2008.

[31] G. Neufeld, T. Cohen, S. Gengrinovitch, and Z. Poltorak. Vascular endothelial growth factor (vegf) and its receptors. *The FASEB Journal*, 13(1):9–22, 1999.

[32] A. Latil, I. Bieche, S. Pesche, A. Valeri, G. Fournier, O. Cussenot, and R. Lidereau. Vegf overexpression in clinically localized prostate tumors and neuropilin-1 overexpression in metastatic forms. *International Journal of Cancer*, 89(2):167–71, 2000.

[33] J. Delli Carpini, A. K. Karam, and L. Montgomery. Vascular endothelial growth factor and its relationship to the prognosis and treatment of breast, ovarian, and cervical cancer. *Angiogenesis*, 13(1):43–58, 2010.

[34] N. Ferrara, K.J. Hillan, and W. Novotny. Bevacizumab (avastin), a humanized anti-vegf monoclonal antibody for cancer therapy. *Biochemical and biophysical research communications*, 333:328–335, 2005.

[35] F. F. Kabbinavar, J. Hambleton, R. D. Mass, H. I. Hurwitz, E. Bergsland, and S. Sarkar. Combined analysis of efficacy: the addition of bevacizumab to fluorouracil/leucovorin improves survival for patients with metastatic colorectal cancer. *Journal of Clinical Oncology*, 23(16):3706–12, 2005.

[36] F. Barlesi, J. de Castro, V. Dvornichenko, J. H. de Kim, A. Pazzola, A. Rittmeyer, A. Vikstrom, L. Mitchell, E. K. Wong, and V. Gorbunova. Avaperl (mo22089): Final efficacy outcomes for patients (pts) with advanced non-squamous non-small cell lung cancer (nsnsclc) randomised to continuation maintenance (mtc) with bevacizumab (bev) or bev plus pemetrexed (pern) after first-line (1l) bev-cisplatin (cis)pem treatment (tx). *Computational Statistics & Data Analysis*, 47:16–16, 2011.

[37] T. J. Perren, A. M. Swart, J. Pfisterer, J. A. Ledermann, E. Pujade-Lauraine, G. Kristensen, M. S. Carey, P. Beale, A. Cervantes, C. Kurzeder, A. du Bois, J. Sehouli, R. Kimmig, A. Stahle, F. Collinson, S. Essapen, C. Gourley, A. Lortholary, F. Selle, M. R. Mirza, A. Leminen, M. Plante, D. Stark, W. Qian, M. K. Parmar, A. M. Oza, and Icon Investigators. A phase 3 trial of bevacizumab in ovarian cancer. *New England Journal of Medicine*, 365(26):2484–96, 2011.

[38] A. Ohtsu, M. A. Shah, E. Van Cutsem, S. Y. Rha, A. Sawaki, S. R. Park, H. Y. Lim, Y. Yamada, J. Wu, B. Langer, M. Starnawski, and Y. K. Kang. Bevacizumab in combination with chemotherapy as first-line therapy in advanced gastric cancer: a randomized, double-blind, placebo-controlled phase iii study. *Journal of Clinical Oncology*, 29(30):3968–76, 2011.

[39] W. A. Spannuth, A. K. Sood, and R. L. Coleman. Angiogenesis as a strategic target for ovarian cancer therapy. *Nature Clinical Practice Oncology*, 5(4):194–204, 2008.

[40] M. M. Ouellette, W. E. Wright, and J. W. Shay. Targeting telomerase-expressing cancer cells. *Journal of Cellular and Molecular Medicine*, 15(7):1433–42, 2011.

[41] C. B. Harley. Telomerase and cancer therapeutics. *Nature Reviews, Cancer*, 8(3):167–79, 2008.

[42] J. W. Shay and W. E. Wright. Role of telomeres and telomerase in cancer. *Seminars in Cancer Biology*, 21(6):349–53, 2011.

[43] C. M. Counter, W. C. Hahn, W. Wei, S. D. Caddle, R. L. Beijersbergen, P. M. Lansdorp, J. M. Sedivy, and R. A. Weinberg. Dissociation among in vitro telomerase activity, telomere maintenance, and cellular immortalization. *Proceedings of the National Academy of Sciences of the United States of America*, 95(25):14723–8, 1998.

[44] K. Masutomi, S. Kaneko, M. Yasukawa, K. Arai, S. Murakami, and K. Kobayashi. Identification of serum anti-human telomerase reverse transcriptase (htert) auto-antibodies during progression to hepatocellular carcinoma. *Oncogene*, 21(38):5946–50, 2002.

[45] P. Mehlen and A. Puisieux. Metastasis: a question of life or death. *Nature Reviews, Cancer*, 6(6):449–58, 2006.

[46] P. S. Steeg. Tumor metastasis: mechanistic insights and clinical challenges. *Nature Medicine*, 12(8):895–904, 2006.

[47] G. P. Gupta and J. Massague. Cancer metastasis: building a framework. *Cell*, 127(4):679–95, 2006.

[48] S. Valastyan and R. A. Weinberg. Tumor metastasis: molecular insights and evolving paradigms. *Cell*, 147(2):275–92, 2011.

[49] S.A. Brooks, H.J. Lomax-Browne, T.M. Carter, C.E. Kinch, and D. Hall. Molecular interactions in cancer cell metastasis. *Acta histochemica*, 112:3–25, 2010.

[50] J. Wels, R.N. Kaplan, S. Rafii, and D. Lyden. Migratory neighbors and distant invaders: tumor-associated niche cells. *Genes & development*, 22:559–574, 2008.

[51] E. C. Nakajima and B. Van Houten. Metabolic symbiosis in cancer: Refocusing the warburg lens. *Molecular Carcinogenesis*, Epub ahead of print, 2012.

[52] R. A. Cairns, I. S. Harris, and T. W. Mak. Regulation of cancer cell metabolism. *Nature Reviews, Cancer*, 11(2):85–95, 2011.

[53] G. Kroemer and J. Pouyssegur. Tumor cell metabolism: cancer's achilles' heel. *Cancer Cell*, 13(6):472–82, 2008.

[54] X. D. Zhang, Z. H. Qin, and J. Wang. The role of p53 in cell metabolism. *Acta Pharmacologica Sinica*, 31(9):1208–12, 2010.

[55] J. W. Kim and C. V. Dang. Cancer's molecular sweet tooth and the warburg effect. *Cancer Research*, 66(18):8927–30, 2006.

[56] L. M. Merlo, J. W. Pepper, B. J. Reid, and C. C. Maley. Cancer as an evolutionary and ecological process. *Nature Reviews, Cancer*, 6:924–35–, 2006.

[57] G. P. Dunn, L. J. Old, and R. D. Schreiber. The three es of cancer immunoediting. *Annual Review of Immunology*, 22:329–60, 2004.

[58] B. Huang, J. Zhao, J. C. Unkeless, Z. H. Feng, and H. Xiong. Tlr signaling by tumor and immune cells: a double-edged sword. *Oncogene*, 27:218–24–, 2008.

[59] N. Chaput, R. Conforti, S. Viaud, A. Spatz, and L. Zitvogel. The janus face of dendritic cells in cancer. *Oncogene*, 27:5920–31, 2008.

[60] M. A. Murphy, J. J. O'Leary, and D. J. Cahill. Assessment of the humoral immune response to cancer. *Journal of Proteomics*, Epub ahead of print, 2012.

[61] S. A. Cannistra. Cancer of the ovary. *New England Journal of Medicine*, 351:2519–29, 2004.

[62] C. Vo and M. E. Carney. Ovarian cancer hormonal and environmental risk effect. *Obstetrics & Gynecology Clinics of North America*, 34(4):687–700, viii, 2007.

[63] I. J. Jacobs and U. Menon. Progress and challenges in screening for early detection of ovarian cancer. *Molecular /& Cellular Proteomics*, 3(4):355–66, 2004.

[64] C. H. Holschneider and J. S. Berek. Ovarian cancer: epidemiology, biology, and prognostic factors. *Seminars in Surgical Oncology*, 19(1):3–10, 2000.

[65] A. Motamed-Khorasani, I. Jurisica, M. Letarte, P. A. Shaw, R. K. Parkes, X. Zhang, A. Evangelou, B. Rosen, K. J. Murphy, and T. J. Brown. Differentially androgen-modulated genes in ovarian epithelial cells from brca mutation carriers and control patients predict ovarian cancer survival and disease progression. *Oncogene*, 26(2):198–214, 2007.

[66] S. Chen, E. S. Iversen, T. Friebel, D. Finkelstein, B. L. Weber, A. Eisen, L. E. Peterson, J. M. Schildkraut, C. Isaacs, B. N. Peshkin, C. Corio, L. Leondaridis, G. Tomlinson, D. Dutson, R. Kerber, C. I. Amos, L. C. Strong, D. A. Berry, D. M. Euhus, and G. Parmigiani. Characterization of brca1 and brca2 mutations in a large united states sample. *Journal of Clinical Oncology*, 24(6):863–71, 2006.

[67] B. Friedenson. Brca1 and brca2 pathways and the risk of cancers other than breast or ovarian. *Medscape General Medicine*, 7(2):60, 2005.

[68] D. Ford, D. F. Easton, D. T. Bishop, S. A. Narod, and D. E. Goldgar. Risks of cancer in brca1-mutation carriers. breast cancer linkage consortium. *Lancet*, 343(8899):692–5, 1994.

[69] J. O. Schorge, S. C. Modesitt, R. L. Coleman, D. E. Cohn, N. D. Kauff, L. R. Duska, and T. J. Herzog. Sgo white paper on ovarian cancer: etiology, screening and surveillance. *Gynecologic Oncology*, 119:7–17–, 2010.

[70] J. H. Choi, A. S. Wong, H. F. Huang, and P. C. Leung. Gonadotropins and ovarian cancer. *Endocrinology Reviews*, 28(4):440–61, 2007.

[71] R. J. Edmondson and J. M. Monaghan. The epidemiology of ovarian cancer. *International Journal of Gynecological Cancer*, 11(6):423–9, 2001.

[72] H. A. Risch. Hormonal etiology of epithelial ovarian cancer, with a hypothesis concerning the role of androgens and progesterone. *Journal of the National Cancer Institute*, 90(23):1774–86, 1998.

[73] J. M. Schildkraut, P. J. Schwingl, E. Bastos, A. Evanoff, and C. Hughes. Epithelial ovarian cancer risk among women with polycystic ovary syndrome. *Obstetrics & Gynecology*, 88(4 Pt 1):554–9, 1996.

[74] M. F. Fathalla. Incessant ovulation–a factor in ovarian neoplasia? *Lancet*, 2:163, 1971.

[75] M. A. Gates, B. A. Rosner, J. L. Hecht, and S. S. Tworoger. Risk factors for epithelial ovarian cancer by histologic subtype. *American Journal of Epidemiology*, 171(1):45–53, 2010.

[76] J. T. Casagrande, E. W. Louie, M. C. Pike, S. Roy, R. K. Ross, and B. E. Henderson. "incessant ovulation" and ovarian cancer. *Lancet*, 2:170–3, 1979.

[77] E. R. Smith and X. X. Xu. Ovarian ageing, follicle depletion, and cancer: a hypothesis for the aetiology of epithelial ovarian cancer involving follicle depletion. *Lancet Oncology*, 9(11):1108–11, 2008.

[78] T. A. Yap, C. P. Carden, and S. B. Kaye. Beyond chemotherapy: targeted therapies in ovarian cancer. *Nature Reviews, Cancer*, 9(3):167–81, 2009.

[79] K. R. Cho and M. Shih Ie. Ovarian cancer. *Annual Review of Pathology*, 4:287–313, 2009.

[80] R. J. Kurman and M. Shih Ie. The origin and pathogenesis of epithelial ovarian cancer- a proposed unifying theory. *American Journal of Surgical Pathology*, 34(3):433–43, 2010.

[81] R. J. Kurman and M. Shih Ie. Molecular pathogenesis and extraovarian origin of epithelial ovarian cancer–shifting the paradigm. *Human Pathology*, 42(7):918–31, 2011.

[82] S. H. Olson, L. Mignone, C. Nakraseive, T. A. Caputo, R. R. Barakat, and S. Harlap. Symptoms of ovarian cancer. *Obstetrics & Gynecology*, 98(2):212–7, 2001.

[83] J. A. Gubbels, N. Claussen, A. K. Kapur, J. P. Connor, and M. S. Patankar. The detection, treatment, and biology of epithelial ovarian cancer. *Journal of Ovarian Research*, 3:8, 2010.

[84] A. P. Singh, S. Senapati, M. P. Ponnusamy, M. Jain, S. M. Lele, J. S. Davis, S. Remmenga, and S. K. Batra. Clinical potential of mucins in diagnosis, prognosis, and therapy of ovarian cancer. *Lancet Oncology*, 9:1076–85–, 2008.

[85] E. L. Moss, J. Hollingworth, and T. M. Reynolds. The role of ca125 in clinical practice. *Journal of Clinical Pathology*, 58(3):308–12, 2005.

[86] D. Gupta and C. G. Lis. Role of ca125 in predicting ovarian cancer survival - a review of the epidemiological literature. *Journal of Ovarian Research*, 2:13–, 2009.

[87] U. Menon, A. Gentry-Maharaj, R. Hallett, A. Ryan, M. Burnell, A. Sharma, S. Lewis, S. Davies, S. Philpott, A. Lopes, K. Godfrey, D. Oram, J. Herod, K. Williamson, M. W. Seif, I. Scott, T. Mould, R. Woolas, J. Murdoch, S. Dobbs,

N. N. Amso, S. Leeson, D. Cruickshank, A. McGuire, S. Campbell, L. Fallowfield, N. Singh, A. Dawnay, S. J. Skates, M. Parmar, and I. Jacobs. Sensitivity and specificity of multimodal and ultrasound screening for ovarian cancer, and stage distribution of detected cancers: results of the prevalence screen of the uk collaborative trial of ovarian cancer screening (ukctocs). *Lancet Oncology*, 10(4):327–40, 2009.

[88] R. G. Moore, M. C. Miller, P. Disilvestro, L. M. Landrum, W. Gajewski, J. J. Ball, and S. J. Skates. Evaluation of the diagnostic accuracy of the risk of ovarian malignancy algorithm in women with a pelvic mass. *Obstetrics & Gynecology*, 118(2 Pt 1):280–8, 2011.

[89] R. Drapkin, H.H. von Horsten, Y. Lin, S.C. Mok, C.P. Crum, W.R. Welch, and J.L. Hecht. Human epididymis protein 4 (he4) is a secreted glycoprotein that is overexpressed by serous and endometrioid ovarian carcinomas. *Cancer research*, 65-6:2162, 2005.

[90] T. Van Gorp, I. Cadron, E. Despierre, A. Daemen, K. Leunen, F. Amant, D. Timmerman, B. De Moor, and I. Vergote. He4 and ca125 as a diagnostic test in ovarian cancer: prospective validation of the risk of ovarian malignancy algorithm. *British Journal of Cancer*, 104(5):863–70, 2011.

[91] B. J. D. Rein, S. Gupta, R. Dada, J. Safi, C. Michener, and A. Agarwal. Potential markers for detection and monitoring of ovarian cancer. *Journal of Oncology*, 2011:475983, 2011.

[92] M. J. Engelen, H. E. Kos, P. H. Willemse, J. G. Aalders, E. G. de Vries, M. Schaapveld, R. Otter, and A. G. van der Zee. Surgery by consultant gynecologic oncologists improves survival in patients with ovarian carcinoma. *Cancer*, 106(3):589–98, 2006.

[93] C. Y. Muller. Doctor, should i get this new ovarian cancer test-ova1? *Obstetrics & Gynecology*, 116:246–7, 2010.

[94] K. Tsung and J. A. Norton. Lessons from coley's toxin. *Surgical Oncology*, 15(1):25–8, 2006.

[95] K. S. Anderson and J. LaBaer. The sentinel within: exploiting the immune system for cancer biomarkers. *Journal of Proteome Ressearch*, 4:1123–33–, 2005.

[96] J. B. Swann and M. J. Smyth. Immune surveillance of tumors. *Journal of Clinical Investigation*, 117(5):1137–46, 2007.

[97] L. Zitvogel, A. Tesniere, and G. Kroemer. Cancer despite immunosurveillance: immunoselection and immunosubversion. *Nature Reviews, Immunology*, 6:715–27, 2006.

[98] G. P. Dunn, L. J. Old, and R. D. Schreiber. The immunobiology of cancer immunosurveillance and immunoediting. *Immunity*, 21:137–48, 2004.

[99] G. P. Dunn, A. T. Bruce, H. Ikeda, L. J. Old, and R. D. Schreiber. Cancer immunoediting: from immunosurveillance to tumor escape. *Nature Immunology*, 3:991–8, 2002.

[100] I. Waldhauer, D. Goehlsdorf, F. Gieseke, T. Weinschenk, M. Wittenbrink, A. Ludwig, S. Stevanovic, H. G. Rammensee, and A. Steinle. Tumor-associated mica is shed by adam proteases. *Cancer Research*, 68:6368–76–, 2008.

[101] M. Jinushi, M. Vanneman, N. C. Munshi, Y. T. Tai, R. H. Prabhala, J. Ritz, D. Neuberg, K. C. Anderson, D. R. Carrasco, and G. Dranoff. Mhc class i chain-related protein a antibodies and shedding are associated with the progression of multiple myeloma. *Proceedings of the National Academy of Sciences of the United States of America*, 105(4):1285–90, 2008.

[102] G. Liu, C. L. Atteridge, X. Wang, A. D. Lundgren, and J. D. Wu. The membrane type matrix metalloproteinase mmp14 mediates constitutive shedding of mhc class i chain-related molecule a independent of a disintegrin and metalloproteinases. *Journal of Immunology*, 184:3346–50, 2010.

[103] O. Ashiru, P. Boutet, L. Fernandez-Messina, S. Aguera-Gonzalez, J. N. Skepper, M. Vales-Gomez, and H. T. Reyburn. Natural killer cell cytotoxicity is suppressed by exposure to the human nkg2d ligand mica*008 that is shed by tumor cells in exosomes. *Cancer Research*, 70:481–9, 2010.

[104] R. W. McGilvray, R. A. Eagle, N. F. Watson, A. Al-Attar, G. Ball, I. Jafferji, J. Trowsdale, and L. G. Durrant. Nkg2d ligand expression in human colorectal cancer reveals associations with prognosis and evidence for immunoediting. *Clinical Cancer Research*, 15:6993–7002–, 2009.

[105] D.H. Raulet and N. Guerra. Oncogenic stress sensed by the immune system: role of natural killer cell receptors. *Nature Reviews, Immunology*, 9:568–580, 2009.

[106] C.L. Sutherland, B. Rabinovich, N.J. Chalupny, P. Brawand, R. Miller, and D. Cosman. Ulbps, human ligands of the nkg2d receptor, stimulate tumor immunity with enhancement by il-15. *Blood - New York*, 108:1313, 2006.

[107] K.E. De Visser, A. Eichten, and L.M. Coussens. Paradoxical roles of the immune system during cancer development. *Nature Reviews, Cancer*, 6:24–37, 2006.

[108] C. M. Koebel, W. Vermi, J. B. Swann, N. Zerafa, S. J. Rodig, L. J. Old, M. J. Smyth, and R. D. Schreiber. Adaptive immunity maintains occult cancer in an equilibrium state. *Nature*, 450:903–7, 2007.

[109] J. M. Reiman, M. Kmieciak, M. H. Manjili, and K. L. Knutson. Tumor immunoediting and immunosculpting pathways to cancer progression. *Seminars in Cancer Biology*, 17:275–87–, 2007.

[110] T. L. Whiteside. The tumor microenvironment and its role in promoting tumor growth. *Oncogene*, 27:5904–12–, 2008.

[111] G. Dranoff. Cytokines in cancer pathogenesis and cancer therapy. *Nature Reviews, Cancer*, 4(1):11–22, 2004.

[112] N. Wegner, K. Lundberg, A. Kinloch, B. Fisher, V. Malmstrom, M. Feldmann, and P. J. Venables. Autoimmunity to specific citrullinated proteins gives the first clues to the etiology of rheumatoid arthritis. *Immunological Reviews*, 233(1):34–54, 2010.

[113] B. T. Kurien and R. H. Scofield. Autoantibody determination in the diagnosis of systemic lupus erythematosus. *Scandinavian Journal of Immunology*, 64(3):227–35, 2006.

[114] S. Zelenay, M. F. Moraes Fontes, C. Fesel, J. Demengeot, and A. Coutinho. Physiopathology of natural auto-antibodies: the case for regulation. *Journal of Autoimmunity*, 29(4):229–35, 2007.

[115] N. Comtesse, D. Heckel, E. Maldener, B. Glass, and E. Meese. Probing the human natural autoantibody repertoire using an immunoscreening approach. *Clinical and Experimental Immunology*, 121(3):430–6, 2000.

[116] A. Coutinho, M. D. Kazatchkine, and S. Avrameas. Natural autoantibodies. *Current Opinion in Immunology*, 7(6):812–8, 1995.

[117] S. D. Fleming. Natural antibodies, autoantibodies and complement activation in tissue injury. *Autoimmunity*, 39(5):379–86, 2006.

[118] R. Schwartz-Albiez, R. C. Monteiro, M. Rodriguez, C. J. Binder, and Y. Shoenfeld. Natural antibodies, intravenous immunoglobulin and their role in autoimmunity, cancer and inflammation. *Clinical & Experimental Immunology*, 158 Suppl 1:43–50, 2009.

[119] C. Backes, N. Ludwig, P. Leidinger, C. Harz, J. Hoffmann, A. Keller, E. Meese, and H. P. Lenhof. Immunogenicity of autoantigens. *BMC Genomics*, 12:340, 2011.

[120] P. H. Plotz. The autoantibody repertoire: searching for order. *Nat Rev Immunol*, 3(1):73–8, 2003.

[121] S. F. Kingsmore. Multiplexed protein measurement: technologies and applications of protein and antibody arrays. *Nature reviews. Drug discovery*, 5:310–20–, 2006.

[122] Biomarkers Definitions Working Group. Biomarkers and surrogate endpoints: preferred definitions and conceptual framework. *Clinical Pharmacology and Therapeutics*, 69:89–95, 2001.

[123] D. Villalta, P. B. Romelli, C. Savina, N. Bizzaro, R. Tozzoli, E. Tonutti, A. Ghirardello, and A. Doria. Anti-dsdna antibody avidity determination by a simple reliable elisa method for sle diagnosis and monitoring. *Lupus*, 12(1):31–6, 2003.

[124] B. P. Corgier, C. A. Marquette, and L. J. Blum. Direct electrochemical addressing of immunoglobulins: immuno-chip on screen-printed microarray. *Biosensors and Bioelectronics*, 22(7):1522–6, 2007.

[125] E. Farng and J. B. Friedrich. Laboratory diagnosis of rheumatoid arthritis. *Journal of Hand Surgery*, 36(5):926–7; quiz 928, 2011.

[126] A. Morell, W. D. Terry, and T. A. Waldmann. Metabolic properties of igg subclasses in man. *Journal of Clinical Investigation*, 49(4):673–80, 1970.

[127] S. Qin, W. Qiu, J. R. Ehrlich, A. S. Ferdinand, J. P. Richie, P. O'Leary M, M. L. Lee, and B. C. Liu. Development of a "reverse capture" autoantibody microarray for studies of antigen-autoantibody profiling. *Proteomics*, 6(10):3199–209, 2006.

[128] Y. Imafuku, G. S. Omenn, and S. Hanash. Proteomics approaches to identify tumor antigen directed autoantibodies as cancer biomarkers. *Disease Markers*, 20(3):149–53, 2004.

[129] H. T. Tan, J. Low, S. G. Lim, and M. C. Chung. Serum autoantibodies as biomarkers for early cancer detection. *The FEBS Journal*, 276:6880–904–, 2009.

[130] S. Gnjatic, L. J. Old, and Y. T. Chen. Autoantibodies against cancer antigens. *Methods in Molecular Biology*, 520:11–9, 2009.

[131] G. Kijanka and D. Murphy. Protein arrays as tools for serum autoantibody marker discovery in cancer. *Journal of Proteomics*, 72:936–44–, 2009.

[132] E. M. Tan and J. Zhang. Autoantibodies to tumor-associated antigens: reporters from the immune system. *Immunological Reviews*, 222:328–40, 2008.

[133] C. A. Casiano, M. Mediavilla-Varela, and E. M. Tan. Tumor-associated antigen arrays for the serological diagnosis of cancer*. *Molecular and Cellular Proteomics*, 5(10):1745–59, 2006.

[134] E. M. Tan. Autoantibodies as reporters identifying aberrant cellular mechanisms in tumorigenesis. *Journal of Clinical Investigation*, 108(10):1411–5, 2001.

[135] Y. Ran, H. Hu, Z. Zhou, L. Yu, L. Sun, J. Pan, J. Liu, and Z. Yang. Profiling tumor-associated autoantibodies for the detection of colon cancer. *Clinical Cancer Research*, 14:2696–700–, 2008.

[136] L. Zhong, K. Ge, J. C. Zu, L. H. Zhao, W. K. Shen, J. F. Wang, X. G. Zhang, X. Gao, W. Hu, Y. Yen, and K. H. Kernstine. Autoantibodies as potential biomarkers for breast cancer. *Breast Cancer Research*, 10:R40–, 2008.

[137] S. Gnjatic, E. Ritter, M. W. Buchler, N. A. Giese, B. Brors, C. Frei, A. Murray, N. Halama, I. Zornig, Y. T. Chen, C. Andrews, G. Ritter, L. J. Old, K. Odunsi, and D. Jager. Seromic profiling of ovarian and pancreatic cancer. *Proceedings of the National Academy of Sciences of the United States of America*, 107:5088–93–, 2010.

[138] K. Ait-Tahar, C. Damm-Welk, B. Burkhardt, M. Zimmermann, W. Klapper, A. Reiter, K. Pulford, and W. Woessmann. Correlation of the autoantibody response to the alk oncoantigen in pediatric anaplastic lymphoma kinase-positive anaplastic large cell lymphoma with tumor dissemination and relapse risk. *Blood*, 115:3314–9–, 2010.

[139] T. Soussi and K. G. Wiman. Shaping genetic alterations in human cancer: the p53 mutation paradigm. *Cancer Cell*, 12:303–12–, 2007.

[140] G. Mor, I. Visintin, Y. Lai, H. Zhao, P. Schwartz, T. Rutherford, L. Yue, P. Bray-Ward, and D. C. Ward. Serum protein markers for early detection of ovarian cancer. *Proceedings of the National Academy of Sciences of the United States of America*, 102:7677–82–, 2005.

[141] H. Suzuki, K. Akakura, T. Igarashi, T. Ueda, H. Ito, M. Watanabe, F. Nomura, T. Ochiai, and H. Shimada. Clinical usefulness of serum antip53 antibodies for prostate cancer detection: a comparative study with prostate specific antigen parameters. *Journal of Urology*, 171:182–6–, 2004.

[142] R. Tang, C. Y. Yeh, J. Y. Wang, C. R. Changchien, J. S. Chen, and L. L. Hsieh. Serum p53 antibody as tumor marker for follow-up of colorectal cancer after curative resection. *Annals of Surgical Oncology*, 16:2516–23–, 2009.

[143] T. Soussi. p53 antibodies in the sera of patients with various types of cancer: a review. *Cancer Research*, 60:1777–88–, 2000.

[144] G. E. Trivers, V. M. De Benedetti, H. L. Cawley, G. Caron, A. M. Harrington, W. P. Bennett, J. R. Jett, T. V. Colby, H. Tazelaar, P. Pairolero, R. D. Miller, and C. C. Harris. Anti-p53 antibodies in sera from patients with chronic obstructive pulmonary disease can predate a diagnosis of cancer. *Clinical Cancer Research*, 2(10):1767–75, 1996.

[145] R. Lubin, G. Zalcman, L. Bouchet, J. Tredanel, Y. Legros, D. Cazals, A. Hirsch, and T. Soussi. Serum p53 antibodies as early markers of lung cancer. *Nature Medicine*, 1:701–2–, 1995.

[146] P. Massoner, A. Lueking, H. Goehler, A. Hopfner, A. Kowald, K. G. Kugler, P. Amersdorfer, W. Horninger, G. Bartsch, P. Schulz-Knappe, and H. Klocker. Serum-autoantibodies for discovery of prostate cancer specific biomarkers. *Prostate*, 72(4):427–36, 2012.

[147] D. J. O'Rourke, D. A. DiJohnson, Jr. Caiazzo, R. J., J. C. Nelson, D. Ure, M. P. O'Leary, J. P. Richie, and B. C. Liu. Autoantibody signatures as biomarkers to distinguish prostate cancer from benign prostatic hyperplasia in patients with increased serum prostate specific antigen. *Clinica Chimica Acta*, 413(5-6):561–7, 2012.

[148] C. Xie, H. J. Kim, J. G. Haw, A. Kalbasi, B. K. Gardner, G. Li, J. Rao, D. Chia, M. Liong, R. R. Punzalan, L. S. Marks, A. J. Pantuck, A. de la Taille, G. Wang, H. Mukouyama, and G. Zeng. A novel multiplex assay combining autoantibodies plus psa has potential implications for classification of prostate cancer from non-malignant cases. *Journal of Translational Medicine*, 9:43, 2011.

[149] X. Wang, J. Yu, A. Sreekumar, S. Varambally, R. Shen, D. Giacherio, R. Mehra, J. E. Montie, K. J. Pienta, M. G. Sanda, P. W. Kantoff, M. A. Rubin, J. T. Wei, D. Ghosh, and A. M. Chinnaiyan. Autoantibody signatures in prostate cancer. *New England Journal of Medicine*, 353(12):1224–35, 2005.

[150] Y. Tang, L. Wang, P. Zhang, H. Wei, R. Gao, X. Liu, and Y. Yu. Detection of circulating anti-mucin 1 (muc1) antibodies in breast tumor patients by indirect enzyme-linked immunosorbent assay using a recombinant muc1 protein containing six tandem repeats and expressed in escherichia coli. *Clinical and Vaccine Immunology*, 17(12):1903–8, 2010.

[151] S. von Mensdorff-Pouilly, A. A. Verstraeten, P. Kenemans, F. G. Snijdewint, A. Kok, G. J. Van Kamp, M. A. Paul, P. J. Van Diest, S. Meijer, and J. Hilgers. Survival in early breast cancer patients is favorably influenced by a natural humoral immune response to polymorphic epithelial mucin. *Journal of Clinical Oncology*, 18(3):574–83, 2000.

[152] S. Lam, P. Boyle, G. F. Healey, P. Maddison, L. Peek, A. Murray, C. J. Chapman, J. Allen, W. C. Wood, H. F. Sewell, and J. F. Robertson. Earlycdt-lung: an immunobiomarker test as an aid to early detection of lung cancer. *Cancer Prevention Research (Phila)*, 4(7):1126–34, 2011.

[153] P. Boyle, CJ Chapman, S. Holdenrieder, A. Murray, C. Robertson, WC Wood, P. Maddison, G. Healey, GH Fairley, and AC Barnes. Clinical validation of an autoantibody test for lung cancer. *Annals of Oncology*, 22:383–389, 2011.

[154] A. Murray, CJ Chapman, G. Healey, LJ Peek, G. Parsons, D. Baldwin, A. Barnes, HF Sewell, HA Fritsche, and JFR Robertson. Technical validation of an autoantibody test for lung cancer. *Annals of Oncology*, 21:1687–1693, 2010.

[155] L. Österberg, K. Levan, K. Partheen, K. Helou, and G. Horvath. Cytogenetic analysis of carboplatin resistance in early-stage epithelial ovarian carcinoma. *Cancer genetics and cytogenetics*, 163:144–150, 2005.

[156] A. Dørum, GB Kristensen, VM Abeler, CG Trope, and P. Møller. Early detection of familial ovarian cancer. *European Journal of Cancer*, 32:1645–1651, 1996.

[157] K. S. Anderson, N. Ramachandran, J. Wong, J. V. Raphael, E. Hainsworth, G. Demirkan, D. Cramer, D. Aronzon, F. S. Hodi, L. Harris, T. Logvinenko, and J. LaBaer. Application of protein microarrays for multiplexed detection of antibodies to tumor antigens in breast cancer. *Journal of Proteome Research*, 7:1490–9, 2008.

[158] H. Shimada, K. Nakashima, T. Ochiai, Y. Nabeya, M. Takiguchi, F. Nomura, and T. Hiwasa. Serological identification of tumor antigens of esophageal squamous cell carcinoma. *International Journal of Oncology*, 26:77–86–, 2005.

[159] E. P. Diamandis. Mass spectrometry as a diagnostic and a cancer biomarker discovery tool: opportunities and potential limitations. *Molecular & Cellular Proteomics*, 3(4):367–78, 2004.

[160] A. Hui, C. How, E. Ito, and F. F. Liu. Micro-rnas as diagnostic or prognostic markers in human epithelial malignancies. *BMC Cancer*, 11:500, 2011.

[161] R. J. Flavin, P. C. Smyth, S. P. Finn, A. Laios, S. A. O'Toole, C. Barrett, M. Ring, K. M. Denning, J. Li, S. T. Aherne, N. A. Aziz, A. Alhadi, B. L. Sheppard, M. Loda, C. Martin, O. M. Sheils, and J. J. O'Leary. Altered eif6 and dicer expression is associated with clinicopathological features in ovarian serous carcinoma patients. *Modern Pathology*, 21(6):676–84, 2008.

[162] M. E. Hudson, I. Pozdnyakova, K. Haines, G. Mor, and M. Snyder. Identification of differentially expressed proteins in ovarian cancer using high-density protein microarrays. *Proceedings of the National Academy of Sciences of the United States of America*, 104:17494–9, 2007.

[163] T. H. Patwa, C. Li, L. M. Poisson, H. Y. Kim, M. Pal, D. Ghosh, D. M. Simeone, and D. M. Lubman. The identification of phosphoglycerate kinase-1 and histone h4 autoantibodies in pancreatic cancer patient serum using a natural protein microarray. *Electrophoresis*, 30:2215–26–, 2009.

[164] A. Heller, I. Zornig, T. Muller, K. Giorgadze, C. Frei, T. Giese, F. Bergmann, J. Schmidt, J. Werner, M. W. Buchler, D. Jaeger, and N. A. Giese. Immunogenicity of serex-identified antigens and disease outcome in pancreatic cancer. *Cancer Immunology, Immunotherapy*, 59:1389–400–, 2010.

[165] A. Fossa, L. Alsoe, R. Crameri, S. Funderud, G. Gaudernack, and E. B. Smeland. Serological cloning of cancer/testis antigens expressed in prostate cancer using cdna phage surface display. *Cancer Immunology, Immunotherapy*, 53(5):431–8, 2004.

[166] C. Desmetz, T. Maudelonde, A. Mangé, and J. Solassol. Identifying autoantibody signatures in cancer: a promising challenge. *Expert review of proteomics*, 6:377–386, 2009.

[167] P. J. Mintz, J. Kim, K. A. Do, X. Wang, R. G. Zinner, M. Cristofanilli, M. A. Arap, W. K. Hong, P. Troncoso, C. J. Logothetis, R. Pasqualini, and W. Arap. Fingerprinting the circulating repertoire of antibodies from cancer patients. *Nature Biotechnology*, 21:57–63–, 2003.

[168] S. Hanash. Harnessing immunity for cancer marker discovery. *Nature Biotechnology*, 21:37–8–, 2003.

[169] K. Martin, C. Ricciardelli, P. Hoffmann, and M. K. Oehler. Exploring the immunoproteome for ovarian cancer biomarker discovery. *International Journal of Molecular Sciences*, 12(1):410–28, 2011.

[170] E. H. Kemp, L. M. Herd, E. A. Waterman, A. G. Wilson, A. P. Weetman, and P. P. Watson. Immunoscreening of phage-displayed cdna-encoded polypeptides identifies b cell targets in autoimmune disease. *Biochemical and Biophysical Research Communications*, 298(1):169–77, 2002.

[171] M. Sioud, M. Hansen, and A. Dybwad. Profiling the immune responses in patient sera with peptide and cdna display libraries. *International Journal of Molecular Medicine*, 6(2):123–8, 2000.

[172] F. Fernandez-Madrid, N. Tang, H. Alansari, J. L. Granda, L. Tait, K. C. Amirikia, M. Moroianu, X. Wang, and R. L. Karvonen. Autoantibodies to annexin xia and other autoantigens in the diagnosis of breast cancer. *Cancer Research*, 64(15):5089–96, 2004.

[173] C. G. Gunawardana, N. Memari, and E. P. Diamandis. Identifying novel autoantibody signatures in ovarian cancer using high-density protein microarrays. *Clinical Biochemistry*, 42(4-5):426–9, 2009.

[174] S. Horn, A. Lueking, D. Murphy, A. Staudt, C. Gutjahr, K. Schulte, A. Konig, M. Landsberger, H. Lehrach, S. B. Felix, and D. J. Cahill. Profiling humoral autoimmune repertoire of dilated cardiomyopathy (dcm) patients and development of a disease-associated protein chip. *Proteomics*, 6:605–13–, 2006.

[175] A. Lueking, O. Huber, C. Wirths, K. Schulte, K. M. Stieler, U. Blume-Peytavi, A. Kowald, K. Hensel-Wiegel, R. Tauber, H. Lehrach, H. E. Meyer, and D. J. Cahill. Profiling of alopecia areata autoantigens based on protein microarray technology. *Molecular & Cellular Proteomics*, 4:1382–90–, 2005.

[176] J. Qiu, J. Madoz-Gurpide, D. E. Misek, R. Kuick, D. E. Brenner, G. Michailidis, B. B. Haab, G. S. Omenn, and S. Hanash. Development of natural protein microarrays for diagnosing cancer based on an antibody response to tumor antigens. *Journal of Proteome Research*, 3(2):261–7, 2004.

[177] J. Madoz-Gurpide, H. Wang, D. E. Misek, F. Brichory, and S. M. Hanash. Protein based microarrays: a tool for probing the proteome of cancer cells and tissues. *Proteomics*, 1(10):1279–87, 2001.

[178] C. P. Paweletz, L. Charboneau, V. E. Bichsel, N. L. Simone, T. Chen, J. W. Gillespie, M. R. Emmert-Buck, M. J. Roth, Iii Ef Petricoin, and L. A. Liotta. Reverse phase protein microarrays which capture disease progression show activation of pro-survival pathways at the cancer invasion front. *Oncogene*, 20(16):1981–9, 2001.

[179] K. Bussow, D. Cahill, W. Nietfeld, D. Bancroft, E. Scherzinger, H. Lehrach, and G. Walter. A method for global protein expression and antibody screening on high-density filters of an arrayed cdna library. *Nucleic Acids Research*, 26:5007–8–, 1998.

[180] O. Stoevesandt. Protein arraying by cell-free expression and diffusion across a fluid-filled gap. *Nature Biotechnology*, 2012.

[181] A. Nand, A. Gautam, J. B. Perez, A. Merino, and J. Zhu. Emerging technology of in situ cell free expression protein microarrays. *Protein Cell*, 3(2):84–8, 2012.

[182] P. Angenendt. Progress in protein and antibody microarray technology. *Drug Discovery Today*, 10(7):503–11, 2005.

[183] M. F. Templin, D. Stoll, J. M. Schwenk, O. Potz, S. Kramer, and T. O. Joos. Protein microarrays: promising tools for proteomic research. *Proteomics*, 3(11):2155–66, 2003.

[184] J. Qiu and S. Hanash. Autoantibody profiling for cancer detection. *Clinics in Laboratory Medicine*, 29:31–46–, 2009.

[185] S. L. O'Kane, J. K. O'Brien, and D. J. Cahill. Optimized autoantibody profiling on protein arrays. *Methods in Molecular Biology*, 785:331–41, 2011.

[186] D. J. O'Connell, M. Bauer, S. Linse, and D. J. Cahill. Probing calmodulin protein-protein interactions using high-content protein arrays. *Methods in Molecular Biology*, 785:289–303–, 2011.

[187] F. I. Staquicini, M. Cardo-Vila, M. G. Kolonin, M. Trepel, J. K. Edwards, D. N. Nunes, A. Sergeeva, E. Efstathiou, J. Sun, N. F. Almeida, S. M. Tu, G. H. Botz, M. J. Wallace, D. J. O'Connell, S. Krajewski, J. E. Gershenwald, J. J. Molldrem, A. L. Flamm, E. Koivunen, R. D. Pentz, E. Dias-Neto, J. C. Setubal, D. J. Cahill, P. Troncoso, K. A. Do, C. J. Logothetis, R. L. Sidman, R. Pasqualini, and W. Arap. Vascular ligand-receptor mapping by direct combinatorial selection in cancer patients. *Proceedings of the National Academy of Sciences of the United States of America*, 108:18637–42, 2011.

[188] N. Olsson, C. Wingren, M. Mattsson, P. James, D. O'Connell, F. Nilsson, D. J. Cahill, and C. A. Borrebaeck. Proteomic analysis and discovery using affinity proteomics and mass spectrometry. *Molecular & Cellular Proteomics*, 10:M110 003962–, 2011.

[189] M. Bauer, M. Maj, L. Wagner, D. J. Cahill, S. Linse, and D. J. O'Connell. Protein networks involved in vesicle fusion, transport, and storage revealed by array-based proteomics. *Methods in Molecular Biology*, 781:47–58, 2011.

[190] M. Han, E. Nagele, C. DeMarshall, N. Acharya, and R. Nagele. Diagnosis of parkinson's disease based on disease-specific autoantibody profiles in human sera. *PLoS One*, 7(2):e32383, 2012.

[191] E. Nagele, M. Han, C. Demarshall, B. Belinka, and R. Nagele. Diagnosis of alzheimer's disease based on disease-specific autoantibody profiles in human sera. *PLoS One*, 6(8):e23112, 2011.

[192] M. A. Murphy, D. J. O'Connell, S. L. O'Kane, J. K. O'Brien, S. O'Toole, C. Martin, O. Sheils, J. J. O'Leary, and D. J. Cahill. Epitope presentation is an important determinant of the utility of antigens identified from protein arrays in the development of autoantibody diagnostic assays. *Journal of Proteomics*, Epub ahead of print, 2012.

[193] D. D. Taylor, C. Gercel-Taylor, and L. P. Parker. Patient-derived tumor reactive antibodies as diagnostic markers for ovarian cancer. *Gynecologic Oncology*, 115(1):112–20, 2009.

[194] A. Gagnon, J. H. Kim, J. O. Schorge, B. Ye, B. Liu, K. Hasselblatt, W. R. Welch, C. A. Bandera, and S. C. Mok. Use of a combination of approaches to identify and validate relevant tumor-associated antigens and their corresponding

autoantibodies in ovarian cancer patients. *Clinical Cancer Research*, 14:764–71, 2008.

[195] E. I. Braicu, J. Sehouli, R. Richter, K. Pietzner, C. Denkert, and C. Fotopoulou. Role of histological type on surgical outcome and survival following radical primary tumour debulking of epithelial ovarian, fallopian tube and peritoneal cancers. *British Journal of Cancer*, 105(12):1818–24, 2011.

[196] J. Ji, A. Forsti, J. Sundquist, P. Lenner, and K. Hemminki. Survival in ovarian cancer patients by histology and family history. *Acta Oncologica*, 47(6):1133–9, 2008.

[197] T. Kaku, S. Ogawa, Y. Kawano, Y. Ohishi, H. Kobayashi, T. Hirakawa, and H. Nakano. Histological classification of ovarian cancer. *Medical Electron Microscopy*, 36(1):9–17, 2003.

[198] J. Kim, D. M. Coffey, C. J. Creighton, Z. Yu, S. M. Hawkins, and M. M. Matzuk. High-grade serous ovarian cancer arises from fallopian tube in a mouse model. *Proceedings of the National Academy of Sciences of the United States of America*, 109(10):3921–6, 2012.

[199] D. D. Bowtell. The genesis and evolution of high-grade serous ovarian cancer. *Nature Reviews, Cancer*, 10(11):803–8, 2010.

[200] K. S. Anderson, J. Wong, A. Vitonis, C. P. Crum, P. M. Sluss, J. LaBaer, and D. Cramer. P53 autoantibodies as potential detection and prognostic biomarkers in serous ovarian cancer. *Cancer Epidemiology, Biomarkers and Prevention*, 19(3):859–68, 2010.

[201] K. Angelopoulou, E. P. Diamandis, D. J. Sutherland, J. A. Kellen, and P. S. Bunting. Prevalence of serum antibodies against the p53 tumor suppressor gene protein in various cancers. *International Journal of Cancer*, 58(4):480–7, 1994.

[202] R. J. Gao, H. Z. Bao, Q. Yang, Q. Cong, J. N. Song, and L. Wang. The presence of serum anti-p53 antibodies from patients with invasive ductal carcinoma of breast: correlation to other clinical and biological parameters. *Breast Cancer Research and Treatment*, 93:111–5–, 2005.

[203] L. Li, K. Wang, L. Dai, P. Wang, X. X. Peng, and J. Y. Zhang. Detection of autoantibodies to multiple tumor-associated antigens in the immunodiagnosis of ovarian cancer. *Molecular Medicine Reports*, 1(4):589–94, 2008.

[204] F. D. Vogl, M. Frey, R. Kreienberg, and I. B. Runnebaum. Autoimmunity against p53 predicts invasive cancer with poor survival in patients with an ovarian mass. *British Journal of Cancer*, 83(10):1338–43, 2000.

[205] K. R. Cho. Ovarian cancer update: lessons from morphology, molecules, and mice. *Archives of Pathology & Laboratory Medicine*, 133:1775–81–, 2009.

[206] M. Tsai-Turton, A. Santillan, D. Lu, R. E. Bristow, K. C. Chan, M. Shih Ie, and R. B. Roden. p53 autoantibodies, cytokine levels and ovarian carcinogenesis. *Gynecologic Oncology*, 114:12–7–, 2009.

[207] B. Piura and E. Piura. Autoantibodies to tumor-associated antigens in epithelial ovarian carcinoma. *Journal of Oncology*, 2009:581939–, 2009.

[208] D. Lu, E. Kuhn, R. E. Bristow, 2nd Giuntoli, R. L., S. K. Kjaer, M. Shih Ie, and R. B. Roden. Comparison of candidate serologic markers for type i and type ii ovarian cancer. *Gynecologic Oncology*, 122(3):560–6, 2011.

[209] A. Gadducci, M. Ferdeghini, F. Buttitta, S. Cosio, A. Fanucchi, C. Annicchiarico, O. Gagetti, G. Bevilacqua, and A. R. Genazzani. Assessment of the prognostic relevance of serum anti-p53 antibodies in epithelial ovarian cancer. *Gynecologic Oncology*, 72(1):76–81, 1999.

[210] K. Angelopoulou, B. Rosen, M. Stratis, H. Yu, M. Solomou, and E. P. Diamandis. Circulating antibodies against p53 protein in patients with ovarian carcinoma. correlation with clinicopathologic features and survival. *Cancer*, 78(10):2146–52, 1996.

[211] E. V. Hogdall, C. K. Hogdall, J. Blaakaer, N. H. Heegaard, E. Glud, L. Christensen, J. E. Bock, B. Norgaard-Pedersen, A. Wiik, and S. K. Kjaer. P53 autoantibodies in sera from danish ovarian cancer patients and their correlation with clinical data and prognosis. *Acta Pathologica, Microbiologica et Immunologica Scandinavica*, 110(7-8):545–53, 2002.

[212] M. Ho, R. Hassan, J. Zhang, Q. C. Wang, M. Onda, T. Bera, and I. Pastan. Humoral immune response to mesothelin in mesothelioma and ovarian cancer patients. *Clinical Cancer Research*, 11(10):3814–20, 2005.

[213] I. Hellstrom, E. Friedman, T. Verch, Y. Yang, J. Korach, J. Jaffar, E. Swisher, B. Zhang, G. Ben-Baruch, M. C. Tan, P. Goedegebuure, and K. E. Hellstrom. Anti-mesothelin antibodies and circulating mesothelin relate to the clinical state in ovarian cancer patients. *Cancer Epidemiology, Biomarkers and Prevention*, 17(6):1520–6, 2008.

[214] J. L. Luborsky, Y. Yu, S. L. Edassery, J. Jaffar, Y. Y. Yip, P. Liu, K. E. Hellstrom, and I. Hellstrom. Autoantibodies to mesothelin in infertility. *Cancer Epidemiology, Biomarkers and Prevention*, 20(9):1970–8, 2011.

[215] K. Milne, R. O. Barnes, A. Girardin, M. A. Mawer, N. J. Nesslinger, A. Ng, J. S. Nielsen, R. Sahota, E. Tran, J. R. Webb, M. Q. Wong, D. A. Wick, A. Wray, E. McMurtrie, M. Kobel, S. E. Kalloger, C. B. Gilks, P. H. Watson, and B. H. Nelson. Tumor-infiltrating t cells correlate with ny-eso-1-specific autoantibodies in ovarian cancer. *PLoS One*, 3:e3409–, 2008.

[216] K. Odunsi, A. A. Jungbluth, E. Stockert, F. Qian, S. Gnjatic, J. Tammela, M. Intengan, A. Beck, B. Keitz, D. Santiago, B. Williamson, M. J. Scanlan, G. Ritter, Y. T. Chen, D. Driscoll, A. Sood, S. Lele, and L. J. Old. Ny-eso-1 and lage-1 cancer-testis antigens are potential targets for immunotherapy in epithelial ovarian cancer. *Cancer Research*, 63(18):6076–83, 2003. 3.

[217] E. Stockert, E. Jager, Y. T. Chen, M. J. Scanlan, I. Gout, J. Karbach, M. Arand, A. Knuth, and L. J. Old. A survey of the humoral immune response of cancer patients to a panel of human tumor antigens. *Journal of Experimental Medicine*, 187(8):1349–54, 1998.

[218] E. Piura and B. Piura. Autoantibodies to tumor-associated antigens in breast carcinoma. *Journal of Oncology*, 2010:264926–, 2010.

[219] R. E. Wang. Targeting heat shock proteins 70/90 and proteasome for cancer therapy. *Current Medicinal Chemistry*, 18(27):4250–64, 2011.

[220] G. Faulds, S. Conroy, M. Madaio, D. Isenberg, and D. Latchman. Increased levels of antibodies to heat shock proteins with increasing age in mrl/mp-lpr/lpr mice. *British Journal of Rheumatology*, 34(7):610–5, 1995.

[221] G. Hayem, M. De Bandt, E. Palazzo, S. Roux, B. Combe, J. F. Eliaou, J. Sany, M. F. Kahn, and O. Meyer. Anti-heat shock protein 70 kda and 90 kda antibodies in serum of patients with rheumatoid arthritis. *Annals of the Rheumatic Diseases*, 58(5):291–6, 1999.

[222] K. Trieb, R. Gerth, G. Holzer, J. G. Grohs, P. Berger, and R. Kotz. Antibodies to heat shock protein 90 in osteosarcoma patients correlate with response to neoadjuvant chemotherapy. *British Journal of Cancer*, 82(1):85–7, 2000.

[223] C. I. Vidal, P. J. Mintz, K. Lu, L. M. Ellis, L. Manenti, R. Giavazzi, D. M. Gershenson, R. Broaddus, J. Liu, W. Arap, and R. Pasqualini. An hsp90-mimic peptide revealed by fingerprinting the pool of antibodies from ovarian cancer patients. *Oncogene*, 23(55):8859–67, 2004.

[224] L. Y. Luo, I. Herrera, A. Soosaipillai, and E. P. Diamandis. Identification of heat shock protein 90 and other proteins as tumour antigens by serological screening of an ovarian carcinoma expression library. *British Journal of Cancer*, 87(3):339–43, 2002.

[225] I. Korneeva, A. M. Bongiovanni, M. Girotra, T. A. Caputo, and S. S. Witkin. Iga antibodies to the 27-kda heat-shock protein in the genital tracts of women with gynecologic cancers. *International Journal of Cancer*, 87(6):824–8, 2000.

[226] J. R. Kanwar, S. K. Kamalapuram, and R. K. Kanwar. Targeting survivin in cancer: the cell-signalling perspective. *Drug Discovery Today*, 16(11-12):485–94, 2011.

[227] J. T. Chang, F. H. Wong, C. T. Liao, I. H. Chen, H. M. Wang, and A. J. Cheng. Enzyme immunoassay for serum autoantibody to survivin and its findings in head-and-neck cancer patients. *Clinical Chemistry*, 50(7):1261–4, 2004.

[228] L. Ma, W. Yue, L. Zhang, Y. Wang, C. Zhang, and X. Yang. [clinical significance and diagnostic value of survivin autoantibody in non-small cell lung cancer patients]. *Zhongguo Fei Ai Za Zhi*, 13(7):706–12, 2010.

[229] A. Yagihashi, K. Asanuma, D. Kobayashi, N. Tsuji, Y. Shijubo, S. Abe, Y. Hirohashi, T. Torigoe, N. Sato, and N. Watanabe. Detection of autoantibodies to livin and survivin in sera from lung cancer patients. *Lung Cancer*, 48(2):217–21, 2005.

[230] A. Yagihashi, T. Ohmura, K. Asanuma, D. Kobayashi, N. Tsuji, T. Torigoe, N. Sato, K. Hirata, and N. Watanabe. Detection of autoantibodies to survivin and livin in sera from patients with breast cancer. *Clinica Chimica Acta*, 362(1-2):125–30, 2005.

[231] D. J. O'Connell, M. C. Bauer, J. O'Brien, W. M. Johnson, C. A. Divizio, S. L. O'Kane, T. Berggard, A. Merino, K. S. Akerfeldt, S. Linse, and D. J. Cahill. Integrated protein array screening and high throughput validation of 70 novel neural calmodulin-binding proteins. *Molecular & Cellular Proteomics*, 9:1118–32–, 2010.

[232] E. F. Petricoin, A. M. Ardekani, B. A. Hitt, P. J. Levine, V. A. Fusaro, S. M. Steinberg, G. B. Mills, C. Simone, D. A. Fishman, E. C. Kohn, and L. A. Liotta. Use of proteomic patterns in serum to identify ovarian cancer. *Lancet*, 359:572–7–, 2002.

[233] A. Lueking, A. Possling, O. Huber, A. Beveridge, M. Horn, H. Eickhoff, J. Schuchardt, H. Lehrach, and D. J. Cahill. A nonredundant human protein chip for antibody screening and serum profiling. *Molecular & Cellular Proteomics*, 2:1342–9–, 2003.

[234] H. Zhu and M. Snyder. Protein chip technology. *Current Opinions in Chemical Biology*, 7(1):55–63, 2003.

[235] S. Lacroix-Desmazes, S. V. Kaveri, L. Mouthon, A. Ayouba, E. Malanchere, A. Coutinho, and M. D. Kazatchkine. Self-reactive antibodies (natural autoantibodies) in healthy individuals. *Journal of Immunological Methods*, 216(1-2):117–37, 1998.

[236] S. Hector, H. Chen, G. Kijanka, F. Murray, and J. H. Prehn. A reverse-elisa for the detection of trim28/kap1 serum autoantibodies in colorectal cancer patients. *Acta Oncologica*, 51(3):394–6, 2012.

[237] M. Nesterova, N. Johnson, C. Cheadle, and Y. S. Cho-Chung. Autoantibody biomarker opens a new gateway for cancer diagnosis. *Biochimica Biophysica Acta*, 1762:398–403–, 2006.

[238] D. Bandah-Rozenfeld, L. Mizrahi-Meissonnier, C. Farhy, A. Obolensky, I. Chowers, J. Pe'er, S. Merin, T. Ben-Yosef, R. Ashery-Padan, E. Banin, and D. Sharon. Homozygosity mapping reveals null mutations in fam161a as a cause of autosomal-recessive retinitis pigmentosa. *The American Journal of Human Genetics*, 87(3):382–91, 2010.

[239] T. Langmann, S. A. Di Gioia, I. Rau, H. Stohr, N. S. Maksimovic, J. C. Corbo, A. B. Renner, E. Zrenner, G. Kumaramanickavel, M. Karlstetter, Y. Arsenijevic, B. H. Weber, A. Gal, and C. Rivolta. Nonsense mutations in fam161a cause rp28-associated recessive retinitis pigmentosa. *The American Journal of Human Genetics*, 87(3):376–81, 2010.

[240] A. Abderrahmani, G. Niederhauser, V. Plaisance, M. E. Roehrich, V. Lenain, T. Coppola, R. Regazzi, and G. Waeber. Complexin i regulates glucose-induced secretion in pancreatic beta-cells. *Journal of Cell Science*, 117(Pt 11):2239–47, 2004.

[241] S. Jutras, M. Bachvarova, M. Keita, J. L. Bascands, A. M. Mes-Masson, J. M. Stewart, L. Gera, and D. Bachvarov. Strong cytotoxic effect of the bradykinin antagonist bkm-570 in ovarian cancer cells–analysis of the molecular mechanisms of its antiproliferative action. *FEBS Journal*, 277(24):5146–60, 2010.

[242] M. R. Rossi, J. Conroy, D. McQuaid, N. J. Nowak, J. T. Rutka, and J. K. Cowell. Array cgh analysis of pediatric medulloblastomas. *Genes Chromosomes Cancer*, 45(3):290–303, 2006.

[243] M. Moghanibashi, F. R. Jazii, Z. S. Soheili, M. Zare, A. Karkhane, K. Parivar, and P. Mohamadynejad. Proteomics of a new esophageal cancer cell line established from persian patient. *Gene*, 500(1):124–33, 2012.

[244] E. K. Lee, H. Cho, and C. W. Kim. Proteomic analysis of cancer stem cells in human prostate cancer cells. *Biochemical and Biophysical Research Communications*, 412(2):279–85, 2011.

[245] H. Chang, S. Y. Rha, H. C. Jeung, J. J. Jung, T. S. Kim, H. J. Kwon, B. S. Kim, and H. C. Chung. Identification of genes related to a synergistic effect of taxane and suberoylanilide hydroxamic acid combination treatment in gastric cancer cells. *Journal of Cancer Research and Clinical Oncology*, 136(12):1901–13, 2010.

[246] T. Hanafusa, A. E. Mohamed, K. Kitaoka, Y. Ohue, E. Nakayama, and T. Ono. Isolation and characterization of human lung cancer antigens by serological screening with autologous antibodies. *Cancer Letters*, 301(1):57–62, 2011.

[247] S. W. Chang, P. Y. Lu, J. H. Guo, T. C. Tsai, Y. P. Tsao, and S. L. Chen. Nrip enhances hpv gene expression via interaction with either gr or e2. *Virology*, 423(1):38–48, 2012.

[248] C. P. Han, M. Y. Lee, S. L. Tzeng, C. C. Yao, P. H. Wang, Y. W. Cheng, S. L. Chen, T. S. Wu, Y. S. Tyan, and L. F. Kok. Nuclear receptor interaction protein (nrip) expression assay using human tissue microarray and immunohistochemistry technology confirming nuclear localization. *Journal of Experimental & Clinical Cancer Research*, 27:25, 2008.

[249] T. C. Tsai, Y. L. Lee, W. C. Hsiao, Y. P. Tsao, and S. L. Chen. Nrip, a novel nuclear receptor interaction protein, enhances the transcriptional activity of nuclear receptors. *Journal of Biological Chemistry*, 280(20):20000–9, 2005.

[250] S. W. Chang, Y. P. Tsao, C. Y. Lin, and S. L. Chen. Nrip, a novel calmodulin binding protein, activates calcineurin to dephosphorylate human papillomavirus e2 protein. *J Virol*, 85(13):6750–63, 2011.

[251] A. Muto, S. Tashiro, O. Nakajima, H. Hoshino, S. Takahashi, E. Sakoda, D. Ikebe, M. Yamamoto, and K. Igarashi. The transcriptional programme of antibody class switching involves the repressor bach2. *Nature*, 429(6991):566–71, 2004.

[252] A. Muto, S. Tashiro, H. Tsuchiya, A. Kume, M. Kanno, E. Ito, M. Yamamoto, and K. Igarashi. Activation of maf/ap-1 repressor bach2 by oxidative stress promotes apoptosis and its interaction with promyelocytic leukemia nuclear bodies. *Journal of Biological Chemistry*, 277(23):20724–33, 2002.

[253] A. Ono, K. Kono, D. Ikebe, A. Muto, J. Sun, M. Kobayashi, K. Ueda, J. V. Melo, K. Igarashi, and S. Tashiro. Nuclear positioning of the bach2 gene in bcr-abl positive leukemic cells. *Genes Chromosomes Cancer*, 46(1):67–74, 2007.

[254] A. Spira, J. E. Beane, V. Shah, K. Steiling, G. Liu, F. Schembri, S. Gilman, Y. M. Dumas, P. Calner, P. Sebastiani, S. Sridhar, J. Beamis, C. Lamb, T. Anderson, N. Gerry, J. Keane, M. E. Lenburg, and J. S. Brody. Airway epithelial gene expression in the diagnostic evaluation of smokers with suspect lung cancer. *Nature Medicine*, 13(3):361–6, 2007.

[255] E. Sakane-Ishikawa, S. Nakatsuka, Y. Tomita, S. Fujita, I. Nakamichi, T. Takakuwa, H. Sugiyama, S. Fukuhara, M. Hino, A. Kanamaru, T. Soma, M. Tsukaguchi, K. Igarashi, Y. Kanakura, K. Aozasa, and Group Osaka Lymphoma Study. Prognostic significance of bach2 expression in diffuse large b-cell lymphoma: a study of the osaka lymphoma study group. *Journal of Clinical Oncology*, 23(31):8012–7, 2005.

[256] A. J. Li, R. G. Elmore, J. C. Pavelka, and B. Y. Karlan. Hyperandrogenism, mediated by obesity and receptor polymorphisms, promotes aggressive epithelial ovarian cancer biology. *Gynecologic Oncology*, 107(3):420–3, 2007.

[257] N.P. Pavletich, K.A. Chambers, and C.O. Pabo. The dna-binding domain of p53 contains the four conserved regions and the major mutation hot spots. *Genes & development*, 7:2556, 1993.

[258] B. Vogelstein and K.W. Kinzler. p53 function and dysfunction. *Cell*, 70:523–526, 1992.

[259] R. C. Sobti and K. Parashar. A study on p53 protein and anti-p53 antibodies in the sera of patients with oesophageal cancer. *Mutation Research*, 422(2):271–7, 1998.

[260] S. Labrecque, N. Naor, D. Thomson, and G. Matlashewski. Analysis of the anti-p53 antibody response in cancer patients. *Cancer Research*, 53(15):3468–71, 1993.

[261] S. F. Winter, J. D. Minna, B. E. Johnson, T. Takahashi, A. F. Gazdar, and D. P. Carbone. Development of antibodies against p53 in lung cancer patients appears to be dependent on the type of p53 mutation. *Cancer Research*, 52(15):4168–74, 1992.

[262] S. Metcalfe, T. K. Wheeler, S. Picken, S. Negus, and A. Jo Milner. P53 autoantibodies in 1006 patients followed up for breast cancer. *Breast Cancer Research*, 2(6):438–43, 2000.

[263] S. Mosolits, U. Harmenberg, U. Ruden, L. Ohman, B. Nilsson, B. Wahren, J. Fagerberg, and H. Mellstedt. Autoantibodies against the tumour-associated antigen ga733-2 in patients with colorectal carcinoma. *Cancer Immunology, Immunotherapy*, 47(6):315–20, 1999.

[264] Y. Li, A. Karjalainen, H. Koskinen, K. Hemminki, H. Vainio, M. Shnaidman, Z. Ying, E. Pukkala, and P. W. Brandt-Rauf. p53 autoantibodies predict subsequent development of cancer. *International Journal of Cancer*, 114:157–60–, 2005.

[265] A. M. Goh, C. R. Coffill, and D. P. Lane. The role of mutant p53 in human cancer. *Journal of Pathology*, 223:116–26, 2011.

[266] B. Schlichtholz, Y. Legros, D. Gillet, C. Gaillard, M. Marty, D. Lane, F. Calvo, and T. Soussi. The immune response to p53 in breast cancer patients is directed against immunodominant epitopes unrelated to the mutational hot spot. *Cancer Research*, 52:6380–4–, 1992.

[267] S. J. Skates, N. K. Horick, J. M. Moy, A. M. Minihan, M. V. Seiden, J. R. Marks, P. Sluss, and D. W. Cramer. Pooling of case specimens to create standard serum sets for screening cancer biomarkers. *Cancer Epidemiology, Biomarkers and Prevention*, 16(2):334–41, 2007.

[268] B. Cahoon-Young, A. Chandler, T. Livermore, J. Gaudino, and R. Benjamin. Sensitivity and specificity of pooled versus individual sera in a human immunodeficiency virus antibody prevalence study. *Journal of Clinical Microbiology*, 27(8):1893–5, 1989.

[269] C. A. Hughes and V. Bennett. Adducin: a physical model with implications for function in assembly of spectrin-actin complexes. *Journal of Biological Chemistry*, 270(32):18990–6, 1995.

[270] K. Gardner and V. Bennett. Modulation of spectrin-actin assembly by erythrocyte adducin. *Nature*, 328(6128):359–62, 1987.

[271] K. L. Barkalow, Jr. Italiano, J. E., D. E. Chou, Y. Matsuoka, V. Bennett, and J. H. Hartwig. Alpha-adducin dissociates from f-actin and spectrin during platelet activation. *Journal of Cell Biology*, 161(3):557–70, 2003.

[272] D. M. Gilligan, R. Sarid, and J. Weese. Adducin in platelets: activation-induced phosphorylation by pkc and proteolysis by calpain. *Blood*, 99(7):2418–26, 2002.

[273] Y. Matsuoka, X. Li, and V. Bennett. Adducin: structure, function and regulation. *Cellular and Molecular Life Sciences*, 57(6):884–95, 2000.

[274] S. C. Kiley, K. J. Clark, S. K. Duddy, D. R. Welch, and S. Jaken. Increased protein kinase c delta in mammary tumor cells: relationship to transformtion and metastatic progression. *Oncogene*, 18(48):6748–57, 1999.

[275] Y. Matsuoka, X. Li, and V. Bennett. Adducin is an in vivo substrate for protein kinase c: phosphorylation in the marcks-related domain inhibits activity in promoting spectrin-actin complexes and occurs in many cells, including dendritic spines of neurons. *Journal of Cellular Biology*, 142(2):485–97, 1998.

[276] H. W. Kaiser, E. O'Keefe, and V. Bennett. Adducin: Ca++-dependent association with sites of cell-cell contact. *Journal of Cell Biology*, 109(2):557–69, 1989.

[277] C. L. Chen, Y. T. Hsieh, and H. C. Chen. Phosphorylation of adducin by protein kinase cdelta promotes cell motility. *Journal of Cell Science*, 120(Pt 7):1157–67, 2007.

[278] Y. Fukata, N. Oshiro, N. Kinoshita, Y. Kawano, Y. Matsuoka, V. Bennett, Y. Matsuura, and K. Kaibuchi. Phosphorylation of adducin by rho-kinase plays a crucial role in cell motility. *Journal of Cell Biology*, 145(2):347–61, 1999.

[279] C. L. Chen, Y. P. Lin, Y. C. Lai, and H. C. Chen. alpha-adducin translocates to the nucleus upon loss of cell-cell adhesions. *Traffic*, 12(10):1327–40, 2011.

[280] D. J. Zabransky, H. A. Smith, C. J. Thoburn, M. Zahurak, D. Keizman, M. Carducci, M. A. Eisenberger, D. G. McNeel, C. G. Drake, and E. S. Antonarakis. Lenalidomide modulates il-8 and anti-prostate antibody levels in men with biochemically recurrent prostate cancer. *Prostate*, 72(5):487–98, 2012.

[281] B. B. Maricque, J. C. Eickhoff, and D. G. McNeel. Antibody responses to prostate-associated antigens in patients with prostatitis and prostate cancer. *Prostate*, 71(2):134–46, 2011.

[282] T. Lorca and A. Castro. The greatwall kinase: a new pathway in the control of the cell cycle. *Oncogene*, Epub ahead of print, 2012.

[283] D. Bataille, L. Heron, A. Virsolvy, K. Peyrollier, A. LeCam, L. Gros, and P. Blache. alpha-endosulfine, a new entity in the control of insulin secretion. *Cellular and Molecular Life Sciences*, 56(1-2):78–84, 1999.

[284] J. R. Von Stetina, S. Tranguch, S. K. Dey, L. A. Lee, B. Cha, and D. Drummond-Barbosa. alpha-endosulfine is a conserved protein required for oocyte meiotic maturation in drosophila. *Development*, 135(22):3697–706, 2008.

[285] S. H. Kim and G. Lubec. Decreased alpha-endosulfine, an endogenous regulator of atp-sensitive potassium channels, in brains from adult down syndrome patients. *Journal of Neural Transmission. Supplementa*, 61(61):1–9, 2001.

[286] V. Syed, X. Zhang, K. M. Lau, R. Cheng, K. Mukherjee, and S. M. Ho. Profiling estrogen-regulated gene expression changes in normal and malignant human ovarian surface epithelial cells. *Oncogene*, 24:8128–43, 2005.

[287] D. Haesen, W. Sents, E. Ivanova, C. Lambrecht, and V. Janssens. Cellular inhibitors of protein phosphatase pp2a in cancer. *Biomedical Research*, 23:197–211, 2012.

[288] N. Ludwig, A. Keller, P. Leidinger, C. Harz, C. Backes, H. P. Lenhof, and E. Meese. Is there a general autoantibody signature for cancer? *European Journal of Cancer*, Epub ahead of print, 2012.

[289] N. Ludwig, A. Keller, S. Heisel, P. Leidinger, S. Rheinheimer, C. Andres, B. Stephan, W. I. Steudel, E. Donauer, N. Graf, B. Burgeth, J. Weickert, H. P. Lenhof, and E. Meese. Novel immunogenic antigens increase classification accuracy in meningioma to 93.84 *International Journal of Cancer*, 128(6):1493–501, 2011.

[290] J. Schmitt, A. Keller, N. Nourkami-Tutdibi, S. Heisel, N. Habel, P. Leidinger, N. Ludwig, M. Gessler, N. Graf, F. Berthold, H. P. Lenhof, and E. Meese. Autoantibody signature differentiates wilms tumor patients from neuroblastoma patients. *PLoS One*, 6(12):e28951, 2011.

[291] P. Leidinger, A. Keller, S. Heisel, N. Ludwig, S. Rheinheimer, V. Klein, C. Andres, A. Staratschek-Jox, J. Wolf, E. Stoelben, B. Stephan, I. Stehle, J. Hamacher, H. Huwer, H. P. Lenhof, and E. Meese. Identification of lung cancer with high sensitivity and specificity by blood testing. *Respiratory Research*, 11:18, 2010.

[292] N. Ludwig, A. Keller, S. Heisel, P. Leidinger, V. Klein, S. Rheinheimer, C. U. Andres, B. Stephan, W. I. Steudel, N. M. Graf, B. Burgeth, J. Weickert, H. P. Lenhof, and E. Meese. Improving seroreactivity-based detection of glioma. *Neoplasia*, 11(12):1383–9, 2009.

[293] E. J. Dunphy, J. C. Eickhoff, C. H. Muller, R. E. Berger, and D. G. McNeel. Identification of antigen-specific igg in sera from patients with chronic prostatitis. *Journal of Clinical Immunology*, 24(5):492–502, 2004.

[294] U. Reineke, C. Ivascu, M. Schlief, C. Landgraf, S. Gericke, G. Zahn, H. Herzel, R. Volkmer-Engert, and J. Schneider-Mergener. Identification of distinct antibody epitopes and mimotopes from a peptide array of 5520 randomly generated sequences. *Journal of Immunological Methods*, 267(1):37–51, 2002.

[295] D.A. Bell. Origins and molecular pathology of ovarian cancer. *Modern pathology*, 18:S19–S32, 2005.

[296] A. L. Gross, R. J. Kurman, R. Vang, M. Shih Ie, and K. Visvanathan. Precursor lesions of high-grade serous ovarian carcinoma: morphological and molecular characteristics. *Journal of Oncology*, 2010:126295, 2010.

[297] B. S. Taylor, M. Pal, J. Yu, B. Laxman, S. Kalyana-Sundaram, R. Zhao, A. Menon, J. T. Wei, A. I. Nesvizhskii, D. Ghosh, G. S. Omenn, D. M. Lubman, A. M. Chinnaiyan, and A. Sreekumar. Humoral response profiling reveals pathways to prostate cancer progression. *Molecular & Cellular Proteomics*, 7:600–11–, 2008.

[298] J. L. Gardy, D. J. Lynn, F. S. Brinkman, and R. E. Hancock. Enabling a systems biology approach to immunology: focus on innate immunity. *Trends in Immunology*, 30(6):249–62, 2009.

[299] D. J. Lynn, G. L. Winsor, C. Chan, N. Richard, M. R. Laird, A. Barsky, J. L. Gardy, F. M. Roche, T. H. Chan, N. Shah, R. Lo, M. Naseer, J. Que, M. Yau, M. Acab, D. Tulpan, M. D. Whiteside, A. Chikatamarla, B. Mah, T. Munzner, K. Hokamp, R. E. Hancock, and F. S. Brinkman. Innatedb: facilitating systems-level analyses of the mammalian innate immune response. *Molecular Systems Biology*, 4:218, 2008.

[300] S. E. Aiyar, J. L. Sun, A. L. Blair, C. A. Moskaluk, Y. Z. Lu, Q. N. Ye, Y. Yamaguchi, A. Mukherjee, D. M. Ren, H. Handa, and R. Li. Attenuation of estrogen receptor alpha-mediated transcription through estrogen-stimulated recruitment of a negative elongation factor. *Genes & Development*, 18(17):2134–46, 2004.

[301] A. Bratt, O. Birot, I. Sinha, N. Veitonmaki, K. Aase, M. Ernkvist, and L. Holmgren. Angiomotin regulates endothelial cell-cell junctions and cell motility. *Journal of Biological Chemistry*, 280(41):34859–69, 2005.

[302] B. Troyanovsky, T. Levchenko, G. Mansson, O. Matvijenko, and L. Holmgren. Angiomotin: an angiostatin binding protein that regulates endothelial cell migration and tube formation. *Journl of Cellular Biology*, 152(6):1247–54, 2001.

[303] W. G. Jiang, G. Watkins, A. Douglas-Jones, L. Holmgren, and R. E. Mansel. Angiomotin and angiomotin like proteins, their expression and correlation with angiogenesis and clinical outcome in human breast cancer. *BMC Cancer*, 6:16, 2006.

[304] L. Holmgren, E. Ambrosino, O. Birot, C. Tullus, N. Veitonmaki, T. Levchenko, L. M. Carlson, P. Musiani, M. Iezzi, C. Curcio, G. Forni, F. Cavallo, and R. Kiessling. A dna vaccine targeting angiomotin inhibits angiogenesis and suppresses tumor growth. *Proceedings of the National Academy of Sciences of the United States of America*, 103(24):9208–13, 2006.

[305] M. Arigoni, G. Barutello, S. Lanzardo, D. Longo, S. Aime, C. Curcio, M. Iezzi, Y. Zheng, I. Barkefors, L. Holmgren, and F. Cavallo. A vaccine targeting angiomotin induces an antibody response which alters tumor vessel permeability and hampers the growth of established tumors. *Angiogenesis*, 15(2):305–16, 2012.

[306] B. J. Mayer, R. Ren, K. L. Clark, and D. Baltimore. A putative modular domain present in diverse signaling proteins. *Cell*, 73:629–30, 1993.

[307] R. J. Haslam, H. B. Koide, and B. A. Hemmings. Pleckstrin domain homology. *Nature*, 363(6427):309–10, 1993.

[308] G. Shaw. The pleckstrin homology domain: an intriguing multifunctional protein module. *Bioessays*, 18(1):35–46, 1996.

[309] A. J. Piekny and M. Glotzer. Anillin is a scaffold protein that links rhoa, actin, and myosin during cytokinesis. *Current Biology*, 18(1):30–6, 2008.

[310] J. Q. Cheng, A. K. Godwin, A. Bellacosa, T. Taguchi, T. F. Franke, T. C. Hamilton, P. N. Tsichlis, and J. R. Testa. Akt2, a putative oncogene encoding a member of a subfamily of protein-serine/threonine kinases, is amplified in human ovarian carcinomas. *Proceedings of the National Academy of Sciences of the United States of America*, 89(19):9267–71, 1992.

[311] S. M. Downs, P. G. Humpherson, and H. J. Leese. Meiotic induction in cumulus cell-enclosed mouse oocytes: involvement of the pentose phosphate pathway. *Biology of Reproduction*, 58(4):1084–94, 1998.

[312] P. Vizan, G. Alcarraz-Vizan, S. Diaz-Moralli, O. N. Solovjeva, W. M. Frederiks, and M. Cascante. Modulation of pentose phosphate pathway during cell cycle progression in human colon adenocarcinoma cell line ht29. *International Journal of Cancer*, 124(12):2789–96, 2009.

[313] H. Y. Zhou, Y. L. Pon, and A. S. Wong. Synergistic effects of epidermal growth factor and hepatocyte growth factor on human ovarian cancer cell invasion and migration: role of extracellular signal-regulated kinase 1/2 and p38 mitogen-activated protein kinase. *Endocrinology*, 148(11):5195–208, 2007.

[314] L. Xu, P. S. Pathak, and D. Fukumura. Hypoxia-induced activation of p38 mitogen-activated protein kinase and phosphatidylinositol 3'-kinase signaling pathways contributes to expression of interleukin 8 in human ovarian carcinoma cells. *Clinical Cancer Research*, 10(2):701–7, 2004.

[315] J. Hayakawa, M. Ohmichi, H. Kurachi, H. Ikegami, A. Kimura, T. Matsuoka, H. Jikihara, D. Mercola, and Y. Murata. Inhibition of extracellular signal-regulated protein kinase or c-jun n-terminal protein kinase cascade, differentially activated by cisplatin, sensitizes human ovarian cancer cell line. *Journal of Biological Chemistry*, 274(44):31648–54, 1999.

[316] K. A. Charles, H. Kulbe, R. Soper, M. Escorcio-Correia, T. Lawrence, A. Schultheis, P. Chakravarty, R. G. Thompson, G. Kollias, J. F. Smyth, F. R. Balkwill, and T. Hagemann. The tumor-promoting actions of tnf-alpha involve tnfr1 and il-17 in ovarian cancer in mice and humans. *Journal of Clinical Investigation*, 119(10):3011–23, 2009.

[317] B. Dobrzycka, S. J. Terlikowski, O. Kowalczuk, and M. Kinalski. Circulating levels of tnf-alpha and its soluble receptors in the plasma of patients with epithelial ovarian cancer. *European Cytokine Network*, 20(3):131–4, 2009.

[318] I. Remy, A. Montmarquette, and S. W. Michnick. Pkb/akt modulates tgf-beta signalling through a direct interaction with smad3. *Nature Cell Biology*, 6(4):358–65, 2004.

[319] J. Luo. Glycogen synthase kinase 3beta (gsk3beta) in tumorigenesis and cancer chemotherapy. *Cancer Letters*, 273(2):194–200, 2009.

[320] S. Bao, G. Ouyang, X. Bai, Z. Huang, C. Ma, M. Liu, R. Shao, R. M. Anderson, J. N. Rich, and X. F. Wang. Periostin potently promotes metastatic growth of colon cancer by augmenting cell survival via the akt/pkb pathway. *Cancer Cell*, 5(4):329–39, 2004.

[321] G. C. Rodriguez, C. Haisley, J. Hurteau, T. L. Moser, R. Whitaker, Jr. Bast, R. C., and M. S. Stack. Regulation of invasion of epithelial ovarian cancer by transforming growth factor-beta. *Gynecologic Oncology*, 80(2):245–53, 2001.

[322] W. Hu, W. Wu, M. A. Nash, R. S. Freedman, J. J. Kavanagh, and C. F. Verschraegen. Anomalies of the tgf-beta postreceptor signaling pathway in ovarian cancer cell lines. *Anticancer Research*, 20(2A):729–33, 2000.

[323] S. D. Yamada, R. L. Baldwin, and B. Y. Karlan. Ovarian carcinoma cell cultures are resistant to tgf-beta1-mediated growth inhibition despite expression of functional receptors. *Gynecologic Oncology*, 75(1):72–7, 1999.

[324] V. Stambolic, A. Suzuki, J. L. de la Pompa, G. M. Brothers, C. Mirtsos, T. Sasaki, J. Ruland, J. M. Penninger, D. P. Siderovski, and T. W. Mak. Negative regulation of pkb/akt-dependent cell survival by the tumor suppressor pten. *Cell*, 95(1):29–39, 1998.

[325] L. A. Hefler, E. Ludwig, A. Lebrecht, R. Zeillinger, D. Tong-Cacsire, H. Koelbl, S. Leodolter, and C. B. Tempfer. Polymorphisms of the interleukin-1 gene cluster and ovarian cancer. *Journal of the Society for Gynecologic Investigation*, 9(6):386–90, 2002.

[326] M. M. Moradi, L. F. Carson, B. Weinberg, A. F. Haney, L. B. Twiggs, and S. Ramakrishnan. Serum and ascitic fluid levels of interleukin-1, interleukin-6, and tumor necrosis factor-alpha in patients with ovarian epithelial cancer. *Cancer*, 72(8):2433–40, 1993.

[327] H. Zeisler, C. Tempfer, E. A. Joura, G. Sliutz, H. Koelbl, O. Wagner, and C. Kainz. Serum interleukin 1 in ovarian cancer patients. *European Journal of Cancer*, 34(6):931–3, 1998.

[328] Y. Kawakami, N. Nagai, S. Ota, K. Ohama, and U. Yamashita. Interleukin-1 as an autocrine stimulator in the growth of human ovarian cancer cells. *Hiroshima Journal of Medical Sciences*, 46(1):51–9, 1997.

[329] S. A. Vlahopoulos, S. Logotheti, D. Mikas, A. Giarika, V. Gorgoulis, and V. Zoumpourlis. The role of atf-2 in oncogenesis. *Bioessays*, 30(4):314–27, 2008.

[330] S. Gehmert, L. Prantl, J. Vykoukal, E. Alt, and Y. H. Song. Breast cancer cells attract the migration of adipose tissue-derived stem cells via the pdgf-bb/pdgfr-beta signaling pathway. *Biochemical and Biophysical Research Communications*, 398(3):601–5, 2010.

[331] J. Yu, C. Ustach, and H. R. Kim. Platelet-derived growth factor signaling and human cancer. *Journal of Biochemistry and Molecular Biology*, 36(1):49–59, 2003.

[332] H. Shimada, M. Arima, K. Nakajima, Y. Koide, S. Okazumi, H. Matsubara, Y. Miyazawa, A. Takeda, H. Hayashi, T. Yoshida, T. Ochiai, and K. Isono. Detection of serum p53 antibodies in mucosal esophageal cancer and negative conversion after treatment. *American Journal of Gastroenterology*, 93(8):1388–9, 1998.

[333] K. Angelopoulou and E. P. Diamandis. Detection of the tp53 tumour suppressor gene product and p53 auto-antibodies in the ascites of women with ovarian cancer. *European Journal of Cancer*, 33(1):115–21, 1997.

[334] S. Kumar, A. Mohan, and R. Guleria. Prognostic implications of circulating anti-p53 antibodies in lung cancer–a review. *European Journal of Cancer Care*, 18(3):248–54, 2009.

[335] A. Takeda, H. Shimada, K. Nakajima, H. Imaseki, T. Suzuki, T. Asano, T. Ochiai, and K. Isono. Monitoring of p53 autoantibodies after resection of colorectal cancer: relationship to operative curability. *European Journal of Surgery*, 167(1):50–3, 2001.

[336] T. Mitsudomi, S. Suzuki, Y. Yatabe, M. Nishio, M. Kuwabara, K. Gotoh, S. Hatooka, M. Shinoda, M. Suyama, M. Ogawa, T. Takahashi, and Y. Ariyoshi. Clinical implications of p53 autoantibodies in the sera of patients with non-small-cell lung cancer. *Journal of the National Cancer Institute*, 90(20):1563–8, 1998.

[337] G. Zalcman, B. Schlichtholz, J. Tredaniel, T. Urban, R. Lubin, I. Dubois, B. Milleron, A. Hirsch, and T. Soussi. Monitoring of p53 autoantibodies in lung cancer during therapy: relationship to response to treatment. *Clinical Cancer Research*, 4(6):1359–66, 1998.

[338] T. Qiu, Q. Yang, X. R. Li, H. Yang, L. L. Qiu, and L. Wang. Detection of serum anti-p53 antibodies from patients with ovarian cancer in china: correlation to clinical parameters. *Cancer Investigation*, 25(7):563–8, 2007.

[339] W. H. Robinson, C. DiGennaro, W. Hueber, B. B. Haab, M. Kamachi, E. J. Dean, S. Fournel, D. Fong, M. C. Genovese, H. E. de Vegvar, K. Skriner, D. L. Hirschberg, R. I. Morris, S. Muller, G. J. Pruijn, W. J. van Venrooij, J. S. Smolen, P. O. Brown, L. Steinman, and P. J. Utz. Autoantigen microarrays for multiplex characterization of autoantibody responses. *Nature Medicine*, 8(3):295–301, 2002.

[340] A. E. Lokshin, M. Winans, D. Landsittel, A. M. Marrangoni, L. Velikokhatnaya, F. Modugno, B. M. Nolen, and E. Gorelik. Circulating il-8 and anti-il-8 autoantibody in patients with ovarian cancer. *Gynecologic Oncology*, 102(2):244–51, 2006.

[341] D. J. Cahill. Protein and antibody arrays and their medical applications. *Journal of Immunological Methods*, 250(1-2):81–91, 2001.

[342] Y. Legros, C. Lafon, and T. Soussi. Linear antigenic sites defined by the b-cell response to human p53 are localized predominantly in the amino and carboxy-termini of the protein. *Oncogene*, 9(7):2071–6, 1994.

[343] B. Schlichtholz, J. Tredaniel, R. Lubin, G. Zalcman, A. Hirsch, and T. Soussi. Analyses of p53 antibodies in sera of patients with lung carcinoma define immunodominant regions in the p53 protein. *British Journal of Cancer*, 69(5):809–16, 1994.

[344] R. Lubin, B. Schlichtholz, D. Bengoufa, G. Zalcman, J. Tredaniel, A. Hirsch, C. Caron de Fromentel, C. Preudhomme, P. Fenaux, G. Fournier, P. Mangin, P. Laurent-Puig, G. Pelletier, M. Schlumberger, F. Desgrandchamps, A. Le Duc, J. P. Peyrat, N. Janin, B. Bressac, T. Soussi, and et al. Analysis of p53 antibodies in patients with various cancers define b-cell epitopes of human p53: distribution on primary structure and exposure on protein surface. *Cancer Research*, 53(24):5872–6, 1993.

[345] B. Abendstein, C. Marth, E. Muller-Holzner, M. Widschwendter, G. Daxenbichler, and A. G. Zeimet. Clinical significance of serum and ascitic p53 autoantibodies in epithelial ovarian carcinoma. *Cancer*, 88(6):1432–7, 2000.

Appendix A

Chapter 3 Appendix

Table A.1: Breakdown of serum used for hEx1 screening

Cohort	Identifier	Stage	Grade	Age	Details
Early	39	IC	2	51	Endometrioid with mucinous foci
Early	66	I	not available	52	Yolk sac tumour in cystic teratoma
Early	99	IA	not available	58	Mixed mullerian tumour
Early	144	IA	2	35	Clear cell
Early	168	IC	not available	83	Mucinous adenocarcinoma
Early	176	IA	2	57	Serous papillary adenocarcinoma
Early	180	IA	1	56	Endometrioid
Early	183	IA	2	34	Endometrioid
Early	223	IC	3	49	Serous papillary adenocarcinoma
Early	257	IC	3	61	Serous papillary adenocarcinoma
Early	268	IC	3	64	Serous papillary adenocarcinoma
Early	277	2B	3	86	Serous papillary adenocarcinoma
Early	294	IC	2	50	Mucinous adenocarcinoma

Cohort	Identifier	Stage	Grade	Age	Details
Late	8	3C	3	59	Serous papillary adenocarcinoma
Late	15	3C	3	60	Serous papillary adenocarcinoma
Late	21	3B	3	42	Serous papillary adenocarcinoma
Late	24	3C	3	64	Serous papillary adenocarcinoma
Late	34	3C	2	74	Serous papillary adenocarcinoma
Late	36	3C	2-3	86	Serous papillary adenocarcinoma
Late	37	3	2	63	Serous papillary adenocarcinoma
Late	55	3C	3	68	Serous papillary adenocarcinoma
Late	65	4	not available	74	Serous papillary adenocarcinoma
Late	71	4	3	41	Serous papillary adenocarcinoma
Late	87	3C	3	60	Serous papillary adenocarcinoma
Late	89	3A	3	44	Serous papillary adenocarcinoma
Late	115	3C	3	61	Serous papillary adenocarcinoma
Late	120	3C	3	60	Serous papillary adenocarcinoma

Cohort	Identifier	Stage	Grade	Age	Details
Late	137	3C	3	51	Serous papillary adenocarcinoma
Late	175	3C	3	79	Serous papillary adenocarcinoma
Late	177	3C	2	76	Serous papillary adenocarcinoma
Late	188	3C	3	74	Serous papillary adenocarcinoma
Late	189	3C	2-3	59	Serous papillary adenocarcinoma
Late	198	4	3	55	Serous papillary adenocarcinoma
Peritoneal	20	4	3	82	Peritoneal serous papillary carcinoma
Peritoneal	40	3C	2	58	Peritoneal serous papillary carcinoma
Peritoneal	62	3C	3	64	Peritoneal serous papillary carcinoma
Peritoneal	68	3C	3	69	Peritoneal serous papillary carcinoma
Peritoneal	86	3C	3	50	Peritoneal serous papillary carcinoma
Benign	22	-	-	44	Mucinous cystadenoma
Benign	47	-	-	52	Cystadenoma
Benign	48	-	-	72	Mucinous cystadenoma

Cohort	Identifier	Stage	Grade	Age	Details
Benign	63	-	-	47	Mucinous cystadenoma
Benign	84	-	-	23	Mucinous cystadenoma
Benign	100	-	-	59	Cystadenoma
Benign	101	-	-	55	Serous cystadenoma
Benign	135	-	-	56	Mucinous cystadenoma
Benign	147	-	-	57	Mucinous cystadenoma
Benign	149	-	-	48	Mucinous cystadenoma and fibroma
Non-remark	N1	-	-	60	
Non-remark	N2	-	-	42	
Non-remark	N3	-	-	56	
Non-remark	N4	-	-	56	
Non-remark	N5	-	-	63	
Non-remark	N6	-	-	53	
Non-remark	N7	-	-	72	

Cohort	Identifier	Stage	Grade	Age	Details
Non-remark	N8	-	-	83	
Non-remark	N15	-	-	62	
Healthy	70077109	-	-	84	
Healthy	70077121	-	-	75	
Healthy	70077127	-	-	72	
Healthy	70077142	-	-	79	
Healthy	70077143	-	-	77	
Healthy	70077151	-	-	81	
Healthy	70077153	-	-	80	
Healthy	Ctr03p	-	-	41	
Healthy	Ctr04p	-	-	58	
Healthy	Ctr05p	-	-	40	
Healthy	Ctr07p	-	-	54	
Healthy	Ctr09p	-	-	66	

Cohort	Identifier	Stage	Grade	Age	Details
Healthy	Ctr10p	-	-	65	
Healthy	Ctr11p	-	-	62	
Healthy	Ctr12p	-	-	73	
Healthy	Ctr13p	-	-	68	
Healthy	Ctr14p	-	-	57	

From the analysis performed by Dr. John O'Brien panels of expression clones were identified to be associated with the different serum cohorts used for screening, these panels and the relevant cohorts are detailed in Table A.2. The panels of clones with the lowest p-value were selected for further analysis, as evident in Table A.2, panels were selected mainly from the ovarian cancer cohorts, i.e. Early ovarian cancer, late ovarian cancer and early/late ovarian cancer associated antigenic panels of clones.

Table A.2: Generated panels of clones of interest and identification of His-tagged

Cohort	Panels of Clones	P-value	Sens	Spec
Early	**528A14** 536F02 **541A01 549G08 579A01** 584O14	2.73E-09	0.9286	0.9016
Early	**528A14** 536F02 **541D13 549G08 579A01** 584O14	2.73E-09	0.9286	0.9016
Early	**528A14** 536F02 **549G08 556J12 579A01** 584O14	2.73E-09	0.9286	0.9016
Early	**528A14** 536F02 **549G08 564H06 579A01** 584O14	2.73E-09	0.9286	0.9016
Early	**506F21 528A14** 536F02 **541A01 579A01** 584O14	7.67E-09	0.9286	0.8852
Early	**506F21 528A14** 536F02 **541D13 579A01** 584O14	7.67E-09	0.9286	0.8852
Early	**506F21 528A14** 536F02 **556J12 579A01** 584O14	7.67E-09	0.9286	0.8852
Early	**506F21 528A14** 536F02 **564H06 579A01** 584O14	7.67E-09	0.9286	0.8852
Early	**513P09 528A14** 536F02 **549G08 579A01** 584O14	7.67E-09	0.9286	0.8852
Early	**521G12 549G08 564H23** 569B16 588M16 597L02	7.67E-09	0.9286	0.8852
Early	**528A14** 529I23 **536F02 549G08 579A01** 584O14	7.67E-09	0.9286	0.8852
Early	**528A14** 536F02 541N20 **549G08 579A01** 584O14	7.67E-09	0.9286	0.8852
Early	**528A14** 536F02 543N20 **549G08 579A01** 584O14	7.67E-09	0.9286	0.8852

Cohort	Panels of Clones	P-value	Sens	Spec
Early	**528A14** 536F02 549E22 **549G08 579A01** 584O14	7.67E-09	0.9286	0.8852
Early	**528A14** 536F02 **549G08 570M24 579A01** 584O14	7.67E-09	0.9286	0.8852
Early	**528A14** 536F02 **549G08 579A01** 584I09 584O14	7.67E-09	0.9286	0.8852
Early	**528A14** 536F02 **549G08 579A01** 584O14 **591M14**	7.67E-09	0.9286	0.8852
Early	**528L15 541D13 541M17 564H23** 582B01 588M16	7.67E-09	0.9286	0.8852
Early	**528L15 541D13 541M17 564H23** 588M16 597L02	7.67E-09	0.9286	0.8852
Early	**528L15 541M17 541N20 564H23** 582B01 588M16	7.67E-09	0.9286	0.8852
Early	**528L15 541M17 541N20 564H23** 588M16 597L02	7.67E-09	0.9286	0.8852
Early	**528L15 541M17 564H06 564H23** 588M16 597L02	7.67E-09	0.9286	0.8852
Early	**528L15 541M17 564H23 570M24** 582B01 588M16	7.67E-09	0.9286	0.8852
Early	**528L15 541M17 564H23 570M24** 588M16 597L02	7.67E-09	0.9286	0.8852
Early	**541D13 541M17** 552J24 **564H23** 582B01 588M16	7.67E-09	0.9286	0.8852
Early	**541D13 541M17** 552J24 **564H23** 588M16 597L02	7.67E-09	0.9286	0.8852
Early	**541D13 549G08 564H23** 569B16 588M16 597L02	7.67E-09	0.9286	0.8852

Cohort	Panels of Clones	P-value	Sens	Spec
Early	**541D13 549G08 564H23** 578M10 588M16 597L02	7.67E-09	0.9286	0.8852
Early	**541M17 541N20** 552J24 **564H23** 582B01 588M16	7.67E-09	0.9286	0.8852
Early	**541M17 541N20** 552J24 **564H23** 588M16 597L02	7.67E-09	0.9286	0.8852
Early	**541M17** 552J24 **564H06 564H23** 588M16 597L02	7.67E-09	0.9286	0.8852
Early	**541M17** 552J24 **564H23 570M24** 582B01 588M16	7.67E-09	0.9286	0.8852
Early	**541M17** 552J24 **564H23 570M24** 588M16 597L02	7.67E-09	0.9286	0.8852
Early	**541N20 549G08 564H23** 569B16 588M16 597L02	7.67E-09	0.9286	0.8852
Early	**541N20 549G08 564H23** 578M10 588M16 597L02	7.67E-09	0.9286	0.8852
Early	543N20 **549G08 564H23** 569B16 588M16 597L02	7.67E-09	0.9286	0.8852
Early	543N20 **549G08 564H23** 578M10 588M16 597L02	7.67E-09	0.9286	0.8852
Early	**549G08** 561J18 **564H23** 569B16 588M16 597L02	7.67E-09	0.9286	0.8852
Early	**549G08 564H06 564H23** 569B16 588M16 597L02	7.67E-09	0.9286	0.8852
Early	**549G08 564H06 564H23** 578M10 588M16 597L02	7.67E-09	0.9286	0.8852
Early	**549G08 564H23 568A19** 569B16 588M16 597L02	7.67E-09	0.9286	0.8852

Cohort	Panels of Clones	P-value	Sens	Spec
Early	**549G08 564H23** 569B16 569L02 588M16 597L02	7.67E-09	0.9286	0.8852
Early	**549G08 564H23** 569B16 **570M24** 588M16 597L02	7.67E-09	0.9286	0.8852
Early	**549G08 564H23** 569B16 574D19 588M16 597L02	7.67E-09	0.9286	0.8852
Early	**549G08 564H23** 569B16 588M16 597L02 602A07	7.67E-09	0.9286	0.8852
Early	**549G08 564H23 570M24** 578M10 588M16 597L02	7.67E-09	0.9286	0.8852
Early/Late	**528A14 549G08 562L16** 582M24 597L02 602D07	8.49E-11	0.8529	0.8780
Early/Late	**528A14** 539C01 **549G08 562L16** 582M24 597L02	8.49E-11	0.8529	0.8780
Early/Late	**528A14 549G08 562L16 571F17** 582M24 597L02	8.49E-11	0.8529	0.8780
Early/Late	**528A14** 533P22 **549G08** 582M24 597L02 602D07	8.49E-11	0.8529	0.8780
Early/Late	**528A14** 533P22 539C01 **549G08** 582M24 597L02	8.49E-11	0.8529	0.8780
Early/Late	**528A14** 539C01 541L07 **549G08** 582M24 597L02	8.49E-11	0.8529	0.8780
Early/Late	**528A14 549G08 556H09 568E16 585H10** 597L02	8.92E-11	0.8235	0.9024
Early/Late	**528A14 549G08** 566B10 **568E16 585H10** 597L02	8.92E-11	0.8235	0.9024
Early/Late	**521G12 528A14 549G08 585H10** 597L02 602D07	8.92E-11	0.8235	0.9024

Cohort	Panels of Clones	P-value	Sens	Spec
Early/Late	**528A14** 542M19 **549G08** 566B10 **585H10** 597L02	8.92E-11	0.8235	0.9024
Early/Late	**521G12 528A14** 545A12 **549G08 585H10** 597L02	8.92E-11	0.8235	0.9024
Early/Late	**514I07 528A14 549G08 568E16 585H10** 597L02	8.92E-11	0.8235	0.9024
Early/Late	**528A14 549G08** 566B10 **585H10 589A08** 597L02	8.92E-11	0.8235	0.9024
Early/Late	**528A14** 539C01 **549G08** 563N03 **585H10** 597L02	8.92E-11	0.8235	0.9024
Early/Late	**514I07 528A14** 539C01 **549G08 585H10** 597L02	8.92E-11	0.8235	0.9024
Early/Late	**521G12 528A14 547B20 549G08 585H10** 597L02	8.92E-11	0.8235	0.9024
Early/Late	**514I07 528A14 547B20 549G08 585H10** 597L02	8.92E-11	0.8235	0.9024
Early/Late	**528A14 549G08 556H09 585H10** 597L02 602D07	8.92E-11	0.8235	0.9024
Early/Late	**528A14 549G08** 566B10 **573P07 585H10** 597L02	8.92E-11	0.8235	0.9024
Early/Late	**528A14 547B20 549G08 556H09 585H10** 597L02	8.92E-11	0.8235	0.9024
Early/Late	**514I07 528A14 549G08** 566B10 **585H10** 597L02	8.92E-11	0.8235	0.9024
Early/Late	515B02 **528A14 549G08** 566B10 **585H10** 597L02	8.92E-11	0.8235	0.9024
Early/Late	**528A14 549G08 556H09 562L16 585H10** 597L02	8.92E-11	0.8235	0.9024

Cohort	Panels of Clones	P-value	Sens	Spec
Early/Late	**514I07 528A14 549G08 562L16 585H10** 597L02	8.92E-11	0.8235	0.9024
Early/Late	**528A14 549G08 562L16** 566B10 **585H10** 597L02	8.92E-11	0.8235	0.9024
Late	**521I11 541H09 578A05** 580K15 **592J02** 602D07	3.65E-14	0.9000	0.9818
Late	**521I11 541H09 544N13 578A05** 580K15 602D07	3.65E-14	0.9000	0.9818
Late	**519O15 521I11** 537B13 577J19 **578A05** 580K15	3.84E-14	0.8500	1.0000
Late	**507H13 519O15 521I11** 549M24 580K15 594A18	3.84E-14	0.8500	1.0000
Late	**519O15 521I11** 524E23 537B13 **578A05** 580K15	3.84E-14	0.8500	1.0000
Late	**519O15** 520M05 **521I11** 580K15 589B01 602D07	3.84E-14	0.8500	1.0000
Late	**519O15 521I11 528N06 578A05** 580K15 602D07	3.84E-14	0.8500	1.0000
Late	**513O07 519O15 521I11** 549M24 **578F13** 580K15	3.84E-14	0.8500	1.0000
Late	**506H06 519O15 521I11** 545D01 **578A05** 580K15	3.84E-14	0.8500	1.0000
Late	**513O07 519O15** 520M05 **521I11** 580K15 602D07	3.84E-14	0.8500	1.0000
Late	**519O15 521I11 533N09 578A05 578F13** 580K15	3.84E-14	0.8500	1.0000
Late	**506H06 519O15 521I11 578A05** 580K15 594A18	3.84E-14	0.8500	1.0000

Cohort	Panels of Clones	P-value	Sens	Spec
Late	**519O15 521I11** 549M24 580K15 589B01 594A18	3.84E-14	0.8500	1.0000
Late	**513O07 519O15 521I11** 545D01 549M24 580K15	3.84E-14	0.8500	1.0000
Late	**519O15 521I11** 549M24 580K15 591H02 **592J02**	3.84E-14	0.8500	1.0000
Late	**507H13 519O15 521I11** 545D01 549M24 580K15	3.84E-14	0.8500	1.0000
Late	**519O15 521I11 533D08 578A05 578F13** 580K15	3.84E-14	0.8500	1.0000
Late	**519O15 521I11 578A05** 580K15 **592J02** 602D07	3.84E-14	0.8500	1.0000
Late	**519O15 521I11 528N06** 549M24 **575J16** 580K15	3.84E-14	0.8500	1.0000
Late	**519O15 521I11 528N06** 549M24 580K15 591H02	3.84E-14	0.8500	1.0000
Late	**519O15 521I11** 537B13 **564L10 578A05** 580K15	3.84E-14	0.8500	1.0000
Late	**519O15 521I11 528N06 547G19** 549M24 580K15	3.84E-14	0.8500	1.0000
Late	**519O15 521I11** 545D01 549M24 **559L09** 580K15	3.84E-14	0.8500	1.0000
Late	**519O15 521I11** 545D01 549M24 580K15 589B01	3.84E-14	0.8500	1.0000
Late	**519O15 521I11 533D08** 545D01 **578A05** 580K15	3.84E-14	0.8500	1.0000
Late	**519O15 521I11 523N01 578A05** 580K15 602D07	3.84E-14	0.8500	1.0000

Cohort	Panels of Clones	P-value	Sens	Spec
Late	**510D19 519O15 521I11** 545D01 549M24 580K15	3.84E-14	0.8500	1.0000
Late	**519O15 521I11** 549M24 **559L09 578F13** 580K15	3.84E-14	0.8500	1.0000
Late	**519O15 521I11 578A05** 580K15 **592M23** 602D07	3.84E-14	0.8500	1.0000
Late	**519O15 521I11** 537B13 574D19 **578A05** 580K15	3.84E-14	0.8500	1.0000
Late	**519O15 521I11 544N13** 549M24 **575J16** 580K15	3.84E-14	0.8500	1.0000
Late	**519O15 521I11 544N13** 549M24 **568E16** 580K15	3.84E-14	0.8500	1.0000
Late	**519O15 521I11 529E13** 544A07 **578A05** 580K15	3.84E-14	0.8500	1.0000
Late	**513O07 519O15 521I11** 580K15 **590G16** 602D07	3.84E-14	0.8500	1.0000
Late	**519O15 521I11** 537B13 541H19 **578A05** 580K15	3.84E-14	0.8500	1.0000
Late	**519O15 521I11 533A02** 537B13 **578A05** 580K15	3.84E-14	0.8500	1.0000
Late	**519O15 521I11** 537B13 545D01 **578A05** 580K15	3.84E-14	0.8500	1.0000
Late	**519O15 521I11** 537B13 **578A05** 580K15 **592J02**	3.84E-14	0.8500	1.0000
Late	**519O15 521I11 528N06 535D07** 549M24 580K15	3.84E-14	0.8500	1.0000
Late	**510D19 519O15 521I11** 580K15 **590G16** 602D07	3.84E-14	0.8500	1.0000

Cohort	Panels of Clones	P-value	Sens	Spec
Late	**519O15** 520M05 **521I11** **559L09** 580K15 602D07	3.84E-14	0.8500	1.0000
Late	**519O15** **521I11** **528N06** 549M24 **568E16** 580K15	3.84E-14	0.8500	1.0000
Late	**519O15** **521I11** 537B13 **578A05** 580K15 584M23	3.84E-14	0.8500	1.0000
Late	**506H06** **519O15** **521I11** **578A05** **578F13** 580K15	3.84E-14	0.8500	1.0000
Late	**519O15** **521I11** **547G19** 549M24 580K15 **592J02**	3.84E-14	0.8500	1.0000
Late	**519O15** **521I11** **525F05** **529E13** **578A05** 580K15	3.84E-14	0.8500	1.0000
Late	**510D19** **519O15** 520M05 **521I11** 580K15 602D07	3.84E-14	0.8500	1.0000
Late	**519O15** **521I11** 537B13 **578A05** 580K15 594D15	3.84E-14	0.8500	1.0000
Late	**519O15** **521I11** **544N13** **578A05** 580K15 602D07	3.84E-14	0.8500	1.0000
Late	**519O15** **521I11** **529E13** **578A05** 580K15 602D07	3.84E-14	0.8500	1.0000
Late	**519O15** **521I11** 537B13 **557B01** **578A05** 580K15	3.84E-14	0.8500	1.0000
Late	**519O15** **521I11** 580K15 589B01 **590G16** 602D07	3.84E-14	0.8500	1.0000
Late	**519O15** **521I11** **533D08** **578A05** 580K15 594A18	3.84E-14	0.8500	1.0000
Late	**519O15** **521I11** **535D07** 549M24 580K15 **592J02**	3.84E-14	0.8500	1.0000

Cohort	Panels of Clones	P-value	Sens	Spec
Late	**519O15 521I11 544N13 547G19** 549M24 580K15	3.84E-14	0.8500	1.0000
Late	**519O15 521I11** 537B13 **578A05 578F13** 580K15	3.84E-14	0.8500	1.0000
Late	**519O15 521I11 535D07 544N13** 549M24 580K15	3.84E-14	0.8500	1.0000
Late	**519O15 521I11 529E13 538A05 578A05** 580K15	3.84E-14	0.8500	1.0000
Late	**507H13 519O15 521I11** 580K15 **590G16** 602D07	3.84E-14	0.8500	1.0000
Late	**519O15 521I11** 537B13 **544N13 578A05** 580K15	3.84E-14	0.8500	1.0000
Late	**513O07 519O15 521I11** 549M24 580K15 594A18	3.84E-14	0.8500	1.0000
Late	**519O15 521I11 544N13** 549M24 580K15 591H02	3.84E-14	0.8500	1.0000
Late	**519O15 521I11 528N06** 537B13 **578A05** 580K15	3.84E-14	0.8500	1.0000
Late	**519O15 521I11** 549M24 **559L09** 580K15 594A18	3.84E-14	0.8500	1.0000
Late	**519O15 521I11** 537B13 **578A05** 580K15 594A18	3.84E-14	0.8500	1.0000
Late	**519O15 521I11** 537B13 **578A05** 580K15 588M16	3.84E-14	0.8500	1.0000
Late	**519O15 521I11** 537B13 **578A05** 580K15 599K03	3.84E-14	0.8500	1.0000
Late	518A20 **519O15 521I11 528N06** 549M24 580K15	3.84E-14	0.8500	1.0000

Cohort	Panels of Clones	P-value	Sens	Spec
Late	**519O15 521I11** 549M24 **578F13** 580K15 589B01	3.84E-14	0.8500	1.0000
Late	**519O15 521I11 533N09** 545D01 **578A05** 580K15	3.84E-14	0.8500	1.0000
Late	**519O15 521I11** 537B13 **578A05** 580K15 597G02	3.84E-14	0.8500	1.0000
Late	**507H13 519O15 521I11** 549M24 **578F13** 580K15	3.84E-14	0.8500	1.0000
Late	**519O15 521I11 533N09 578A05** 580K15 594A18	3.84E-14	0.8500	1.0000
Late	**510D19 519O15 521I11** 549M24 **578F13** 580K15	3.84E-14	0.8500	1.0000
Late	**519O15 521I11 559L09** 580K15 **590G16** 602D07	3.84E-14	0.8500	1.0000
Late	**519O15 521I11** 549M24 **575J16** 580K15 **592J02**	3.84E-14	0.8500	1.0000
Late	518A20 **519O15 521I11 544N13** 549M24 580K15	3.84E-14	0.8500	1.0000
Late	**519O15 521I11** 537B13 **578A05** 580K15 582K12	3.84E-14	0.8500	1.0000
Late	518A20 **519O15 521I11** 549M24 580K15 **592J02**	3.84E-14	0.8500	1.0000
Late	**507H13 519O15** 520M05 **521I11** 580K15 602D07	3.84E-14	0.8500	1.0000
Late	**519O15 521I11** 549M24 **568E16** 580K15 **592J02**	3.84E-14	0.8500	1.0000
Late	512F01 **521I11 533D08 544N13 553F06 568E16** 597L02	2.88E-16	1.0000	0.9636

Cohort	Panels of Clones	P-value	Sens	Spec
Late	512F01 **521I11 533D08 549M22 568E16** 597F24 597L02	2.88E-16	1.0000	0.9636
Late	512F01 **521I11 533D08 544N13 549M22 568E16** 597L02	2.88E-16	1.0000	0.9636
Late	**521I11** 545E16 **546G19 568E16** 582B01 **601P03** 602D07	2.88E-16	1.0000	0.9636
Late	512F01 **521I11 525J13 553F06 568E16** 570C14 597L02	2.88E-16	1.0000	0.9636
Late	512F01 **521I11 525J13 549M22 568E16** 570C14 597L02	2.88E-16	1.0000	0.9636
Late	512F01 **521I11 533D08 553F06 568E16 592J02** 597L02	2.88E-16	1.0000	0.9636
Late	512F01 **521I11 533D08 553F06 568E16** 597F24 597L02	2.88E-16	1.0000	0.9636
Late	512F01 **521I11 549M22 568E16** 570C14 597L02 602D07	2.88E-16	1.0000	0.9636
Late	512F01 **521I11 533D08 549M22 568E16 592J02** 597L02	2.88E-16	1.0000	0.9636
Late	**521I11 525J13** 545E16 **546G19 568E16** 582B01 **601P03**	2.88E-16	1.0000	0.9636
Late	512F01 **521I11 553F06 568E16** 570C14 **597L02** 602D07	2.88E-16	1.0000	0.9636
Benign	**511O10 525D04 528B14** 556L11 **592F05**	1.21E-12	1.0000	1.0000
Benign	**511O10 525D04 528B14 530C03 592F05**	1.21E-12	1.0000	1.0000
Benign	**511O10 525D04 528B14 592F05** 598I03	1.21E-12	1.0000	1.0000

Cohort	Panels of Clones	P-value	Sens	Spec
Benign	511O10 525D04 528B14 552J04 592F05	1.21E-12	1.0000	1.0000
Benign	511O10 525D04 528B14 541J04 592F05	1.21E-12	1.0000	1.0000
Benign	511O10 525D04 528B14 533D01 592F05	1.21E-12	1.0000	1.0000
Benign	511O10 525D04 528B14 546G11 592F05	1.21E-12	1.0000	1.0000
Benign	511O10 525D04 528B14 578I03 592F05	1.21E-12	1.0000	1.0000
Benign	511O10 525D04 528B14 573P04 592F05	1.21E-12	1.0000	1.0000
Benign	507D22 511O10 525D04 528B14 592F05	1.21E-12	1.0000	1.0000
Peritoneal	589N14 594M05 601E12	3.48E-07	1.0000	0.9857
Peritoneal	552K12 601E12 602A21	1.22E-06	1.0000	0.9714
Peritoneal	528M16 552K12 601E12	1.22E-06	1.0000	0.9714
Peritoneal	589N14 592F05 601E12	1.22E-06	1.0000	0.9714
Peritoneal	523G13 578B14 601E12	1.22E-06	1.0000	0.9714
Peritoneal	532L19 553C06 601E12	3.24E-06	1.0000	0.9571
Peritoneal	589A21 589N14 601E12	3.24E-06	1.0000	0.9571

Cohort	Panels of Clones	P-value	Sens	Spec
Peritoneal	532L19 589N14 601E12	3.24E-06	1.0000	0.9571
Peritoneal	549G07 589N14 601E12	3.24E-06	1.0000	0.9571
Peritoneal	552K12 589N14 601E12	3.24E-06	1.0000	0.9571

Table A.3: Identities and details of antigens of interest

N	Clone	Product	PAGE Sizing	Seq Sizing
1	506F21	DDB1- and CUL4-associated factor 6 isoform d	60	18
2	506H06	alpha-adducin	25	22
3	507H13	endosulfine alpha	23	19
4	510D19	endosulfine alpha	23	19
5	511O10	Putative RNA-binding protein 15B	27	not available
6	513O07	endosulfine alpha	23	19
7	513P09	tetratricopeptide repeat domain 3	25	23
8	514I07	FTH1 protein	17	17
9	519O15	myosin light chain 6B	30	28
10	521G12	cadherin-related 23	17	15
11	521I11	prefoldin 5	20	20
12	523N01	ADP-ribosylhydrolase like 2	40	40
13	525D04	FGF13	32	30
14	525F05	RNA binding motif protein 22	32	not available
15	525J13	mitogen-activated protein kinase 11	15	not available
16	528A14	complexin 1	26	23
17	528B14	zinc finger protein 6	28	28
18	528L15	tripartite motif containing 37 protein	32	27
19	528M16	Bromodomain containing 9	37	38
20	528N06	NGFI-A-binding protein 2	28	21
21	529E13	dematin	18	18
22	530C03	RPLP1	18	17
23	533A02	kinesin light chain 1	26	25
24	533D01	PDZD4 protein	70	36
25	533D08	Calcium channel, voltage-dependent, beta 1 subunit	33	25
26	533N09	Calcium channel, voltage-dependent, beta 1 subunit	37	30
27	535D07	ankyrin repeat and MYND domain-containing protein 2	24	22

N	Clone	Product	PAGE Sizing	Seq Sizing
28	538A05	RNA binding motif protein 22	26	41
29	541A01	tetratricopeptide repeat domain 3	20	19
30	541D13	formin-binding protein 4	40	36
31	541H09	myosin light chain 6B	30	25
32	541J04	coiled-coil domain-containing protein 12	27	22
33	541M17	dematin	17	15
34	541N20	BCL2-associated athanogene 5	19	18
35	544N13	zinc finger protein 207	15	31
36	546G11	ADP-ribosylation factor binding protein GGA1	20	36
37	546G19	zyxin	30	41
38	547B20	39S ribosomal protein L27	35	not available
39	547G19	Cellular tumour antigen p53	35	28
40	549G07	KIF18B protein	18	15
41	549G08	DDB1 and CUL4 associated factor 6	65	39
42	549M22	leucine-rich repeat-containing protein 42	23	21
43	552J04	ADP-ribosylation factor binding protein GGA1	70	41
44	552J24	Potential novel protein	12	10
45	553F06	peptidyl-prolyl cis-trans isomerase NIMA-interacting 1	22	22
46	556H09	Ferritin heavy chain	18	not available
47	556J12	TPRD	22	20
48	557B01	single-stranded DNA binding protein 2	36	32
49	559L09	endosulfine alpha	23	19
50	562L16	sperm-associated antigen 7	27	29
51	564H06	drebin 1	27	29
52	564H23	GON-4-like protein	16	22
53	564L10	coiled-coil domain containing 94	36	28
54	568A19	Serine/threonine-protein kinase D2	100	not available
55	568E16	Cellular tumour antigen p53	26	24
56	570M24	RNA-binding protein 6	100	not available

N	Clone	Product	PAGE Sizing	Seq Sizing
57	571F17	RD RNA binding protein	45	36
58	573P04	WW and C2 domain containing 1	17	19
59	573P07	praja ring finger 1	45	24
60	575J16	MBOAT7 protein	32	29
61	578A05	coiled-coil domain containing 92	40	38
62	578F13	HIP1R	16	17
63	578I03	microtubule-associated protein 1S	60	36
64	579A01	B-cell lymphoma/leukemia 11B	10	5
65	585H10	zinc finger FYVE domain-containing protein 27	15	13
66	589A08	Creatine kinase B-type	45	not available
67	590G16	Meis homeobox 2	40	29
68	591M14	Formin binding protein 4	70	31
69	592F05	protein FAM161A	24	24
70	592J02	transcription regulator protein BACH2	35	31
71	592M23	Calcium binding and coiled-coil domain 2	32	33
72	594M05	mitochondrial ribosomal protein S11	24	23
73	601E12	SAP domain containing ribonucleoprotein	30	27
74	601P03	XAP-5 protein	37	37

Comparison of Protein Purification Methodologies

For protein purification IMAC was the method of choice as the hEx1 protein are all His-tagged Two different metals, nickel and zinc, were examined in this study to determine the optimum purification method. Comparison of both metal agaroses revealed similar proportions of contaminating *E-coli* proteins compared to the yield of hEx1 protein. However the nickel agarose has a higher histidine binding affinity and the resulting purified protein yield was much higher compared to zinc agarose purified proteins. Hence protein purification using nickel agarose was the favoured method.

To purify the proteins two different purification methods were investigated, purification using pH change and purification using concentration change. The pH purification method was performed under denaturing conditions with pellet lysis in 6M guanidine hydrochloride and protein purification in 8M urea, as outlined in Section 2.4.4. The concentration gradient method was performed under the following conditions, pellet lysis in 6M guanidine hydrochloride and protein washing with imidazole (20mM), and protein elution with imidazole (250mM). From the comparative results of these two different purification methods, the methods were relatively interchangeable in terms of protein yield. However, protein stability was greatly improved in the urea buffer, hence due to ease of handling, purification using pH change was favoured.

As the protein storage buffer may have implications on protein folding and hence recognition of antigens in the secondary techniques, buffer exchange was also interrogated in this study. The urea prepared purified proteins underwent buffer exchange to PBS buffer using filtration spin columns with a molecular weight cut-off (~10kDa) to remove urea. However, this step resulted in decreased protein yield and was very time intensive. Also, the buffer exchange did not seem to effect the results attained in the secondary validation methods when compared to the urea proteins. The loss of the urea buffer, decreased the storage-life of the protein (3-4 days at 4°), making storage more

difficult. Hence the buffer exchange step was not routinely performed for interrogation of the purified antigens.

Table A.4: Breakdown of serum used for hEx1 protein microarray screening

Cohort	Serum	Stage	Grade	Age	Details
Early	39	IC	2	51	Endometrioid with mucinous foci
Early	99	IA	not available	58	Mixed mullerian tumour
Early	114	IA	low	42	Endometrioid
Early	144	IA	2	35	Clear cell
Early	168	IC	not available	83	Mucinous adenocarcinoma
Early	176	IA	2	57	Serous papillary adenocarcinoma
Early	180	IA	1	56	Endometrioid
Early	183	IA	2	34	Endometrioid
Early	201	IC	1	51	Mucinous adenocarcinoma
Early	214	IA	not available	69	Clear cell with adenofibroma
Early	223	IC	3	49	Serous papillary adenocarcinoma
Early	224	IC	not available	70	Clear cell with adenofibroma
Early	236	IA	1	69	Mucinous adenocarcinoma
Early	239	IC	not available	60	Clear cell with adenofibroma
Early	257	IC	3	61	Serous papillary adenocarcinoma
Early	258	IC	not available	47	Granulosa theca cell tumour
Early	268	IC	3	64	Serous papillary adenocarcinoma
Early	277	2B	3	86	Serous papillary adenocarcinoma
Early	294	IC	2	50	Mucinous adenocarcinoma
Early	347	IC	3	50	Serous papillary adenocarcinoma
Late	8	3C	3	59	Serous papillary adenocarcinoma
Late	15	3C	3	60	Serous papillary adenocarcinoma
Late	21	3B	3	42	Serous papillary adenocarcinoma
Late	24	3C	3	64	Serous papillary adenocarcinoma
Late	34	3C	2	74	Serous papillary adenocarcinoma
Late	36	3C	2-3	86	Serous papillary adenocarcinoma
Late	37	3	2	63	Serous papillary adenocarcinoma
Late	55	3C	3	68	Serous papillary adenocarcinoma
Late	65	4	not available	74	Serous papillary adenocarcinoma
Late	71	4	3	41	Serous papillary adenocarcinoma
Late	83	4	3	65	Clear cell
Late	87	3C	3	60	Serous papillary adenocarcinoma
Late	89	3A	3	44	Serous papillary adenocarcinoma
Late	95	3C	not available	40	Clear cell
Late	96	3C	3	58	Clear cell
Late	115	3C	3	61	Serous papillary adenocarcinoma
Late	120	3C	3	60	Serous papillary adenocarcinoma
Late	137	3C	3	51	Serous papillary adenocarcinoma
Late	175	3C	3	79	Serous papillary adenocarcinoma
Late	177	3C	2	76	Serous papillary adenocarcinoma
Late	188	3C	3	74	Serous papillary adenocarcinoma
Late	189	3C	2-3	59	Serous papillary adenocarcinoma

Cohort	Serum	Stage	Grade	Age	Details
Late	198	4	3	55	Serous papillary adenocarcinoma
Benign	22	-	-	44	Mucinous cystadenoma
Benign	25	-	-	50	Follicular cyst
Benign	47	-	-	52	Cystadenoma
Benign	48	-	-	72	Mucinous cystadenoma
Benign	63	-	-	47	Mucinous cystadenoma
Benign	84	-	-	23	Mucinous cystadenoma
Benign	100	-	-	59	Cystadenoma
Benign	101	-	-	55	Serous cystadenoma
Benign	107	-	-	44	Fibroid
Benign	118	-	-	39	Endometriosis
Benign	135	-	-	56	Mucinous cystadenoma
Benign	147	-	-	57	Mucinous cystadenoma
Benign	149	-	-	48	Mucinous cystadenoma and fibroma
Benign	151	-	-	34	Endometriotic cyst
Benign	382	-	-	58	Serous cystadenoma
Benign	383	-	-	42	Serous cystadenoma, fibroma
Benign	398	-	-	31	Serous cystadenoma
Benign	412	-	-	28	Serous cystadenoma
Benign	420	-	-	57	Serous cystadenoma
Benign	429	-	-	43	Serous cystadenoma
Non-remark	N1	-	-	60	
Non-remark	N2	-	-	42	
Non-remark	N3	-	-	56	
Non-remark	N4	-	-	56	
Non-remark	N5	-	-	63	
Non-remark	N6	-	-	53	
Non-remark	N7	-	-	72	
Non-remark	N8	-	-	83	
Non-remark	N9	-	-	70	
Non-remark	N10	-	-	70	
Non-remark	N11	-	-	82	
Non-remark	N12	-	-	85	
Non-remark	N13	-	-	52	
Non-remark	N15	-	-	62	
Non-remark	N16	-	-	48	

Appendix B

Chapter 4 Appendix

Table B.1: Ovarian cancer associated antigens of interest (individual serum analysis)

These antigens were identified from individual ovarian cancer serum screening. AAbs to these antigens were present in ovarian cancer patient serum and not present in the non-remarkable serum

60S ribosomal protein L9
adducin alpha
C6orf153 protein
CDC42 binding protein kinase beta (DMPK-like)
Endosulfine alpha
eukaryotic translation elongation factor 2
FK506 binding protein 3
FTH1 protein ferritin
homeobox protein Meis
KIF18B
Metastasis associated 1
mitochondrial ribosomal protein
MYC-associated zinc finger protein
Cellular tumour antigen p53
prefoldin subunit
PRO0890
semaphorin-4C (SEMA4C)
Septin
TATA box binding protein (TBP)-associated factor
zinc finger HIT domain-containing protein

Table B.2: Ovarian cancer associated antigens of interest (pooled serum analysis)

These antigens were identified from pooled ovarian cancer serum screening. AAbs to these antigens were present in the ovarian cancer pooled serum and not present in the non-remarkable pooled serum.

ADP-ribosylation factor
bolA-like protein
cytoplasmic protein
endosulfine alpha
inhibitor of growth protein
coiled-coil domain protein
F-box protein
transmembrane protein
zinc finger protein
spliceosomal protein
Cellular tumour antigen p53
ephexin protein
Coiled-coil containing protein
Non-ATPase protein
transcription factor
Cerebellar degeneration-related protein
staufen protein
Rab interacting protein
Novel protein
peptidylprolyl isomerase protein
spectrin protein
stathmin protein
Nuclear GTPase activating protein
UDP-glucose like protein
40S ribosomal protein
ral guanine nucleotide related protein
methyl binding domain protein
ubiquitin modifier enzyme
dihydropyrimidinase-like protein
B-cell and lymphoma antigen protein
Adducin alpha
nuclear receptor coactivator
Selenoprotein
amino-terminal protein

Commercial anti-p53 antibody incubation of 200ng per lane Western blots

Western immunoblotting was carried out as per materials and methods, however instead of serum, anti-p53 antibody (Calbiochem, OP43) was diluted (1:1000 dilution) in 10ml

2% milk-TBS-T and blot was incubated in antibody for 1 hour on slow rock at RT. From this stage the blot was washed and imaged as per the other Western blots.

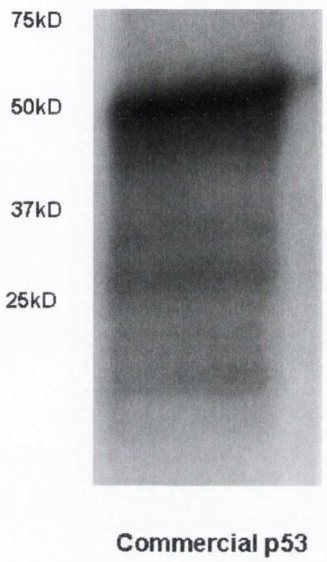

Figure B.1: Commercial p53 Western blot, probed with commercial anti-p53 antibody

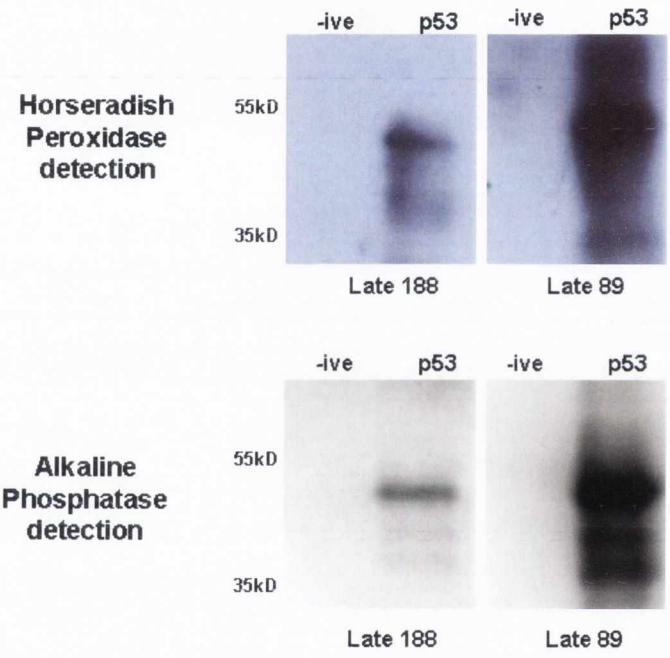

Figure B.2: Comparison of detection methodologies

Appendix C

Chapter 5 Appendix

Table C.1: Identification of antigens associated with cohorts

Late OC only	Early OC only	Non-Remark only	Benign only
Pleckstrin homology domain-containing family O member 2	LIM domain and actin-binding protein 1	family with sequence similarity 21, member C	Protein DGCR6L
Ral GEF with PH domain and SH3 binding motif 1	ubiquitin protein ligase E3A (UBE3A)	Serine/threonine-protein kinase 25	protein tyrosine phosphatase, non-receptor type 12
anillin, actin binding protein	enoyl Coenzyme A hydratase domain containing 1	RAD51 associated protein 1	Small proline-rich protein 3
glial fibrillary acidic protein	pelota homolog (Drosophila)	SH3 domain-binding protein 2	hypothetical protein MGC4473

Late OC only	Early OC only	Non-Remark only	Benign only
	Metastasis-associated protein MTA1	family with sequence similarity 90, member A1	C-jun-amino-terminal kinase-interacting protein 2
	Protein phosphatase Slingshot homolog 3	Activin receptor type-2B	CWF19-like 2, cell cycle control (S. pombe)
	3'-phosphoadenosine 5'-phosphosulfate synthase 2	cysteine and glycine-rich protein 2	
	chimeric cDNA clone	SH2 domain protein 2A	
	nuclear receptor binding factor 2	Hematopoietic lineage cell-specific protein	
	chromosome 9 open reading frame 37	mitochondrial ribosomal protein L28	

Late OC only	Early OC only	Non-Remark only	Benign only
	homer homolog 2 (Drosophila)	La ribonucleoprotein domain family, member 7, transcript variant 1	
	superoxide dismutase 2, mitochondrial	active BCR-related gene (ABR), transcript variant 1	
	JTV1 gene	Microtubule-associated protein 9	
	Isovaleryl-CoA dehydrogenase, mitochondrial	Uncharacterized protein C19orf44	
	potassium channel tetramerisation domain containing 6	chromosome 11 open reading frame 63, transcript variant 2	
	AF4/FMR2 family, member 4	Ataxin-7-like protein 3	
	transcription elongation factor A (SII)-like 8		
	stromal membrane-associated protein 1		

Late OC only	Early OC only	Non-Remark only	Benign only
	CWC15 homolog (S. cerevisiae)		
	Uncharacterized protein C20orf96		
	centaurin, beta 2		
	AT rich interactive domain 3A		
	Rap guanine nucleotide exchange factor 3		
	Proline-rich protein 16		
	Kanadaptin		
	Glucose-6-phosphate isomerase		
	holocarboxylase synthetase		
	Mevalonate kinase		
	Rho GTPase activating protein 17, transcript variant 1		

Late OC only	Early OC only	Non-Remark only	Benign only
	aldehyde dehydrogenase 7 family, member A1		
	chromogranin B		
	6-phosphofructo-2-kinase/fructose-2,6 biphosphatase 1		
	RD RNA binding protein		
	DEAD (Asp-Glu-Ala-Asp) box polypeptide 1		
	Transducin-like enhancer protein 4		
	nudix-type motif 21		
	Kelch-like ECH-associated protein 1		
	leucine rich repeat containing 6		
	inositol(myo)-1(or 4)-monophosphatase 2		

Late OC only	Early OC only	Non-Remark only	Benign only
	glutamate receptor, ionotropic, NMDA-like 1A, transcript variant 1		
	Zinc finger CCHC domain-containing protein 8		
	TBC1 domain family member 22B		
	coiled-coil domain containing 99		
	solute carrier family 4, member 1, adaptor protein		
	zinc finger protein 496		
	chorionic gonadotropin, beta polypeptide 1		
	glutamic pyruvate transaminase 2		
	cortactin, transcript variant 2		

Late OC only	Early OC only	Non-Remark only	Benign only
	chromosome 1 open reading frame 87		
	potassium inwardly-rectifying channel, subfamily J, member 1, transcript variant rom-k2		
	ADP-ribosylation factor GTPase activating protein 1, transcript variant 2		
	protein phosphatase 2, regulatory subunit Bγ, transcript variant 4		
	La ribonucleoprotein domain family, member 4, transcript variant 3		
	Splicing factor 1		
	family with sequence similarity 102, member A, transcript variant 2		

Late OC only	Early OC only	Non-Remark only	Benign only
	regulator of calcineurin 1, transcript variant 2		
	PREDICTED: Homo sapiens hypothetical gene supported by BC047417, transcript variant 1		
	PREDICTED: Homo sapiens hypothetical LOC401363		

Table C.2: Identification of antigens common to all cohorts

Common Antigens
Ig lambda chain C regions
Immunoglobulin heavy constant gamma 1 (G1m marker)
CD3D
IGK
immunoglobulin heavy constant mu
Fc fragment of IgG, low affinity IIIa, receptor
immunoglobulin heavy constant gamma 1
Matrilin-2
CD79A
immunoglobulin heavy constant gamma 1
Ig gamma-1 chain C region
family with sequence similarity 84, member A
immunoglobulin kappa constant
IGK
IGL, immunoglobulin lambda locus
CD7
IGK
immunoglobulin heavy constant gamma 3 (G3m marker)
immunoglobulin kappa constant
immunoglobulin kappa variable 1-5
immunoglobulin kappa variable 1-5
immunoglobulin heavy constant mu
EGF-like repeats and discoidin I-like domains 3
immunoglobulin heavy variable 4-31
immunoglobulin kappa constant
Ig kappa chain C region
immunoglobulin kappa constant
Ig gamma-1 chain C region
immunoglobulin kappa constant region
Ig gamma-1 chain C region
Ig gamma-1 chain C region
twinfilin, actin-binding protein, homolog 1 (Drosophila)
tripartite motif-containing 21
LIM and senescent cell antigen-like-containing domain protein 1
hematopoietic SH2 domain containing
recombination signal binding protein for immunoglobulin kappa J region
Recombinant human CTLA-4/Fc

Tables C.3, C.4 and C.5 outline the relative AAb frequency of the cohort associated antigens identified from ProtoArray screening.

Table C.3: Autoantibody frequency of benign associated antigens

	Non-Remarkable					Benign					Early OC					Late OC				
	N1	N3	N5	N15	N16	382	383	398	420	429	176	223	257	268	347	87	89	120	189	198
Protein DGCR6L								Y	Y											
protein tyrosine phosphatase, non-receptor type 12	Y								Y	Y		Y								
Small proline-rich protein 3		Y						Y	Y						Y					
hypothetical protein MGC4473									Y	Y				Y						
C-jun-amino-terminal kinase-interacting protein 2			Y				Y	Y												
CWF19-like 2, cell cycle control (S. pombe)								Y	Y						Y					

Table C.4: Autoantibody frequency of early OC associated antigens

	Non-Remarkable					Benign					Early OC					Late OC				
	N1	N3	N5	N15	N16	382	383	398	420	429	176	223	257	268	347	87	89	120	189	198
LIM domain and actin-binding protein 1				Y									Y		Y					
ubiquitin protein ligase E3A (UBE3A)													Y		Y	Y				
enoyl Coenzyme A hydratase domain containing 1													Y		Y					
pelota homolog (Drosophila)													Y		Y					
Metastasis-associated protein MTA1												Y	Y							
Protein phosphatase Slingshot homolog 3													Y		Y					Y
3'-phosphoadenosine 5'-phosphosulfate synthase 2									Y				Y	Y	Y					
chimeric cDNA clone													Y	Y						
nuclear receptor binding factor 2	Y										Y				Y					
chromosome 9 open reading frame 37													Y		Y					
homer homolog 2 (Drosophila)													Y		Y	Y				
superoxide dismutase 2, mitochondrial		Y											Y		Y					
JTV1 gene														Y	Y					

	Non-Remarkable					Benign					Early OC					Late OC				
	N1	N3	N5	N15	N16	382	383	398	420	429	176	223	257	268	347	87	89	120	189	198
Isovaleryl-CoA dehydrogenase, mitochondrial									Y				Y	Y	Y					
potassium channel tetramerisation domain containing 6													Y		Y					
AF4/FMR2 family, member 4	Y							Y					Y	Y						
transcription elongation factor A (SII)-like 8												Y			Y					
stromal membrane-associated protein 1											Y				Y					
CWC15 homolog (S. cerevisiae)											Y	Y	Y							
Uncharacterized protein C20orf96													Y	Y	Y					
centaurin, beta 2													Y		Y					
AT rich interactive domain 3A													Y	Y						
Rap guanine nucleotide exchange factor 3											Y		Y							
Proline-rich protein 16												Y		Y	Y					
Kanadaptin									Y		Y				Y					
Glucose-6-phosphate isomerase												Y	Y							
holocarboxylase synthetase		Y									Y				Y					

	Non-Remarkable					Benign					Early OC					Late OC				
	N1	N3	N5	N15	N16	382	383	398	420	429	176	223	257	268	347	87	89	120	189	198
Mevalonate kinase														Y	Y					
Rho GTPase activating protein 17, transcript variant 1	Y								Y			Y	Y		Y					
aldehyde dehydrogenase 7 family, member A1		Y							Y					Y	Y					
chromogranin B											Y			Y						
6-phosphofructo-2-kinase/fructose 2,6 biphosphatase 1								Y				Y	Y		Y	Y				
RD RNA binding protein													Y	Y						
DEAD (Asp-Glu-Ala-Asp) box polypeptide 1												Y			Y					
Transducin-like enhancer protein 4											Y		Y		Y	Y				
nudix-type motif 21								Y				Y			Y					
Kelch-like ECH-associated protein 1									Y		Y				Y					
leucine rich repeat containing 6													Y		Y					
inositol(myo)-1(or 4)-monophosphatase 2									Y				Y		Y					
glutamate receptor, ionotropic, NMDA-like 1A, transcript variant 1									Y				Y		Y					

	Non-Remarkable					Benign					Early OC					Late OC				
	N1	N3	N5	N15	N16	382	383	398	420	429	176	223	257	268	347	87	89	120	189	198
Zinc finger CCHC domain-containing protein 8				Y					Y				Y		Y					
TBC1 domain family member 22B			Y						Y				Y		Y					Y
coiled-coil domain containing 99											Y				Y					
solute carrier family 4, member 1, adaptor protein									Y		Y				Y					
zinc finger protein 496												Y			Y					
chorionic gonadotropin, beta polypeptide 1													Y		Y					
glutamic pyruvate transaminase 2							Y						Y		Y					
cortactin, transcript variant 2			Y						Y		Y			Y	Y					
chromosome 1 open reading frame 87						Y					Y				Y					
potassium inwardly-rectifying channel, subfamily J, member 1, transcript variant rom-k2											Y		Y							
ADP-ribosylation factor GTPase activating protein 1, transcript variant 2													Y		Y					

	Non-Remarkable					Benign					Early OC					Late OC				
	N1	N3	N5	N15	N16	382	383	398	420	429	176	223	257	268	347	87	89	120	189	198
protein phosphatase 2, regulatory subunit B\gamma, transcript variant 4													Y		Y					
La ribonucleoprotein domain family, member 4, transcript variant 3							Y				Y		Y			Y				
Splicing factor 1												Y	Y							
family with sequence similarity 102, member A, transcript variant 2			Y										Y	Y						
regulator of calcineurin 1, transcript variant 2													Y		Y					
PREDICTED: Homo sapiens hypothetical gene supported by BC047417, transcript variant 1													Y		Y	Y				
PREDICTED: Homo sapiens hypothetical LOC401363													Y		Y					

Table C.5: Autoantibody frequency of non-remarkable associated antigens

	Non-Remarkable					Benign					Early OC					Late OC				
	N1	N3	N5	N15	N16	382	383	398	420	429	176	223	257	268	347	87	89	120	189	198
family with sequence similarity 21, member C			Y	Y																
Serine/threonine-protein kinase 25	Y			Y																
RAD51 associated protein 1		Y	Y							Y	Y									
SH3 domain-binding protein 2	Y		Y						Y							Y				
family with sequence similarity 90, member A1	Y	Y																		
Activin receptor type-2B	Y				Y															
cysteine and glycine-rich protein 2	Y				Y															
SH2 domain protein 2A			Y	Y			Y							Y						
Hematopoietic lineage cell-specific protein		Y			Y										Y					
mitochondrial ribosomal protein L28			Y	Y																
La ribonucleoprotein domain family, member 7, transcript variant 1				Y	Y															
active BCR-related gene (ABR), transcript variant 1		Y	Y																	
Microtubule-associated protein 9		Y	Y						Y						Y					
Uncharacterized protein C19orf44		Y	Y																	
chromosome 11 open reading frame 63, transcript variant 2		Y	Y																	
Ataxin-7-like protein 3																				

Table C.6: Autoantibody frequency antigens associated with all cohorts

	Non-Remarkable					Benign					Early OC					Late OC				
	N1	N3	N5	N15	N16	382	383	398	420	429	176	223	257	268	347	87	89	120	189	198
Ig lambda chain C regions	Y	Y	Y	Y	Y	Y	Y		Y	Y	Y	Y	Y	Y	Y	Y	Y	Y	Y	Y
Immunoglobulin heavy constant gamma 1 (G1m marker)	Y	Y	Y	Y	Y	Y	Y	Y	Y	Y	Y	Y	Y	Y	Y	Y	Y	Y	Y	Y
CD3D	Y	Y	Y	Y	Y	Y	Y	Y	Y	Y	Y	Y	Y	Y	Y	Y	Y	Y	Y	Y
IGK	Y	Y	Y	Y	Y	Y	Y	Y	Y	Y	Y	Y	Y	Y	Y	Y	Y	Y	Y	Y
immunoglobulin heavy constant mu	Y	Y	Y	Y	Y	Y	Y	Y	Y	Y	Y	Y	Y	Y	Y	Y	Y	Y	Y	Y
Fc fragment of IgG, low affinity IIIa, receptor	Y	Y	Y	Y	Y	Y	Y		Y			Y	Y	Y	Y	Y		Y	Y	Y
immunoglobulin heavy constant gamma 1	Y	Y			Y		Y		Y	Y	Y	Y	Y	Y	Y	Y			Y	Y
Matrilin-2	Y		Y	Y	Y	Y	Y	Y	Y	Y	Y	Y		Y		Y		Y	Y	Y
CD79A	Y	Y	Y	Y	Y	Y	Y	Y	Y	Y	Y	Y	Y	Y	Y	Y	Y	Y	Y	Y
immunoglobulin heavy constant gamma 1		Y	Y	Y		Y		Y	Y	Y	Y	Y	Y	Y	Y	Y	Y	Y		Y
Ig gamma-1 chain C region	Y	Y	Y	Y	Y	Y	Y	Y	Y	Y	Y	Y	Y		Y	Y	Y	Y	Y	Y
family with sequence similarity 84, member A	Y	Y	Y	Y	Y	Y	Y	Y	Y	Y	Y	Y	Y	Y	Y	Y	Y		Y	
immunoglobulin kappa constant	Y	Y	Y		Y	Y	Y		Y	Y	Y	Y	Y	Y	Y	Y	Y		Y	Y
IGK	Y	Y	Y	Y	Y	Y	Y	Y	Y	Y	Y	Y	Y	Y	Y	Y	Y	Y	Y	Y
IGL, immunoglobulin lambda locus	Y	Y	Y	Y	Y	Y	Y	Y	Y	Y	Y	Y	Y	Y	Y	Y	Y	Y	Y	Y

	Non-Remarkable					Benign					Early OC					Late OC				
	N1	N3	N5	N15	N16	382	383	398	420	429	176	223	257	268	347	87	89	120	189	198
CD7	Y	Y	Y	Y	Y	Y	Y	Y	Y	Y	Y	Y	Y	Y	Y	Y	Y	Y	Y	Y
IGK	Y	Y	Y	Y	Y	Y	Y	Y	Y	Y	Y	Y	Y	Y	Y	Y	Y	Y	Y	Y
immunoglobulin heavy constant gamma 3 (G3m marker)	Y	Y	Y	Y	Y	Y	Y	Y	Y	Y	Y	Y	Y	Y	Y	Y	Y	Y	Y	Y
immunoglobulin kappa constant	Y	Y	Y	Y	Y	Y	Y	Y	Y	Y	Y	Y	Y	Y	Y	Y	Y	Y	Y	Y
immunoglobulin kappa variable 1-5	Y	Y	Y		Y	Y	Y	Y	Y	Y	Y	Y	Y	Y	Y		Y	Y	Y	Y
immunoglobulin kappa variable 1-5	Y	Y	Y	Y	Y	Y	Y	Y	Y	Y	Y	Y	Y	Y	Y	Y	Y	Y	Y	Y
immunoglobulin heavy constant mu	Y	Y	Y	Y	Y	Y	Y		Y	Y	Y	Y	Y	Y	Y	Y	Y	Y	Y	Y
EGF-like repeats and discoidin I-like domains 3	Y	Y	Y	Y	Y	Y	Y		Y	Y	Y	Y	Y	Y	Y	Y	Y	Y	Y	Y
immunoglobulin heavy variable 4-31	Y	Y	Y	Y	Y	Y	Y	Y	Y	Y	Y	Y	Y	Y	Y	Y	Y	Y	Y	Y
immunoglobulin kappa constant	Y	Y	Y	Y	Y	Y	Y		Y	Y	Y	Y	Y	Y	Y	Y	Y	Y	Y	Y
Ig kappa chain C region	Y	Y	Y	Y	Y	Y	Y	Y	Y	Y	Y	Y	Y	Y	Y	Y	Y	Y	Y	Y
immunoglobulin kappa constant	Y	Y	Y			Y	Y	Y	Y	Y	Y	Y	Y	Y	Y	Y	Y	Y	Y	Y
Ig gamma-1 chain C region	Y	Y	Y	Y	Y	Y	Y	Y	Y	Y	Y	Y	Y	Y	Y	Y	Y	Y	Y	Y
immunoglobulin kappa constant region	Y	Y		Y	Y		Y		Y	Y	Y	Y	Y	Y	Y	Y	Y	Y	Y	Y

	Non-Remarkable					Benign					Early OC					Late OC				
	N1	N3	N5	N15	N16	382	383	398	420	429	176	223	257	268	347	87	89	120	189	198
Ig gamma-1 chain C region	Y	Y	Y	Y	Y		Y	Y	Y		Y	Y	Y	Y	Y	Y	Y	Y	Y	Y
Ig gamma-1 chain C region	Y	Y	Y	Y	Y		Y		Y	Y		Y	Y	Y	Y	Y	Y	Y	Y	Y
twinfilin, actin-binding protein, homolog 1 (Drosophila)	Y	Y	Y			Y	Y	Y	Y	Y	Y		Y		Y	Y	Y			Y
tripartite motif-containing 21	Y	Y	Y	Y	Y	Y	Y	Y	Y	Y	Y	Y	Y	Y	Y	Y	Y	Y	Y	Y
LIM and senescent cell antigen-like-containing domain protein 1	Y	Y	Y			Y	Y		Y	Y	Y	Y	Y	Y	Y	Y	Y			Y
hematopoietic SH2 domain containing	Y	Y	Y	Y	Y	Y	Y	Y	Y	Y	Y	Y	Y	Y	Y	Y	Y	Y	Y	Y
recombination signal binding protein for immunoglobulin kappa J region	Y	Y	Y	Y	Y	Y	Y	Y	Y	Y	Y	Y	Y	Y	Y	Y	Y	Y	Y	Y
Recombinant human CTLA-4/Fc	Y	Y	Y	Y	Y						Y	Y	Y	Y	Y	Y	Y	Y	Y	Y